How suboptimal are retail products? An analysis of different sources of suboptimality

Von der Mercator School of Management, Fakultät für Betriebswirtschaftslehre, der

Universität Duisburg-Essen

zur Erlangung des akademischen Grades

eines Doktors der Wirtschaftswissenschaft (Dr. rer. oec.)

genehmigte Dissertation

von

Stefan Kaltepoth

aus

Duisburg

Referentin: Prof. Dr. Antje Mahayni

Korreferent: Prof. Dr. Peter Anker

Tag der mündlichen Prüfung: 08.12.2015

Contents

List of Figures

List of Tables

CHAPTER 1

Introduction of the thesis

1.1 Motivation and structure of the thesis

During recent decades, the variety of financial products has continuously grown. Besides the number of financial products, their complexity has also increased. Indeed, this development holds for different classes of financial products. For example, we can refer to structured products (resp. certificates) which play a major role in the financial markets. In Germany, the volume of certificates has leveled off between 80 and 100 billion euro since 2009. Before the financial crises began in 2007[1], the volume reached a peak level at 139 billion euro. However, the current level is almost twice as high as at the beginning of the statistic in 2004.[2]

Of course, the number of special certificates and their complexity have both increased. Evidence is provided by the Swiss Market, where the number of observed products classes rose from 18 to 26 from 2007 to 2014.[3]

Other financial products have undergone a comparable development; for instance, insurance contracts began to change in the 20th century. Forced by factors including demographic changes in the population, insurance companies had to reorganize their business to ensure future liabilities. However, the current period of low interest rate is more challenging, which started during the financial crises. Here, insurance companies have adjusted their range

1 When we mention the financial crises, we mean the crises beginning in 2007, which also includes the default of the investment bank "Lehman Brothers".

2 The relevant statistics about certificates in Germany are published by the "Deutsche Derivate Verband"(DDV) at "www.derivateverband.de/DEU/Start". Comparable statistics for the European Structured Investment Products Association are published at www.eusipa.org.

3 The figures are given by reports from the Swiss Structured Products Association ("www.svsp-verband.ch"). They classify each new product in categories and rank it by a special risk grade.

of products with insurance contracts in a style of a financial product often linked to the movement on an equity market.[4]

The variety and complexity of the financial products offered depends on different factors. First, increasingly more issuers of financial products are operating in the financial markets. As a natural result, the number of products has increased. Second, the issuers are forced by the high competition to develop new products. However, it is observed that new products become more complex than the older ones. Of course, the issuer uses the complexity in their investment product to make them incomparable to other products. Carlin [Car09] mentioned that the more complex a product, the higher the profit that an issuer could engross.
Finally, regulatory requirements also influence the development of new investment products. In particular, German insurance companies have to develop contracts offering a guarantee as well as participation in an equity market to meet the requirements of some governmental schemes.[5] Such products enlarge classical insurance contracts and make them increasingly comparable to other investment strategies.
Owing to this development, an investor has to choose between many different investment opportunities. We observe an investor with a finite time horizon who tries to maximize her utility. More precisely, we assume that the investor's preferences can be described by the expected utility of terminal wealth. In particular, for utility functions with constant relative risk aversion, retail products can be compared by comparing the expected utility of the returns.

However, we assume that the financial market is complete from the perspective of the product provider (the issuer of the products). In a Black and Scholes model setup, we assume that the provider can generate any payoff profile by dynamic trading in two basis assets, namely a risky asset and a risk-free asset. In principle, the product provider could offer an "overall" optimal product to the retail investor.
By contrast, we assume that the financial market is incomplete for the retail investor. She has to resort to a restricted class of products since she cannot generate her optimal product through a dynamic trading strategy.
However, within the restricted class of offered products (payoff profiles, respectively), the investor can choose her optimal one.

4 A detailed description of the developments of insurance contracts can be found in Schneider [Sch11].
5 e.g. Schneider [Sch11] mentions that pension schemes from the second pillar of retirement savings have to offer a guarantee in Germany.

Nonetheless, the optimal choice of a payoff profile generated by the offered retail products will generally differ from the theoretically overall optimal product for the investor.
In summary, from the investor's perspective there exists an overall optimal payoff profile that suits her preferences. However, given that she suffers from an incomplete market, she can only choose between the offered retail products.

Of course, it is an adequate assumption that an investor could only choose from a fixed number of stylized products offered by the issuing companies.[6] In general, the investor will suffer from the suboptimality of the stylized products. Even if the investor chooses the optimal product among the traded ones, this is suboptimal compared to the overall optimal solution (which is not available to the investor). In addition to the suboptimality caused by the restricted set of products, the investor faces additional sources of suboptimality.
The question is how the product is influenced by these exogenous sources. More importantly, what is the influence on the investor's utility?

Thus, this thesis examines different sources of suboptimality and their influence on the investor utility. By quantifying the levels of suboptimality for varying financial products, we can classify which sources most strongly influence the investor's utility.
For this reason, it is an appropriate assumption that the investors know their optimal investment strategy. More precisely, we always assume an expected constant relative risk aversion (CRRA) utility maximizing investor under the assumptions of the Black and Scholes model where the optimal payoff profile is given by a Constant-Mix strategy.[7] A Constant-Mix strategy is a strategy where the fraction of portfolio wealth invested in the risky asset is constant during the entire investment period. Note that each CRRA investor can be classified by the risk aversion parameter γ. Thus, the optimal Constant-Mix strategy can be defined by the assumed γ.[8] In particular, we use the corresponding utility of the Constant-Mix payoff profile as an optimal "benchmark" utility.
In our analysis, we compare the utility of terminal wealth of the retail products observed with an overall optimal Constant-Mix utility using realistic market data. If a product is not optimal for the investor, we will assess the grade of suboptimality by a loss rate, which

6 The issuer could be a bank, an insurance company or another financial institution.
7 cf. Merton [Mer71] as well as Proposition 1 in Section 3.3.3.
8 More precisely, a Constant-Mix strategy is defined by a constant investment fraction on the entire investment period. Assuming a fixed drift parameter, volatility and risk-free interest rate, the optimal constant investment fraction can be stated as a function of γ.

describes the discrepancy of the calculated utility from the optimal one.

Furthermore, we observe real traded retail products. Since we assume an arbitrage-free and complete financial market from the issuer's perspective, we are able to calculate "fair" model prices of the observed traded payoff profiles.[9] Here, we are able to compare the calculated Black and Scholes model price with the real market price. For this reason, we introduce a special loss rate that separates the utility loss depending on a mispricing and the loss regarding the suboptimal structure of the product.

For our observation, we assume the following sources of suboptimality.
We define the problem of disposability of the optimal product: in other words, we assume that the investor knows the optimal product class, as well as the optimal product specification that fits her risk aversion γ. However, the optimal products digress from the required product specification. In this case, even the stylized products offered are optimal for another γ, whereby the observed investor suffers by investing in a sub-optimal product.

Furthermore, we acknowledge that the variety of financial products (resp. structured products) available to the investor has continuously grown. In particular, we observe structured stylized product that allow additional payoff specifications written on the corresponding value process of the optimal Constant-Mix strategy. Thus, we combine the optional investment strategy with a guarantee, a cap or even an additional path-dependent payoff feature. By definition, the adjusted product will be suboptimal for the CRRA investor. We analyze this effect of additional product features and value them with the defined loss rate, which describes the mismatch compared to the optimal utility.

Moreover, we account for margins, i.e. an unfair pricing of the stylized and structured stylized products. Since the complete market assumption holds for the issuer, she knows the fair (arbitrage-free) price of a product. Therefore, she can offer a product for a higher price at issue date.[10] For this reason, we define the relevant product margin owing to an overvaluation at issue date. Since the offered (unfair) products have a lower fair price, they

9 Remember, that we assume that the issuer can generate any payoff profile by dynamic trading in two basis assets. Thus, we can also calculate the initial value (resp. model price) of the investment strategy that generates the observed payoff profile.

10 More precisely, we assume that all products are offered for the same price: the nominal amount of the product. Thus for an embedded margin the fair (arbitrage-free) price has to be below the nominal amount.

have to differ from the fair product design which results in the nominal amount. Thus, we analyze how the adjusted specification (e.g. a lower guarantee resp. lower cap) influences the utility of the investor.

Furthermore, we consider a Black and Scholes model with default risk in Chapter 6.[11] By contrast to the standard Black and Scholes model, where the solvency of the issuer is not observed, we explore a structured stylized product including issuer default risk.[12] Note, a default of an issuer will influence the payoff profile of a product in such a manner that e.g. the guarantee is not paid. In the case of a default, we calculate the payoff by multiplication of the theoretical product payoff and the assumed recovery rate. In general, the investor suffers a huge loss, since the recovery rate is typically below 50.0 %.[13]
We assume that the financial market is complete from the perspective of the the issuer. Thus, the issuer knows her solvency at issue date and can offer fair products including her probability of default. With the application of the model and the complete market assumption for the issuer, we are able to compare payoff profiles for different solvencies. Assuming that the optimal Constant-Mix strategy is not affected by any default risk, the investor could suffer from the suboptimal structure of the offered product and an optional default of the issuer, although the payoff profile looks more attractive.[14]

Chapter 3 focuses on stylized products as well as structured stylized products. First, we analyze the suboptimality pertaining to the problem of disposability of the optimal stylized products. Second, we use a Constant-Mix strategy resp. the value process of a Constant-Mix strategy (which is optimal for $\gamma = 2$) as the underlying asset for structured stylized products. We use guarantees and caps to distort the optional payoff profile. Furthermore, we combine the observed products with path-dependent payoff features that rely on a minimum or averaged calculation method. Finally, we allow an embedded margin

11 Goetz et al. [Goe10] introduced a Black and Scholes model where the issuer of a retail product can become insolvent during the entire investment period.
12 In general, structured stylized product (resp. certificates) are structured as bearer bonds. This means that the products are influenced by the solvency of the issuer. For instance, structured products from the issuing company Lehman Brothers were almost worthless in September 2008 when the company became insolvent.
13 cf. Section 6.2.4.
14 Of course, allowing a default of the issuer influences the fair price of a product. However, comparing model prices and observed market prices, we define the difference of the market price and the model price as an embedded margin in the product.

so that the product specification has to be adjusted. More precisely, we assume that the nominal amount of all observed products is identical; thus, the issuer will deteriorate the payoff profile to gain a margin.
For all analyzed products, we quantify the suboptimality by a loss rate. The loss rate illustrates the utility loss of an investor who invests in a suboptimal product. More precisely, the loss rate puts the expected utility of the suboptimal product and the expected utility of the optimal product in relation with each other.[15] For the analysis of the embedded margin, we also illustrate our result by a special loss rate separating the influence of the margin and the influence of the suboptimal product design.

In Chapters 4 and 5, we consider two existing classes of structured products and assume that the dynamics of the risky asset (serving together with one risk-free asset as the basis assets of the financial market) satisfy the assumptions of the Black and Scholes model (and Heston model, respectively). In contrast to Chapter 3, we use an equity index as the underlying asset rather than the value process of the optimal Constant-Mix strategy.[16] Thus, the focus is on the suboptimality of the product specification in combination with a suboptimal underlying asset. In both analysis, we assume that the investor has to resort to the restricted class of the observed structured products. Thus, the financial market is incomplete for the investor. While the investor can choose the optimal product within the restricted class, her choice differs from her overall optimal solution.

The specific class of Best Garant Certificates (BGCs) is analyzed in Chapter 4. The certificates are characterized by a guaranteed rate, a cap rate and a best-entry strike. Two of the three observed BGCs offer a best-entry strike derived by a path-dependent calculation of the underlying price during an observation period. Beside the analysis of fair product design and the return rate distribution at maturity, we focus on the suboptimality of the products by calculating the utility loss compared to the optimal investment strategy of a CRRA investor. The analysis also contain a calculation referring to real market date.

Chapter 5 focus on the class of Globally Capped Garant Certificates (GCGC) and Lo-

15 In this regard, we use the certainty equivalent rather than the expected utility in the following. The certainty equivalent is defined by the certain amount that makes the investor indifferent between achieving this certain amount (at maturity) or choosing the product.
16 This is along the lines of the actual design of the observed certificates.

cally Capped Garant Certificates (LCGC)[17]. Both certificates offer a guarantee amount at maturity. The special payoff feature of the LCGC is calculated with a fix number of sub-period returns where each observed return of the underlying is bounded, so that in the final calculation a combination of effective returns and a number of capped returns are relevant. Our analysis is analogous to the BGC. The main focus is on the loss rate associated with the special product features. Beside the level of guarantees, we focus on different observation periods that define the rate of path-dependence. Furthermore, we also consider the influence of different volatility levels.

An extension of the BGC observation (cf. Chapter 4) is given in Chapter 6, whereby we analyze the class of defaultable Best Garant Certificate (DBGC) in a Black and Scholes model with default risk. Here, we use the identical assumption for the issuer and the investor as in the previous chapters. Thus, we assume that the financial market is complete from the perspective of the issuer of the defaultable products. By contrast, we assume that the financial market is incomplete for the retail investor. Accordingly, she is restricted to the class of defaultable Best Garant Certificates. We highlight the adjustments regarding the fair product design and the simulated return rate at maturity of the three DBGCs. On the one hand, we calculate the loss rates based upon the fair product design. On the other hand, we analyze real trade DBGCs assuming regarding real market data. We separate two source of suboptimality for the real traded DBGC. Thus, we finally mention the ratio between the loss emanate from the structure of the certificates and the loss belongs to the unfair market price.

Finally, an observation combining the preference of the investor and the issuer is made in Chapter 7. We assume that the offered product are always overvalued at issue date due to an embedded margin. Assuming this constraint, we try to answer the question of whether any product designs are optimal for both the investor and the issuer. For the relating calculation, we introduce a sales margin as well as a hedging margin. While the sales margin is constant, the hedging margin that an issuer requires depends on the Value-at-Risk approach. We illustrate the optimal product design under consideration, as well as the calculated certainty equivalent for the investor.

17 A first analysis is made by Bernard et al. [Ber11b] where a different description for the observed certificates are used. On the one hand, they use the description of Locally-Capped and Globally-Capped Contracts. On the other hand, they refer to existing products called locally-capped globally floored index link notes. In our analysis, the corresponding certificates are named Locally resp. Globally Capped Garant Certificates, which highlights that the certificates belongs to the class of garant certificates.

The main results of the thesis are as follows. Chapter 3 illustrates different sources of supoptimality which are related to the imcomplete market assumption for the investor who has to select from a restricted set of products offered by the issuer. Focusing on stylized products, the problem of disposability leads in the best case to a loss rate that is almost zero if one of the offered products fits the investor's preference; otherwise, the minimum loss rate varies between $l_T = 0.27$ % and $l_T = 0.44$ % in our observation. We assume an exemplary CRRA investor (with $\gamma = 2$) for structured stylized products written on the value process of her optimal investment strategy (resp. the optimal stylized product). We ascertain that a loss rate close to zero is possible if we assume a very low guaranteed rate resp. a very high cap rate. Under this product specification, the payoff distribution is almost identical to the optimal strategy. However, in general the investor suffers from an investment in a guarantee product (GP), a capped product (CP) or a product with guarantee and cap (GCP). Our examples illustrate a loss rate of $l_T = 0.42$ % for a GP that grants the nominal amount and $l_T = 0.961$ % for the comparable GCP. Although the GCPs show the highest level of suboptimality (resp. highest loss rate), we ascertain that the investor can lower her utility loss if she selects a more risky underlying asset. However, selecting the most risky underlying asset only improves the loss rate from $l_T = 0.961$ % to $l_T = 0.894$ %.
The results based upon the path-dependent products significantly differ. The loss rates for the observed investor are always above $l_T = 0.5$ % for all path-dependent products, while the highest loss rates are observed for the path-dependent GCP. The averaging feature leads to a loss rate of 1.0 % and above. However, for all minimum calculation features, $l_T > 1.7$ % holds.
The impact of the embedded margin could be noticed as a parallel shift of the loss rate. However, the separated loss rate by margin does not show an explicit trend. For the observed investor, an exemplary margin ($M_2 = 2$ %) will lead to the separated loss rate by margin of at least $l_T^{(\text{margin})} = 0.4$ % for the selected guarantee products. If we focus on the selected path-dependent capped products we identify a $l_T^{(\text{margin})}$ that is on average below 0.4 %.

For the class of BGCs (which includes path-dependent and path-independent certificates) analyzed in Chapter 4, we ascertain the following. First, it is seen that the entry strike (resp. the path-dependent feature) does not necessary improve the return distribution. An entry strike that tends to be lower also generates a lower fair cap rate. We identify for

all BGCs that over three-quarters of the simulated return rates at maturity are equal to the guaranteed rate or the cap rate. The highest weight is observed for the minimum strike setting at the corresponding cap rate (where this cap rate is the lowest of all BGCs). Thus, the investor has to decide whether to select a product that gives a moderately good return relatively often or one that can obtain a higher good return less often.
Second, we observe that the optimal guaranteed rate of a BGC for a CRRA investor (with assumed risk aversion parameter $\gamma = 5$) is not necessarily equal to zero. In addition, we calculate a high loss rate for the minimum entry strike BGC compared to the fixed entry strike setting without any path-dependence. The calculated loss rates lie between 0.2 % and 0.4 % for a small guaranteed rate. However, the fair cap rates and the loss rates calculated in the Black and Scholes model look more attractive than the results based upon the Heston model.
Regarding the real traded BGCs, we could mention that the calculated model prices are always above the nominal amount at issue date, which seems to result from our assumption. Nevertheless, we illustrate that separated loss rates rely on the structure of the product, as well as the loss rate derived from the market price. On average, the investor suffers from an investment in a BGC by almost $l_T = 0.1$ %, although the products are undervalued at issue date.

The analysis in Chapter 5 highlights the huge influence of path-dependence on the class of Locally Capped Garant Certificates (LCGC). Of course, the fair locally caps are lower for higher guaranteed rates. However, the calculated fair locally caps are higher for longer observation period resp. smaller numbers of observation dates. Note that the combination of locally caps and the number of observation date defines the maximum return rates of the LCGCs.
We ascertain that the return rates at maturity of the LCGCs always have an accumulation at the guaranteed rate, but there is no point mass at a specific positive return rate. Below the corresponding maximum return, we observed a more-or-less smooth development of positive return rate. However, it emerges that the higher the theoretical maximum return (resp. the higher the locally cap), the higher the weight at the guaranteed rate and the lower the weights at the relative good positive returns. Thus, the investor has to decide whether she is confident about a good return or if she requires a very high return with the side effect that the probability of simply getting the guaranteed rate is higher.
In addition, we show that the assumed volatility has a huge influence on the results, where a higher volatility results in a significantly higher locally cap rate. At once, the simulated

average return rates and median are clearly worse.
The calculated loss rates show that all LCGCs are suboptimal for the assumed CRRA investor (with $\gamma = 5$). Here, the loss rates are especially high in the case of short observation periods. In particular, the minimal loss rate is calculated for a guaranteed rate above zero. Depending on the length of the observation period, it is identified between $l_T = 0.35$ % and $l_T = 0.45$ % in the Black and Scholes model and $l_T = 0.55$ % and $l_T = 0.75$ % in the Heston model.

Chapter 6 refers to the analysis of the BGCs. By taking into account default risk which means that the issuer of the BGC can become insolvent before maturity, we calculate significantly higher fair cap rates than in Chapter 4. However, most results regarding the product design are analogous with Chapter 4, only differing in the corresponding level. Focusing on the return rate distribution, we identify a third accumulation point which illustrates a negative return rate generated by a default event. Thus, besides the choice of the different entry strike setting, the investor could select an issuer who is more solvent than another issuer. Although the product specification looks less attractive, the simulated return rates illustrate the merits of a more solvent issuer. In the case of an issuer default, the investor will suffer from a negative return rate, which is significantly below the defined guaranteed rate. Accordingly, it holds that the higher the probability of an issuer's default, the higher the fair cap rates. Thus, an additional aspect influences the investor's loss rate. It is seen that the entry strike setting is inconsiderable in comparison to the optimal default of the issuer. The calculated loss rates are above $l_T = 2.75$ %. In addition, the loss rate is strictly decreasing with higher a guaranteed rate, which could be explained by a higher recovery rate in the case of a default. By taking into account default risk, we are able to repeat the analysis of the real trade DBGC under more realistic assumptions. It results that all DBGC are highly overpriced at issue date. The fair model prices lie between 92.0 % and 94.5 % of the nominal amount. The loss rates for the traded products are all above $l_T = 4.0$ %. Furthermore, we illustrate the separated loss rates and mention that over 93 % of the overall loss rate is explained by the suboptimal product design of the DBGC.

The results of Chapter 7 are summarized as follows. We focus on two sources of suboptimality assuming products with guarantees and caps. The CRRA investor who is restricted on the offered products suffers from the suboptimal product specification and by an embedded margin of the issuer. We determine the optimal product design and the corresponding certainty equivalents for three constraints and two underlying asset V_t and

S_t. However, the illustrated optimal product design from the investor's perspective only holds for the restricted class of products with guarantees and caps. Nonetheless, the optimal product design will generally differ from the theoretically overall product design of the investor.

First, we observe the fair product design without a margin. In the calculation of the fair combination of guaranteed rate, cap rate and participation rate, it emerges that the optimal solution can result in such low guaranteed and high cap rates which have only a marginal influence on the payoff distribution of the product. For example, this happens if we assume an underlying that is already optimal for an investor. In this case, the investor does not suffer from any suboptimality. However, all other observed investors find an optimal solution for the assumed product, but their certainty equivalents are at least 0.25 % lower than the optimal one. Thus, even we assume a fair product design, the investor suffers by a lower certainty equivalent with depends on the product specification using guarantees and caps.

The results relying on the embedded margin are as follows. If we assume a fixed sales margin of 2.0 % we will identify that for all risk aversion parameter the adjustment are identical. Compared to the optimal fair product design the guaranteed rate, the cap rate as well as the participation rate decreases by a fixed amount for each risk aversion parameter. Thus, also the adjusted certainty equivalents result from a parallel shift. Additionally to the utility loss caused by suboptimal product specification, all investors suffer from the sales margin by a adjusted certainty equivalent p.a. which is 0.4 % lower.

Finally, we assume a hedging margin derive from a Value-at-Risk approach. In this observation, we identify different results depending on the assumed underlying asset. Once, it is optimal for the investor if the issuer increase the cap rate and the guaranteed rate, but at the same time decrease the participation rate; otherwise, we observe a lower guaranteed and cap rate while the participation rate is higher for the other underlying. However, we identify optimal product design with lower hedging margin compare to the theoretical hedging margin of the optimal fair product. However, the investor always suffer from an embedded hedging margin, although the overall grade depends on the assumed underlying asset.

1.2 Summary of the thesis

In **Chapter 3** we analyze different classes of products regarding the investor's utility.

First, we give a short overview of the general market model and some basic information of

the observed product design. Additionally, we show some well-known investments strategies with their special characteristics.
To start the analysis of the different products from the investor's perspective, we state the investment problem and the optimization problem of maximum expected utility. This problem was first mentioned and solved by Merton [Mer71]. We apply his results and use them for a CRRA investor, whereby a Constant-Mix strategy is optimal in a complete Black and Scholes model. However, in our analysis we assume that the financial market is incomplete for the retail investor. Thus, the investor has to resort to a restricted class of products since she cannot generate her optimal product by herself.
Of course, she can choose her optimal product within the restricted class of payoff profiles, but it will differ from the theoretical, overall optimal product for the investor. For each of the observed products, we try to determine how the investor's utility is influenced by the considered sources of suboptimality. Thus, we use the optimal solution (Constant-Mix strategy) which holds in a complete financial market for the calculation of the benchmark utility.

We analyze stylized product and quantify the problem of disposability of the optimal product. We observe four stylized product and state the resulting decision problem for the investor. In general, an investor suffers by investing in one of the offered stylized products owing to their digression from the required optimal product specification. Thus, we can quantify the utility loss of the investor, which results in the suboptimal product design.
Furthermore, we allow additional payoff specification written on the optimal investment strategy. Regarding the huge variety of structured products, we combine the optional investment strategy with a guarantee, a cap or even an additional path-dependent payoff feature and give an overview of the relevant fair product design. Using the value process of the optional investment strategy as the underlying asset, we can focus on the separated influence of the corresponding product specification. Of course, the structured stylized products are suboptimal for the CRRA investor since the investor do not required any additional features.
On the one hand, we analyze the effect of the additional product features and value them with the defined loss rate, which describes the mismatch to the optimal utility. Exemplary, we show that an expected CRRA utility maximizing investor suffer from any additional guarantee.
On the other hand, we select one product of each observed product class that would lead to a utility loss for the investor. For this selection, we try to calculate if a more risk seeking

resp. a more risk aversion underlying asset will result in a lower utility loss.
Finally, we allow an embedded margin in the selected products. For this reason, we define the relevant product margin as a result of an overvaluation at issue date. Since the products have a lower fair price which is calculated by the issuer under complete financial market conditions, they have to be differ from the fair product design. Thus, we analyze how a lower guarantee resp. a lower cap influence the utility of the investor. More precisely, we separate a loss rate depending on the specific structure of the product (loss rate by structure) and a loss rate owing to the embedded margin (loss rate by margin). It emerges that the overall loss rate looks comparable to the loss rate by structure. For the loss rate by margin, we cannot identify a clear trend.

In particular, this chapter encourages the analysis in the following two chapters. In Chapters 4 and 5, we have a detail look at two different structured products, which includes a guarantee, a cap as well as a path-dependent payoff feature. By assumption, the financial market is incomplete for the investor. Thus, she has to resort to the restricted class of the observed structured products. While the investor can choose the optimal product within the restricted class, her choice differs from her overall optimal solution

In **Chapter 4**, we analyze BGC advertised in Germany[18] by attractive return characteristics achieved by best-entry prices/strikes. In addition to a guaranteed rate, the investor participates on the excess return that is measured regarding the so-called entry strike. Nonetheless, the investor gives up some of her upward participation for the entry strike, as well as the guarantee. We consider three cases for the (entry) strike setting: fixed, average and minimum entry strike.
Our main contributions are as follows. We derive and analyze fair combinations of guaranteed and cap rates for all entry strike settings in a Black and Scholes and a Heston model setup.
Based upon the observation that both, an entry price which tends to be lower and a higher guaranteed rate, afford a lower (fair) cap rate, the *best* entry strike does not necessarily improve the return distribution of the BGC in the context of fair contracts. Therefore, we consider the question of whether an investor benefits from the best-entry strike setting and the guarantee.
We analyze the optimality (suboptimality) of the entry strike setting and the overall

18 The corresponding BGCs were offered between 2009 and 2010.

product design for an expected CRRA utility maximizing investor who is restricted to the class of BGCs. Interestingly, it emerges that a Best Garant investor does not necessarily suffer from a higher guaranteed rate. In the case of a fair cap rate, the utility of a BGC increases with the guaranteed rate for small guaranteed rates but decreases after some (optimal) guarantee level. In addition, we show that the *best* entry feature, i.e. the minimum strike setting and the average strike setting, are suboptimal compared to the fixed strike setting for low guaranteed rates. We illustrate our results by means of real market data. We consider the model prices at issue date and loss rates implied by traded BGCs. It is observed that all certificates are undervalued at issue date, which could result from our assumed parameter. However, we use a special loss rate calculation and ascertain that some certificates seems inefficient for the CRRA investor although they are issued above their nominal amount.

In **Chapter 5** we focus on the class of Globally Capped Garant Certificates (GCGC) and Locally Capped Garant Certificates (LCGC)[19]. Analogous to the BGCs, the main feature of these certificates is the combination of a guarantee, a cap and a path-dependent underlying observation. The payoff is floored at the nominal amount or at an amount above, so that the investor receives independently from the underlying performance an amount greater than or equal to her initial investment. With an additional amount, the investor participates in the performance of the underlying asset. However, rather than simply calculating the excess return of the underlying between the issue date and maturity, a fix number of sub-period returns is observed and finally combined. As the special feature, each observed return of the underlying is bounded, whereby a combination of effective returns and a number of capped returns are relevant in the final calculation.

We observe five different calculation sequences: monthly, quarterly, semi-annual, annual and globally. The globally sequence includes that there is no sub-periodical calculation, e.g. only the terminal return at maturity is taken into account for the certificate. We analyze fair combination of a guaranteed rate and a locally cap for all of the certificates. For the analysis, we again refer to the Black and Scholes model, as well as the Heston model, which allows stochastic volatility.
It is seen that shorter observation periods (more sub-period returns are calculated) include the opportunity for higher payoffs a maturity. We identify that the shorter the observation

19 This type of certificates were first analyzed by Bernard et al. [Ber11b]

period the higher the theoretical maximum payoff. We analyze the optimality resp. suboptimality of these payoffs for an expected CRRA utility maximizing investor, knowing that all payoff profiles of the LCGCs resp. GCGCs differ from the overall optimal payoff profil of a CRRA investor. On the one hand, we ascertain that the investor could suffer from the short observation period in terms of a high loss rate. On the other hand, we mention that there is an optimal guarantee rate above zero where the investor benefits most of a corresponding structure.

Furthermore, we consider the influences of different volatility (resp. variance) levels. Although an assumed higher volatility includes higher caps and consequently higher theoretical maximum payoffs, the simulated figures under the real world measure show changes in the payoff distribution at maturity, which could be interpreted as suboptimal for the investor. For instance, the number of the simulated payoffs only paying the guarantee amount significantly increases with higher volatility.

In **Chapter 6**, we conduct an additional analysis for the class of BGC since we take into account default risk. Using the identical assumption concering the completeness and incompleteness of financial markets, our main contributions are analogous to Chapter 4. However, we rely on a Black and Scholes model under default risk. For this reason, we apply the model setup introduced in Goetz et al. [Goe10].
Regarding the characteristics of the issuing company, we use a recovery rate as well as an initial debt, which describes the debt of the issuer at the corresponding issue date.
Beside the standard payoff profiles, we illustrates the return rates in the case of an possible issuers default regarding the guaranteed rate, the cap rate and the entry strike setting. We should mention that the price for all DBGCs is significantly influenced by the issuer depending parameter. The price of the DBGC is decreasing with a higher initial debt of the issuer and is increasing with a higher recovery rate.

In addition to the question of whether a DBGC investor benefits from the best-entry strike setting and the guarantee, we illustrated the risk comes along with an issuing company which could become insolvent during the time to maturity. Again, we analyze the optimality (suboptimality) of the entry strike setting and the product design for an expected utility maximizing CRRA investor. Interestingly, it emerges that a Best Garant investor could profit from a higher guaranteed, which results in a lower cap rate. In the case of a fair product specification, the utility of a DBGC increases with the guaranteed

rate. This could be explained by the fact that with a higher guaranteed amount also the amount calculated by the recovery rate in the case of an issuers default is higher.
In addition, we show that the *best* entry feature, i.e. the minimum strike setting and the average strike setting, are suboptimal compared to the fixed strike setting.
We illustrate our results by means of real market data and take into account default risk. We consider the model prices at issue date and loss rates implied by traded DBGCs. It is observed that all certificates are highly overvalued at issue date, although the path-dependent DBGCs are relatively more overvalued than the DBGCs with the fixed strike setting.
In addition, the loss cause by a suboptimal product design, which results from the comparison to the *non-defaultable* optimal Constant-Mix strategy is significantly higher compared with the loss, given that the certificates include margins. We compare our results to the product design of currently offered BGCs.

In **Chapter 7**, we consider the optimal product design of products with guarantees and caps from the both investor's and the issuer's perspective, allowing an embedded margin.
We assume that an issuer do not offer any products for free. Thus, we will explore an adjustment of the fair product design, which implies an embedded margin. Nevertheless, we suggest that the issuer try to offer products that fit the investor's preference.
The embedded margins define an addition source of suboptimality for the investor. However, we differ between two margins: an exogenously given sales margin $M_{(sales)}$ and an issuer's hedging margin $M_{(hedge)}$. On the one hand, we presume a sales margin which is more-or-less given exogenously. On the other hand, we use a hedging margin, which the issuer has to apply. In our observation, we assume a hedging margin that increases with the Value-at-Risk of the return rate distribution of the product.
We observe products characterized by a guaranteed rate g, a participation rate α and a cap rate c.[20] In our analysis, we allow two different underlying assets where both can be interpreted as Constant-Mix strategies. V_t is the value process of the optimal Constant-Mix strategy for the risk aversion $\gamma = 2$ and S_t describes a Constant-Mix strategy which invests the complete amount in the risky asset.[21]
However, we calculate the optimal product design for an investor who is restricted to the set

20 By contrast to Chapter 3, we allow a variable participation rate α.
21 The underlying S_t can be compared to an equity index which is often used in practice.

of offered products under the constraint of an embedded margin. To classify the preference of the investor, we presume that her utility could be described by a CRRA utility function. Our analysis relies on a formulated optimization problem, where we calculate the (g,c,α)-tuple that maximizes the CRRA investor utility under constraints. The constraints are given by the fair product design or an adjusted product design, which responds to the embedded margin.

We calculate the optimal fair product design of the corresponding products. For each underlying asset, we calculate the corresponding certainty equivalent for a range of risk aversion parameter and compare the results to the overall optimal certainty equivalent.

Beyond the fair product design, the application of the optimization problem result in an adjustment of the product specification. Thus, we calculated the optimal (g,c,α)-tuple generated under the embedded margin constraint. It results that all investor suffer from the embedded margin, albeit in their optimal product design. However, it is seen that a constant sales margin influences all observed products in the same way, while a hedging margin is followed by different product adjustments. Here, it is proven that a change of the relevant underlying could gain in a higher certainty equivalent of the investor.

CHAPTER 2

Review of related literature

This chapter gives a review of related literature. We group this overview in several sections to classify the literature for each chapter separately. However, we abdicate a review of related literature for Chapter 7 since it is motivate by the result of the previous chapters.

2.1 About Chapter 3

Chapter 3 initiates the models and concepts used in this thesis. At the beginning, we illustrate the general market model assumptions, whereby we essentially refer to a standard Black and Scholes economy. The corresponding mathematical background can be found in any standard book concerning mathematical finance. For our analysis, we refer to Protter [Pro90], Karatzas et al. [Kar99] and Dana et al. [Dan07].

Subsequently, we summarize the most popular investment strategies. The characteristics of the Buy-and-Hold (B&H) strategy, The Constant-Mix (CM) strategy and The Constant Proportion Portfolio Insurance (CPPI) strategy are illustrated. Perold et al. [Per88] compare all strategies and summarize which strategy is the best dependent on the investor's risk tolerance, the volatility and the trend in the markets. However, they also group the investment strategies according to whether they result in a concave or convex payoff.

Since our focus is on quantifying the grade of suboptimality of the investment product, we want to illustrate some relating literature that also concentrates on the optimality and efficiency of financial products. Without postulating completeness, we first refer to recent work with a more technical view of suboptimality where always complete financial market condition are used.

An analysis of the optimality of a strategy without using investors' preference is stated in Dybvig [Dyb88b] and Dybvig [Dyb88a]. They derive a cost efficient strategy that offers the identical payoff distribution compared to other strategies with the lowest initial cost. Of course, the cost efficient strategy will be chosen from all investors who prefer more than less. Bernard et al. [Ber12] state the explicit representation of the cost efficient strategy with a given payoff distribution. Furthermore, for any non-cost efficient strategy, they built a strategy with financial derivatives that dominate the inefficient strategy.

More general, it is shown in Cox et al. [Cox00] that in a given one dimensional Black and Scholes market all path-dependent structures are inefficient resp. suboptimal for a risk aversion investor with finite time horizon. Bernard et al. [Ber11a] extend the result to a multi-dimensional Black-Scholes market. Furthermore Vanduffel et al. [Van09] enlarge the result from Cox et al. [Cox00] to general Levy markets.
Kassberger et al. [Kas12] generalizing the result from Cox et al. [Cox00] as well as from Vanduffel et al. [Van09] by analyzing the suboptimality of a path-dependent payoff. It is shown that a risk averse investor with finite investment horizon will prefer path-independent payoff rather than a path-dependent payoff, when the pricing kernel is a function of the terminal underlying price. However, they also mention that the model used for the underlying dynamics is less important for the suboptimalitiy; instead, the price kernel influences the level of suboptimality most.
They also assume incomplete market conditions where various pricing kernel exists. In this case, there is a martinal measure, which make a given path-dependent payoff attractive.
Larsen et al. [Lar12] analyze the cost of suboptimal strategies in a general model of return dynamics. Among others, they ascertain that an investor will suffer by a utility loss if she ignores the intertemporal hedging demand. Furthermore, also omitting some assets from the investment strategy lead to a significant utility loss.
It is seen that path-dependence take a major role in the evaluation of suboptimality. However, a quantification of the corresponding utility loss is missing in the illustrated works.
Beside the examples show the suboptimality of path-dependence, Jensen et al. [Jen15] illustrate an example of another source of suboptimality, which we also take into account in a modified way. They analyze the problem of disposability of the optimal strategy by assuming a sharing rule that two CRRA investors have to accept (e.g. Pension funds). If the manager uses a geometric mean of the two investors risk aversion parameter, the relative loss in wealth is identical for both. Of course, they ascertain that the losses will be

larger if the corresponding risk aversion parameters significantly differ. Furthermore, they find numerically a Pareto optimal solution for both investors.

Now, we also want to mention some explicit results for optimal strategies, which we in parts use for our analysis.
It is well known that Merton [Mer71] mentioned the Constant-Mix strategy as optimal for a CRRA investor. Furthermore, Branger et al. [Bra10] show that a protective put on the optimal Constant-Mix strategy is optimal for a CRRA investor when the investment strategy includes a guarantee. In addition, they mention that a CPPI will be optimal if a hyperbolic absolute risk aversion (HARA) investor with a required guarantee amount is assumed (cf. Basak [Bas02] and El Karoui et al. [EK05]).

For the analysis of the (structured) stylized products, we assume fair product design. We call a product fair if the no-arbitrage price at issue date of the corresponding product payoff is equal to the nominal amount. More precise, we use the expected discounted payoff under the risk-neutral resp. equivalent martingale measure of the observed product (cf. Harrison et al. [Har79] and Harison et al. [Har81]). For this reason, we use the no-arbitrage options pricing formula introduced in Black et al. [Bla73][1]. We should mention that there always exist a self-financing investment strategy in the complete Black and Scholes setup to replicate the options payoff.
The overview of the literature with special focus on structured products is given in the next section where we concentrate on real traded certificates.

In our analysis, we consider a general financial product that could be dedicated as a mutual fund or a structured product upon glance. However, we should mention that also insurance contracts could be part of the observed products. Thus, we refer to some works highlight the connection between an insurance contract and a financial product. Embrechts [Emb00] illustrates a comparison of the classical actuarial approach of pricing an insurance to the modern one, which relies on a financial pricing model using expectations under the risk-neutral measure. Schneider [Sch11] gives an overview of the development of insurance contracts. Furthermore, she focuses on structured life insurance where the contracts provide a guarantee amount for the investor and a payoff, which depends on a risky underlying. The suboptimality of an investment strategy is observed by calculating a

1 An overview of option pricing theory is also given in Hull [Hul09]

loss rate comparable to our analysis. Thus, it is mentioned that a CRRA investor suffers from selecting a CPPI strategy. While the observation in Schneider [Sch11] is restricted on guarantee schemas, we conduct a more general survey also including capped and path-dependent products.
Another overview in a recent work is given in Branger et al. [Bra10] who analyze different insurance contracts with embedded guaranteed schemes including B&H, CM and CPPI strategies. They analyzed which investment strategy is optimal for an insured who would like to maximize her expected utility. It results that the optimal insurance contract with guaranteed interest rate for an CRRA investor is given by a protective put on a Constant-Mix strategy.

Although we will focus on a CRRA investor where the optimal strategy is a Constant-Mix, it is important to note that CPPI strategy plays an important role in the literature of dynamic portfolio insurance strategies that offer a given guarantee at maturity. A first introduction is given in Black et al. [Bla87]. For a detailed presentation of dynamic CPPI, we refer to Black et al. [Bla92]. They show the basic characteristics of CPPI strategies. Furthermore, they analyze the effects of transaction cost as well as borrowing limits on the strategy.
In Basak [Bas02] it is proved that for a HARA utility investor who requires a guarantee the CPPI strategy with the corresponding guarantee is the optimal investment strategy. However Dersch [Der10] mentions some critiques on the CPPI e.g. the fixed time horizon, the inability to take profits as well as the recover from a major drawback. Subsequent, he introduce some potential advanced features as lock-in levels and transaction filters.[2]

Finally, we want to refer to some basic literature, since we observe optimal investment strategies and utility function in Chapter 3.
We refer to the work of Von Neumann et al. [VN53], in which the fundamental framework of expected utility theory is introduced. In addition to the ordinal utility theory, they use probability theory to observe the investor's preference of an investment. In summary, they calculate the expectation of a function that assigns any final wealth to a real number. A detailed introduction in utility theory is given in Lengwiler [Len06]. Here, at full length the development from ordinal utility theory to the von Neumann-Morgenstern utility is illustrated.

2 Of course, a transaction filter is not needed if we do not respect to transaction cost.

We mention the classical *Merton problem* which seeks the optimal investment strategy to maximize the expected utility of terminal wealth (cf. MERTON [Mer71]). As previously mentioned, MERTON [Mer71] proves that the Constant-Mix strategy is the best solution in a Black and Scholes framework for an expected CRRA utility maximizing investor. A detailed illustration of the Merton problem and further variations can be found in ROGERS [Rog13].

2.2 About Chapters 4 and 5

In Chapters 4 and 5, we analyze Best Garant Certificates as well as Locally resp. Globally Capped Garant Certificates.

Thus, it is meaningful to give an overview of the literature of structured products first. A lot of analysis with focus on structured product and certificates are made. The main focus of the following literature is on pricing structured product. To our knowledge, the optimality of the product is in general only mentioned in accordance with fair pricing. They do not refer to imcomplete markets conditions from the investor's perspective who has to choose a product of a restricted set.

Without postulating completeness, we refer for example to the studies of CHEN et al. [Che90a] and CHEN et al. [Che90b], who analyze structured products with and without capital guarantee offered in the United States and find an overvaluation at issue date. CHEN et al. [Che90a] analyze a sample of 18 Market Index Certificates of Deposits that are linked to the S&P 500. They mentioned inconsistencies in the pricing of the products among product types, time to maturity and issuer. CHEN et al. [Che90b] conclude that S&P 500 Index Notes are overpriced by 5.0 % at issue date and during a first subperiod. An analysis from BAUBONIS et al. [Bau93] concentrate on equity-linked certificates of deposit. They show that an issuer could earn a margin between 2.5 % and 4.0 % in the primary market.

For the European markets, most empirical studies are focused on the Swiss stock market. For example, GRUENBICHLER et al. [Gru05] and BURTH et al. [Bur01] examine certificates without capital guarantee and find evidence that at issue date the average of their samples are overvalued, i.e. they are to the disadvantage of the investor. In BURTH et al. [Bur01] the average difference of price lie at 1.91 %.

WASSERFALLEN et al. [Was96] derive the result by analyzing structured products with a capital guarantee. WILKENS et al. [Wil03] discover for German Stock market that Discount Certificates as well as Reverse Convertibles are overpriced at their issue date, having analyzed more than 900 structured products. On average, the products are priced 3.0 %

above their duplicating strategy by the issuer.
In Robinson [Rob98] the costs/inefficiencies of other types of guaranteed investment products are discussed. It is mentioned that the cost arise not with the provision of the guarantees but with the feature of path-dependency. Depending on the grade of path-dependence, the inefficiency costs are stated between 0.7 % and 2.4 %.
Doehrer et al. [Doe13] make an extensive analysis of structured products in Germany. They use a reprehensive sample of over 3,000 structured products and calculate the average margin for each product category. The average expected issuer margin is 0.36 % per annum, where the smallest margin is identified for capital protection products with a coupon (0.14 % p.a.). Significantly higher margins are calculated for e.g. uncapped capital protection certificates (0.73 % p.a.), Reverse Convertibles (0.65 % p.a.) and Discount Certificates (0.50 % p.a.).

Some works in the literature focus on the marketing of structured products. Wallmeier [Wal11] mentioned that the issuer work to make the products look attractive to the investor. In general, the products are advertised with an illustration of a payoff diagram. He mentioned that an additional return probability distribution could be helpful to understand the characteristics of a given product.
He shows an analysis including the return distribution and the probability density function, which give an in-depth view of the risk return profile of a structured product. In parts, we enlarge his analysis by illustrating the return rate distribution of the BGC and the LCGC. Especially the calculation regarding the LCGC highlights the results of Wallmeier [Wal11], since we prove that the probability to receive the maximum payoff is almost zero for some LCGCs.
Chang et al. [Cha10] analyze the substantial amount of structured products with special regard concerning CLNs and CDOs.[3] They ascertain using data from Hong Kong that more financially literate investors allocated less structured products in their portfolios. They suggest that the volume of structured product is pulled by distribution companies, which is along the lines of Wallmeier [Wal11].
Doskeland et al. [Dos08] try to explain the demand for structured products in a utility framework. They do not find any evidence, but they mentioned that including parts of the cumulative prospect theory could influence the preferences.[4] Among others, they quantify

3 The abbreviations stand for Credit Linked Notes and Collateralized Debt Obligations.
4 We will not focus on cumulative prospect theory in this thesis. For detailed information, we refer to some standard work e.g. Kahneman et al. [Kah79] and Tversky et al. [Tve92]

the loss for a CRRA investor, albeit without a comparison to an optimal strategy. They prove that the highest loss in a pension insurance comes with introducing annual guarantees.

Referring to the topic of marketing structured products, we want to inform about current regulatory developments. In the European Union (EU), there are disclosure practices in progress concerning packaged retail investment products (PRIPs), which will include all products with elements of packaging or wrapping on an underlying investment. CFA Institute [CFA13] show the main focus is on illustrating the overall cost of an investment in a comparable way. Additionally, there should be a standardized illustration of risk and performance. National implementation are already given in e.g. Germany where a standard product information sheet is required for all products (excluding mutual funds). Here, an issuer estimate value of a product is illustrated for the investor. Furthermore a scenario analysis is required where all relevant cost are included, so that the investor has an overview of her optional net return rates at maturity.[5]

In the next step, we refer to some work providing the fundament for the analysis of the certificates.
BGCs are characterized by a guaranteed, a cap and a path-dependent best-entry feature. Thus, the analysis requires some theoretical knowledge about the joint distribution of minimum asset prices and (terminal) asset prices. The corresponding mathematical fundamentals that are necessary in the analysis of BGCs can be found in Shreve [Shr04] and Dana et al. [Dan07]. Additionally, Harrison [Har85] analyzes the distribution of the difference between the Brownian motion and its minimum. An application of the joint distribution on options can be found in He et al. [He98]. In the special case, where the observation period is equal to the time to maturity and continuous asset price observations, Goldman et al. [Gol79b] and Goldman et al. [Gol79a] provide closed-form solution for the BGC regarding a minimum strike $K^{(\min)}$.

Furthermore, we focus on the class of LCGC, which is also analyzed by Bernard et al. [Ber11b]. Thus, Bernard et al. [Ber11b] provides the preparatory work for our analysis, focusing on different aspects of locally capped globally floored Certificates issued in the United States. They mention that the observed products are very complicated to

5 The illustrated requirement are formulated in the BaFin Circular 4/2013 (WA)- Interpretation of statutory requirements for preparation of information sheets pursuant to sections 31(3a) WpHG, 5a WpDVerOV.

understand for retail investors. Furthermore, they show that the illustrated payoffs in the products prospectus are extremely optimistic, meaning that an investor has an unrealistic view about the certificate. Finally, they prove that the observed certificates were highly overpriced at issue date, on average. However, we enlarge the observation of Bernard et al. [Ber11b] by an analysis analogous to the BGCs. Exemplary, we quantify the utility loss of a CRRA investor who invest in a LCGC. Due to the special payoff feature of the LCGCs, we have to use Monte Carlo simulation (cf. Irle [Irl03]) for the pricing of the certificate.

With the analysis relying on the Heston model, we take into account stochastic volatility. For the implementation of the Heston model, we refer to Heston [Hes93] where the quasi-closed-form solution of a call option is introduced. He derives the characteristic function of the logarithmic stock price and obtains European option prices via inverse Fourier transformation. We use time efficient simulation techniques along the line with Van Haastrecht et al. [VH08] and Anderson [And06], where the variance process is calculated by the non-central chi-square distribution. Finally, the stock price is determined with an Euler scheme, which leads us to the option price by averaging. An overview of different simulation schemes can be found in Zhu [Zhu10]. The setting for optimal portfolio process in the Heston model is based upon Lui [Lui07]. It results that the optimal portfolio process is not constant, but rather is independent from the variance process and only changes with the remaining time to maturity.

2.3 About Chapter 6

The analysis in Chapter 6 also focus on Best Garant Certificate. However, in contrast to Chapter 4, we assume a Black and Scholes model with default risk. Therefore, we take into account that the issuer of a BGC could become insolvent during the time to maturity. Since we simply change the corresponding model compared to Chapter 4, we will only illustrate some related literature on this topic default risk.

Long before the financial crises began, the literature considered a possible default of an issuer of a financial product. Accordingly, some works with the view of modeling the default risk are detailed as follows.

Hull et al. [Hul95] show how data on bonds could be used to calculate defaultable options for the relevant counterparty. They are following the idea of Johnson et al. [Joh87] where the assets of the issuer as well as the asset underlying of the options are described by stochastic processes. They also assume that in case of a default of the issuer the holder

receives all the assets of the issuer. Looking at this assumption HULL et al. [Hul95] extended this idea by permitting equal ranking claims on the assets of the issuer.
JARROW et al. [Jar95] observe two sources of credit risk resp. default risk. On the one hand the risk that the asset underlying could default and on the other hand that the writer of the option become insolvent. The special assumption of the existence of other liabilities is allowed by KLEIN [Kle96]. The recovery is calculated proportional of nominal claims in the default event. Therefore, he combine the payoff ratio to the total value of the assets of the issuer. Thus, he takes into account a correlation between the underlying asset and the issuer's assets.
KLEIN et al. [Kle01] make an extension to JOHNSON et al. [Joh87] and KLEIN [Kle96], by considering an influence of the potential liability of the written option on the default event.
The model uses in Chapter 6 refers to GOETZ et al. [Goe10]. They follow the idea from KLEIN [Kle96] and KLEIN et al. [Kle01] to calculated closed-form solution of standard option with default risk. Finally, they use the standard option to analyze some types of structured product under their model assumption. GOETZ et al. [Goe10] also illustrate an analysis of different classes of structured products regarding their pricing issues, although they do not have a focus on the suboptimality of the defaultable certificate. In our analysis of the defaultable BGC, we will consider the corresponding fair product specification and the CRRA investor's utility. More precisely, we explain the utility loss that results by taking into account default risk by comparing the certificate to the optimal Constant-Mix strategy, which is not exposed to default risk.

Further results including default risk with explicit focus on financial products are given in WALLMEIER [Wal11] and DOSKELAND et al. [Dos08].
WALLMEIER [Wal11] mentioned that many investors were not aware of the credit risk in structured financial products. Thus, he advises improved product information for the investors. BAULE et al. [Bau08] conclude that up to 42 % of the overall margin in structured product depends on the value of credit risk.
DOSKELAND et al. [Dos08] observe the case where the company could default. They calculate that for a CRRA investor, a fair contract with a guarantee including the default risk of the company can be more attractive than a protective put strategy, due to the downside risk.
In general, default risk is analyzed in relation to corporate yield. In a recent work, LONGSTAFF et al. [Lon05] use data from Credit Default Swaps to analyze corporate yield spreads. They ascertain that the major part of the corporate spreads could be ex-

plained by the default component. More precisely, the default component explains 51 % of the spread for the best rated bond and over 83 % for lower ratings. This results are in contrast with e.g. HUANG et al. [Hua03] and DELIANEDIS et al. [Del01]. HUANG et al. [Hua03] use historical default data and conclude that credit risk accounts only for 20 % of the observed yield spreads. In DELIANEDIS et al. [Del01] it is mentioned that the major components are given by e.g. taxes, jumps, liquidity and market risk factor, whereby default and recovery risk could be neglected.

Beside the analysis concentrate on the influence of default risk on corporate debt, VASSALOU et al. [Vas04] focus on the effect of default risk on equity returns. They use default likelihood indicators for companies using equity data rather than data from the bond markets. It result that default risk depends on the size as well as the book-to-markets characteristics of a company. However, they mentioned that the size effect is only identified for companies with very high default risk. The effect for the book-to-market also holds for the same class of very high default risk companies.

CHAPTER 3

The suboptimality of stylized and structured stylized products

This chapter starts with a short overview of the general market model and some basic definition. We illustrate some exemplary investment strategies and their characteristics. Furthermore, we denominate the investor's decision problem and present a brief overview of utility theory.
In the main part of this chapter, we focus on the suboptimality of stylized products as well as structured stylized products. First, we analyze the suboptimality pertaining to the problem of disposability of the optimal stylized products. Second, we observe suboptimal structured stylized products written on the value process of the optimal investment strategy. We use guarantees and caps to distort the optimal payoff. Furthermore, we combine the observed product with path-dependent payoff features, which rely on a minimum or an average calculation method. Finally, we allow an embedded margin so that the fair product specification has to be adjusted. For all analyze products, we quantify the suboptimality by a loss rate. For the analysis of the embedded margin, we also illustrate our result by a special loss rate separating the influence of the margin and the influence of the suboptimal product design.

3.1 Fundamentals

This section gives a short overview of the market model and some basic definition. In the following, we confine the model to have two assets. Namely, the risk-free asset and the risky asset. Under this assumption, we illustrate some investment strategies that are well known in practice. Furthermore, we denominate the investor's decision problem to find the optimal investment strategy. For this reason, we present an overview of utility theory as well as the classical Merton problem. Finally, we state two optimal investment strategy assuming an expected CRRA utility maximizing investor in a complete financial market.

3.1.1 The market model

We assume a multi-dimensional Black and Scholes model setup with finite time horizon T. We define all stochastic processes on a filtered probability space $(\Omega, \mathcal{F}, (\mathcal{F}_t)_{t\geq 0}, P)$. The filtration $(\mathcal{F}_t)_{t\geq 0}$ satisfies the usual conditions. P is the real world measure.[1]

The observed financial market differs between risky assets and one risk-free asset. The risk-free asset S_0 is defined by the so-called risk-free interest rate r given by

$$dS_{t,0} = S_{t,0} r dt, \quad S_{0,0} = s_0 \tag{3.1}$$

Furthermore, we assume n risky assets which could be denote as *the stocks*. Each stock S_i satisfies the stochastic differential equation

$$dS_{t,i} = S_{t,i} \left(\mu_i dt + \sum_{j=1}^{n} b_{ij} dW_{t,j} \right), \quad S_{0,i} = s_i \text{ for } i = 1,...,n \tag{3.2}$$

where $W = (W_{t,1},...W_{t,n})_{t\geq 0}$ denotes the standard n-dimensional Brownian motion under the real world measure P. μ_i describes the drift parameter under the real world measure P for each risky asset S_i. For all $i = 1,...,n$ it holds that $0 \leq r < \mu_i$.

While b_{ij} is a constant, we write $\sigma_i^2 = \sum_{j=1}^{n} b_{ij}^2$ and $\sigma_{ij} = \sum_{k=1}^{n} b_{ik} b_{kj}$ as the quadratic variation of S_i and the covariation of S_i and S_j. It results

$$\sigma = \begin{pmatrix} \sigma_1^2 & \sigma_{12} & \cdots & \sigma_{1n} \\ \sigma_{21} & \sigma_2^2 & & \vdots \\ \vdots & & \ddots & \vdots \\ \sigma_{n1} & \cdots & \cdots & \sigma_n^2 \end{pmatrix} \tag{3.3}$$

which is known as the variance covariance matrix.

We will observe investment strategies consisting on the risk-free as well on risky assets. For this reason, we use a definition analogous to Bjoerk [Bjo96].

1 cf. Protter [Pro90], Karatzas et al. [Kar99] and Dana et al. [Dan07]

Definition 1 (Investment strategy, value process and self-financing) *We define*

(i) A investment strategy (resp. portfolio process) is any locally bounded predictable vector process

$$\pi = (\pi_0,\pi_1,...,\pi_n)\,. \tag{3.4}$$

(ii) The value process corresponding to the portfolio process π is defined by

$$(V_t^\pi)_{t\geq 0} := \sum_{i=0}^{n} \pi_{i,t} S_{i,t}. \tag{3.5}$$

(iii) A portfolio process π is called self-financing if the following holds

$$dV_t^\pi = \sum_{i=0}^{n} \pi_{i,t} dS_{i,t}. \tag{3.6}$$

Analogous to Mahayni et al. [Mah13], if the self-financing strategy π does not allow any short position in the assets, we will denote π as a *admissible* investment strategy. [2] The value process can be written by

$$V_t = V_0 + \sum_{i=0}^{n} \int_0^t \pi_{i,t} dS_{i,t} \tag{3.7}$$

with π the investment strategy defined by Definition 1 and V_0 any initial investment amount.

3.1.2 Product design

In the following we differentiate between the issuer's and investor's perspectives. For the issuer, we assume a complete and arbitrage-free financial market with two assets (cf. Section 3.1.1 for $n = 2$). Thus, there is only one risky asset, which we denote with S. For the risk-free asset, we use the denomination B. Of course, the issuer can generate any payoff profile by dynamic trading in the two assets.
Furthermore, we assume that the financial market is incomplete for the retail investor. She has to resort to a restricted class of products the issuer offers since she cannot generate

2 Mahayni et al. [Mah13] call an investment strategy admissible if the strategy is self-financing and any short positions are prohibited.

her optimal product through a dynamic trading strategy.
Now, we focus on the issuer's perspective and illustrate different product designs.
We consider the standard Black and Scholes assumptions. It follows that the dynamics of the two price processes under the real world measure P can be illustrated by

$$dS_t = \mu S_t dt + \sigma S_t dW_t \text{ and} \tag{3.8}$$

$$dB_t = B_t r dt \tag{3.9}$$

where $(W_t)_{0\leq t\leq T}$ is a standard Brownian motion under the real world measure P. μ is the drift of the risky asset and σ is the corresponding volatility of that process. Furthermore, r is the risk-free interest rate. In the model setup we assume μ, σ and r are constant. Furthermore, we assume that there are no dividend payments.
Note that Equation (3.8) implies that the dynamics of the stock prices under the equivalent martingale measure (resp. the risk-neutral measure)[3] P^* are

$$dS_t = rS_t dt + \sigma S_t dW_t^*, \tag{3.10}$$

where $(W_t^*)_{0\leq t\leq T}$ is a standard Brownian motion under the equivalent martingale measure P^*. We will use (3.10) if we calculate fair products and fair product specification, which is specified by Definition 2

Definition 2 (Fair product) *Let N be the nominal amount of the product at time t_0 and r the risk-free interest rate. The product V with maturity T is called fair if the no-arbitrage t_0-price of the corresponding payoff V_T at maturity is equal to the nominal amount, whereby*

$$N = E_{P^*}\left\{e^{-r(T-t_0)}V_T\right\} \tag{3.11}$$

where E_{P^*} denotes the expectation under the equivalent martingale measure.

We assume that an issuer could offer any possible fair investment strategy. The corresponding predictable process (cf. Definition 1) can be described by $(\pi_t)_{t\leq 0\leq T} = \left(\pi_t^S, \pi_t^B\right)$ on the risky asset S and the risk-free asset B.
While π_t^S and π_t^B describe the number of shares invested in the risky and the risk-free asset, we can also introduce the investment strategy by the predictable process illustrating

3 cf. Harrison et al. [Har79] and Harison et al. [Har81]

the relevant investment fraction invested in S and B. To attain self-financing requirement for the investment fraction φ_t^S and φ_t^B, it must always hold that $\varphi_t^B = \left(1 - \varphi_t^S\right)$ for all $t \in [0,T]$. In the following, let $\varphi_t = \varphi_t^S$ the proportion invested in the risky asset. Here, we can write the corresponding value process by

$$dV_t = \varphi_t dS_t + (1 - \varphi_t) dB_t \tag{3.12}$$

Applying (3.8), it holds that

$$dV_t = V_t \left((r + \varphi_t (\mu - r)) \, dt + \varphi_t \sigma dW_t \right). \tag{3.13}$$

In the following, we illustrate a couple of optional investment strategies.

3.2 Investment strategies resp. stylized products

We illustrate several investment strategies that an issuer could offer. Here, we introduce the so-called Buy-and-Hold (B&H) strategy, the Constant-Mix (CM) strategy and the Constant Proportion Portfolio Insurance (CPPI) strategy.[4]

It is evident that the final wealth of all strategies is path-independent in the assumed Black and Scholes model. Thus, for comparison of the different strategies, we decide to plot the payoff V_T with respect to the final price of the risky asset S_T as well as the development of the investment fraction φ and the number of shares invested in S_T. For the sake of convenience we assume $S_0 = 1$ as well as $V_0 = 1$.

3.2.1 The Buy-and-Hold (B&H) strategy

The B&H strategy is more-or-less one of the simplest investment strategies.
For a Buy-and-Hold strategy holds that the number of shares $\pi_t^{B\&H}$ invested in the risky asset S_t is fixed during the time to maturity, but the fraction of investment $\varphi_t^{B\&H}$ in S_t depends on the dynamics of the price S_t.
However, the number of shares invested in S_t is constant given by $\pi_t^{B\&H} = \frac{\varphi_0^{B\&H} V_0}{S_0}$ for $0 \leq t \leq T$. But the investment fraction is dynamic calculated with $\varphi_t^{B\&H} = \varphi_0^{B\&H} \frac{\frac{S_t}{S_0}}{\frac{V_t}{V_0}}$.
The corresponding value process V_t of the B&H strategy during the entire investment

4 All the strategies are well-known. Exemplary works with a focus on all strategies include Perold et al. [Per88] and Branger et al. [Bra10]

period is given by

$$V_t = V_0 \left(\pi_0^{B\&H} \frac{S_t}{S_0} + \left(1 - \pi_0^{B\&H}\right) e^{rt} \right). \tag{3.14}$$

In summary, the issuer chooses the proportion at the beginning of the contract resp. at issue date of the product and renounced any changes during the lifetime of the B&H strategy. In a worst case scenario, the value invested in the risky asset S_t could become worthless. In this case, the remaining amount at time T is simple the amount invested in the risk-free asset plus the corresponding interest rate $(1 - \varphi_0^{B\&H})e^{rT}V_0$. In particular, this amount could be identified as a guarantee.

We illustrate the payoff V_T of two different B&H strategies depending on the final

Figure 3.1: Overview of the two selected Buy-and-Hold strategies

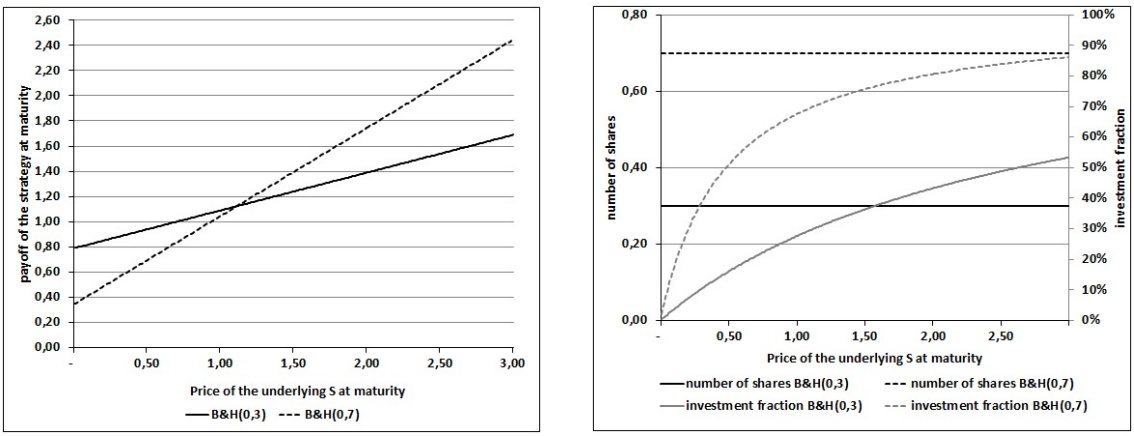

The payoffs of the Buy-and-Hold strategies with respect to the final price of the risky asset S_T for $\pi^{B\&H} = 0.3$ and $\pi^{B\&H} = 0.7$ are illustrated in the left plot. The corresponding development of the number of shares $\pi^{B\&H}$ as well as the investment fraction $\varphi^{B\&H}$ is given in the right plot.

price of S_T in the left plot of Figure 3.1. On the one hand, we assume a Buy-and-Hold strategy where 30 % of the initial wealth is invested in the risky asset. Thus, for this strategy it holds that $\varphi_0^{B\&H} = 30$ % and $\pi_0^{B\&H} = 0.3$. We denote this strategy by $B\&H(0.3)$. On the other hand, we consider a more risky Buy-and-Hold strategy ($B\&H(0.7)$) with $\varphi_0^{B\&H} = 70$ % as well as $\pi_0^{B\&H} = 0.7$.

As assumed, the final payoffs of the strategies are rising with a constant factor which is given by $\pi^{B\&H}$. Of course, the higher the number of shares invested in S_t the steeper is the payoff graph. We have already mentioned the worst case scenario with $S_T = 0$. Due to the interest payment, we identify a corresponding worst case payoff of $V_T^{B\&H(0.3)} = 0.792$ and $V_T^{B\&H(0.7)} = 0.345$ for the observed strategies.

Nevertheless, we also show in the right plot of Figure 3.1 the development of $\varphi_T^{B\&H}$ and $\pi_T^{B\&H}$ with respect to S_T.
By definition of the $B\&H$ strategy, $\pi_T^{B\&H}$ is constant. The graph of the investment fraction $\varphi_T^{B\&H}$ is positively correlated with S_T, resulting in a concave function. It is seen that $\pi_T^{B\&H} < \pi_0^{B\&H}$ for $S_T = S_0$ owing to the fraction invested in the risk-free asset, which grows with $e^{r\Delta t}$.

3.2.2 The Constant-Mix (CM) strategy

In comparison to a B&H strategy, the CM strategy requests dynamic adjustments of the portfolio constellation.

For the Constant-Mix strategy, it holds that the investment fraction φ_t^{CM} is constant during the entire investment period. The number of shares invests in S_t depends on the dynamics of the price process S_t.
Therefore, the fraction invested in S_t is defined with $\varphi_t^{CM} = \varphi_0^{CM}$, which is constant for $0 \leq t \leq T$. The number of shares of S_t is dynamically calculated with $\pi_t^{CM} = \frac{\varphi_t^{CM} V_t}{S_t}$.
In other words, if the stock price rises, the issuer will sell parts of the risky assets. Of course, if the stock market rises continuously the CM strategy is significantly worse compared to an investment strategy in which the number of shares is constant.
The corresponding value process V_t of the CM strategy results from a straightforward calculation (cf. Balder et al. [Bal10]). Referring to (3.13) and with $\varphi = \varphi_t^{CM}$ we can write

$$V_t = V_0 e^{\left(r+\varphi(\mu-r)-\frac{1}{2}\varphi^2\sigma^2\right)T+\varphi\sigma W_T}. \tag{3.15}$$

Using the standard Black and Scholes solution for the stock price S_t with

$$\begin{aligned} \ln\left(\frac{S_T}{S_0}\right) &= \left(\mu - \frac{1}{2}\sigma^2\right) + \sigma W_T \\ \Leftrightarrow \sigma W_T &= \ln\left(\frac{S_T}{S_0}\right) - \left(\mu - \frac{1}{2}\sigma^2\right) \end{aligned} \tag{3.16}$$

we could write

$$V_t = V_0 e^{\left(r+\varphi(\mu-r)-\frac{1}{2}\varphi^2\sigma^2\right)T+\varphi\left(\ln\left(\frac{S_T}{S_0}\right)-\left(\mu-\frac{1}{2}\sigma^2\right)\right)}. \tag{3.17}$$

Immediately follows

$$V_t = V_0 e^{(1-\varphi)\left(r+\varphi\frac{1}{2}\sigma^2\right)t}\left(\frac{S_t}{S_0}\right)^{\varphi}. \tag{3.18}$$

Looking at the value process, we identify that V_T is always larger than V_0 if $S_T = S_0$ holds for the risky asset. Obviously, the dynamic rebalancing is followed by a outperformance especially in more-or-less no performing markets.
In Figure 3.2 we illustrate comparable graphs to the B&H strategy. For this reason, we choose two CM strategies with constant investment fractions $\varphi^{CM} = 30\ \%$ and $\varphi^{CM} = 70\ \%$. The strategies will be denoted by CM(30 %) as well as CM(70 %). As mentioned in Perold

Figure 3.2: Overview of the two selected Constant-Mix strategies

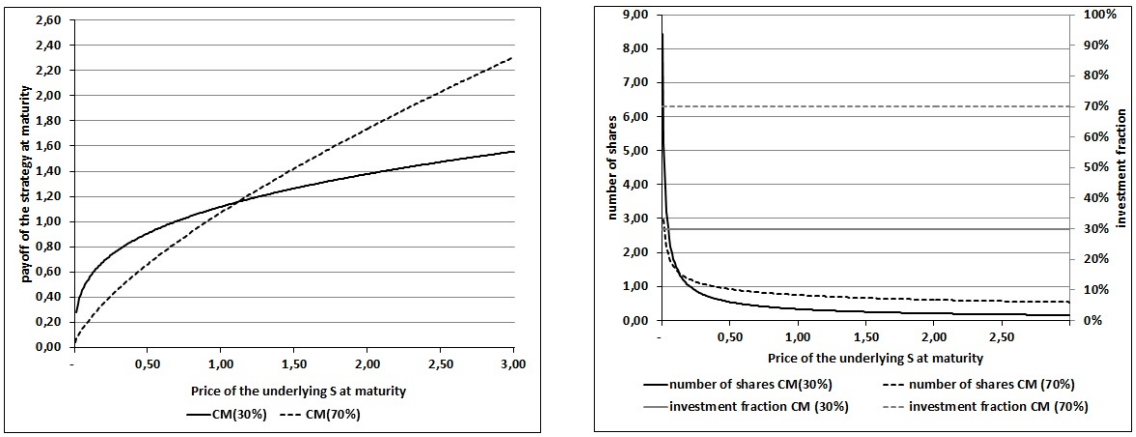

The payoffs of the Constant-Mix strategies with respect to the final price of the risky asset S_T for $\varphi^{CM} = 30\ \%$ and $\varphi^{CM} = 70\ \%$ is illustrated in the left plot. The corresponding development of the number of shares π^{CM} as well as the investment fraction φ^{CM} is given in the right plot.

et al. [Per88] the Constant-Mix strategy results in a concave payoff function regarding S_T. It holds that the CM strategy do not offer a guarantee for the investor. If the price of risky asset S_t fall, the issuer has to buy additional shares of the stock to rebalance the investment fraction φ^{CM}. To sum up the effect, the value of the CM strategies could become very small if the risky asset is decreasing continuously. In particular, the sensitivity to the development of the risky asset is unchanged with a lower price of S_t, but a higher

number of shares is necessary.
This development is highlighted in the right plot of Figure 3.2. To assure that the investment fraction remains constant for a lower price S_t, the issuer will increase her position continuously in the risky asset by buying further shares. Of course, the number of shares could be very high at maturity if the underlying S_t falls until maturity.

3.2.3 The Constant Proportion Portfolio Insurance (CPPI) strategy

The Constant Proportion Portfolio Insurance strategy makes use of two additional parameter: a guarantee G and a multiplier m. For this strategy the investment fraction as well as the number of shares held during the time to maturity is flexible.[5]
The main focus of a CPPI strategy is granting the amount G at maturity. However, the strategy should always invest the difference between the current t-value of the strategy V_t and the t-value of the guarantee $G_t = e^{e-r(T-t)}G$ in the risky asset S_t to allow some upward participation. The difference $C_t = V_t - e^{-r(T-t)}G$ is called *cushion*. In the Black and Scholes model setup where we assume continuous trading opportunities for the issuer of such strategy, it is feasible to use a multiplier m to invest a higher amount in S_t. Thus, the investment fraction of V_t is defined with $\varphi_t^{CPPI} = \frac{m\left(V_t - e^{-r(T-t)}G\right)}{V_t}$. Here, the number of shares invested in S_t is $\pi_t^{CPPI} = \frac{m\left(V_t - e^{-r(T-t)}G\right)}{S_t}$. Of course, the investment fraction as well as the number of shares depends on the combination of m and G. For constant multiplier m the investment fraction and the number of shares are higher the lower the guarantee. On the other hand, π_t^{CPPI} as well as φ_t^{CPPI} is higher for higher m if G is constant.
For the sake of completeness, we illustrate the corresponding value process of a CPPI strategy. Thus, V_t of the CPPI strategy during the time to maturity is given by[6]

$$V_t = Ge^{-r(T-t)} + \left(V_0 - Ge^{-rT}\right) e^{(1-m)\left(r+m\frac{1}{2}\sigma^2\right)t} \left(\frac{S_t}{S_0}\right)^m. \tag{3.19}$$

Intuitively, the CPPI strategy follows a pro-cyclical investment approach. Analogous to the other observed strategies, we show the terminal payoff of two exemplary CPPI strategies in Figure 3.3. We assume a multiplier of $m = 3$ for both strategies. Furthermore, we consider a guarantee of $G = 0.9$ for the first CPPI strategy and a guarantee equal to the nominal

5 For an overview of the CPPI strategy, we refer to Black et al. [Bla87], Black et al. [Bla92] and Balder et al. [Bal09]
6 The derivation of V_t could be done analogous to the calculation of the CM strategy. For this reason, the cushion process C_t has to be observed, so that V_t follows indirectly with the corresponding guarantee (cf. Balder et al. [Bal10]).

amount ($G = 1.0$) for the second strategy. The strategies are named CPPI($G = 0.9; m = 3$) and CPPI($G = 1.0; m = 3$).

We identify in the left plot of Figure 3.3 that the CPPI payoff is a convex function regarding

Figure 3.3: Overview of two selected CPPI strategies

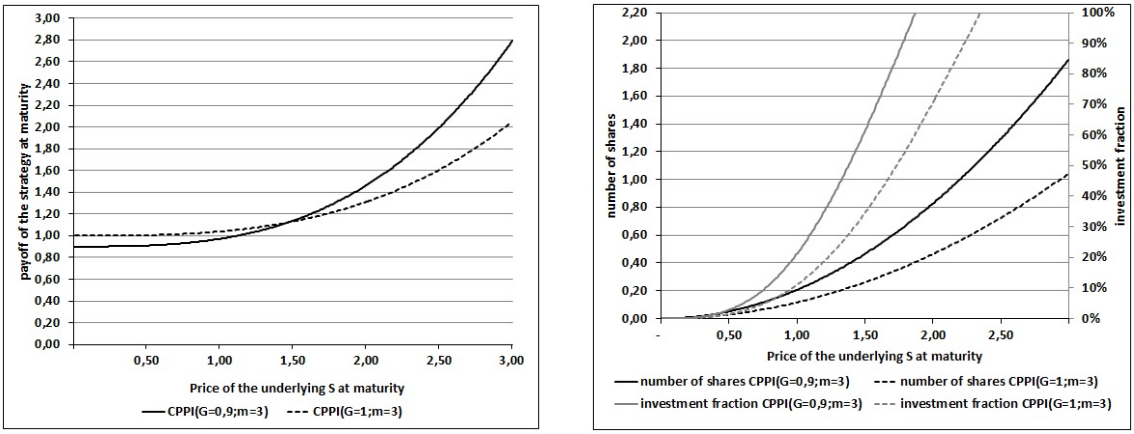

The payoff of the CPPI strategies with respect to the terminal price of the risky asset S_T for the tuple ($G = 0.9$,$m = 3$) and ($G = 1.0$,$m = 3$) is illustrated in the left plot. The corresponding development of the number of shares π as well as the investment fraction φ is given in the right plot.

the terminal price S_T. Since we assume the same multiplier m for both strategies, we could see the dependency of the payoff function slope from the guarantee. As previously mentioned, the lower the guarantee, the higher the participation in the price of S_T. Nevertheless, if we consider the case $S_T = S_0$, we will find an interesting difference in the performance of the two strategies. While CPPI($G = 0.9; m = 3$) result in a small loss with $V_T^{CPPI(G=0.9)} = 0.97$ the more conservative CPPI can report a positive performance ($V_T^{CPPI(G=1.0)} = 1.04$).

The difference of the two CPPI strategies can be also highlighted by the investment fraction and the number of shares (Figure 3.3 (right plot)). For the lower guarantee, $\varphi_t^{CPPI(G=0.9)}$ and $\pi_t^{CPPI(G=0.9)}$ are almost higher for all terminal prices S_T. Independently from the guarantee, both parameter will reach a significantly higher level compared to the level at issue date ($t_0 = 0$) if S_T show a positive development.[7]

7 We should mention that a standard CPPI strategy allows investment fraction above 100 % which is in opposite to our assumption. However, since we want to maintain the nature of a CPPI, we decide to resign this assumption in this illustration.

3.2.4 Summary of the investment strategies

We mentioned that the final payoff of all strategies is path-independent in the Black and Scholes model. In the Buy-and-Hold strategy no transactions are made during the time to maturity, so that the issuer choose the number of shares of S_t and invest the remaining amount in the risk-free asset. The investment proportion is derived by the development of S_t. If the price of S_t boost the investment proportion could rise rapidly. In a scenario where the risky asset becomes valueless, only the amount invested in the risk-free asset remains in the portfolio. Accordingly, this amount is comparable with a chosen guarantee. In both scenarios the B&H strategy will outperform the CM strategy since the Constant-Mix strategy adjusts the number of shares continuously in such a manner that the investment fraction at time t is always equal to φ_0^{CM}. It follows that an exceedingly increasing or decreasing asset price S_t result in a "sell high, buy low" behavior of the CM strategy which brings the underperforms compared to the B&H strategy.[8] However, a more-or-less trendless development (with only a small increase or decrease of the stocks) results in an outperformance of the CM strategy compared to the B&H strategy. To be more precise, the volatility defines an interval about the value S_0 where the CM strategy is better than the Buy-and-Hold strategy.

The CPPI strategy includes a fix guarantee G, which significantly influences the strategy results. The number of shares π_t^{CPPI} invested in S_t and the corresponding investment fraction φ_t^{CPPI} is dynamic and depends on G and m as well as the development of the risky asset S_t. Therefore, in comparison to the B&H and the CM neither the number of invested shares nor the investment fraction is constant.
With a look at the calculation, we identify the alikeness to the other illustrated strategies. If no guarantee is required ($G = 0$), the CPPI will be equal to the CM strategy. Furthermore, it results in a B&H strategy if a multiplier of $m = 1$ is chosen.

3.3 Optimization problem and utility function

In this section, we illustrate the optimization problem of an investor who wants to maximize the utility of her investment decision. For this observation from the investor perspective, we have to assume a complete financial market. We define the result as the overall optimal stategy. It is used as a benchmark when we analyze suboptimal strategy in incomplete

8 The underperformance results from the adjustment of the φ_t^{CM}. In an increasing market situation, the agent always reduces the fraction of the performing asset. By contrast, the agent always buys a new fraction of a decreasing asset.

market conditions.

We refer to the work of Von Neumann et al. [VN53] where the fundamental framework of expected utility theory is introduced. In addition to the ordinal utility theory, they use probability theory to observe the investor's preference of an investment. In summary, they calculate the expectation of a function which assigns any final wealth to a real number.[9]
Furthermore, we mention the classical *Merton problem* which seeks for the optimal investment strategy to maximize the expected utility of terminal wealth.[10]
In the following, we will set up the specific optimization problem for our assumptions. Before we state the solution in the Black and Scholes model for the investor's investment problem, we illustrate a selection of well-known utility function and their characteristics.

3.3.1 The optimization problem

The standard *Merton problem* that describes a stochastic optimal control problem allows finite and infinite time horizon. Furthermore, the investor's utility depends on the terminal wealth as well as intertemporal consumption. We observe a simplified optimization problem. First, we can rely on complete market assumptions in a standard Black and Scholes model. Second, we assume an investor who would like to maximize the expected utility of her investment strategy depending only on the terminal wealth of the investment strategy (where no intertemporal consumption is allowed). In this simple manner, the optimization problem of the maximum expected utility will be given by

$$\max_{\varphi \in A} E_P \left\{ u(V_T^{\varphi}) \right\} \tag{3.20}$$

where A describes the set of all self-financing investment strategies φ. The utility function u is define as a continuous and monotonic non-decreasing real-valued function. More precisely, a utility function u assign a terminal wealth V_T^{φ} to the investor's utility $u(V_T^{\varphi}) \in \mathbb{R}$. Hereby, u uses an additional risk aversion parameter explaining whether the investor is risk seeking, risk neutral or risk averse.

In other words, we assume that the investor's decision problem of selecting an optimal

9 A detailed introduction in utility theory is given in Lengwiler [Len06].
10 cf. Merton [Mer71]. Additional illustration of the Merton problem and further variations can be found in Rogers [Rog13].

investment strategy do not depend on the expected terminal wealth of the corresponding investment strategy but rather on the investor's individual utility.

A solution of (3.20) for some classes of utility function is given in MERTON [Mer71]. After illustrate different utility function we will calculated the explicit solution of the optimization problem for a CRRA investor.

3.3.2 Exemplary utility functions

In the following, we illustrate three exemplary utility functions, all of which belong to the class of hyperbolic absolute risk aversion (HARA) utility function. This specification is given in Definition 3.

Definition 3 (HARA utility function) *For a function $u : \mathbb{R} \to \mathbb{R}$ and the Absolute Risk Aversion (ARA) defined by*

$$ARA(u(x)) = -\frac{u''(x)}{u'(x)} = \frac{1}{ax+b} \tag{3.21}$$

for constant parameter a,$b \in \mathbb{R}$ holds. The function u is called a hyperbolic absolute risk aversion (HARA) utility function if the ARA is hyperbolic.

If $a \neq 0$ and $b = 0$, we will observe the Constant-Relative-Risk-Aversion (CRRA) utility function given by

$$u^{CRRA}(x) = \begin{cases} \frac{x^{1-\gamma}}{1-\gamma} & \text{for } \gamma \in [0,\infty) \setminus \{1\} \\ \ln(x) & \text{for } \gamma = 1 \end{cases} \tag{3.22}$$

The description of the CRRA utility function relates to the Arrow-Pratt-De Finetti (APF) measure of relative risk aversion, which is defined by $-x\frac{u''(x)}{u'(x)}$. In the case of the CRRA utility function, the APF measure is equal to γ.
For the CRRA utility function $u^{CRRA}(x)$, the investor's utility is independent of her initial wealth. As a direct result, it is possible to concentrate on the resulting return rates of an observed strategy.

For $a = 0$ and $b \neq 0$ results a so-call exponential utility function, which can be writ-

ten as

$$u^{Exp}(x) = -e^{-\kappa x} \tag{3.23}$$

where $\kappa = \frac{1}{\beta}$. It is seen that the exponential utility function has a constant ARA.

The third illustrated utility function, with $a \neq 0$ and $b \neq 0$, is known as the Decreasing Relative Risk Aversion (DRRA) utility function. u^{DRRA} is often used as an extension to the CRRA utility function where a future consumption or a required guarantee G is integrated. The function is given by

$$u^{DRRA}(x) = \frac{(x-G)^{1-\nu}}{1-\nu}. \tag{3.24}$$

We should mention that Basak [Bas02] and Branger et al. [Bra10] state that a CPPI is the optimal strategy for an investor with utility function $u^{DRRA}(x)$.

3.3.3 Optimal investment

In the following, we restrict ourselves on expected CRRA utility maximizing investor, since we would like to analyze the investor's preference independently from her initial wealth. Therefore, we focus on the expected utility $EU_T^{CRRA,\varphi} = E_P(u^{CRRA}\left(V_T^{\varphi}\right))$ for a corresponding strategy. Here, we consider the optimization problem (cf. (3.20)) given by

$$\max_{\varphi \in A} E_P\left\{u^{CRRA}(V_T^{\varphi})\right\} \tag{3.25}$$

where A describes the set of all self-financing investment strategies φ. Furthermore, we determine the certainty equivalent of the analyzed strategies. The certainty equivalent is defined by

$$CE_T^{CRRA,\varphi} = \left[(1-\gamma)\, EU_T^{CRRA,\varphi}\right]^{\frac{1}{1-\gamma}}. \tag{3.26}$$

Furthermore, using (3.13) and (3.22) immediately follows

$$CE_T^{CRRA,\varphi} = v_0 e^{\left(r+\varphi(\mu-r)-\frac{1}{2}\gamma\varphi^2\sigma^2\right)T}. \tag{3.27}$$

$CE_T^{CRRA,\varphi}$ describes the relevant return rate at maturity that makes the investor indifferent about investing in the strategy φ or getting this return.

We now present the solution of the previous optimization problem. The result is stated in Proposition 1 and refers to MERTON [Mer71].

Proposition 1 (Optimal investment strategy) *For $\gamma > 1$, the optimal investment strategy resp. portfolio process φ^* for an investor with CRRA utility function $u(x) = \frac{x^{1-\gamma}}{1-\gamma}$ is given by the Constant-Mix (CM) strategy, where the investment fraction is given by*

$$\varphi^{*,CM} = \frac{\mu - r}{\gamma \sigma^2} \tag{3.28}$$

The result is called the Merton strategy (cf. MERTON *[Mer71]).*

Additionally the certainty equivalent of the optimal strategy is given by

$$CE_T^* = v_0 e^{\left(r + \frac{1}{2\gamma}\left(\frac{\mu - r}{\sigma}\right)^2\right)T} \tag{3.29}$$

Proof 1 *The proof is a straightforward to the Black and Scholes assumption for V_t, which is illustrated in Appendix A.1.*

As an additional result, we illustrate the optimal investment solution for an expected CRRA utility maximizing investor where the investment strategy includes a guarantee amount. Before we illustrate the proposition, we have to define the contribution guarantee schema. Both the definition and the following proposition can be found in BRANGER et al. [Bra10].

Definition 4 (The contribution guarantee schema) *Let V_0 be the initial wealth of an investment strategy φ_t with value process V_t with a time to maturity T and the final payoff V_T. A corresponding guarantee amount $G(T,V_0,g)$ is defined by*

$$G = G(T,V_0,g) := V_0 e^{g(T-t_0)} \tag{3.30}$$

where g describes the guaranteed interest rate. Then, the contribution guarantee schema for a time to maturity of T, a guarantee amount G and a participation rate α applied on the investment strategy φ_t with value process V_t is given by

$$CG\left(V_T,\alpha,G\right) := \max\left\{\alpha V_T, G\right\} = G + \left(\alpha V_T - G\right)^+ = \alpha V_T + \left(G - \alpha V_T\right)^+ . \tag{3.31}$$

Now, Proposition 2 shows that the optimal investment strategy with guarantee is a contribution guarantee schema.

Proposition 2 (Optimal investment strategy with guarantee) *Let $G \geq 0$ a guarantee amount, so that $V_T \geq G$ must hold at maturity. Then, the optimal investment strategy for an investor with CRRA utility function $u(x) = \frac{x^{1-\gamma}}{1-\gamma}$ is given by a contribution guarantee schema applied on the Constant-Mix (CM) strategy $V_t^{\varphi^*}$ from Proposition 1.*
The payoff can be illustrated by

$$X_T^{\varphi^*} = CG\left(V_T^{\varphi^*}, \alpha, G\right) = \max\left\{G, \alpha V_T^{\varphi^*}\right\} \tag{3.32}$$

with $\alpha \in \mathbb{R}$ fulfill the initial wealth condition.

Proof 2 *The proof is given in Appendix A.2.*

3.3.4 Definition of loss rate

In the following, we analyze optimal investment strategies for an expected CRRA utility maximizing investor with risk aversion parameter γ. In reality, retail investors do not have the opportunity to trade such dynamics strategies by their selves. Thus, we assume that the financial market is incomplete for the investor. In particular, each investor is restricted on a set of stylized products offered by investment companies.[11] Since the overall optimal solution for each investor is not necessarily available, we identify a utility loss. We will determine this utility loss by defining a loss rate that results from a discrepancy of the product's certainty equivalent, which in turn results from the optimal Constant-Mix strategy (Merton strategy).

Definition 5 (Loss rate) *Let CE^{φ} the certainty equivalent of an investment strategy φ. We define for a CRRA investor the loss rate l_T by*

$$l_T = \frac{\ln\left(\frac{CE^*}{CE^{\varphi}}\right)}{T} \tag{3.33}$$

where CE^* is the optimal certainty equivalent for the optimal Constant-Mix strategy with φ^* as the optimal investment fraction in risky assets for given risk aversion γ defined in (3.29). As a straightforward result from (3.27), if φ is a Constant-Mix strategy for a

11 Issuers of such stylized products could be banks, insurance companies or other financial institutions.

dissenting risk aversion, the loss rate is given by

$$l_T = \frac{1}{2}\gamma\sigma^2 \left(\varphi^* - \varphi\right)^2 . \tag{3.34}$$

3.4 Market assumptions and Data

For our analysis, we use the following parameters, which we derived from the observed products in Chapter 4. For the derivation of the parameter, we focus on the period from October 2009 to February 2010.[12] We will assume a time to maturity of $T = 5$ years and a risk-free interest rate $r = 2.4$ %. The risk-free interest rate is calculated as the average of the five-year Germany Government Bonds return, which we identify with the risk-free investment.

To gain a realistic estimation for the volatility in the Black and Scholes setting we observed the implied volatility of traded option on the Euro Stoxx 50 between October 2009 and February 2010 with strikes between 1,800 and 3,900 index points[13] and a time to maturity close to five years. The calculation results an implied volatility in a range between $\sigma_1 = 24.50$ % and $\sigma_2 = 22.50$ %. Due to the small difference between the two calculated volatilities, it seems sufficient simply to use the mean value of both for the following analysis. Accordingly, we decide to use $\sigma = 23.50$ %.
To define the drift parameter μ, we need to assume a realistic risk premium. Based upon the Capital Asset Price Model (CAPM), the data provider FACTSET calculates a risk premium for the Euro Stoxx 50 on a monthly basis. The average risk premium in the observed period is fixed at 6.6 %, whereby we finally use $\mu = 9.0$ %.

3.5 Analysis of stylized products

In this section, we focus on suboptimal stylized products. Here, we begin with an observation of stylized products where the problem of disposability is quantified. More precisely, the investor has to resort to the restricted class of stylized products offered by the issuer. Of course, the optimal choice within the restricted class will differ from her overall optimal product. Finally, we quantify the suboptimality by a loss rate.
We observe different "optimal" products (resp. CM strategies) invest a fraction φ in the risky asset S_t and $1 - \varphi$ in the risk-free asset B_t. As described, we assume $\mu = 9.00$ % and

12 This is the range of time when the observed BGCs in Chapter 4 were issued.
13 With this range, the observation includes out-of-the-money, at-the-money as well as in-the-money call options.

$\sigma = 23.5$ %. It follows that the parameter μ, σ and r are given and we could calculated $\gamma(\varphi)$ as the optimal investors risk aversion for a given CM strategy.

We focus on four exemplary Stylized Products A, B, C and D characterized by the investment fraction φ which are offered for retail investors (cf. Table 3.1). The first product is defined by the most risk averse investment opportunity illustrated by $\varphi = 0$ %. Second, the most risk seeking product allow the investor to invest directly in the risky asset S_t with $\varphi = 100$ %. Furthermore, we choose the corresponding products for $\varphi = 30$ % and $\varphi = 70$ %. A summary of the four stylized products is shown in Table 3.1. With the selection of φ, we define the (μ,σ)-tuple for the relevant stylized product.
As previously mentioned, we calculated the optimal risk aversion parameter γ for each product. Furthermore, we illustrated the optimal certainty equivalent for an investor with the matching risk aversion parameter γ.
Of course, all investors with a dissenting γ will suffer by a utility loss which we represent by the loss rate defined in Definition 5. We denote that the calculated loss rate is only influenced by the problem of disposability. For this reason, we will show in the left plot of Figure 3.4 the optimal certainty equivalent for different risk aversion parameter γ based upon the optimal Constant-Mix strategy. It is seen, the certainty equivalent is a strictly

Figure 3.4: Optimal Constant-Mix CE and loss rates resulting by stylized products

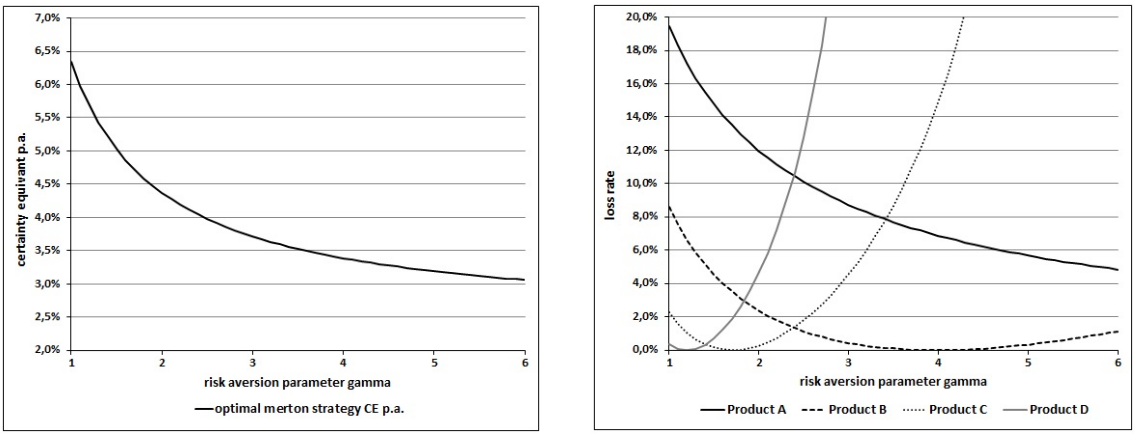

Optimal certainty equivalents calculated for the optimal Constant-Mix strategy resp. Merton strategy (left plot) and the derived loss rates (right plot) are illustrated for different level of risk aversion.

decreasing function of γ. For $\gamma = 1$, the calculated CE^* is 6.34 %. The CE^* will fall to a

Table 3.1: Summary of the stylized products

Stylized product ID	φ in %	μ in %	σ in %	opt. γ^*	$CE(\gamma^*)$ in %
A	0	2.4	0	∞	2.4
B	30	4.38	7.05	3.98	3.39
C	70	7.02	16.45	1.71	4.71
D	100	9.0	23.5	1.195	5.70

Summary of the observed stylized products

level of 3.09 % if we choose $\gamma = 6$. We should mention that this amount is only 0.39 % above the risk-free interest rate. As illustrated in Table 3.1, the certainty equivalent is equal to risk-free interest rate for $\lim_{\gamma\to\infty}$.

The right plot of Figure 3.4 illustrates the calculated loss rates based upon the investor's risk aversion for the four available stylized products. We identify that the loss rate is zero if the offered product exactly suits the risk preference of the investors. For these investors, the problem of disposability does not exist. All other investors have to choose a product that does not match her risk aversion perfectly.
For the following analysis, we define four exemplary investors by the risk aversion parameter $\gamma \in \{2,3,4,5\}$. Assuming that the investor could only choose between the four offered stylized product, we could calculate the corresponding loss rates for each combination of investor and product. The results are shown in Table 3.2.
We identify that Product B is almost optimal of the investor with $\gamma = 4$. Theoretically, the investor will require an investment proportion of $\varphi = 29.88$ %. As calculated, the small difference to $\varphi = 30.00$ % results in a loss rate of $l_T = 0.0001$ %.
All other investors suffer from an investment in one of the offered product. Indeed, the corresponding lowest loss rates lie between $l_T = 0.27$ % and $l_T = 0.44$ %. It is meaningful to mention that all other calculated loss rates are significantly higher. Thus, the utility loss could boost if only one of the products is not available. For example, if the investor with $\gamma = 3$ cannot choose Product B, she have to switch to Product C, for which the corresponding loss rate ($l_T = 4.54$ %) is ten times higher.
We should mention that there are combinations for which no loss rate could be calculated. For $\gamma = 4$ and $\gamma = 5$ the certainty equivalent of Product D is lower than the nominal amount: in other words, the CE p.a. is negative, meaning that the investor would prefer a small loss rather than investing in the corresponding product.

Table 3.2: Resulting loss rates for the exemplary investors

loss rate in %	A	B	C	D
$\gamma = 2$	11.99	2.37	0.27	4.58
$\gamma = 3$	8.74	0.44	4.54	32.92
$\gamma = 4$	6.88	0.0001	14.89	X
$\gamma = 5$	5.68	0.32	50.53	X

Observation of the calculated loss rates

In summary, we show that the observed stylized product are generally not optimal for an expected CRRA utility maximizing investor due to a bounded product variety. For an exemplary investor, the calculated loss rate is a decreasing function of the number of stylized products. The loss rate could be very high for a low number of products.
In the following, we extend the observation with structured stylized products, whereby we also allow embedded options written on the value process of the optimal investment strategy V_t.

3.6 Analysis of structured stylized products

In this section, we observe different structured stylized products and analyze them regarding their loss rates, which result from the deviation from the optimal product which an investor would require in complete market conditions. Thus, we quantify the loss results by the difference between the optimal product offered to the retail investor and her overall optimal product. Our calculations rely on three basic product specifications.
First, we observe products with a kind of capital guarantee. Such a guarantee product offers the investor a protection feature and a participation in the return of the underlying asset.[14] Second, we focus on capped products that grant the investor participation in the investment underlying until a defined boundary resp. cap. In the third observation, both (the guarantee and the cap) are combined.

For this analysis, our focus is on an investor with risk aversion parameter $\gamma = 2$[15] and the corresponding value process V_t of the optimal Constant-Mix strategy $\varphi^{*,CM}$. We denote her with investor Γ. Thus, in the benchmark case V_t is used as the underlying asset

14 The observed guarantee product is identical to the contribution guarantee schema illustrated in Definition 4.

15 We refer to Chiappori et al. [Chi11] where a constant risk aversion parameter of $\gamma = 1.7$ is proven by a panel analysis in Italy. Thus, we use $\gamma = 2$ as a sufficient approximation.

for the observed structured stylized products. In particular, we use the relevant parameter $\mu = 6.34$ % and $\sigma = 14.04$ % of the optimal investment strategy $\varphi^{*,CM}$ result by our market assumption. Of course, we also use the risk-free interest rate $r = 2.4$ % as well as the time to maturity of $T = 5$ for our calculation.

3.6.1 General definition

We assume products which can be describes analogous to Mahayni et al. [Mah13].
The payoff and the return rates at maturity depends on the development of the underlying V_t. A product could offer a guarantee amount G_T which is defined by the guaranteed rate g with $G_T = Ne^{gT} = e^{gT}$. Furthermore, an optional product feature is a cap C_T which is given by a cap rate c with $c > g$, so that the maximum payoff is bounded at $C_T = e^{cT}$. We also use the participation rate α with $\alpha \in \mathbb{R}_+$. α controls the level to which the investor participates in the excess return of V_t.

In addition to the two schemata from Mahayni et al. [Mah13]

$$X_T^{(1)} = \max\{G_T, \alpha V_T\} \quad \text{and} \tag{3.35}$$

$$X_T^{(2)} = \min\{\max\{G_T, V_T\}, C_T\} \tag{3.36}$$

which we denote as special investment processes, we also observe a schema where no guarantee exists. This process is given by

$$X_T^{(3)} = \min\{\alpha V_T, C_T\}. \tag{3.37}$$

Thus, $X_T^{(1)}$ describes an uncapped product with guarantee amount and participation rate, which define the class of guarantee products (GPs). With $X_T^{(2)}$, we observe products with guarantee and cap (GCPs). For this class, we assume a fixed participation rate $\alpha = 1$. A product without a guarantee is given by $X_T^{(3)}$. Notice, this class of product is summarized by capped products (CPs), where the cap rate and the participation rate characterize the relevant product specification.
A corresponding general case that can describe all products is given by

$$X_T^{(gen)} = G_T + (\alpha V_T - G_T)^+ - (\alpha V_T - C_T)^+. \tag{3.38}$$

We should also mention that path-dependent payoff features or other construction could be made. More general, we could use the description

$$X_T^{(gen)} = G_T + h\left(G_T, V_{T,\alpha}^{\rightarrow}\right) - \hat{h}\left(C_T, V_{T,\alpha}^{\rightarrow}\right) \tag{3.39}$$

where $V_{T,\alpha}^{\rightarrow}$ is a vector which describes the relevant return rates resp. the underlying prices during the time to maturity T (resp. in an observation period). h and $\hat{h}$ are the corresponding path-dependent payoff function.

Mahayni et al. [Mah13] use the Black and Scholes model to illustrate the t-price of the products by

$$X_t^{(gen)} = e^{(g-r)(T-t)} + \alpha\left(Call^V\left(t, \frac{e^{gT}}{\alpha}\right) - Call^V\left(t, \frac{e^{cT}}{\alpha}\right)\right) \tag{3.40}$$

where $Call^V(t, \frac{e^{gT}}{\alpha})$ describes the t-call price on V with strike $K = \frac{e^{gT}}{\alpha}$, initial time to maturity of T and remaining time $(T-t)$.

If not mentioned otherwise, we consider that the product are fair priced (cf. Definition 2) with a nominal amount of $N = 1$.

3.6.2 Calculation of the certainty equivalent / loss rate

In this section we show a closed-form solution for the expected utility of CRRA investor in the Black and Scholes model which is given in the following Proposition 3.

Proposition 3 (Expected utility and certainty equivalent) *For an expecting CRRA utility maximizing investor with investment horizon T holds in the Black and Scholes model*

(i) For the guaranteed rate g, the cap rate c and the participation rate α the expected

utility $EU^{X^{(gen)}}$ *for the product* $X^{(gen)}$ *is given by*

$$
\begin{aligned}
EU^{X^{(gen)}} &= E_P\left[u\left(e^{gT} + \left[\alpha V_T - e^{gT}\right]^+ - \left[\alpha V_T - e^{cT}\right]^+\right)\right] \qquad (3.41)\\
&= \frac{1}{1-\gamma}\left[e^{(1-\gamma)gT}\mathcal{N}\left(\frac{gT + \ln\alpha - (\mu - \frac{1}{2}\sigma^2)T}{\sigma\sqrt{T}}\right)\right.\\
&+ e^{(1-\gamma)cT}\mathcal{N}\left(-\frac{cT + \ln\alpha - (\mu - \frac{1}{2}\sigma^2)T}{\sigma\sqrt{T}}\right) \quad + \alpha^{1-\gamma}e^{(1-\gamma)\left(\mu - \frac{1}{2}\gamma\sigma^2\right)T}\\
&\left.\left(\mathcal{N}\left(\frac{cT + \ln\alpha - (\mu + (\frac{1}{2} - \gamma)\sigma^2)T}{\sigma\sqrt{T}}\right) - \mathcal{N}\left(\frac{gT + \ln\alpha - (\mu + (\frac{1}{2} - \gamma)\sigma^2)T}{\sigma\sqrt{T}}\right)\right)\right]
\end{aligned}
$$

(ii) The certainty equivalent $CE_T^{X^{(gen)}}$ *of a product is given by*

$$CE_T^{X^{(gen)}} = \left[(1-\gamma)EU^{X^{(gen)}}\right]^{\frac{1}{1-\gamma}} \qquad (3.42)$$

Proof 3 *The proof is given in Appendix A.3.*

With the corresponding certainty equivalent $CE_T^{X^{(gen)}}$, we are able to calculate the loss rate l_T defined in Definition 5 to classify the optimality or suboptimality of a product.

In the following, we observe different structured stylized products and analyze their corresponding loss rates.

3.6.3 Guarantee products (GPs)

We know from the previous section that an expected CRRA utility maximizing investor suffers by a utility loss if the available product do not suit to her corresponding optimal Constant-Mix strategy with her individual risk aversion parameter γ. A product with a guarantee will generate a loss rate by definition since a CRRA investor requires no capital protection.

Referring to (3.40), we use $c = \infty$ to calculate fair (g,α)-tuple of GPs at issue date $(t_0 = 0)$. The corresponding pricing formula is given by

$$GP_{t_0} = X_{t_0}^{(1)} = e^{(g-r)(T-t_0)} + \alpha\left(Call^V\left(t_0, \frac{e^{gT}}{\alpha}\right)\right) \qquad (3.43)$$

since the second call option is equal to zero. We show the fair (g,α)-tuple for the parameter $(r = 2.4\ \%,\ \sigma = 14.04\ \%$ and $T = 5)$ in the left plot of Figure 3.5. Interestingly, we find no

Figure 3.5: Fair (g,α)-tuple for GPs and loss rates for selected stylized GPs

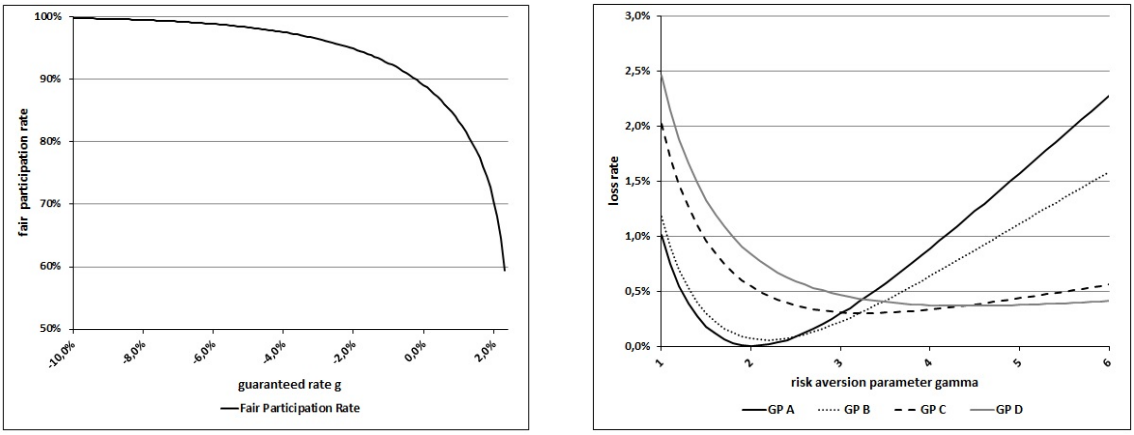

The fair (g,α)-tuple for GPs are illustrated in the left plot. The resulting loss rates for the selected stylized GPs are shown for a risk aversion parameter of $\gamma \in [1,6]$ (right plot).

fair participation rate above 100 % in the range of $g = -10.0$ % to $g = 2.4$ %.[16]
However, the fair α lie near to 100 % for very low guaranteed rates. Note that the smaller the guaranteed rates, the lower the strike prices of the embedded call options. This results in call options that are deep-in-the-money for such low guaranteed rates. Finally, the sum of the "low" guaranteed amounts and the option prices do not significantly change for different low guaranteed rates g, so that also the fair α do not change much.
In the cases where the guaranteed rate lies above $g = -4.5$ % the option starts to get expensive. Thus, we recognize that α will fall to 60 % if the guarantee increases.

To analyze the investor's loss rates, we choose four exemplary stylized GPs with guaranteed rates between $g = -10$ % and $g = 1.0$ %. The selected stylized products are as follows:
GP A $= (-10\%, 99.789\%)$, GP B $= (-5\%, 98.322\%)$,
GP C $= (0\%, 89.122\%)$ and GP D $= (1\%, 83.354\%)$.

In Figure 3.5 (right plot) we show the calculated loss rates for investor Γ and further risk aversion parameters $\gamma \in [1,6]$.

16 In our observation a guaranteed rate of $g = -10.0$ % results in a guaranteed amount of only 60.7 % of the nominal amount. These low guarantee amount should highlight that also GPs are observed for more risk seeking investors.

We identify that the guarantee product with the lowest guaranteed rate (GP A) is the best for investor Γ. The observed loss rate is slightly above $l_T = 0.0$ %. In other words, investor Γ (with $\gamma = 2$) could choose the structured stylized GP A as an alternative to her optimal Constant-Mix strategy. The higher the guaranteed rate, the higher the loss rate for the observed investor. Of course, looking at the fair participation α, we identify that a GP with $G_T \to 0$ converse to the corresponding Constant-Mix strategy.
Of course, other investors will suffer from an investment in GP A. The products with higher guaranteed rate g are suboptimal for all illustrated γ (resp. investors).

Now, we assume that only GP C with guaranteed rate $g = 0.0$ % is available for the investor. This GP results in a loss rate of $l_T = 0.55$ %. To optimize her utility the investor can choose different underlying assets for the GP C. Since the guaranteed rate is higher than the investor requires, we analyze whether a more risky underlying asset could lower the investor's loss rate.

Figure 3.6: Calculated loss rates for GP C with varying underlying asset

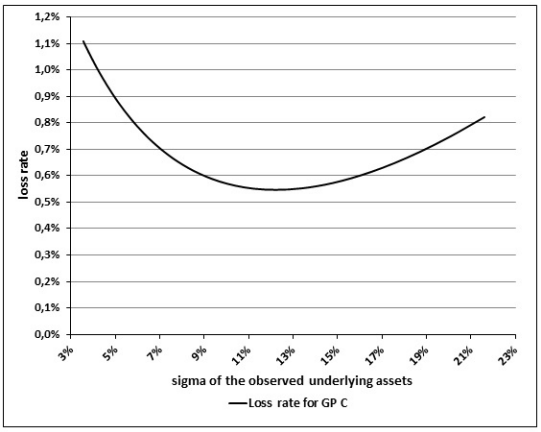

Calculated loss rate for the guarantee product with $g = 0.0$ % (GP C) for different underlying assets resp. different volatility levels.

Figure 3.6 shows that the lowest loss rate is still calculated for $\sigma = 14.04$ %, which is the volatility of the optimal Constant-Mix strategy. This seems unconvenient at the first glance, but the result is along the lines with Proposition 2. Since the guaranteed rate $g = 0.0$ % is exogenously given, the optimal investment strategy is given by a contribution guarantee schema (cf. Definition 4) on the corresponding value process V_t of the optimal

Constant-Mix resp. Merton strategy .[17]

3.6.4 Capped products (CPs)

As already mentioned, a CRRA investor does not require a guarantee nor a cap. Nevertheless, it is meaningful to consider CPs to analyze how the cap influences the utility of the investor. CPs can be describe by the specification of (3.40).
For the class of CPs we set $g = -\infty$, so that the guarantee amount $G_T = e^{gT} = 0$. Furthermore, the strike of the long call option is zero. It results a zero-strike-call with the characteristics of the underlying asset itself.[18]
We observe the following pricing formula at issue date

$$\begin{aligned} CP_{t_0} = X_{t_0}^{(3)} &= \alpha \left(Call^V (t_0, 0) - Call^V \left(t_0, \frac{e^{cT}}{\alpha} \right) \right) \\ &= \alpha \left(V_{t_0} - Call^V \left(t_0, \frac{e^{cT}}{\alpha} \right) \right). \end{aligned} \tag{3.44}$$

Analogous to the illustration for the GPs, we will show fair (c,α)-tuple of the CPs. Furthermore, we calculate the corresponding loss rates for investor Γ for the selected structured stylized CPs and compare them to risk aversion parameters between $\gamma = 1$ to $\gamma = 6$.
We illustrate the development of the fair (c,α)-tuple in the left plot of Figure 3.7. The maximum α is about 140 % calculated for the lowest cap rate of $c = 3.0\%$. For higher c, the participation rate converge to $\alpha = 100$ %. For the highest observed cap rate ($c = 23.0$ %) we calculate $\alpha = 100.01$ %. In comparison to the guarantee products, we simply illustrated participation rates above 100 % for the CPs, while all α are shown for the GPs are below that level.

We now focus on the following four CPs, which we assume are offered by the issuer:
CP A $= (3\%, 141.73\%)$, CP B $= (7\%, 106.96\%)$,
CP C $= (10\%, 102.45\%)$ and CP D $= (15\%, 100.37\%)$.

Analogous to Figure 3.5, we illustrate the resulting loss rates calculated by (Definition 5) for the selected stylized CPs in the right plot of Figure 3.7.

17 Under our assumptions, the Put-Call Parity proves that the payoff of the GP (cf. (3.43)) is equal to the contribution guarantee schema on V_t.

18 We should mention that in general a zero-strike-call differ from the underlying while the underlying pays dividends. Since we assume a no-dividend paying underlying asset the development of the underlying price and the zero-strike-call are equal.

Figure 3.7: Fair (c,α)-tuple for CPs and loss rate for selected stylized CPs

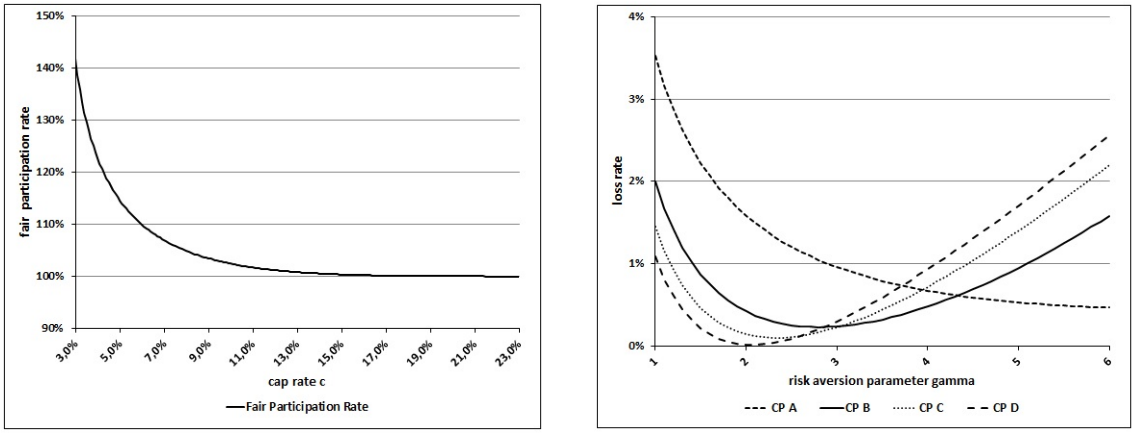

The fair (c,α)-tuple for a CP are illustrated in the left plot. The resulting loss rates for the stylized CP are shown for a risk aversion parameter of $\gamma \in [1,6]$ (right plot).

For the observed investor (investor Γ), CP D would be the best choice of the selection. We should mention that the higher the cap rates, the closer the corresponding CP is to the optimal Constant-Mix. To be more precise, the calculated loss rates for CP D and GP A do not significantly differ. Of course, for the observed investor, the lower the cap rates the higher her utility loss.

Analogous to the calculation for the GPs, we assume a fixed cap rate of $c = 7.0$ % (CP B). Investor Γ could choose different underlyings asset for the corresponding CP. The loss rate using the underlying V_t is given by $l_T = 0.42$ %. Figure 3.8 show the different variation. Interestingly, we identify the same development for the CPs as observed for the GPs. The minimum loss rate is related to the corresponding Constant-Mix strategy V_t with is optimal for the assumed investor. In summary, the exogenous cap influences the investor's utility, although her optimal underlying asset remains the same.

3.6.5 Products with guarantee and cap (GCPs)

In opposite to CPs and GPs, GCPs combine a guaranteed rate with a cap rate. Thus, we assume $c < \infty$ as well as $g > -\infty$. In the following, we set $\alpha = 1$ and calculate the fair

Figure 3.8: Calculated loss rates for CP B with varying underlying asset

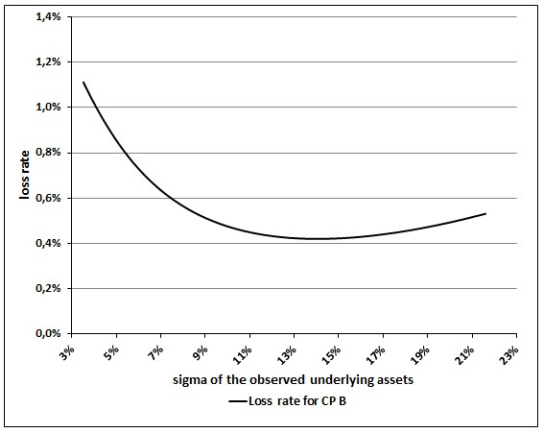

Calculated loss rate for the CP with $c = 7.0$ % (CP B) for different underlying assets resp. different volatility levels.

(g,c)-tuple for general GCPs. The corresponding t_0-price is calculated by

$$GCP_{t_0} = X_{t_0}^{(2)} = e^{(g-r)(T-t_0)} + \left(Call^V\left(t_0, e^{gT}\right) - Call^V\left(t_0, e^{cT}\right)\right) \tag{3.45}$$

As in the previous analysis we will give an overview of the fair (g,c)-tuple. Furthermore, we observe exemplary stylized GCP to calculate the corresponding loss rate for investor Γ.

We illustrate the fair (g,c)-tuple for the GCPs in the left plot of Figure 3.9. It is seen that for a higher guaranteed rate g the fair cap rate c decreases. Additionally, the development looks more-or-less linear. The lowest observed guaranteed rate of $g = -10$ % result in a fair cap rate of $c = 16.30$ %. We should mention that such low guaranteed rates in combination with the calculated high cap rates do not have a significant influence of the products price since the relevant component has a very low price.
Here, we assume for these combinations of g and c that the loss rate is very close to the product GP A or CP D.
If the guaranteed rate goes to $r = 2.4$ % also the fair cap rate converge to the risk-free interest rate. Finally, the corresponding GCP could be identify with a zerobond investment, which is almost independent from the development of the underlying asset.

For the calculation of the loss rate, we define the following four stylized GCP:
GCP A $= (-10\%, 16.297\%)$, GCP B $= (-5\%, 10.991\%)$,

Figure 3.9: Fair (g,c)-tuple for GCPs and loss rate for selected stylized GCPs

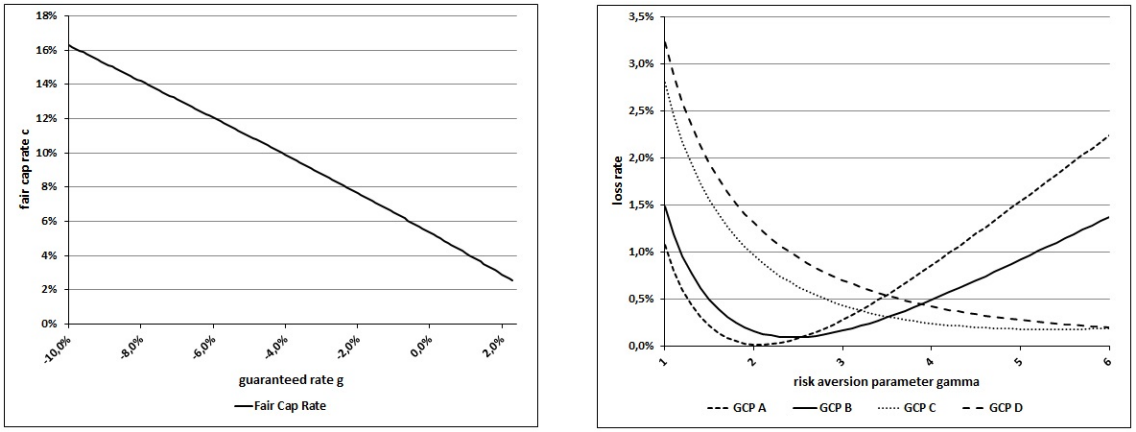

The fair (g,c)-tuple for a product with guarantee and cap are illustrated in the left plot. The resulting loss rates for the stylized GCP are shown for a risk aversion parameter of $\gamma \in [1,10]$ (right plot).

GCP C= $(0\%, 5.355\%)$ and GCP D = $(1\%, 4.152\%)$.

The development of the calculated loss rates are illustrated in the right plot of Figure 3.9. For investor Γ holds that GCP A results in the lowest loss rate. To be more precise, the loss rate of GCP A for investor Γ is $l_T = 0.017$ %. Notice that the development of the loss rate for GCP A is very similar to the loss rates calculated for GP A and CP D. For higher guaranteed rates (GCP B, GCP C or GCP D) the loss rate for investor Γ rises up to $l_T = 1.31$ %. Of course, an investor with a significantly higher risk aversion will profit from the higher guaranteed rate in combination with a lower fair cap rate.
Finally, we observe GCP C, which leads to a loss rate of $l_T = 0.961$ % for investor Γ. Once again, we calculate if a deviation of the assumed underlying V_t could reduce the investor's loss rate. The result is illustrated in Figure 3.10. In contrast to the other observed structured stylized product (e.g. GP and CP), the GCP investor Γ can optimize her utility by an adjustment of the underlying asset for GCP C. We identify that each underlying asset with $\sigma > 14.04$ % will lead to a lower loss rate. In our observed volatility range, the optimal underlying asset is given by stylized product D with $\varphi = 100$ %.[19]

19 Of course, this development is influenced by the assumed guaranteed rate. An overview with different guaranteed rate is given in Appendix A.1.

Figure 3.10: Calculated loss rates for GCP C with varying underlying asset

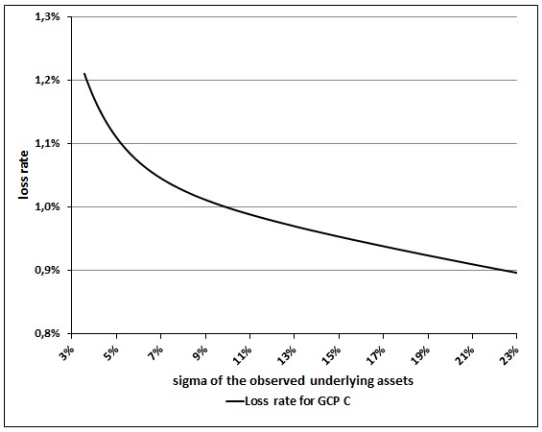

Calculated loss rate for the GCP with guaranteed rate $g = 0$ % (GCP C) for different underlying assets resp. different volatility levels.

3.6.6 Summary of the structured stylized products

Although we assume incomplete market conditions for the investor, we could mention that there are product specifications for all three observed structured stylized products that guide to very low loss rate. Therefore, the investor has to select a product for which the payoff distribution is close to the optimal Constant-Mix strategy. Intuitively, this holds for very low guaranteed rates (GP), very high cap rates (CP) or a combination of the two (GCP). Obviously, the calculated loss rates for investor Γ rely on GP A, CP D and GCP A highlight this effect.

Furthermore, we answer the question of whether a variation of the underlying asset could result in a lower loss rate for a given product specification.

For the GPs and CPs holds that the underlying asset V_t (derived from the optimal Constant-Mix strategy) always results in the lowest loss rate. Thus, Proportion 2 also holds for an exogenous cap. For the selected GCP C, we show that the observed investor will reduce her utility loss by choosing a more risky underlying asset.

3.7 Analysis of path-dependent structured stylized products

As mentioned, many products use path-dependence as an additional payoff feature. Thus, for the calculation of the payoffs and the return rate of a product, the development of the underlying is observed during the time to maturity (or in a sub-period). We will analyze two

classes of path-dependent products which define the restricted set of suboptimal products the investor can choose. On the one hand, we observe products where the minimum price of the underlying is taken into account for the calculation of the final payoff. Of course, there are different opportunities to integrate a minimum calculation in such a path-dependent structured stylized products. We will observe the specification where the strike price is derived by the minimum underlying price due to an observation period (and a number of observation dates).
On the other hand, we focus on products with an asianing feature. For these path-dependent payoff features, an average of observed underlying prices (resp. return rates) is used for the calculation of the payoff. Theoretically, the averaging method could be used either for the calculation of the strike price of the embedded option or for the excess return of the underlying itself. In the following, we will focus on the second case, where the strike is fixed.
For the minimum and the average calculation, we have to rely on a specific observation frequency. Our calculation are based upon a monthly, quarterly, semi-annual or annual observation period.[20]

We modify the illustrated structured stylized products from Section 3.6 by the corresponding features of path-dependence. However, we focus on different observation frequency as well as two separate path-dependent calculations. In the following, we will analyze path-dependent products $\mathrm{P}(\xi,\psi)$ where ξ describe the observation period and ψ denotes the specific path-dependent calculation method. The monthly, quarterly, semi-annual or annual observation periods is noticed by $\xi \in \{m, q, s, a\}$. Furthermore, we focus on an average and a minimum calculation illustrated by $\psi = a$ and $\psi = m$. The following products will be describe by (3.39).
However, there does not exist a close form solution for the observed path-dependent products. Thus, we will only illustrate the payoff function in the following. Furthermore, we rely on Monte Carlo simulation to calculate the fair tuples as well as the corresponding loss rates.

20 To be more precise, the observation period resp. the observation frequency defines regarding the time to maturity T the number of observation date where the underlying price or a corresponding return rate is calculated. It holds that the shorter the observation period, the higher the number of observed underlying prices resp. return rates responsible for the payoff at maturity.

3.7.1 Path-dependent guarantee products (PGPs)

In the case of a path-dependent guarantee product (P(ξ,ψ)GP), we calculate the excess return based upon the development of the underlying while assuming a guaranteed amount which is entirely independent of the underlying performance. Furthermore, the payoff resp. return rate of the P(ξ,ψ) GP is not capped.

Path-dependent GPs with averaging feature (P(ξ,a) GPs)

We first assume a function h (cf. 3.39) which integrates the calculation of an average return of the underlying during the entire investment period in a GP. We denote this product by P(ξ,$\psi = a$)GP. The payoff is given by[21]

$$P\left(\xi,a\right) GP_T = G_T + h\left(G_T, V^{\rightarrow}_{T,\alpha}\left(\xi,a\right)\right) \tag{3.46}$$

with

$$h\left(G_T, V^{\rightarrow}_{T,\alpha}\left(\xi,a\right)\right) = \max\left\{0; V^{\rightarrow}_{T,\alpha}\left(\xi,a\right) - G_T\right\} \text{ and } V^{\rightarrow}_{T,\alpha}\left(\xi,a\right) = \alpha \frac{1}{n} \sum_{i=1}^{n} V_{t_i,\alpha} \tag{3.47}$$

where ξ specifies the number of summands n and $t_i \in \{t_1,t_2,...t_n = T\}$ are the resulting observation dates.[22]

To compare our result to the standard stylized GPs (resp. path-independent stylized GPs), we assume the same four guaranteed rates which are used to define GP A, GP B, GP C and GP D.[23] Since we observe different observation periods, we have to calculate the fair participation rate α for each combination of guaranteed rate and observation period. We illustrate the fair (g,α)-tuple of general path-independent GPs in the left plot of Figure 3.19.

We identify that the calculated α is lower for a higher guaranteed rate which is already known from Section 3.6.3. Furthermore, it is seen that α is lower for longer observation period (resp. a lower number of observation dates).

21 For the family of path-dependent GPs, it holds that $C_T = e^{cT} = \infty$ which implies $\hat{h}\left(C_T = \infty, V^{\rightarrow}_{T,\alpha}\left(\xi,\psi\right)\right) = 0$ for all $V^{\rightarrow}$.

22 Of course, a longer observation period results in a smaller number of observation dates which are used for the averaging calculation. In other words, for $\xi = m$ follows $n = 60$. Thus, with a monthly observation we will calculate an average based upon 60 observed sub-period prices. For example, $\xi = a$ results in an averaging of only five sub-period prices.

23 We use the guaranteed rates $g_A = -10$ %, $g_B = -5$ %, $g_C = 0$ % and $g_D = 1$ %.

Figure 3.11: Fair (g,α)-tuple for P(ξ,a)GPs and loss rate for selected stylized P(q,a)GPs

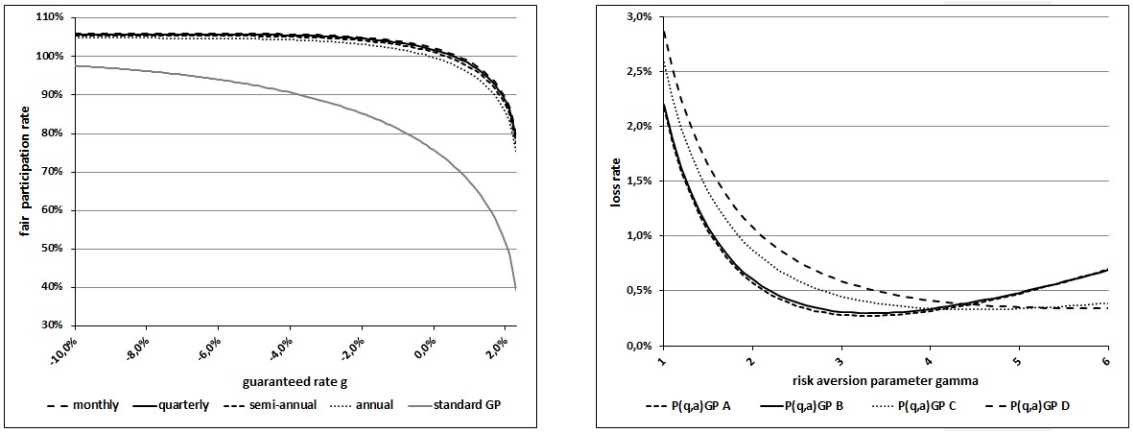

The fair (g,α)-tuple for the path-dependent guarantee product (P(ξ,a)GP) for varied observation periods and the fair (g,α)-tuple for the path-independent GP are illustrated (left plot). The resulting loss rates for the path-dependent stylized P(q,a) GP with a quarterly observation period are shown for a risk aversion parameter of $\gamma \in [1,10]$ (right plot).

However, in comparison to the standard stylized GP (cf. Section 3.6.3), we notice higher fair participation rates α for all guaranteed rates. For a better overview, we integrate the fair (g,α)-tuple of the path-independent GP into the left plot of Figure 3.19.
We show that each graph looks very similar compared to the illustration of the standard stylized GP. But overall, the fair participation rates are higher for the path-dependent guarantee product (P(ξ,a)GP). In the path-independent case, the lowest guaranteed rate $g = -10$ % (GP A) results a fair α of 97.613% while the corresponding fair α for P(ξ,a)GP lie between 104.83 % and 105.99 %.
The results show the sensitivity regarding the observation periods. On the one hand, we could mention that all path-dependent GPs have a higher α regardless which calculation method is used. On the other hand, the number of observation dates resp. the length of the observation period has an additional impact on the calculation. Although the difference is marginal, we ascertain that the fair α is lower the longer the observation period.

The analysis of the resulting loss rates for investor Γ focus on $\xi = q$. To compare the result to the standard stylized guarantee product, we observe the following path-dependent GPs with quarterly averaging feature:
P(q,a)GP A= $(-10\%, 105.990\%)$, P(q,a)GP B= $(-5\%, 105.655\%)$,

P(q,a)GP C= $(0\%, 101.748\%)$ and P(q,a)GP D= $(-1\%, 78.763\%)$.

The calculated loss rates for investor Γ and further risk aversion parameter are shown in the right plot of Figure 3.19. We should mention that the development of the calculated loss rates for P(q,a)GP A and P(q,a)GP B is more-or-less the same. From the investor's perspective, P(q,a)GP A is the best product in this selection. However, the loss rate ($l_T = 0.57$ %) is clearly above the loss rate of the path-independent GP A. Furthermore, we identify that the loss rate of all P(q,a)GPs find their minimum at a risk aversion level above the observed investor risk aversion ($\gamma = 2$), although the optimal value process V_t is used.
It seems that the path-dependent features make the PGP more attractive for higher risk aversion parameter.

Since investor Γ will suffer by investing in one of the selected PGPs, it is meaningful to analyze if she could lower her utility loss. For this analysis, we give her the choice to change the underlying asset. Analogous to the calculation for the GPs, we assume the product with guaranteed rate of $g = 0.0$ % (PGP(q,a) C) which leads to a loss rate of $l_T = 0.87$ % for the underlying asset V_t.
By the varying σ we ascertain that a more risky underlying asset would lower the loss rate of investor Γ which we illustrate in Figure 3.12. This development could be explained

Figure 3.12: Calculated loss rates for P(q,a)GP C with varying underlying asset

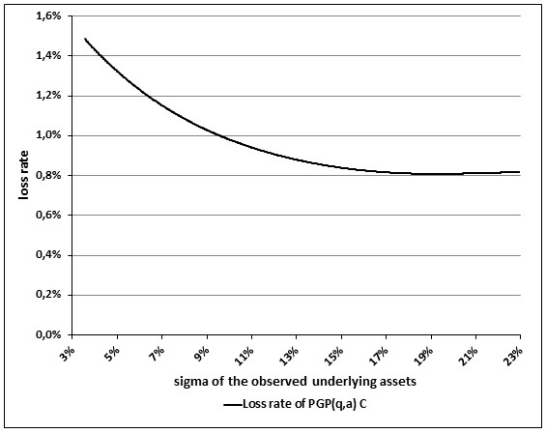

Calculated loss rate for the PGP with $g = 0.0$ % (P(q,a)GP C) for different underlying assets resp. different volatility levels.

as follows. Of course, the averaging calculation makes the product less risky by their

smoothing character. The investor could counteracts this development by selecting a more risky underlying asset. The minimum loss rate of $l_T = 0.804$ % is calculated for $\sigma = 19$ %.

Path-dependent GPs with minimum feature (P(ξ,m)GPs)

Next, we illustrated a path-dependent guarantee product which uses minimum calculation: P(ξ,m)GP. Applying (3.38), the payoff can be described by

$$P\left(\xi,m\right) GP_T = G_T + h\left(G_T, V^{\rightarrow}_{T,\alpha}\left(\xi,m\right)\right) \tag{3.48}$$

with

$$h\left(G_T, V^{\rightarrow}_{T,\alpha}\left(\xi,m\right)\right) = \max\left\{0; \alpha \frac{V_T}{\min_{i=1,\ldots,n} V_{t_i}} - G_T\right\} \tag{3.49}$$

where ψ describes the number of observation dates taken into account for the minimum calculation and $t_i \in \{t_1,t_2,\ldots t_n = T\}$ are the resulting observation dates.
We illustrated the fair (g,α)-tuple for all possible P(ξ,m)GPs in the left plot of Figure 3.21. Again, we compare the calculated tuple with the resulting graph of the standard stylized GP.

Figure 3.13: Fair (g,α)-tuple for P(ξ,m)GPs and loss rate for selected stylized P(q,m)GPs

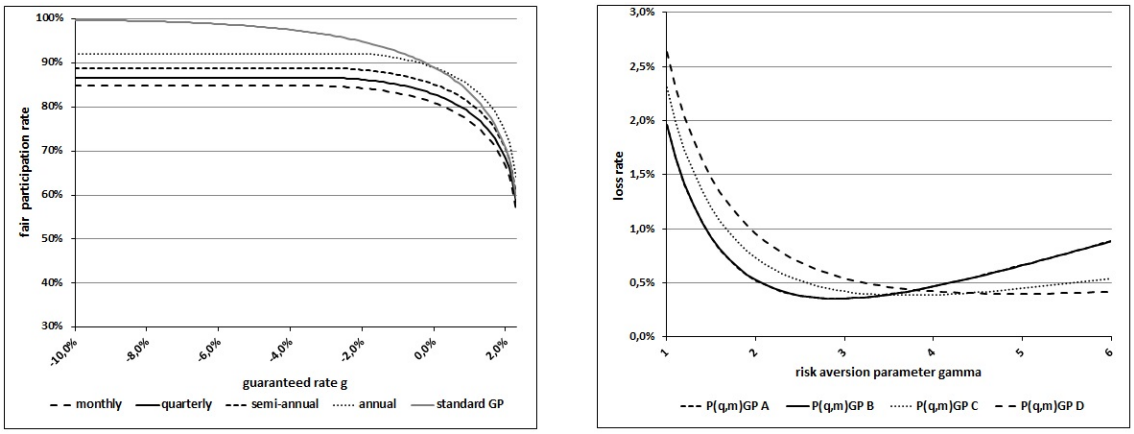

The fair (g,α)-tuple for a path-dependent guarantee product with an minimum return calculation (P(ξ,m)GP) and varied observation period are illustrated in the left plot. The resulting loss rates for the path-dependent stylized P(q,m)GP are shown for a risk aversion parameter of $\gamma \in [1,10]$ (right plot).

Regarding the illustrated development, we could mention the following characteristics.

With the exception of a very small range of guaranteed rates, all calculated α are smaller than the comparable participation rates of the standard stylized GP. Again, the shorter the observation period, the smaller the fair α and the larger the difference compared to the calculated α for the standard stylized GP.
As previously mentioned, the fair participation rate is near to 100 % if we assume the lowest guaranteed rate of $g = -10$ % for the path-independent GP. Instead, the fair participation rates for the P(ξ,m)GP lie between 73.6 % and 83.5 % for $g = -10$ %.
Interestingly, the fair α are constant for a range of lower guaranteed rates. This result could be explained by the following observation.
By definition, the fraction of the terminal underlying price and its minimum at the corresponding observation dates (including $t_n = T$) is always greater than 1. In addition, for $\alpha > G_T = e^{gT}$ holds that

$$\alpha \frac{V_T}{\min_{i=1,\dots,n} V_{t_i}} - e^{gT} > 0 \tag{3.50}$$

which results in a simplified payoff of

$$P\,(\xi,m)\,GP_T = \alpha \frac{V_T}{\min_{i=1,\dots,n} V_{t_i}} \tag{3.51}$$

where the guaranteed amount $G_T = e^{gT}$ become irrelevant. To be more precise, the minimum calculation prevents negative return rate based upon the underlying development. Thus, this calculation has a kind of guarantee feature since the calculated fraction is always above 1. For some low guaranteed rates, the minimum calculation in combination with the fair participation rate results in a higher guaranteed amount than the guaranteed rate itself.
Nevertheless, for higher guaranteed rates the calculated participation rate significantly decreases.

Using the common four guaranteed rates[24], we calculate loss rates which we illustrate in the right plot of Figure 3.21. The resulting loss rate for investor Γ are based upon the fair tuple (g,α) for the quarterly observation period:
P(q,m)GP A= $(-10\%, 86.693\%)$, P(q,m)GP B= $(-5\%, 86.693\%)$,
P(q,m)GP C= $(0\%, 82.938\%)$ and P(q,m)GP D= $(-1\%, 78.763\%)$.

24 $g_A = -10$ %, $g_B = -5$ %, $g_C = 0$ % and $g_D = 1$ %

We identify that P(q,m)GP A and P(q,m)GP B have the identical loss rate for all observed risk aversion parameter (including investor Γ). This is a direct results from the fair product design where α is equal for $g = -10$ % and $g = -5$ %. However, investor Γ will suffer from a utility loss by at least $l_T = 0.525$ %. Furthermore, we ascertain that all of the selected P(q,m)GPs are more suitable for investors with higher risk aversion than investor Γ. The corresponding minimum for the P(q,m)GPs are calculated between $\gamma = 2.9$ and $\gamma = 4.9$.

As in the calculations before, we allow investor Γ the change the underlying asset to lower her loss rate. Thus, we observe P(q,m)GP C and calculate the loss rate for varying σ and the corresponding fair participation rate. The result is illustrated in Figure 3.14.

Figure 3.14: Calculated loss rates for P(q,m)GP C with varying underlying asset

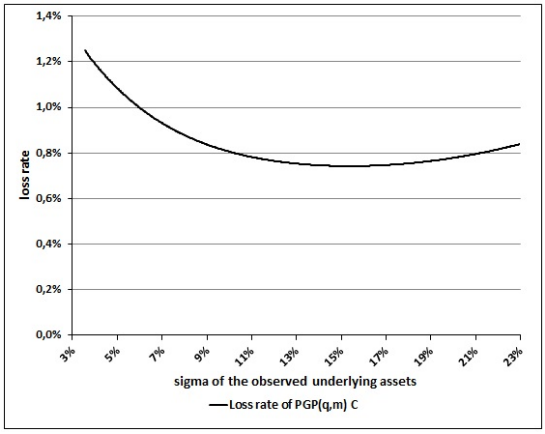

Calculated loss rate for the PGP(q,m) with $g = 0.0$ % (PGP(q,m) C) for different underlying assets resp. different volatility levels.

It is seen that a slightly riskier underlying ($\sigma = 15$ %) could lower the loss rate from $l_T = 0.74$ % to $l_T = 0.73$ %. In particular, it seems that the underlying derived from the optimal Constant-Mix strategy is more-or-less optimal for the observed PGP(q,m) C.

The investor's choice to find the optimal path-dependent GP remains complicated. The observed investor suffers from the path-dependent feature, while an investor with a significantly higher risk aversion would benefit. For investor Γ, both calculation methods lead to a loss rate from almost $l_T = 0.5$ % which is clearly above the loss rates calculate for the path-independent GPs. Of course, this results from the assumed utility function, since a CRRA investor do not required a path-dependent payoff. However, we prove that for a

path-dependent GP an adjustment of the underlying asset can lower the investor's loss rate, although the relative utility gain is margin.

3.7.2 Path-dependent capped products (PCPs)

Path-dependent capped products ($P(\xi,\psi)$ CPs) combine the payoff of a standard capped product (cf. Section 3.6.4) with the applied path-dependent calculation method. In the following, we will observe the capped products which imply the average calculation $P(\xi,a)$CPs and path-dependent CPs where the payoffs rely on the minimum calculation of the underlying ($P(\xi,m)$CPs).

Path-dependent CPs with averaging feature (P(ξ,a)CPs)

Analogous to the other path-dependent structures, the payoff is given by (3.39):

$$P(\xi,a)\,CP_T = V^{\rightarrow}_{T,\alpha}(\xi,a) - \hat{h}\left(C_T, V^{\rightarrow}_{T,\alpha}(\xi,a)\right) \tag{3.52}$$

with

$$\hat{h}\left(C_T, V^{\rightarrow}_{T,\alpha}(\xi,a)\right) = \max\left\{0; V^{\rightarrow}_{T,\alpha}(\xi,a) - C_T\right\} \text{ and } V^{\rightarrow}_{T,\alpha}(\xi,a) = \alpha\frac{1}{n}\sum_{i=1}^{n} V_{t_i} \tag{3.53}$$

where n the number of observation date depending on ξ and t_i with $i = 1,...,n$ the corresponding observation dates.[25]

We illustrate the development of the calculated fair α in Figure 3.15 where the fair (c,α)-tuple w.r.t. P(ξ,a)CP are compared to the tuple derived for the standard capped product.
In comparison to the path-dependent GPs, we cannot find a trend regarding the length of the observation period. For cap rates below $c = 6.0$ %, the highest α is calculated for the annual observation period. However, for higher cap rates hold, the longer the observation period the lower the participation rates. Furthermore, we identify that the fair participation rate for the standard CP is above the calculated α until the cap rate of almost 7.0 %. Subsequently, α lie below the other participation rates and converge to 100 %. The limit for the path-dependent case is calculated between $\alpha = 105.99$ % and $\alpha = 104.83$ %.

25 By applying (3.39), we use $G_T = e^{gT} = 0$. It follows that $h\left(0,V^{\rightarrow}_{T,\alpha}(\xi,a)\right) = V^{\rightarrow}_{T,\alpha}(\xi,a)$.

Figure 3.15: Fair (c,α)-tuple for P(ξ,a)CPs and loss rate for selected stylized P(q,a)CPs

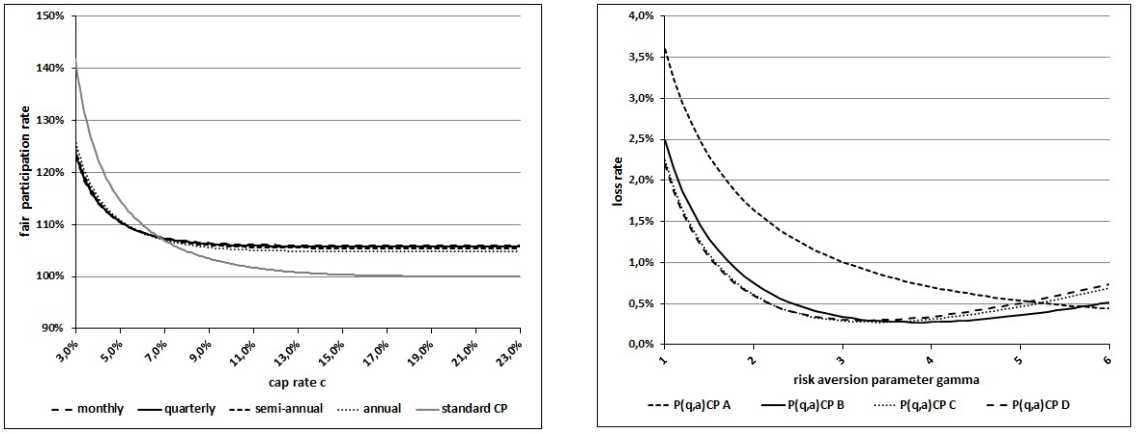

The fair (c,α)-tuple for general PCPs with an average return calculation (P(ξ,a)CP) for varied observation period are illustrated (left plot). The resulting loss rates for the selected path-dependent structured stylized P(q,a)CP are shown for a risk aversion parameter of $\gamma \in [1,6]$ (right plot).

Now, we consider the corresponding loss rate for investor Γ. For this reason, we observe four exemplary stylized path-dependent CPs with averaging features. The selection assumes the cap rates which are used in Section 3.6.4. Thus, we use the following fair tuple:
P(q,a)CP A= $(3\%, 123.974\%)$, P(q,a)CP B= $(7\%, 107.344\%)$,
P(q,a)CP C= $(10\%, 106.044\%)$ and P(q,a)CP D= $(15\%, 105{,}788\%)$.

The resulting loss rate for the observed investor (investor Γ with $\gamma = 2$) is shown in the right plot of Figure 3.15. We see that the investor's loss rate lie between $l_T = 0.594$ % and $l_T = 1.641$ %. Analogous to the analysis of P(q,a)GPs, we ascertain that the loss rate of two selected products (P(q,a)CP C and P(q,a)CP D) are identical.
However, investor Γ suffer from the averaging feature. Thus, we try to ascertain whether another underlying asset could change her utility. In Figure 3.16, we calculate the corresponding loss rates for investor Γ assuming different underlying assets and the resulting fair participation rates α for P(q,a)CP B. It is evident that a underlying asset with higher volatility will lead to a lower loss rate for investor Γ. If V_t is used as the underlying asset, the observed product will result in a loss rate of $l_T = 0.746$ %. By choosing a riskier underlying with a volatility of $\sigma = 20$ % the investor can reduce her loss rate to $l_T = 0.696$ %.

Figure 3.16: Calculated loss rates for P(q,a)CP B with varying underlying asset

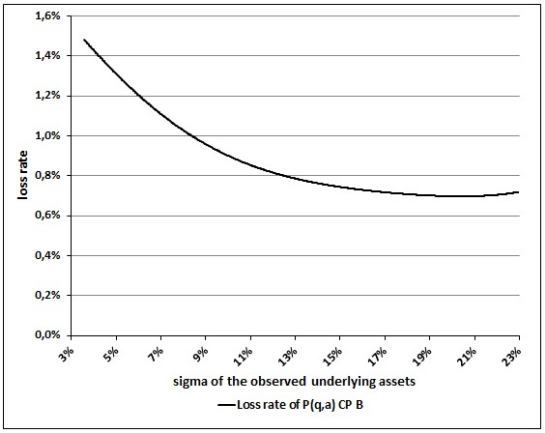

Calculated loss rate for the P(q,a)CP with $c = 7.0$ % (P(q,a)CP B) for different underlying assets resp. different volatility levels.

Path-dependent CPs with minimum feature (P(ξ,m)CPs)

Subsequently, we consider the PCPs that imply the minimum calculation. The payoff is given

$$P\left(\xi,m\right) CP_T = V_{T,\alpha}^{\rightarrow}\left(\xi,m\right) - \hat{h}\left(C_T, V_{T,\alpha}^{\rightarrow}\left(\xi,m\right)\right) \tag{3.54}$$

with

$$\hat{h}\left(C_T, V_{T,\alpha}^{\rightarrow}\left(\xi,m\right)\right) = \max\left\{0; V_{T,\alpha}^{\rightarrow}\left(\xi,m\right) - C_T\right\} \text{ and } V_{T,\alpha}^{\rightarrow}\left(\xi,m\right) = \alpha\frac{V_T}{\min_{i=1,\ldots,n} V_{t_i}} \tag{3.55}$$

As in the other description, the number of the relevant observation dates n depends of the chosen ξ.

We illustrate the development of the calculated fair α as well as the (c,α)-tuple for the standard CP in Figure 3.17.

For all P(ξ,m)CPs, we identify a development of the fair participation rates which starts for the lowest assumed cap rate near to $\alpha = 100$ %, whereby the annual observation leads to the highest participation rate of $\alpha = 105.21$ %. With increasing c the corresponding fair participation rate α are decreasing to a range between $\alpha = 85$ % and $\alpha = 92$ %, whereby

Figure 3.17: Fair (c,α)-tuple for P(ξ,m)CPs and loss rate for the selected stylized P(q,m)CPs

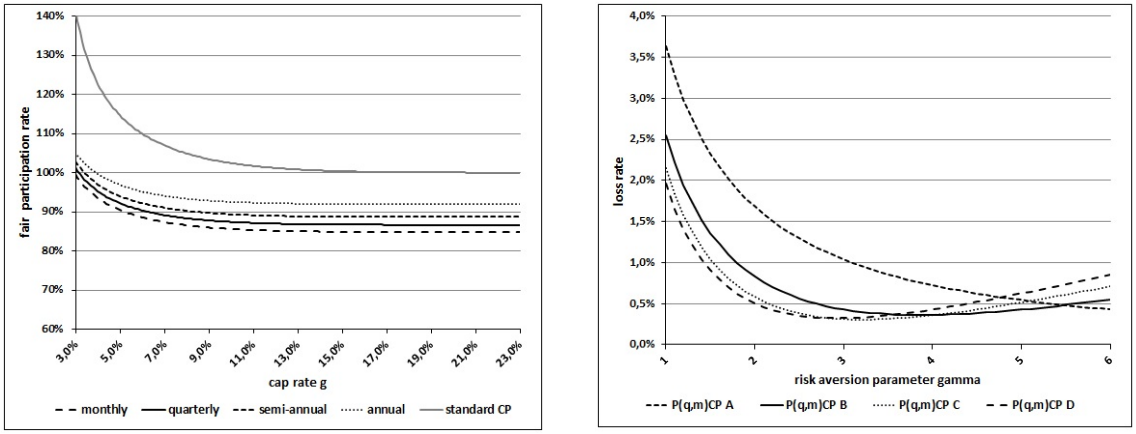

The fair (c,α)-tuple for general path-dependent capped products with an minimum return calculation (P(ξ,m)CPs) for varied observation period are illustrated (left plot). The resulting loss rates for the selected path-dependent stylized P(q,m)CPs are shown for a risk aversion parameter of $\gamma \in [1,6]$ (right plot).

the shorter observation period results in the lower participation rates. The difference with the standard CP without any path-dependent feature is huge, which is along the lines of the results for the observed GP, where the minimum calculation is also significantly lower α.

The loss rates for investor Γ as well as for further risk aversion parameter are calculated regarding four selected P(q,m)CPs and shown in the right plot of Figure 3.17. The selection is given by:
P(q,m)CP A= (3%,101.345%), P(q,m)CP B= (7%, 89.144%),
P(q,m)CP C= (10%, 87.410%) and P(q,m)CP D= (15%, 86.738%).

It is seen that all observed P(q,m)CPs results in a loss rate for investor Γ above $l_T = 0.5$ %. The highest loss rate ($l_T = 1.75$ %) is identified for P(q,m)CP A which offers the lowest cap rate of the selection. This result is along the line with the observation of the CPs as well as the P(q,a)CPs. However, the minimum calculation feature makes the product more interesting for investors who have a higher risk aversion compared to investor Γ. This result prompts the question of whether the investor can lower her loss rate by choosing another underlying asset.
The calculation is illustrated in Figure 3.18. We use the capped product P(q,m)CP B with

the corresponding cap rate of $c = 7.0$ % for this analysis.

In particular, the investor can influence her loss rate by an adjustment of the underlying

Figure 3.18: Calculated loss rates for P(q,m)CP B with varying underlying asset

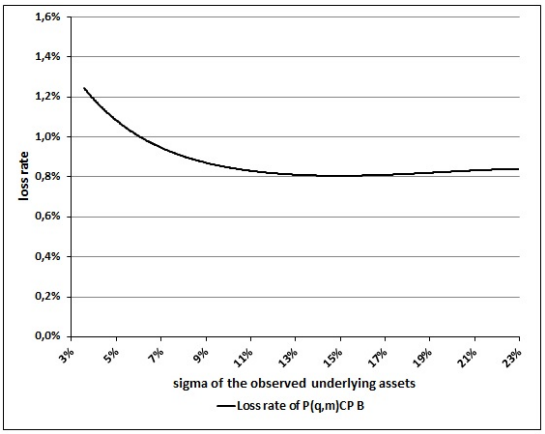

Calculated loss rate for the P(q,m)CP with $c = 7.0$ % (P(q,m)CP B) for different underlying assets resp. different volatility levels.

asset. However, the utility gain is significantly lower compared to the other PCPs with averaging calculation. Increasing the volatility of the underlying asset from 14 % to 15 % can lower the loss rate from $l_T = 0.82$ % to $l_T = 0.81$ %. However, this result is along the line with the analysis of the P(q,m)GP C.

The results quantifying the suboptimality of the PCPs are analogous to the PGPs. The loss rate is always above $l_T = 0.5$ % for investor Γ regardless if we focus on the minimum or average calculation. Nevertheless, we find an opportunity to improve the investor's utility by adjusting the underlying asset. However, the calculated loss rate is only a few basis point lower.

3.7.3 Path-dependent products with guarantee and cap (PGCPs)

Finally, we consider path-dependent products with a guarantee and cap. As in the previous section, we will first observe the path-dependent calculation method based upon an averaging of the underlying prices. Subsequently, we analyze the PGCP with the minimum calculation.

Path-dependent GCPs with average feature (P(ξ,a)GCPs)

Of course, the payoff function could be describe analogous to the other path-dependent product (cf. (3.39))

$$P\,(\xi,a)\,GCP_T = G_T + h\,(G_T, V_T^{\rightarrow}\,(\xi,a)) - \hat{h}\,(C_T, V_T^{\rightarrow}\,(\xi,a)) \tag{3.56}$$

$$\text{with } h\,(G_T, V_T^{\rightarrow}\,(\xi,a)) = \max\{0; V_T^{\rightarrow}\,(\xi,a) - G_T\}$$
$$\hat{h}\,(C_T, V_T^{\rightarrow}\,(\xi,a)) = \max\{0; V_T^{\rightarrow}\,(\xi,a) - C_T\} \text{ and } V_T^{\rightarrow}\,(\xi,a) = \frac{1}{n}\sum_{i=1}^{n} V_{t_i}$$

where the number of the relevant observation dates n depends of ξ.

We illustrate the fair (g,c)-tuple in the left plot of Figure 3.19.
For our assumption, it is impossible to calculate fair cap rates for lower guaranteed rates (especially for $g < 0$ %). This development results from the averaging calculation, which makes the product less risky. However, we show the resulting fair tuple for guaranteed rates $g \in [0.0\%, 2.4\%]$.

Figure 3.19: Fair (g,c)-tuple for P(ξ,a)GCPs and loss rate for the selected stylized P(q,a)GCPs

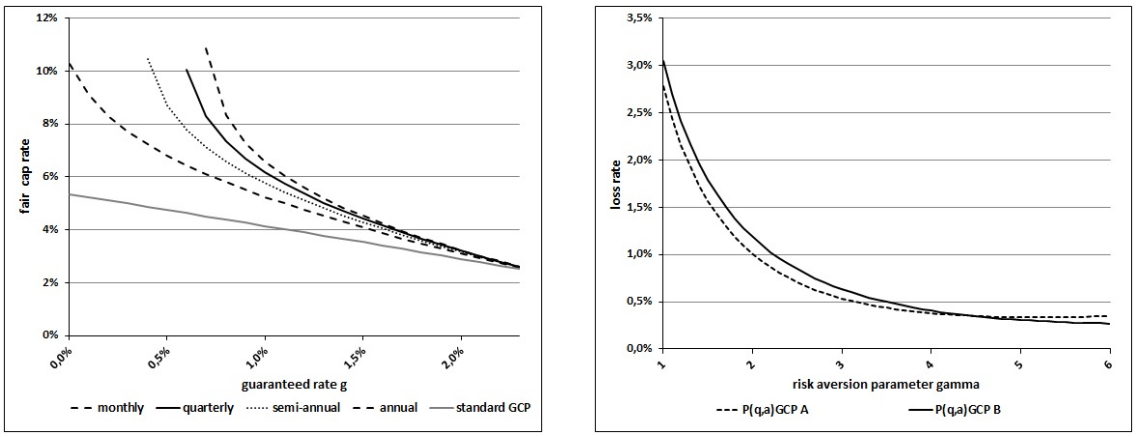

The fair (g,c)-tuple for general path-dependent products with guarantee and cap with an average return calculation (P(ξ,a)GCP) for varied observation period are illustrated (left plot). The resulting loss rates for the selected path-dependent stylized P(q,a)GCPs are shown for a risk aversion parameter of $\gamma \in [1,6]$ (right plot).

For a better overview, we integrate the corresponding (g,c)-tuple for the path-independent

GCP. It is seen that the fair cap rates are higher the shorter the observation period. Furthermore, we should mention that for a guaranteed rate of $g = 0.0$ % only P(a,a)GCP results a fair cap rate c.
Analogous to the path-independent GCP, we consider a selection regarding the quarterly observation. In particular, there are no fair (g,c)-tuple for $g = -10$ %, $g = -5$ % and $g = 0$ %. Thus, we concentrate on the following two products:
P(q,a)GCP A $= (0.6\%, 10.059\%)$, P(q,a)GCP B$= (1\%, 6.185\%)$.

The corresponding loss rates are shown in the right plot of Figure 3.19. Obviously, both products are suboptimal for investor Γ, since the loss rate is clearly above $l_T = 1.0$ %. However, P(q,a)GCP A and P(q,a)GCP B seems more suitable for investors with higher risk aversion.

In the following, we observe the case where investor Γ could adjust the relevant underlying asset to improve her utility. Thus, we observe P(q,a)GCP A with $g = 0.6$ % and calculated the fair cap rates as well as the loss rates depending on different level of volatility. Figure 3.20 shows the result.

Figure 3.20: Calculated loss rates for P(q,a)GCP A with varying underlying asset

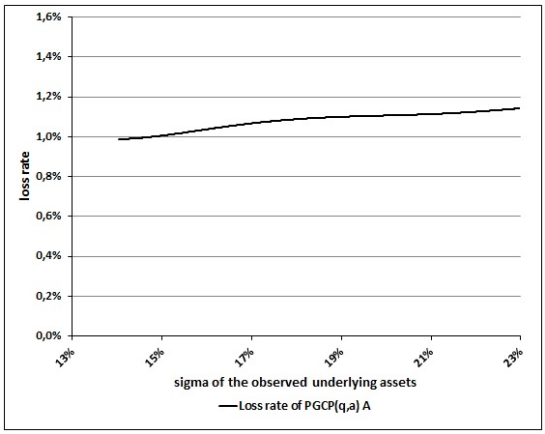

Calculated loss rate for the P(q,a)GCP with $g = 0.6$ % (P(q,a)GCP A) for different underlying assets resp. different volatility levels.

Interestingly, the loss rates rises for higher σ, which is somewhat surprising upon first glance. Note that the fair cap rates c are lower for higher volatility. Therefore, for the assumed guaranteed rate $g = 0.6$ %, there is no opportunity the from investor's Γ perspective to optimize her loss rate. However, we should mention that only a few product specification were available in this analysis. Especially, the missing lower guaranteed rate influences the

utility of the observed investor.

Path-dependent GCPs with minimum feature (P(ξ,m)GCPs)

Finally, we analyze (P(ξ,m)GCPs. The payoff depends on a minimum observation of the underlying asset until maturity. It holds that

$$P\left(\xi,m\right)GCP_T = G_T + h\left(G_T, V_T^{\rightarrow}\left(\xi,m\right)\right) - \hat{h}\left(C_T, V_T^{\rightarrow}\left(\xi,m\right)\right) \tag{3.57}$$

$$\begin{aligned} &\text{with } h\left(G_T, V_T^{\rightarrow}\left(\xi,m\right)\right) = \max\left\{0; V_T^{\rightarrow}\left(\xi,m\right) - G_T\right\} \\ &\hat{h}\left(C_T, V_T^{\rightarrow}\left(\xi,m\right)\right) = \max\left\{0; V_T^{\rightarrow}\left(\xi,m\right) - C_T\right\} \text{ and } V_T^{\rightarrow}\left(\xi,m\right) = \frac{V_T}{\min_{i=1,\ldots,n} V_{t_i}} \end{aligned} \tag{3.58}$$

where ξ defines the number of the relevant observation dates n. Now, Figure 3.21 shows the fair (g,c)-tuple for general P(ξ,m)GCPs and the resulting loss rates for a selection of P(q,m)GCPs with quarterly observation.

We restrict the illustration of the fair (g,c)-tuple on a range between $g = -2.0$ % and

Figure 3.21: Fair (g,c)-tuple for P(ξ,m)GCPs and loss rate for the selected stylized P(q,a)GCPs

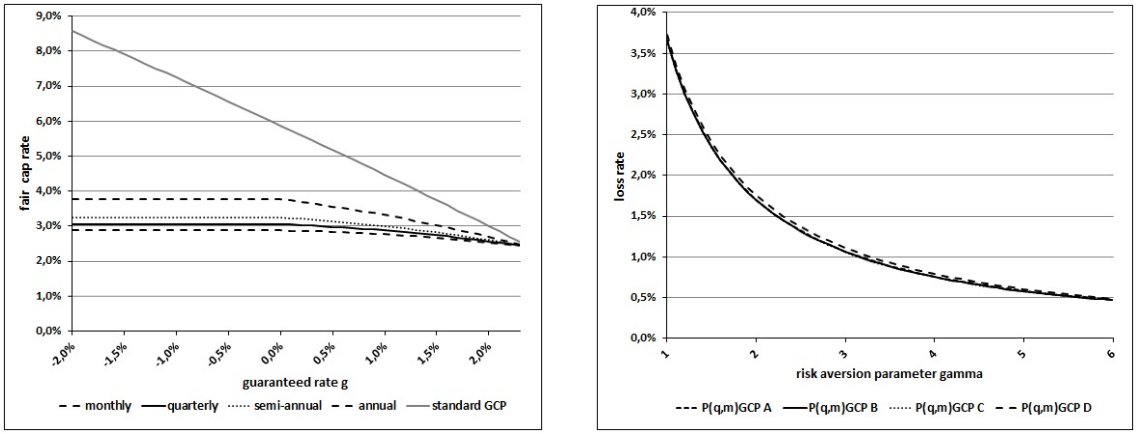

The fair (g,c)-tuple for general path-dependent product with guarantee and cap with a minimum return calculation (P(ξ,m)GCP) for varied observation period are illustrated (left plot). The resulting loss rates for the selected path-dependent stylized P(q,m)GCPs are shown for a risk aversion parameter of $\gamma \in [1,6]$ (right plot).

$g = -2.4$ % since the fair cap rates are constant for all lower guaranteed rates. Notice, this development is along the lines with the results calculated for P(ξ,m)GP. It is seen again

that shorter observation periods results in lower fair cap rates. As previously mentioned, for all guaranteed rates below $g = 0.0$ %, the fair cap rates are constant between $c = 2.872$ % and $c = 3.767$ % for all observation periods. For $g > 0.0$ % the fair cap rates decreasing with higher guaranteed rate.
The loss rate calculation in the left plot of Figure 3.21 relies on the following selection of P(q,m)GCPs:
P(q,m)GCP A= $(-10\%, 3.049\%)$, P(q,m)GCP B= $(-5\%, 3.049\%)$,
P(q,m)GCP C= $(0\%, 3.049\%)$ and P(q,m)GCP D= $(1\%, 2.881\%)$.

The selection uses the same guaranteed rates as the path-independent GCPs from the previous section. Therefore, the first three PGCPs have the same cap rate. It is evident that the calculate loss rates for P(q,m)GCP A, P(q,m)GCP B and P(q,m)GCP C lying upon each other. We see again that the observed investor would suffer from an investment in such a product. We identify a loss rate development which is comparable to the PGCP(q,a).

Furthermore, we analyze the loss rate for different underlying volatilities and the corresponding fair cap rates. This time, it results that the investor will suffer less if she chooses a more risk aversion underlying. Figure 3.22 shows a strictly increasing loss rate depending on the level of volatility. To explain the preference of investor Γ, we should highlight that the fair cap rates are lower for higher volatility.

Figure 3.22: Calculated loss rates for P(q,m)GCP C with varying underlying asset

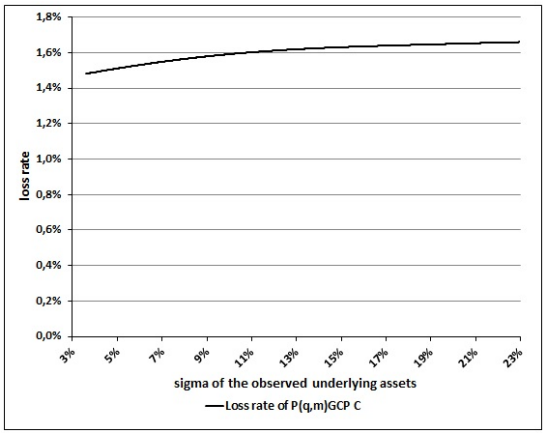

Calculated loss rate for the P(q,m)GCP with $g = 0.0$ % (P(q,m)GCP C) for different underlying assets resp. different volatility levels.

In summary, we ascertain that the analysis of path-dependence in combination with a

guarantee and a cap is complicated. For the averaging feature, we are unable to calculate fair cap rate for a negative guaranteed rate. Assuming the minimum calculation, we identify that the fair cap rate is more-or-less constant for lower guaranteed rate. However, the loss rates calculated for investor Γ are significantly higher than for the other path-dependent features.
Furthermore, the optimal adjustment of the underlying asset shows a differing result compared to the other path-dependent product. However, the observed investor would suffer if she selects an underlying asset with higher volatility.

3.7.4 Summary of the path-dependent products

In this section, we assume that the investor could only choose of the restrictd class of path-dependent products. However, we illustrate the characteristics of different path-dependent products. We show fair parameter combination for all products specification. We ascertain that no fair tuples are available for some product specifications. However, there are also specifications that result in constant parameter solutions. Both developments can be referred to the corresponding path-dependent calculation feature.
In addition, we calculate the corresponding loss rate for the assumed investor Γ who could only invest in the offered path-dependent products. We could summarize that investor Γ suffers from all analyzed path-dependent products. In comparison to the path-independent product, we cannot find any product specification resulting in a loss rate close to $l_T = 0.0\,\%$. Furthermore, we observe that the averaging and the minimum calculation influence the investor's utility regarding the optimal underlying asset. For PGP and PCP, it holds that an underlying asset with higher volatility will result in a lower loss rate. However, we should mention that the potential gain is margin. The loss rates seem to be dominated by the path-dependence of the product.
In addition, we should mention that for each feature, the chosen observation period has a subordinate role in the derivation of the fair tuple. The comparison of the different products and varied observation periods show that the structure is more important. As already mentioned, the important choice is not which path-dependent observation feature is selected, but rather whether a path-dependence is selected in the first place.

3.8 Analysis of the influence of embedded margin

In general, all products observed in Section 3.5, Section 3.6 and Section 3.7 are offered by a financial institution. Thus, we have to assume that they will not offer the product for free. We consider that the issuers offer the product at a price which is overvalued compared

to the arbitrage-free t_0-price (cf. Definition (2)). The difference is denoted as the margin M.

Of course, there are various components of an embedded margin in stylized products and structured stylized products. On the one hand, a part of the margin could be appropriate for the structuring and hedging of the product. On the other hand, an additional margin could be integrated in a product as a profit for the distribution unit.[26]

In the following, we will only concentrate on the influence of embedded margins on the investor's utility. Here, we assume that the financial market is complete from the perspective of the issuer. Thus, she can generate any payoff profile by dynamic trading in the basis assets. Furthermore, the issuer can offer unfair products to the retail investor. By contrast, we assume that the financial market is incomplete for the retail investor. She has to resort to a restricted class of products even the products include margins.
However, we assume that the embedded margin does not influence the issue price but the corresponding product specification offered at issue date. Without losing generality, we use the price $N = 1$ for each observed product.
First, we have a short look how a margin will influence a Constant-Mix strategy. Second, we observe some exemplary structured stylized product. Assuming an exogenous margin, we try to find out which adjustment of the product specification could be optimal for the investors.

For the further analysis, we assume a margin that is paid entirely at issue date, whereby the following holds

$$\hat{X}_{t_0}^{(gen)} + M^{(gen)} = 1 \text{ with } \hat{X}_{t_0}^{(gen)} < X_{t_0}^{(gen)} = 1 \tag{3.59}$$

where $M^{(gen)}$ describe the absolute margin of the corresponding product. $X_{t_0}^{(gen)}$ could be identified as a fair product specification and $\hat{X}_{t_0}^{(gen)}$ is the adjusted product such that equation (3.59) holds. We use the following three margin in our analysis: $M_1 = 1.0$ %, $M_1 = 2.0$ % and $M_1 = 3.0$ %.

26 A more detailed view concerning optional margins is given in Chapter 7, where we introduce a special calculation method to calculate and integrate margins.

3.8.1 Stylized products with embedded margin

We already mentioned that a Constant-Mix strategy is the optimal product for an expected CRRA utility maximizing investor. If an embedded margin is used in such a product, the initial investment in the strategy is lower than in the fair product design. However, we can calculate the corresponding certainty equivalent of the stylized product with an embedded margin by

$$CE_T^* = \hat{V}_0 e^{\left(r+\frac{1}{2\gamma}\left(\frac{\mu-r}{\sigma}\right)^2\right)T} \tag{3.60}$$

where $\hat{V}_0$ describes the reduced initial investment amount calculated by $\hat{V}_0 = V_0 - M_i$ with $i = \{1,2,3\}$. Figure 3.23 (left plot) shows that the development of the corresponding

Figure 3.23: Certainty equivalents and loss rates for a Constant-Mix strategy with an embedded margin

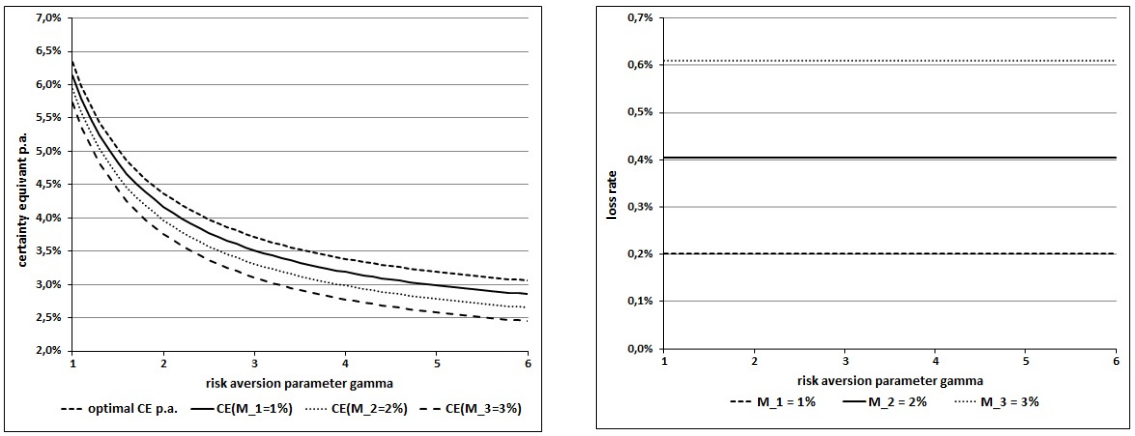

Calculated certainty equivalents (left plot) and loss rates (right plot) for the optimal Constant-Mix strategy rely on different risk aversion parameter assuming three embedded margins.

certainty equivalents are derived by a simple parallel swift of the optimal (margin-free) certainty equivalent. Recall that the CEs are calculated by (3.60). As a direct result, we identify that the corresponding loss rate are constant for all observed risk aversion parameter (cf. Figure 3.23 (right plot)).

Now, we consider investor Γ and the four selected stylized products illustrated in Section 3.5.

Figure 3.24: Calculated loss rates or selected stylized products with an embedded margin and derived loss rates by varying σ

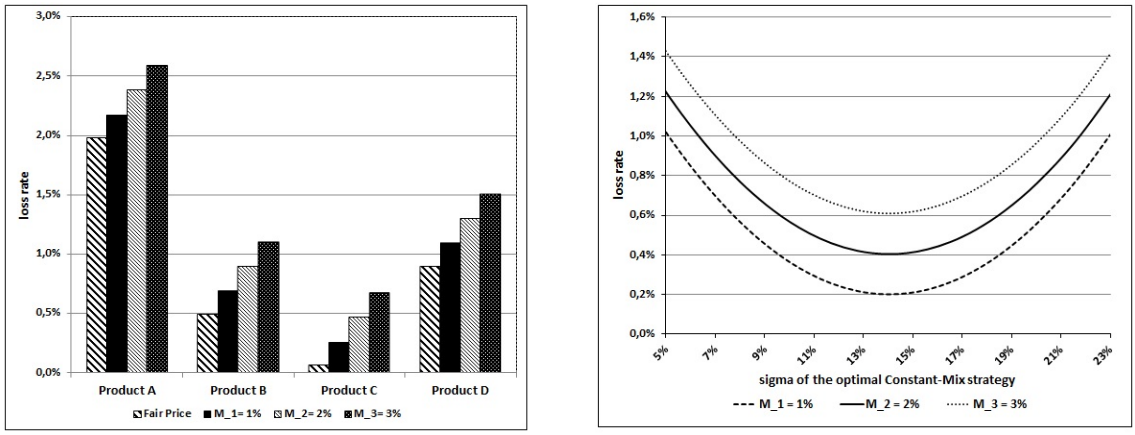

Calculated loss rates for the four selected stylized products for varying margin are illustrated in the left plot, while the calculated loss rate for the stylized products for different underlying assets resp. different volatility levels are illustrated in the right plot.

We already know from Section 3.5 that none of the selected stylized products is optimal for investor Γ. The loss rate calculated in the previous section is compared with the derived loss rates depend on the embedded margin M_i in the left plot of Figure 3.24. It is seen that the embedded margin could lead to a significantly higher loss rate for the observed investor Γ. Since the loss rate is proportional to the assumed margin, we should mention that the relative loss by the margin is higher if the fair stylized product has a low loss rate. This means for product C that the lowest assumed margin M_1 leads to an increase of the loss rate from $l_T = 0.06$ % to $l_T = 0.26$ % which is not less than a quadruplication. Regarding product B, we identify a loss rate that rises by about 40 % from $l_T = 0.49$ % to $l_T = 0.69$ %.
However, if we assume that different stylized products have varying margins, investor Γ will suffer less by investing in a more suboptimal product without an embedded margin (or with a low margin) rather than investing in the almost optimal product with a margin. Exemplary, this could the case, when we compare product C including M_3 with the fair product B. Here, the choose of product C will lead to a loss rate which is 0.19 % higher.

Finally, we calculated the loss rates for investor Γ regarding the volatility of the op-

timal investment strategy.[27] Thus, the right plot of Figure 3.24 is more-or-less a continuous representation of the left plot. Here, it is highlight how the influence of the embedded margin corresponds with the derivation of the volatility. Therefore, it is seen that an embedded margin of $M_1 = 1.0$ % will lead to a higher loss rate compare to the optimal Constant-Mix strategy (with $\sigma = 14.04$ %) with $M_2 = 2.0$ % if the volatility is lower than $\sigma = 9.5$ % or higher then $\sigma = 18.5$ %. It also results, if an investor must choose a suboptimal strategy, she is indifferent about selecting a strategy with 5 % higher or lower σ since the illustrated loss rate development is symmetric.

3.8.2 Structured stylized products with embedded margin

In this section, we illustrate how the product design of structured stylized products is changed by the embedded margin. Furthermore, we compare the calculated loss rates to the results based upon the fair product design. For the comparison, we use a specific description of the loss rate. We define

$$l_T = \frac{\ln\left(\frac{CE_T^*}{C\tilde{E}_T}\right)}{T} + \frac{\ln\left(\frac{C\tilde{E}_T}{CE_T^{\text{margin}}}\right)}{T} \tag{3.61}$$

where $C\tilde{E}_T$ describes the certainty equivalent of the a fair product $\mathrm{X}_t^{(\text{gen})}$[28], and CE_T^{margin} is the certainty equivalent of the corresponding product with an embedded margin. CE_T^* illustrates the certainty equivalent of the optimal Constant-Mix strategy.

With this definition, we are able to separate a loss rate depending on the specific structure of the product (loss rate by structure ($l_T^{(\text{structure})}$) and a loss rate owing to the embedded margin (loss rate by margin ($l_T^{(\text{margin})}$)). Thus, we can also analyze the influence of the assumed margin on the investor's utility.

Now, we make this analysis for some exemplary products. On the one hand, we observe the standard GP, which we analyzed in Section 3.6.3. On the other hand, we consider one of the path-dependent products. Thus, we focus on P(q,a)CP illustrated in Section 3.7.2. For both calculation we use $\eta \in \{M_1, M_2, M_3\}$.

27 Of course, it make no different if we use the proportion of risky asset or the volatility of the strategy since both parameter are proportional to each other. Thus, this calculation is analogous to the previous section.

28 In the first step, we define the corresponding fair product by using the same guaranteed rate resp. cap rate. Applying (3.38) finally results in the fair participation rate. The relevant certainty equivalent is calculated with (3.42).

3.8.3 Guaranteed products with embedded margin

First, we want to illustrate the influence by an embedded margin on the (g,α)-tuple. Thus, we let the guaranteed rate remain unchanged and calculate the participation rates that result in an embedded margin. Second, we use the assumed guaranteed rates from Section 3.6.3 to make a selection of four structured stylized guarantee products with embedded margins. For this calculation of the loss rates, we use M_2.

We illustrate the corresponding (g,α)-tuple relying on the defined margin and compare them to the fair (g,α)-tuple in Figure 3.25 (left plot). The development of the adjusted

Figure 3.25: Calculated (g,α)-tuple for GP(η)s with an embedded margin and loss rates for selected stylized GP(M_2)s

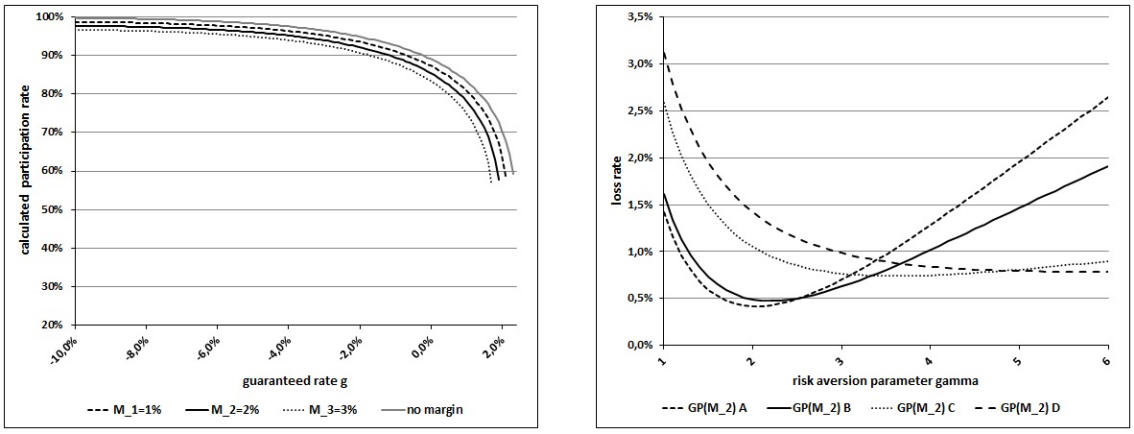

The calculated (g,α)-tuple for general guarantee products with an embedded margin (GP(η)s) for varied margin rates are illustrated (left plot). The resulting loss rates for the selected GP(M_2)s are shown for a risk aversion parameter of $\gamma \in [1,6]$ (right plot).

participation rates is unsurprising. For all guaranteed rates, we recognize that the participation rate decreases with higher margins. Depending on the level of the margin, we cannot calculated a participation rate for very high guaranteed rates. Of course, this problem will occur if the sum of the t_0-price of the guarantee amount $G_T = e^{gT}$ and the margin M is above the nominal amount of $N = 1$.

Now, we focus on the selected GPs with a margin of $M_2 = 2.0$ %. Thus, we use the adjusted stylized products:

GP(M_2) A = $(-10\%, 97.752\%)$, GP(M_2) B = $(-5\%, 96.083\%)$,
GP(M_2) C = $(0\%, 85.432\%)$ and GP(M_2) D = $(1\%, 78.111\%)$.

Looking at the right plot of Figure 3.25, we identify a development comparable to the loss rates of guarantee products without margin. The lower the guaranteed rate, the lower the loss rate for investor Γ. Nevertheless, the illustrated loss rates seem to result from a parallel shift, which depends on the margin. Exemplary, GP(M_2) A and GP(M_2) B results in a loss rate of $l_T = 0.41$ % and $l_T = 0.49$ % for the observed investor Γ while the corresponding loss rates for GP A and GP B are $l_T = 0.01$ % and $l_T = 0.08$ %.
However, we can calculated the separated loss rate $l_T^{(\text{structure})}$ and $l_T^{(\text{margin})}$ using (3.61). If

Figure 3.26: Separation of the loss rate for the selected stylized GP(M_2)s

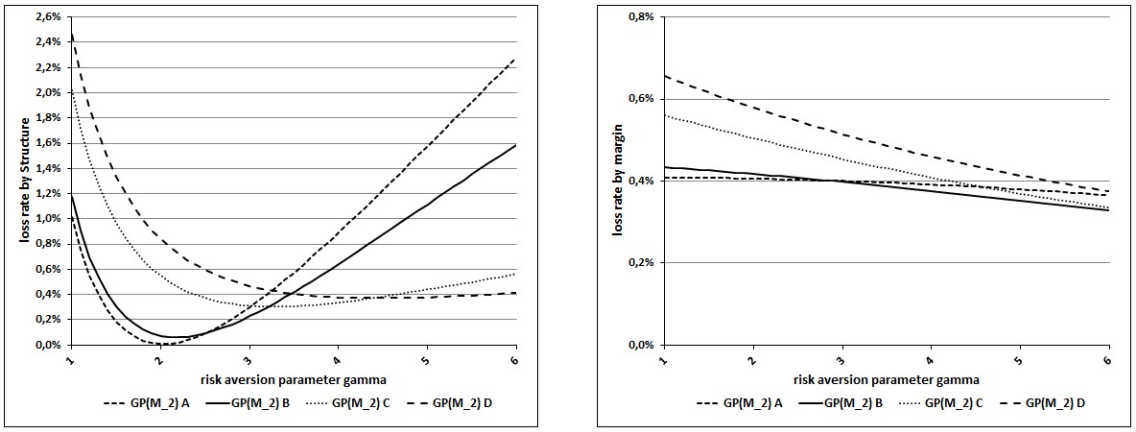

The loss rate by structure (left plot) and the loss rate by margin (right plot) is illustrated for the selected GP with an embedded margin $M_2 = 2.0$ %.

we analyze the separated loss rates shown in Figure 3.26 from the perspective of investor Γ we will ascertain that the margin has a different relative influence on the loss rate.
In the left plot of Figure 3.26, the loss rate by structure $l_T^{(\text{structure})}$ is illustrated. Recall, $l_T^{(\text{structure})}$ is identical to the overall loss rate in the case of fair products (cf. Figure 3.5). A more surprising result is seen in the right plot of Figure 3.26. The development of $l_T^{(\text{margin})}$ does not result of a parallel shift.
For investor Γ holds, the smaller $l_T^{(\text{structure})}$ the smaller is $l_T^{(\text{margin})}$ for the corresponding GPs. More precise, it results that $l_T^{(\text{margin})}$ for GP(M_2) A and GP(M_2) B are significantly lower than the loss rates by margin of GP(M_2) C and GP(M_2) D, which is the same development observed of $l_T^{(\text{structure})}$.

However, all loss rates by margin are decreasing with higher risk aversion parameter. Therefore, the observed development for investor Γ cannot transfer to investor with dissenting risk aversion. The results can be explained by the unchanged guaranteed rate. Since only the participation rate is reduced by the embedded margin the ratio of the component responsible for the guaranteed amount rises. Of course, more risk aversion investor suffer less than the observed investor Γ for this adjustment.

Now, we try to ascertain whether a better product adjustment exists from the investor's perspective when we allow adjusting the participation rate α and the guaranteed rate g. First, we observed all possible (g,α) of GP(η) C and calculate the corresponding loss rate. Second, we make the additional assumption that the relevant margin will not result in a better guarantee rate resp. participation rate for GP(η) C. Technically, we start with the fair (g,α)-tuple of GP C. Then, we calculate all possible combination of $(\bar{g}, \bar{\alpha})$ with $\bar{g} \leq g$ and $\bar{\alpha} \leq \alpha$.
Remember, investor Γ suffer from investing in the fair GP C with a utility loss of $l_T = 0.55$ %.
In the left plot of Figure 3.27 it is illustrated that investor Γ has the lowest utility loss

Figure 3.27: Calculated loss rates for GP(η) C regarding different parameter adjustments

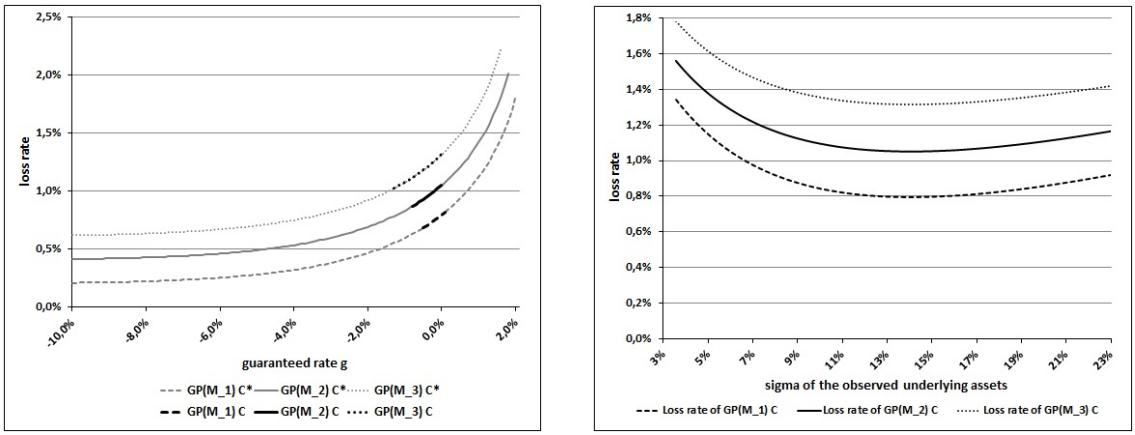

Calculated loss rate for the GP(η) C for different parameter adjustments methods (left plot). Calculated loss rate for different underlying assets resp. different volatility levels (right plot).

if only the guaranteed rate is changed. This development holds for both observation. We denote the products result by an adjustment without the constraint with GP* and simply GP otherwise. With the constraint $\bar{g} \leq g$ and $\bar{\alpha} \leq \alpha$. The minimum loss rates are between

$l_T = 0.685$ % and $l_T = 1.023$ %. Of course, the investor's utility loss is significantly lower if we reject the constraint. Then, the loss rate is on average 0.45 % lower. This calculation shows that an issuer has different possibility to make a product look attractive although it is offered for an unfair price.

Finally, we repeat the analysis relying on the underlying assets. Focusing on GP(η) C with fixed guaranteed rate $g = 0.0$ % we have a look if a more risk averse or a more risk seeking underlying asset can optimize investor Γ utility. The answer is along the line with Proportion 2 where the optimal strategy with guarantee is introduced. We can withdraw from Figure 3.27 (right plot) that we always find the minimal loss rate for investor Γ when we use the optimal underlying asset V_t.

3.8.4 Path-dependent Capped Products with averaging feature and embedded margin

In a last step, we repeat to observation from Section 3.8.3 for a PCPs with averaging feature. We assume the margin M_1, M_2 and M_3 from the previous analysis. We denote the observed product family with P(q,a)CP(η). In comparison to the observed GPs with an embedded margin, we use the parameter from Section 3.7.2 to calculate the corresponding products. Here, we use the following cap rates: $c_{\mathrm{A}} = 3.0$ %, $c_{\mathrm{B}} = 7.0$ %, $c_{\mathrm{C}} = 10.0$ % and $c_{\mathrm{D}} = 15.0$ %. In particular, we only adjust the participation rate α and let the assumed cap rates unchanged.
The complete development of the adjusted participation rates is illustrated in the left plot of Figure 3.28. The swift of the calculated (c,α)-tuple (left plot of Figure 3.28) is unsurprising, given that the calculated participation rates are lower for higher embedded margins. The development whereby the α decreases for higher cap rates has already been identified.
In opposite to the guarantee product with an embedded margin (GP(η)), all assumed cap rates provide tuples that could be offered. Of course, this results from the missing guarantee amount, which could be an expensive component of the product.

We now consider the right plot of Figure 3.28. We illustrate four selected path-dependent CPs where the average calculation refers to a quarterly observation period. All products imply the margin $M_2 = 2.0$ %. Analogous to GP(η), the development is comparable to the illustration in Figure 3.15. Again, the loss rate seems to be shifted by the embedded margin.
Thus, it is meaningful to consider the separated loss rate defined by (3.61). The separated

Figure 3.28: Calculated (c,α)-tuple for P(q,a)CP(η)s with an embedded margin and loss rates for selected stylized P(q,a)CP(M_2)s

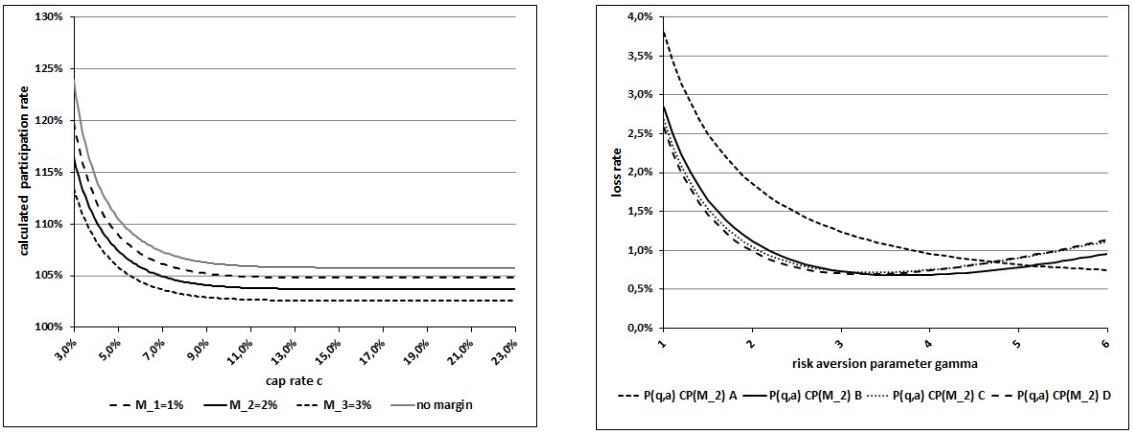

The calculated (c,α)-tuple for general path-dependent capped products with an averaging feature and an embedded margin (P(q,a)CP(η)s) for varied margin rates are illustrated (left plot). The resulting loss rates for the selected P(q,a)CP(M_2)s are shown for a risk aversion parameter of $\gamma \in [1,6]$ (right plot).

loss rates are shown in Figure 3.29. Of course, the loss rate by structure is identical to the P(q,a)CP with fair product design. Focusing on investor Γ, we identify in the right plot that the product with the highest $l_T^{(\text{structure})}$ leads to lower $l_T^{(\text{margin})}$. This development is in contract to the observation of GP(η). This result from our adjustment method, since we leave the cap rate unchanged.

In the following, we will allow an adjustment of the participation rate α and the cap rate c. For this observation we focus on P(q,a)CP(η) B. The calculation is analogous to Section 3.8.3. First, we consider the fair (c,α)-tuple. Second, we assume the margins and calculate the corresponding loss rates depending on the possible combination of α and c. Finally, we make the following constraint, so that only ($\bar{c}$,$\bar{\alpha}$)-tuple are allowed with $\bar{c} \leq c$ and $\bar{\alpha} \leq \alpha$. The left plot of Figure 3.30 show the results. The loss rates based upon the restriction are illustrated within the black graph. Here, we identify a minimum loss rate between $l_T = 0.947$ % and $l_T = 1.347$ %, which all result from an unchanged cap rate. Without the constraint the loss rate lie in a range of $l_T = 0.780$ % and $l_T = 1.217$ % illustrated by the gray graphs (e.g. P(q,a)CP(M_1) B). It holds that the loss rate for investor Γ investing in the fair product is $l_T = 0.746$ %. Thus, the influence of the lowest margin cannot compensate by a permissible adjustment of the product specification.

Figure 3.29: Separation of the loss rates for the selected stylized P(q,a)CP(M_2)s

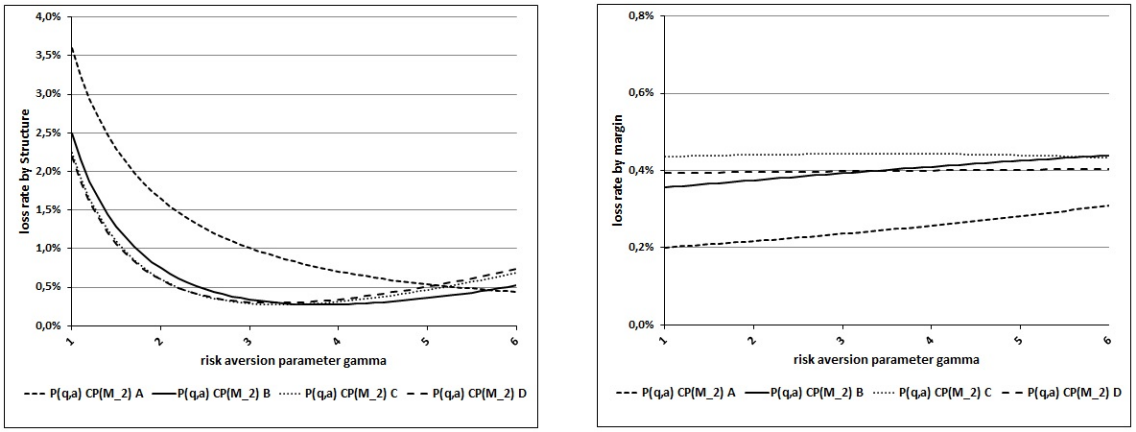

The loss rate by structure (left plot) and the loss rate by margin (right plot) is illustrated for the selected P(q,a)CP(M_2) with an embedded margin $M_2 = 2.0$ %.

In the observation of the fair product design, we ascertain that the observed investor would profit by choosing a more risky underlying asset. The same development holds if we assume an embedded margin. The result is illustrated in Figure 3.30 (right plot). It is seen that the minimum loss rates are calculated for $\sigma = 20$ %. However, the investor's gain is again bounded. According to the assumed margin, she could lower her loss rate on average by 0.06 %.

In this section, we analyze the influence of an embedded margin on the product specification as well as the investor's utility who is restricted on the class of products with an embedded margin. Observing the stylized products, a parallel swift is identified, whereby the calculated loss rates are equal for all illustrated risk aversion parameters. However, investor Γ could profit from an investment in a suboptimal stylized product if the corresponding embedded margin is significant lower than in the most optimal stylized product. Nevertheless, if we assume a fixed margin, the optimal stylized product will be always the same.
In addition, we focus on two exemplary structured stylized products and derive separated loss rates relying on the structure of the product as well as the embedded margin. For the GP, it holds that the higher $l_T^{(\text{structure})}$, the higher that $l_T^{(\text{margin})}$ is. The development regarding the path-dependent CP is in opposite, although this could due to our adjustment method, since we only calculate a suitable participation rate for both products.

Figure 3.30: Calculated loss rates for P(q,a)CP(η) B regarding different parameter adjustments

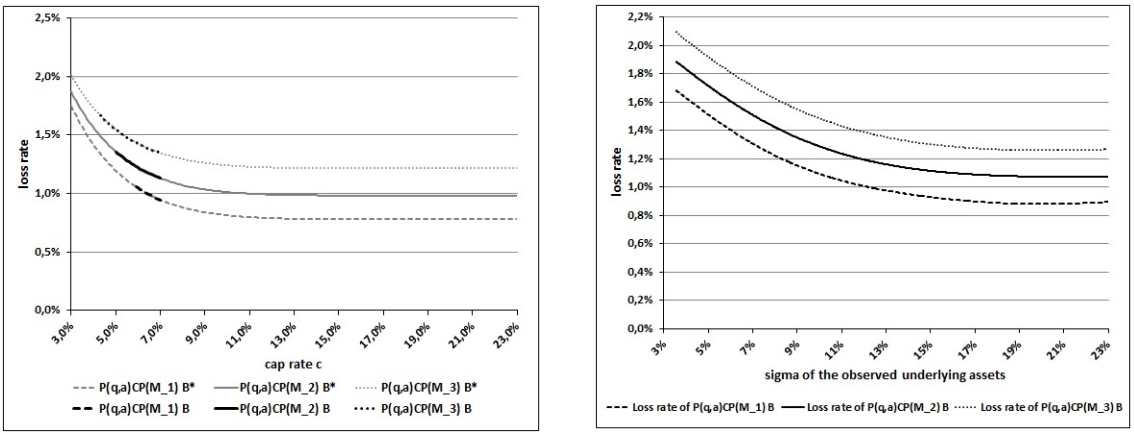

Calculated loss rate for the P(q,a)CP(η) B for different parameter adjustments methods (left plot). Calculated loss rate for different underlying assets resp. different volatility levels (right plot).

Furthermore, we distinguish two alternative method for the adjustment of the product parameter. It is seen that a variation of the relevant product parameter could significantly reduce the loss rate.

3.9 Conclusion

In this chapter, we analyze different sources of suboptimality regarding stylized products as well as on structured stylized products.

For the reason, we assume complete market conditions for the issuer of the products. In a Black and Scholes model setup, we assume that the issuer can generate any payoff profile by dynamic trading. In principle, the product provider could offer an "overall" optimal product to the retail investor.

By contrast, we assume an incomplete financial market from the investor's perspective. She has to resort to a restricted class of products since she cannot generate her optimal product through a dynamic trading strategy.

However, the optimal choice of an offered product will generally differ from the theoretically overall optimal product for the investor. Thus, we can analyze and quantify the suboptimality of the offered retail products.

The main focus in the observation of stylized products is the problem of disposability of the optimal product. Even if an investor knows her overall optimal product, she would suffer a utility loss if the offerings do not suit to her preference. We show that the loss rate could be almost zero when a suitable stylized product is offered. Otherwise, the observed investor suffers by the suboptimality of the product with a loss rate of at least $l_T = 0.27$ %. However, the minimum loss rate will be significantly higher if a lower number of products are offered. Thus, it is illustrated that the loss rates strongly depend on the number of observed products.

The analysis of the structured stylized products takes into account further sources of suboptimality. To obtain a lower loss rate, the investor has to choose products for which the payoff distribution is close to the optimal Constant-Mix strategy. Of course, this is only possible for the structured stylized products without a path-dependent feature. Thus, we find the corresponding product specification (very low guaranteed rates (GP) for very high cap rates (CP) or a combination of both (GCP)), which leads to a loss rate of almost zero. In general, the investor will suffer from any additional feature by a loss rate of e.g. $l_T = 0.42$ % for a GP.
In the case of a structured stylized product with a guarantee and cap, we show that a variation of the optimal underlying asset can gain the investor's utility. However, this is not possible for the guarantee or the capped products.

The loss rates for the observed investor who has to choose a path-dependent stylized product are always above $l_T = 0.5$ % for all path-dependent products. The more additional features that are assumed, the higher the resulting loss rates. Thus, the highest losses are observed for the path-dependent products with guarantee and cap. The averaging feature leads to a loss rate of 1.0 % while all GCP with minimum calculation features leads to a loss of at least $l_T = 1.7$ %.

Finally, we give an overview of the suboptimality forced by margins. Of course, there will be no optimal product if the issuer uses an embedded margin. However, investor Γ could benefit from an investment in a suboptimal stylized product. This could be the case if the corresponding embedded margin is significantly lower than in the most suitable stylized product. The separation of the loss rate into the loss rate by structure and the loss rate by margin shows the following. On the one hand, we identify that the development of the loss rate by structure is more-or-less identical to the overall loss rate. This explains the notion

that the suboptimal product design generally has greater influence on the investor's loss rate than an embedded margin.
On the other hand, we cannot identify a clear development of the loss rate by margin. For the GP, the loss rate by margin is proportional to the loss rate by structure. However, assuming a path-dependent CP, the development stands in contrast.

CHAPTER 4

Best Garant Certificates–Is best entry really better?

4.1 Introduction

Recently, increasingly more structured products are being offered that give an upward participation on the return of an underlying while simultaneously granting a guarantee. Our main focus is on products that are also advertised by granting a special return feature. Here, the benchmark return of the underlying is not measured in terms of the initial price of the underlying; instead, the entry price is determined according to the minimum (or average) price based upon some observation period.[1] These certificates are called Best Garant Certificates (including Best-In and Best-Entry Garant Certificates), which belong to the family of Garant Certificates. The underlying of a Best Garant Certificate is normally an equity index; for example, traded Best Garant Certificates are written on DJ Euro Stoxx 50.

The protection feature usually refers to the nominal amount of the certificate. The Best Garant Certificate's payoff is floored by the nominal amount, regardless of how the underlying evolves during the investment horizon.[2] In addition, the investor participates in the excess return of the underlying. A special feature is given by determining the excess return with respect to a *best* (resp. minimum) entry or average entry price. In the case of the best-entry price, the return is measured in terms of the quotient implied by the terminal price of the underlying and the minimum price of the underlying with respect to some observation period. Alternatively, there are also variants of Best Garant Certificates

1 Typically, the length of the observation period is between three and six months, where the price of the underlying is observed weekly or monthly. The length of the investment horizon varies between three and year years.

2 More precisely, this is only true if we do not take into account default risk, i.e. the nominal guarantee only prevails if the issuer remains solvent at maturity.

in which the return is measured with respect to the average price determined during the observation period.
However, neither the guarantee nor the additional feature in form of the *entry strike* come for free; indeed, the investor pays an implicit premium by giving up some of her upward participation, i.e. the payoff is also capped. In particular, the return of the underlying (the upward participation) is capped at a rate c, which is higher than the guaranteed rate g. In summary, the payoff of a Best Garant Certificate is specified in terms of the observation period $\underline{T}^{\text{obs}}$ (with last observation date t_N), the contract horizon T with $T > t_N$, the guaranteed rate g and the cap rate c with $c > g$. In addition, the contract also specifies how the entry strike is determined, whereby we distinguish between a fixed strike $K^{(\text{fix})}$, average strike $K^{(\text{ave})}$ and minimum strike $K^{(\text{min})}$ setting.[3]

Obviously, the contract value with an average entry strike $K^{(\text{ave})}$ is - ceteris paribus - lower than that implied with a minimum strike $K^{(\text{min})}$ ($K^{(\text{min})} \leq K^{(\text{ave})}$), since the price of a call option increases with the lower strike. Independent of the model assumptions, the value of a Best Garant Certificate increases with the guaranteed rate g, although it decreases with the cap rate c.
We call a contract fair if the initial value of the payoff coincides with the nominal value. In general, this implies that the lower the fair cap rate c^*, the higher the value of the guarantee (the higher g) and the higher the value of the entry feature.

Our main contributions are as follows. We derive and analyze fair combinations of guaranteed and cap rates in a Black and Scholes and a Heston model setup. For this reason, we assume that the financial market is complete for the issuer. More precisely, the issuer can generate any payoff profile by a dynamic strategy in the risky and risk-free assets. Thus, all fair BGC contracts can be replicated by the issuer. Based upon the observation that both an entry price - that tends to be lower - and a higher guaranteed rate afford a lower (fair) cap rate, the *best* entry strike does not necessarily improve the return distribution of the Best Garant Certificate in the context of fair contracts. Therefore, we consider the question of whether an investor benefits from the best-entry strike setting and the guarantee. Here, we assume incomplete market conditions for the investor. The investor cannot trade dynamically in the two assets. Moreover, she has to choose one of the BGCs offered by the issuer. We analyze the optimality (suboptimality) of the entry strike setting

3 Unless otherwise mentioned, the nominal value is set equal to one, i.e. $N = 1$.

and the overall product design for an expected utility maximizing CRRA investor. Interestingly, it emerges that a Best Garant investor does not necessarily suffer from a higher guaranteed rate. In the case of a fair cap rate, the utility of a BGC increases with the guaranteed rate for small guaranteed rates but decreases after some (optimal) guarantee level. In addition, we show that the *best* entry feature, i.e. the minimum strike setting and the average strike setting, are suboptimal compared to the fixed strike setting for low guaranteed rates. We illustrate our results by means of real market data. We consider the model prices at issue date and loss rates that are implied by traded BGCs. It is observed that all certificates are undervalued at their issue date, which could result from our assumed parameter.[4] In addition, we use a special loss rate calculation and find that some certificates are inefficient for the CRRA investor, despite being issued below their fair model price.

Note that the BGC can also be interpreted as a bullish vertical spread that comprises a long position and a short position of a (plain vanilla) call option.[5] The strike of the long call is lower than the strike of the short call. For a fixed strike setting, we can thus rely on closed-form call price formula in the case of the Black and Scholes model and quasi closed-form solutions in the case of the Heston model. However, for the minimum and average strike setting, the best-entry feature implies that the strikes of the BGC depend upon the asset prices during the observation period. Therefore, the values of the Best Garant Certificates (the fair cap rates, respectively) depend upon the joint distribution of the asset prices during the observation period and the terminal asset price. Regarding the Black and Scholes model, the joint distribution can be stated in closed form for the minimum price setting.[6] By contrast, this is not possible for the average price setting. Even in the case of a simple Black and Scholes model setup, the pricing affords numerical methods. If necessary, we use Monte Carlo simulations to determine the model prices.

Older empirical studies always find a huge overvaluation of the traded structured products, which has changed in more recent literature. We believe that these results form a more

4 The undervaluation can also result by the assumption that we do not take into account default risk; cf. Chapter 6.

5 In particular, the payoff structure is mixed in the sense that the payoff is neither a convex nor a concave function regarding all terminal asset prices. Consequently, the value of a fixed strike Best Garant Certificate is not monotonous in the volatility of the underlying.

6 More precisely, the joint distribution is well known in the case of a continuous asset price monitoring. However, there are also recent works on quasi closed–form solutions for the joint densities in the case of discrete–time monitoring, cf. for example Fusai et al. [Fus06].

competitive market, where the margins for the issuers are significant lower. However, the assumption of the relevant realistic parameter has a strong influence. An overview of the relating literatur is given in Section 2.2.

The remainder of the chapter is organized as follows. In Section 4.2.1, the payoff structure of Best Garant Certificates - including the fixed strike, average strike and minimum strike settings - is stated. In Section 4.2.2, we consider the pricing of Best Garant Certificates with a fixed, average and minimum strike setting regarding a Black and Scholes model setup. In Section 4.2.3, we provide a brief summary about the Heston model used to price the Best Garant Certificate when taking into account stochastic volatility. The assumed market data are summarized in Section 4.3.1. Sections 4.3.2 and 4.3.3 focus on the return distributions of the BGCs in the Black and Scholes and the Heston model. The CRRA investor's perspective is illustrated in Sections 4.3.4 and 4.3.5. Illustrative results based upon market prices can be found in Section 4.4, before Section 4.5 concludes the chapter.

4.2 Product specification and pricing of fair contracts

4.2.1 Product specification

As mentioned in the introduction, the payoff of a Best Garant Certificate is specified in terms of the observation period $\underline{T}^{\text{obs}}$ (with last observation date t_N), the contract horizon T ($T > t_N$), the guaranteed rate g and the cap rate c ($c > g$). The guaranteed rate and the cap rate prevail regarding the nominal contract amount N. At T, the investor receives a payoff at least equal to the guaranteed amount Ne^{gT}. However, she does not receive a payoff higher than the maximal amount Ne^{cT} ($c > g$). The entry strike is determined according to an observation period, which is denoted by $\underline{T}^{\text{obs}}$, where

$$\underline{T}^{\text{obs}} = \{t_0 = 0 < t_1 \ldots < t_N\} \tag{4.1}$$

and $t_N < T$. In the following, we consider three possibilities concerning how the entry strike is determined, i.e. we distinguish between a fixed strike $K^{(\text{fix})}$, average strike $K^{(\text{ave})}$

and minimum strike $K^{(\min)}$ setting. In particular, we use the conventions

$$K^{(\text{fix})} := K^* > 0 \tag{4.2}$$

$$K^{(\text{ave})} := \frac{1}{N+1}\sum_{i=0}^{N} S_{t_i} \tag{4.3}$$

$$\text{and } K^{(\min)} := \min_{i=0,\ldots,N} S_{t_i} \tag{4.4}$$

where S_{t_i} denotes the price of the underlying at time t_i ($t_i \in [0,t_N]$). For the sake of simplicity, we normalize $S_{t_0} = 1$.

Definition 6 (Payoff of Best Garant Certificate) *The payoff of a Best Garant Certificate with a nominal amount N, observation period $\underline{T}^{obs}$, maturity T, guaranteed rate g and cap rate c ($c \geq g$) is given by*

$$h(S_{t_0},\ldots,S_{t_N},S_T) = N\left(e^{gT} + \left[\frac{S_T}{K^{(w)}} - e^{gT}\right]^+ - \left[\frac{S_T}{K^{(w)}} - e^{cT}\right]^+\right) \tag{4.5}$$

where $w \in \{fix, ave, min\}$.

Unless otherwise mentioned, we set $N = 1$. A contract is called fair if

$$1 = PV_{t_0,T}\left(e^{gT} + \left[\frac{S_T}{K^{(w)}} - e^{gT}\right]^+ - \left[\frac{S_T}{K^{(w)}} - e^{cT}\right]^+\right) \tag{4.6}$$

where $PV_{t_0,T}(.)$ denotes the arbitrage free t_0–value of a payoff received at time T.
Thus, a tuple (g^*,c^*) of a guaranteed and cap rate that satisfies condition (4.6) defines a fair contract. Under the assumption that the interest rate r is a constant, we immediately obtain that $g^* \leq r$. In particular, $g^* = r$ also implies $c^* = r$. In addition, observe that the payoff (4.5) is increasing in g and decreasing in c. Pricing by no arbitrage immediately implies that for $g < r$ there exists a $c^*(g) > g$ such that the contract is fair in the sense of (4.6). It is also obvious that for two fair tuples (g_1^*,c_1^*) and (g_2^*,c_2^*) with $g_1^* < g_2^*$, it holds that $c_1^* > c_2^*$. However, the functional form $c^*(g)$ depends upon the assumed pricing model.

4.2.2 Pricing in the Black and Scholes model

For simplicity, we first assume a Black and Scholes model setup with no dividends. The pricing in a stochastic model setup is straightforward and is subsequently described regarding a Heston model setup.

Under the Black and Scholes assumptions, the price of the underlying S_t satisfies the stochastic differential equation

$$dS_t = \mu S_t dt + \sigma S_t dW_t, \tag{4.7}$$

where $\{W_t\}_{0\leq t\leq T}$ is a standard Brownian motion under the real world measure P. Note that equation (4.7) implies that the dynamics of the stock prices under the risk-neutral measure P^* are[7]

$$dS_t = rS_t dt + \sigma S_t dW_t^* \tag{4.8}$$

where $\{W_t^*\}_{0\leq t\leq T}$ is a standard Brownian motion under the equivalent martingale measure P^*.

Proposition 4 (Pricing) *For an entry strike setting $K^{(w)}$ where $w \in \{fix, ave, min\}$, the no–arbitrage t_0–price of the Best Garant Certificate (BGC) is given by*

$$\begin{aligned} BGC_{t_0}^{(w)} &= e^{(g-r)T} \\ &\quad + e^{-rt_N} E_* \left[\frac{1}{K^{(w)}} \left(\mathcal{B}^{Call}\left(S_{t_N},t_N,r,e^{gT}K^{(w)},T\right) - \mathcal{B}^{Call}\left(S_{t_N},t_N,r,e^{cT}K^{(w)},T\right)\right)\right] \end{aligned} \tag{4.9}$$

$\mathcal{B}^{Call}(S_t,t,r,K,T)$ denotes the t–price of a European call–option with underlying S, maturity T and strike K, i.e.

$$\begin{aligned} &\mathcal{B}^{Call}(S_t,t,r,K,T) \\ =&S_t\mathcal{N}\left(h^{(1)}\left(t,\frac{S_t}{e^{-r(T-t)}K}\right)\right) - e^{-r(T-t)}K\mathcal{N}\left(h^{(2)}\left(t,\frac{S_t}{e^{-r(T-t)}K}\right)\right) \end{aligned} \tag{4.10}$$

$\mathcal{N}(.)$ denotes the one–dimensional cumulative distribution function of the standard normal distribution and

$$h^{(1)}(t,z) := \frac{\ln z + \frac{1}{2}\sigma^2(T-t)}{\sigma\sqrt{T-t}},\ h^{(2)}(t,z) := h^{(1)}(t,z) - \sigma\sqrt{T-t} \tag{4.11}$$

Proof 4 *The proof is given in the appendix, cf. Appendix B.1.*

The above proposition states that the price of a BGC is given by the expected discounted (over the observation period) value of the price difference between a call with strike $K_1 = e^{gT}K^{(w)}$ and a call with strike $K_2 = e^{cT}K^{(w)}$. Intuitively, this is obvious: The entry

7 cf. Harrison et al. [Har79] and Harison et al. [Har81]

strike is known if the observation period is over. Subsequently, the payoff of the BGC is given by the payoff of a *bullish vertical spread*, i.e. the payoff of a portfolio comprising a long position in a call option and a short position in a call option with a higher strike.

In particular, we do not need the outer expectation in the case of a fixed strike setting, i.e. for $w = \text{fix}$, we simply have $K^{(\text{fix})} = K^*$ and $t_N = t_0$ with

$$BGC_{t_0}^{(\text{fix})} = e^{(g-r)T} + \frac{1}{K^*}\left(\mathcal{B}^{\text{Call}}\left(S_{t_0},t_0,r,e^{gT}K^*,T\right) - \mathcal{B}^{\text{Call}}\left(S_{t_0},t_0,r,e^{cT}K^*,T\right)\right)$$

Using condition (4.6) gives the fair tuples (g,c). These are illustrated in Figure 4.1 for

Figure 4.1: Fair (g,c)–tuple for fixed strike setting

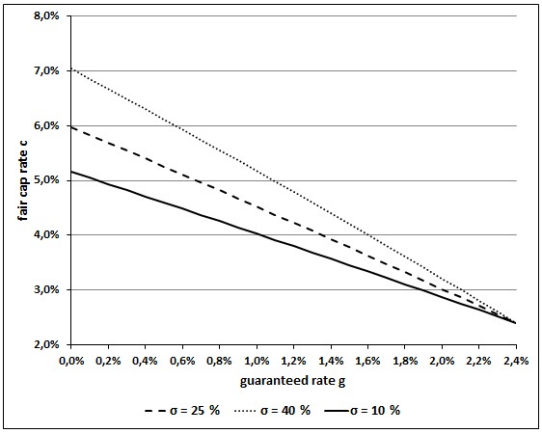

Fair (g,c)-tuple for three different volatility levels. The time to maturity of the BGC is $T = 5$ years, while the interest rate is $r = 2.4$ %.

$K^{(\text{fix})} = S_{t_0} = 1$ and for different levels of volatility. The time to maturity of the BGC is $T = 5$ years, while the interest rate is $r = 2.4$ %. Observe that the fair cap level c^* - independent from the assumed volatility - decreases with the guaranteed rate g. Recall that a lower cap rate means that the payoff is capped *earlier*, i.e. the payoff becomes cheaper. Thus, to compensate for a higher guarantee, we have to lower the cap level. In addition, recall that the bullish vertical spread comprises a long call and a short call, both of which increase with the volatility. The direction of the overall effect of the volatility on the BGC price (and on the fair contract tuples) is ambiguous. In our setup, the fair cap rates are higher the higher the volatility is, i.e. the concave part of the payoff profile dominates.

In order to calculate the t_0–price regarding the minimum strike and the average strike, we need the joint distribution of S_{t_N} and $\min_{i=0,\dots,N} S_{t_i}$ and $\frac{1}{N+1}\sum_{i=0}^{N} S_{t_i}$, respectively. For $w = \min$, Proposition 4 immediately gives

$$BGC_{t_0}^{(\min)} = e^{(g-r)T} + \int_0^\infty \int_0^\infty \frac{e^{-rt_N}}{x} \left(\mathcal{B}^{\text{Call}}\left(y,t_N,r,e^{gT}x,T\right) - \mathcal{B}^{\text{Call}}\left(y,t_N,r,e^{cT}x,T\right) \right) f^{(\min)}(x,y)\, dx\, dy$$

where $f^{(\min)}(x,y)$ denotes the joint density function for $K^{(\min)} = \min\{S_{t_0},\dots,S_{t_N}\} = x$ and $S_{t_N} = y$. In the case of the Black and Scholes model and continuous asset price observations, the density $f^{(\min)}$ is well known, i.e.[8]

$$f^{(\min)}(x,y) = \frac{2ln\frac{x}{S_0} - 4ln\frac{y}{S_0}}{\sigma^3\sqrt{t^3}xy}\phi\left(\frac{-ln\frac{x}{S_0} + (\mu - \frac{1}{2}\sigma^2)t}{\sigma\sqrt{t}}\right) exp\left(\frac{2ln\frac{x}{S_0}ln\frac{y}{S_0} - 2ln\frac{y}{S_0}^2}{\sigma^2 t}\right)$$

Note that the minimum decreases with the number of observations. Therefore, the price of a Best Garant Certificate with discrete–time observations is bounded from above by that with a continuous–time observation, which is given in quasi closed–form. In order to approximate the exact price in the case of discrete-time observations, we rely on the Monte Carlo method, i.e. for k sample paths of $(S_{t_1},\dots,S_{t_N})$, we obtain (for $j = 1,\dots k$) $\hat{y}_j = S_{t_N}(\omega_j)$ and $\hat{x}_j = \min_{i=0,\dots,N} S_{t_i}(\omega_j)$ and use

$$BGC_{t_0}^{(\min)} \approx e^{(g-r)T} + \frac{1}{k}\sum_{j=1}^{k} \frac{e^{-rt_N}}{\hat{x}_j} \left(\mathcal{B}^{\text{Call}}\left(\hat{y}_j,t_N,r,e^{gT}\hat{x}_j,T\right) - \mathcal{B}^{\text{Call}}\left(\hat{y}_j,t_N,r,e^{cT}\hat{x}_j,T\right) \right) \tag{4.12}$$

Figure 4.2 illustrates the fair contract tuples (g,c) for the minimum strike setting. The left plot results from monthly observations of the asset prices, whereby three volatility levels are considered. The observation horizon is $t_N = 0.5$, the time to maturity is $T = 5$ years and the interest rate is $r = 2.4$ %. Qualitatively, the observations are the same as for fixed priced setting, i.e. the fair cap levels decrease with the guaranteed rate. In the right plot of Figure 4.2, we vary the frequencies of asset price observations during the observation period. Since the BGC–price increases with the observation frequency, the lower the fair cap level, the higher the observation frequency. We also consider the length of the observation period

8 For the sake of completeness, the derivation of the density is given in the appendix, cf. Appendix B.5, Corollary 2.

and illustrate the implied (g,c)-tuple in the appendix, cf. Appendix B.6.

Now, consider the average entry strike setting, which also affords the calculation of the outer expectation, cf. Proposition 4, i.e.

$$BGC_{t_0}^{(\text{ave})} = e^{(g-r)T} + \int_0^\infty \int_0^\infty \frac{e^{-rt_N}}{x} \left(\mathcal{B}^{\text{Call}}\left(y,t_N,r,e^{gT}x,T\right) - \mathcal{B}^{\text{Call}}\left(y,t_N,r,e^{cT}x,T\right) \right) f^{(\text{ave})}(x,y)\, dx\, dy$$

where $f^{(\text{ave})}(x,y)$ denotes the joint density for $K^{(\text{ave})} = x$ and $S_{t_N} = y$. However, even in the case of a Black and Scholes model, the density cannot be stated in closed form. As above, we use a price approximation (cf. 4.12) whereby we use $\hat{x}_j = \frac{1}{N+1} \sum_{i=0}^{N} S_{t_i}(\omega_j)$ rather than the minimum $\hat{x}_j = \min_{i=0,\ldots,N} S_{t_i}(\omega_j)$. In particular, we use

$$BGC_{t_0}^{(\text{ave})} \approx e^{(g-r)T} + \frac{1}{k} \sum_{j=1}^{k} \frac{e^{-rt_N}}{\hat{x}_j} \left(\mathcal{B}^{\text{Call}}\left(\hat{y}_j,t_N,r,e^{gT}\hat{x}_j,T\right) - \mathcal{B}^{\text{Call}}\left(\hat{y}_j,t_N,r,e^{cT}\hat{x}_j,T\right) \right) \tag{4.13}$$

for the following calculation. Analogous the illustrations of the fixed and minimum strike setting, the resulting fair (g,c)–tuple are illustrated in Figure 4.3. Intuitively, it is to be expected that the average strike setting does not imply results that are significantly different from a fixed strike setting where $K^{(\text{fix})} = S_{t_0}$. This is also immanent in the observation that the fair (g,c)–tuple are very similar for different observation periods, cf. right plot of Figure 4.3. To sum up the effects of the different strike settings that are immanent in Best Garant Certificates, we compare the fair contract tuples in all three cases, cf. Figure 4.4. As argued before, for a given guaranteed rate, the fair cap level is the lower the lower the strike. Thus, the fair cap rate regarding the minimum strike setting is well below that concerning the fixed strike setting. In particular, the investor pays a substantial (implicit) premium for the best-entry strike. The same is true if one compares the average and the minimum price setting ($K^{(\text{min})} < K^{(\text{ave})}$). The fair cap rate regarding the minimum strike is also well below the fair cap rate concerning the average strike. By contrast, a comparison of the fixed strike and the average strike provides ambiguous results. For high levels of volatility (here 25 % or 40 %), the fair cap rate regarding the average strike setting is slightly above the fair cap rate in terms of the fixed strike setting, cf. Figure 4.4. By contrast, a low volatility level (10 %) implies a fair cap rate regarding the average strike setting, which is

Figure 4.2: Fair (g,c)–tuple for minimum strike setting

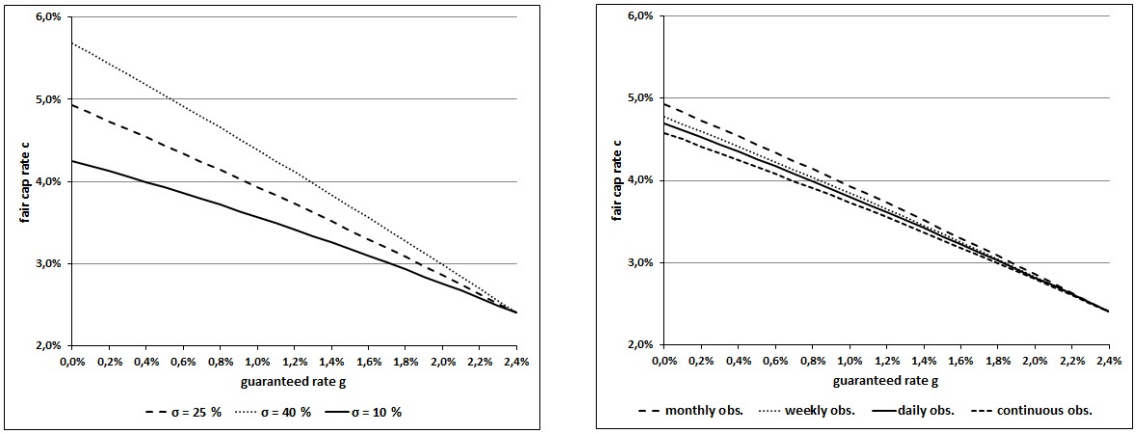

Fair (g,c)–tuple for different volatility levels (left plot) and different observation frequencies (right plot). The observation horizon is $t_N = 0.5$, the time to maturity is $T = 5$ years and the interest rate is $r = 2.4$ %.

far beyond the fair cap rate concering the fixed strike setting.

4.2.3 Pricing in the Heston model

It emerged that the volatility has a crucial impact on the pricing and fair contract design. Thus, in order to calculate realistic BGC prices, it is necessary to take into account stochastic volatility. However, the main lines of the procedure are still as described above.

In the following, we refer to the Heston model, i.e. we use

$$dS_t = S_t \left((r + \lambda_t)dt + \sqrt{V_t} d\widehat{W}_t^{(2)} \right) \tag{4.14}$$

$$dV_t = \kappa \left(\theta - V_t \right) dt + \sigma_v \sqrt{V_t} d\widehat{W}_t^{(1)} \tag{4.15}$$

which describe the asset price and volatility dynamics under the real world measure P.

$\{\widehat{W}^{(1)}\}_{0 \leq t \leq T}$ and $\{\widehat{W}^{(2)}\}_{0 \leq t \leq T}$ denote two one–dimensional correlated Brownian motions with correlation coefficient ρ. The parameter θ describes the long-term variance of the underlying. κ is the rate that controls how fast V_t reverts to the long-term variance θ. In addition, σ_v specify the volatility of the particular variance process and r again represents the risk-free interest rate.

In addition, $(r + \lambda_t)$ can be interpreted as the counterpart of the Black and Scholes drift

Figure 4.3: Fair (g,c)–tuple for average entry strike

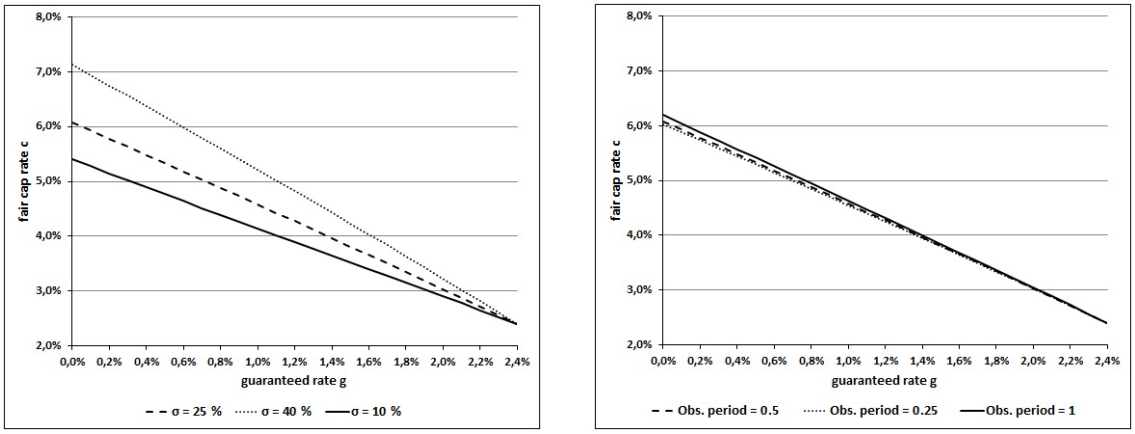

Fair (g,c)-tuple for different volatility levels (left plot) and different observation periods (right plot). For the left plot, the observation horizon is $t_N = 0.5$ and for the right plot we use $\sigma = 25$ %. In both plots, the time to maturity is $T = 5$ years, and the interest rate is $r = 2.4$ %.

parameter μ. We define the process λ_t by $\lambda_t := \overline{\lambda} V_t$ with $\overline{\lambda} \in \mathbb{R}$.

In this context, the market price of risk ε_t is unbounded with

$$\varepsilon_t := \frac{\lambda_t}{\sqrt{V_t}} = \overline{\lambda}\sqrt{V_t} \tag{4.16}$$

To attain to the dynamics under the risk-neutral measure, we refer to the equivalent Cholesky decomposition and apply the Girsanov theorem. The related calculations are illustrated in Appendix B.2. Finally, the dynamics of asset price and variance under the risk-neutral measure P^* are described by

$$dS_t = rS_t dt + S_t\sqrt{V_t}(\rho dW_t^{(1)} + \sqrt{1-\rho^2}dW_t^{(2)}) \tag{4.17}$$

$$dV_t = \kappa^*\left(\theta^* - V_t\right)dt + \sigma_v\sqrt{V_t}dW_t^{(1)} \tag{4.18}$$

Now, $\{W^{(1)}\}_{0\leq t\leq T}$ and $\{W^{(2)}\}_{0\leq t\leq T}$ denote two independent one–dimensional Brownian motions. The long-term variance of the underlying and the rate that controls how fast V_t reverts to the long-term variance are defined by the two parameters κ^* and θ^*, which can

Figure 4.4: Fair (g,c)-tuple for all three entry strike settings of a BGC

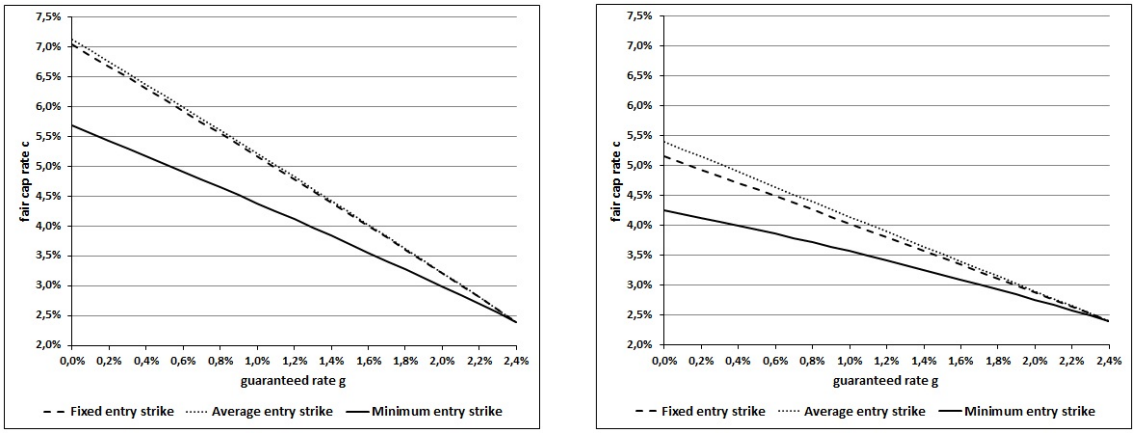

Fair (g,c)-tuple for all observed BGC for $\sigma = 40$ % (left plot) and $\sigma = 10$ % (right plot). In both plots, the time to maturity is $T = 5$ years, the interest rate is $r = 2.4$ % and the observation horizon (for the minimum and the average strike setting) is $t_N = 0.5$.

be calculated by

$$\kappa^* = \kappa + \sigma_v \overline{\lambda} \text{ and } \theta^* = \frac{\kappa\theta}{\kappa + \sigma_v \overline{\lambda}} \tag{4.19}$$

The price approximation by means of the Monte Carlo method is comparable to (4.12) resp. (4.13), whereby the asset price path during the observation period is generated according to (4.17). Rather than the Black and Scholes option pricing formulas $\mathcal{B}^{\text{Call}}$, we use the quasi closed-form solutions $\mathcal{B}^{\text{Call, Heston}}$.
Details concerning the change of measure and the implementation are provided in the appendix, cf. Appendix B.2.

We illustrate the fair (g,c)-tuple, which are based upon a Heston model whereby we use a model parametrization that allows a comparison with the above Black and Scholes framework. Based upon the observation that[9]

$$E(V(T)|V(t)) = \theta + (V(t) - \theta)e^{-\kappa(t_t)}, \tag{4.20}$$

9 Cf. for example Anderson [And06]

we set $\sqrt{\theta} = \sqrt{V_0} = \sigma$ such that with $\theta = V_0 = 0.0625$, the initial variance is equal to the long-term variance. The risk-free interest rate is again $r = 2.40$ %, the remaining parameters are chosen along the lines of BROADIE et al. [Bro06] by $\kappa = 2.0$, $\rho = -0.3$ and the so-called *vol of vol* with $\sigma_v = 1.0$. Thus, we calculate the fair tuple under the risk-neutral measure using $\theta^* = 0.0608$ and $\kappa^* = 2.06$.
A comparison of the fair (g,c)–tuple based upon the Heston and the Black and Scholes model ($\sigma = 25.00$ %) is given in Figure 4.5. Across all strike settings, the fair cap rates

Figure 4.5: Fair (g,c)-tuple: Heston and Black & Scholes model

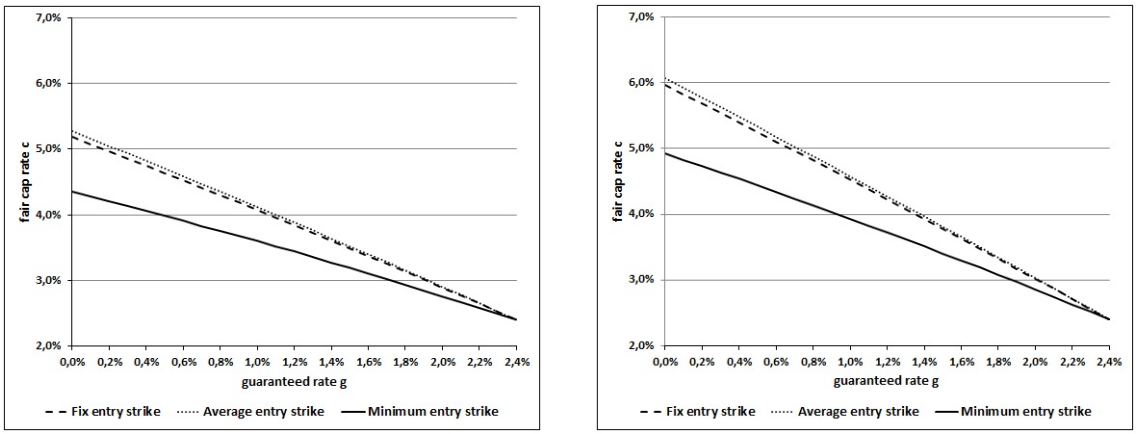

Comparison of model based fair (g,c)-tuple for the Heston model (left plot) and the Black and Scholes model (right plot) with a risk-free interest rate of $r = 2.4$ %, a time to maturity of $T = 5$ year, an observation horizon of $t_N = 0.5$ (for the path-dependent BGC) and volatility of $\sigma = 25$ % in the Black and Scholes model, as well as the comparable variance for the Heston model.

based upon the Heston model are below the fair cap rate regarding the Black and Scholes framework. Although most parameters are chosen in such a way that a comparison of the two model is feasible, we must not undervalue the influence of ρ, κ and σ_v, which we absorb from BROADIE et al. [Bro06]. Naturally, a lower vol of vol would lead to higher cap rates, which are more similar to the Black and Scholes observation. Nonetheless, as long as the calculated results enable further analysis, we will retain this parameter.

4.3 Analysis from the Perspective of the investor

Essentially, the decision problem of a BGC investor is to choose among the return distributions that can be generated by the products under consideration. While the pricing is based upon the risk-neutral measure, the return distributions that are relevant for the investor

are given under the so-called *real world measure* or any subjective measure assumed by the investor. We assume that the investor is restricted to the class of BGCs. Thus, she has to choose a BGC payoff profile which generally differs from her overall optimal payoff profil. Of course, she can choose among all fair contract designs, i.e. the products are fairly priced. For now, our main focus is on the BGC contracts and the payoff distributions obtainable via a fair BGC in the case of a fixed, minimum and average price setting. First, we provide some illustrative examples of payoff distributions, before we optimize the contract design for a CRRA investor who maximizes her expected utility within the class of BGCs.

4.3.1 Assumed Market Data

For further analysis, we use the following parameters. Especially for the calculation in Section 4.4, it seems meaningful to use parameters derived from real market data, if possible. For the derivation of the parameter, we focus on the period from October 2009 to February 2010, which is significant for the three observed Best Garant Certificates in Section 4.4. Furthermore, we will take into account that the time to maturity of each observed BGC is $T = 5$ years. Unless specified otherwise, we assume $t_N = 0.5$ and a monthly observation period for the minimum and average strike setting. Since the investor invests in a structured product with capital guarantee, we assume a conservative risk aversion parameter of $\gamma = 5$.

For both the Black and Scholes and the Heston model, we use the risk-free interest rate $r = 2.4$ %. This is calculated as an average of the five year Germany Government Bonds return, which we will identify with the risk-free investment.
To obtain a realistic estimation for the volatility in the Black and Scholes setting, we observed the implied volatility of traded option on the Euro Stoxx 50 between October 2009 and February 2010, with strikes between 1,800 and 3,900 index points and a time to maturity close to five years. The calculation results in an implied volatility of the at-the-money call option of $\sigma_1 = 24.50$ % [10]. The second relevant call has an implied volatility of $\sigma_2 = 22.50$ % [11]. Due to the minor difference between the two calculated volatilities, it seems sufficient to simply use the mean value of both for the following analysis. Accordingly, we decide to use $\sigma = 23.50$ %. To define the drift parameter μ, we need to assume a realistic risk premium. Based upon the CAPM, the data provider

10 We use a call option issued by the Dresdener Bank, e.g. (WKN DR15RJ) with a strike at 2,800 index points.

11 With a strike at 3,900 index point, the DR15RV was between 34 % and 39.5 % out-of-the-money, whereby this option can be used to identify a realistic implied volatility for the option that is needed for the construction of the cap.

FACTSET calculates a risk premium for the Dow Jones Euro Stoxx 50 on a monthly basis. The average risk premium between the three different issue dates is fixed at 6.6 %, whereby we finally use $\mu = 9.0$ %.

The parameter in the Heston model should allow us to make a comparison with the above Black and Scholes framework. Under the real world measure P, we define θ and V_0 in the same sense as in Section 4.2.2. With $\sqrt{\theta} = \sqrt{V_0} = \sigma$ we set $\theta = V_0 = 0.0552$.
Regarding the other parameters, we considered the existing literature[12] and choose the parametrization of Broadie et al. [Bro06], which is illustrated in Table 4.1.

The parameter for the risk-neutral measure P^* are due to (4.19) and the calculation in Appendix B.2.
As a benchmark we use $\overline{\lambda} = 1.2$, such that for the expectation holds $E\left(r + \overline{\lambda}\sqrt{V_t}\right) \approx \mu$. With these $\overline{\lambda}$, we arrive close to the initial weight of the risky asset in our observation in Sec. 4.3.4. Since we also use $\mu = 7.0$ % for a better overview in the Black and Scholes model, we sometimes define $\overline{\lambda} = 0.85$ to analyze the sensitivity of our results.

4.3.2 Illustration of return distribution in the Black and Scholes Model

The following return distributions under the real world measure P in the Black and Scholes model setting are approximated by means of the Monte Carlo method. We illustrate and compare the final returns for each of the different strike settings of a BGC. For each one, we focus on the tuples $(0,c^{(w)})$. The results for the benchmark case ($\mu = 9.0$ %) and a lower drift parameter are illustrated in Figure 4.6. Due to the payoff description of a BGC, cf. Definition 6, there is point mass on a low return, defined by the guaranteed rate g, as well as point mass on a high return, defined by the cap rate c. Thus, for a fair contract, the maximum return of a BGC is lower in the case of a minimum strike setting than in the case of an average price setting or fixed price setting. For the fixed strike, 79 % of the sample paths yield the minimum or the maximum return. The minimum strike has more weight at the boundaries (≈ 84 %). The average strike stands with 78 % below the two. Table 4.2 summarizes the mean return rates, the median of the return rates and the percentage of return observations that are equal to the minimum and maximum returns defined by the guaranteed and cap rate.
As Figure 4.6 shows, the ratio between the weight at the boundaries strongly depends upon the assumed drift parameter resp. risk premium. For a fixed strike and a drift parameter

12 We found that the parameter significantly varies in the literature, e.g. [Mik03] assumed $\sigma_v = 0.2$, which we think is far too low for our observed time period.

Table 4.1: Overview of the parameter used in the Heston setting

	real world measure P	risk-neutral measure P^*
r in %	2.4	2.4
κ / κ^*	2.0	2.06
ρ	-0.3	-0.3
σ_v	1. 0	1.0
θ / θ^*	0.0552	0.0537
$\overline{\lambda}$	1.2	

Assumed parameter in the Heston model

Figure 4.6: Simulated return rates w.r.t. the fixed strike BGC - BS model

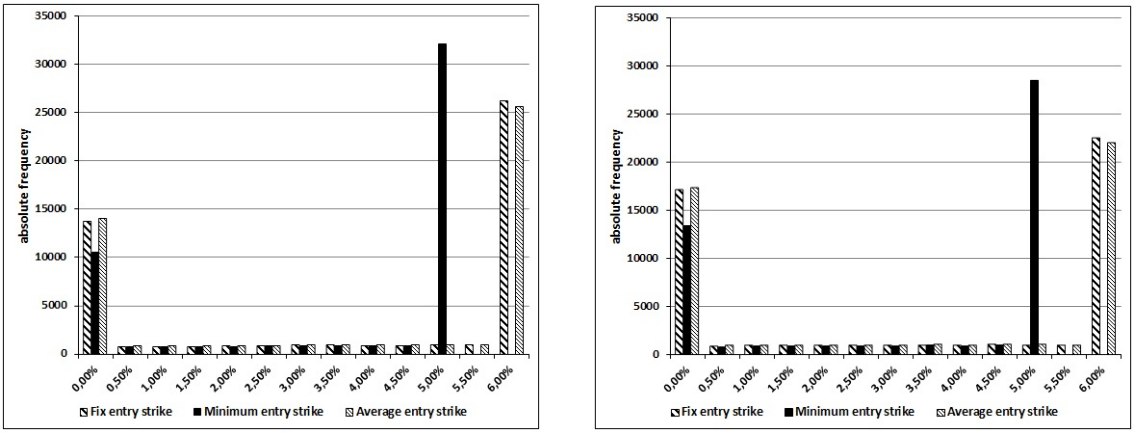

Simulated return rate distribution for the different features of the BGC, with $c^{(\text{fix})} = 5.879$, $c^{(\min)} = 4.850$ and $c^{(\text{avg})} = 5.982$; $\mu = 9.0$ % (benchmark case, left plot) and $\mu = 7.0$ % (right plot).

of less than $\mu = 5.7$ %, the weight on the low return (guaranteed rate) is higher than the weight on the high return (cap rate). The same is true for the minimum entry strike and a drift parameter of $\mu = 2.9$ % or less. For the average entry strike, the turning point is slightly above 6.0 %. For a drift parameter below 5.3 %, the average return of the minimum strike rises above the average return of the fixed strike.

Furthermore, observe that the higher the volatility, the smaller the weight at the cap rate and the higher the weight at the guaranteed rate. While this seems counter-intuitive upon first glance, the effect is easily understood if one recalls the fair contract design that defines the fair cap rate as a function of g. In our benchmark case, the cap rate of the lower volatility is higher than the cap rate of the higher volatility. In particular, the average

Table 4.2: Overview of the return rate distribution - BS model

	fixed	minimum	average
fair cap rate in %	5.88	4.85	5.98
average return in %	3.65	3.46	3.64
median in %	5.88	4.85	5.83
return = guaranteed rate (in %)	27.66	21.09	28.21
return = cap rate (in %)	51.34	63.07	49.72

An overview of the return rate distribution for all entry strike settings of a BGC is illustrated. The calculation assumes a drift of $\mu = 9.0$ % and a volatility of $\sigma = 23.50$ %

return decreases with a higher volatility. Table 4.3 shows the huge differences obtained by setting $\sigma = 10.00$ % and $\sigma = 40.00$ %. Besides the difference in the average return and the median where the volatility parameter $\sigma = 10.00$ % illustrates significant better results, the weight at the left side of the distribution, which only pays the guarantee rate, decreases to 3.00 % or below for all entry strike settings. Considering the minimum strike setting, almost 87 % of the sample paths pay the cap rate, whereby this investment behaves more as a bond than an equity investment in comparison. The higher volatility changes the figures in a completely different way (cf. Table 4.3).

Figures 4.7 plot the payoff of the certificates for each simulated terminal price of the underlying. Since the fixed price setting implies a path–independent payoff, we focus on the two other strike settings, namely the minimum and average strike setting.

Again, it is illustrated that the minimum price setting more commonly provides the high return. However, the high return is lower than in the case of the other price setting mechanisms.

4.3.3 Illustration of return distribution in the Heston Model

Now, we compare the results with the accordant calculations in the Heston model. Again, we use the relevant fair tuple $(0,c^{(w)})$ for the simulation. In Figure 4.8, it is shown that the simulated return rate distribution is very similar to the Black and Scholes model. The study of different levels of θ results in the same effect as observed in the Black and Scholes model. Table 4.4 summarizes the results of the benchmark case.

Finally, Figure 4.9 demonstrates the return rate for a minimum and an average entry strike in the Heston model. However, it is necessary to bear in mind that each maximum payoff rate in the Heston model is below the maximum payoff rate in the Black and Scholes model.

In a simplified manner, the decision problem between a minimum and fixed (respec-

Table 4.3: The influence of the volatility on the return rates

$\sigma = 10.00\ \%$ / $\sigma = 40.00\ \%$	fixed	minimum	average
fair cap rate %	5.16 / 7.04	4.25 / 5.68	5.40 / 7.13
average return in %	4.62 / 3.12	3.99 / 3.10	4.75 / 3.12
median in %	5.16 / 0.93	4.25 / 4.86	5.40 / 0.86
return = guaranteed rate (in %)	2.83 / 47.82	1.78 / 38.97	3.02 / 48.07
return = cap rate (in %)	77.67 / 36.87	87.15 / 48.20	73.19 / 35.80

An overview of the return rate distribution for all entry strike settings of a BGC is illustrated. The calculation assumes a drift of $\mu = 9.0\ \%$ and a volatility of $\sigma = 10.00\ \%$, as well as $\sigma = 40.00\ \%$

Figure 4.7: Simulated return rates w.r.t the minimum and average strike BGC - BS model

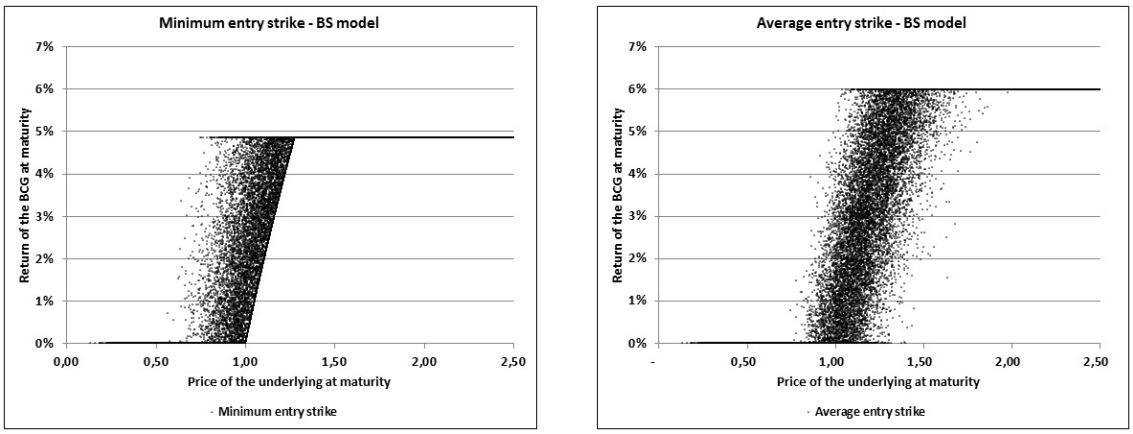

Simulated return rates at maturity depending upon the simulated underlying price for the minimum strike (left plot) and the average strike setting (right plot) in the Black and Scholes model.

tively average strike setting) can be stated as follows. Either one prefers a contract design that gives a moderately good return relatively often or alternatively one can obtain a higher good return, albeit less often. The next section tackles the optimality of the strike price setting mechanism on a more solid basis, i.e. we consider an expected utility maximizing CRRA investor.

Figure 4.8: Simulated return rates w.r.t. the fixed strike BGC - Heston model

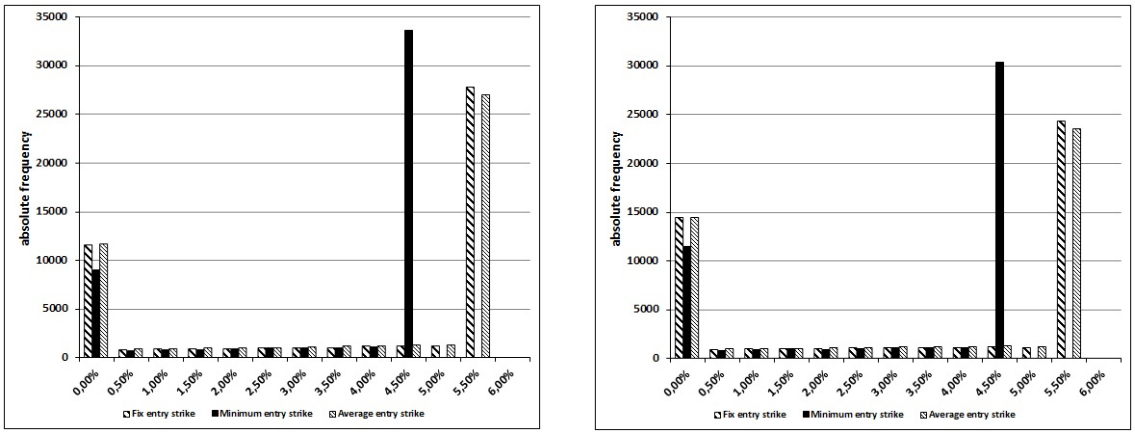

Simulated return rate distribution for the different features of the BGC, with $c^{(\text{fix})} = 5.213$, $c^{(\text{min})} = 4.364$ and $c^{(\text{avg})} = 5.292$; $\overline{\lambda} = 1.2$ (benchmark case, left plot) and $\overline{\lambda} = 0.85$ (right plot).

Table 4.4: Overview of the return rate distribution - Heston model

	fixed	minimum	average
average return in %	3.47	3.25	3.46
median in %	5.21	4.36	5.29
return = guaranteed rate (in %)	23.17	17.96	23.36
return = cap rate (in %)	54.73	65.88	53.00

Calculated for $r = 2.40$ %, $\overline{\lambda} = 1.2$, $\theta = 0.0552$, $\sigma_v = 1.0$, $\rho = -0.3$ and $\kappa = 2.0$

4.3.4 Expected utilities and loss rates in the Black and Scholes model

We consider an expected CRRA utility maximizing investor. As already mentioned, we assume that the financial market is incomplete for the investor, e.g. she has to resort to the restricted class of BGC since she cannot generate her optimal product through a dynamic trading strategy. However, we benchmark the expected utility obtained by an investment in the Best Garant Certificate against the expected utility obtained by the so–called *Merton strategy*, which is optimal regarding a complete Black and Scholes model and a CRRA utility function. Now, we review the basic results concerning the optimal investment in complete market conditions of a CRRA investor in a Black and Scholes model. The Black and Scholes case is used as a benchmark case, i.e. we subsequently define the loss rate implied by the Best Garant Certificate regarding the certainty equivalent, which is implied by the optimal certainty equivalent given by the *Merton strategy*, cf. MERTON [Mer71].

Figure 4.9: Simulated return rates w.r.t the minimum and average strike BGC - Heston model

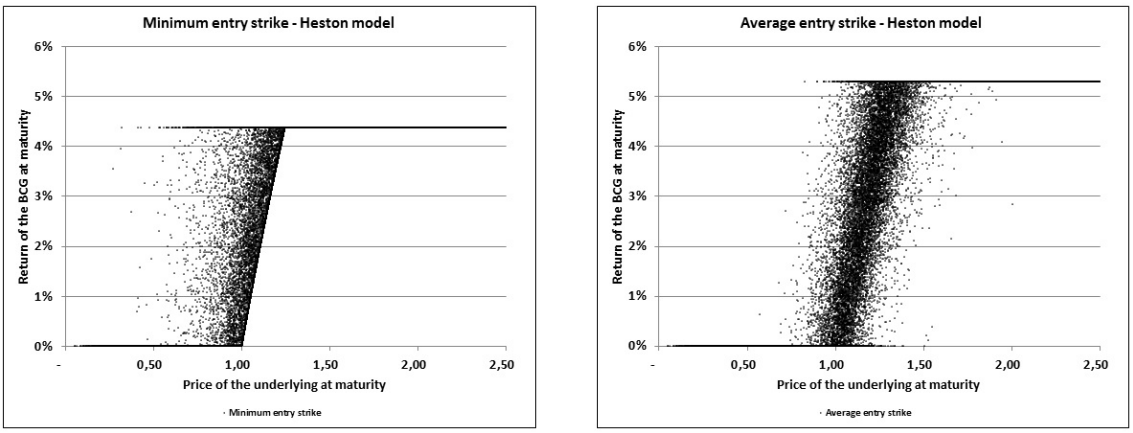

Return rates at maturity depending on the simulated underlying price for the minimum strike (left plot) and the average strike setting (right plot) in the Heston model.

In the case of a Black and Scholes model, the overall optimal investment decisions are well known for the special case of a CRRA utility function $u(w) = \frac{w^{1-\gamma}}{1-\gamma}$ for $w > 0$ and $u(w) = -\infty$ for $w \leq 0$. Here, the optimal proportion of wealth φ^* which is invested in the risky asset S is constant during the observed period $[0,T]$, i.e.

$$\varphi^* = \frac{\mu - r}{\gamma \sigma^2} \tag{4.21}$$

where μ is the assumed drift parameter, r the risk-free interest rate, σ the volatility of the underlying S and γ describe the risk aversion of the investor.
The terminal value V_T^{φ} of any Constant-Mix strategy, which is characterized by a constant investment faction of φ and initial wealth V_0, is given by

$$V_T^{\varphi} = V_0 \, e^{\left(r+\varphi(\mu-r)-\frac{1}{2}\varphi^2\sigma^2\right)T+\varphi\sigma W_T}.$$

The expected utility (under the real world measure P) is

$$E_P\left[u(V_T^{\varphi})\right] = \frac{(V_0)^{1-\gamma}}{1-\gamma} e^{(1-\gamma)\left(r+\varphi(\mu-r)-\frac{1}{2}\gamma\varphi^2\sigma^2\right)T}.$$

The certainty equivalent CE_T^{φ}, which is defined by the certain amount that makes the investor indifferent between achieving this certain amount (at T) or using the strategy φ, i.e.

$$u\left(CE_T^{\varphi}\right) = E_P\left[u\left(V_T^{\varphi}\right)\right]$$

is subsequently

$$CE_T^{\varphi} = V_0 e^{\left(r+\varphi(\mu-r)-\frac{1}{2}\gamma\varphi^2\sigma^2\right)T}.$$

In particular, the benchmark certainty equivalent is

$$CE_T^{*} = V_0 e^{\left(r+\frac{1}{2\gamma}\left(\frac{\mu-r}{\sigma}\right)^2\right)T}. \tag{4.22}$$

Now, we consider the expected utility derived by an investment in a BGC. In the case of a fixed strike K, the expected utility of the Best Garant Certificate can be calculated in closed–form. In addition, the following proposition also yields a simplified procedure to approximate the expected utility by means of the Monte Carlo method.

Proposition 5 (BGC$^{(\mathbf{fix})}$: Expected utility, certainty equivalent and loss rate)

(i) The expected utility $EU^{BGC,fix}$ of a fixed entry strike Best Garant Certificate is given by

$$\begin{aligned} EU^{BGC,fix} &= E_P\left[u\left(e^{gT}+\left[\frac{S_T}{K}-e^{gT}\right]^+-\left[\frac{S_T}{K}-e^{cT}\right]^+\right)\right] \qquad (4.23)\\ &= \frac{1}{1-\gamma}\left[e^{(1-\gamma)gT}\mathcal{N}\left(\frac{gT+\ln K-(\mu-\frac{1}{2}\sigma^2)T}{\sigma\sqrt{T}}\right)\right.\\ &+ e^{(1-\gamma)cT}\mathcal{N}\left(-\frac{cT+\ln K-(\mu-\frac{1}{2}\sigma^2)T}{\sigma\sqrt{T}}\right) \;+\left(\frac{s_0}{K}\right)^{1-\gamma} e^{(1-\gamma)\left(\mu-\frac{1}{2}\gamma\sigma^2\right)T}\\ &\left.\left(\mathcal{N}\left(\frac{cT+\ln K-(\mu+(\frac{1}{2}-\gamma)\sigma^2)T}{\sigma\sqrt{T}}\right)-\mathcal{N}\left(\frac{gT+\ln K-(\mu+(\frac{1}{2}-\gamma)\sigma^2)T}{\sigma\sqrt{T}}\right)\right)\right] \end{aligned}$$

(ii) The certainty equivalent $CE_T^{BGC,fix}$ of a fixed strike Best Garant Certificate is given by

$$CE_T^{BGC,fix} = \left[(1-\gamma)EU^{BGC,fix}\right]^{\frac{1}{1-\gamma}} \tag{4.24}$$

(iii) The loss rate l_T of a fixed strike Best Garant Certificate (benchmarked against the certainty equivalent of the optimal Merton strategy) is given by

$$l_T = \frac{\ln\left(\frac{CE_T^*}{CE_T^{BGC,fix}}\right)}{T} \tag{4.25}$$

where $CE_T^* = V_0 e^{\left(r+\frac{1}{2\gamma}\left(\frac{\mu-r}{\sigma}\right)^2\right)T}$ *and* $V_0 = BGC_{t_0}^{fix}$

Proof 5 *The proof is given in the appendix, cf. Appendix B.3.*

Note that Proposition 5 can also be used to determine the expected utility, the certainty equivalent and the loss rate for the average and minimum strike setting. One can improve the Monte Carlo simulation by restricting the simulation to the observation period, i.e. only the underlying prices S_{t_n} and strikes $K^{(\min)}$ and $K^{(\text{ave})}$ are simulated. Subsequently, the expected utility is calculated according to part (i) of the proposition with the remaining time to maturity (time to maturity after the observation period) and an slight modification of the formular.[13] Averaging across all simulated utilities gives the result.

Now, we illustrate the loss rates l_T of the three price settings observed for BGCs. As above, the cap rates are calculated such that the contracts are fair. Figure 4.10 shows the loss rates for a CRRA investor for $\mu = 9.0$ % as well as for $\mu = 7.0$ %, for comparison. Based upon the assumed risk aversion parameter $\gamma = 5$ and the two different drift parameter μ, the optimal proportion of risky asset in the Merton resp. Constant-Mix strategy is 23.9 % in the benchmark case and 16.7 % in the second calculation.
First, the left plot of Figure 4.10 shows that a Best Garant Certificate investor does not necessarily suffer from a higher guaranteed rate, i.e. the loss rate does not monotonously increase with the guaranteed rate.[14] In the case of a fair cap rate, the utility of a BGC increases with the guaranteed rate for small guaranteed rates but decreases after some (optimal) guarantee level. The loss rate for the minimum entry strike setting finds its (local) minimum for the guaranteed rate of $g = 0.0$ %. The turning point for the fixed and the average entry strike BGC is identified for $g = 0.5$ %.
Second, we observe that the loss rate due to the fixed strike setting is lower than those

13 With the change from t_0 to t_n, not only the time parameter has to be adjusted. We will include $\ln S_{t_n}$ in each numerator in the terms of the cumulative distribution function. Details are provided in Appendix B.3.

14 This might be expected since the CRRA investor generally does not want a guarantee.

Figure 4.10: Analysis of the loss rates for fair BGCs - BS model

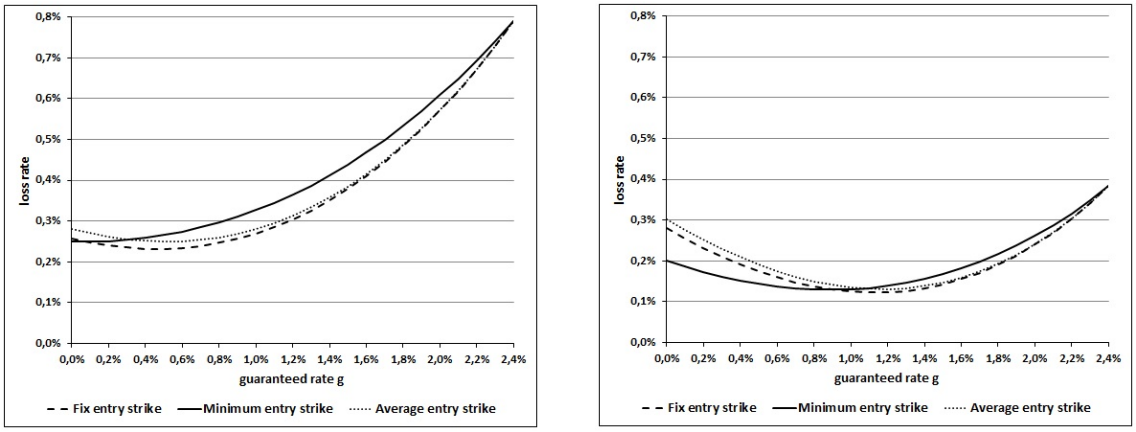

Loss rates for a risk aversion of $\gamma = 5$; $\mu = 9.0$ % (benchmark case, left plot) and $\mu = 7.0$ % (right plot).

obtained by the average and minimum price setting. For the lower guaranteed rate, the difference between the loss rate regarding the average strike setting and the loss rate concerning the fixed entry strike setting is clear. However, with a higher guarantee, where the payoffs are less dependent on the development of the underlying, the graphs converge. Since the average price setting gives similar pricing results to those of the fixed strike setting, this may be explained by the path-dependence, which is suboptimal for a CRRA investor regarding a Black and Scholes model setup. The development of the path-dependent minimum entry strike is quite different. The loss rate regarding the minimum entry strike setting lies on the loss rate concerning the fixed strike setting for the lowest and the highest guaranteed rate. In the range between, the loss rate is significant higher.

By comparison, the right plot illustrates the results for the exemplary low drift $\mu = 7.0$ %. Again, it is seen that all loss rate first decreases and subsequently increases after an optimal guaranteed rate. The different development between the fixed and the average entry strike remains the same. Nonetheless, we should mention that the minimum strike setting seems more attractive for the lower μ. This can be explained by the fact that the minimum feature will outperform the other BGCs if the underlying price does not boost.

While the observation that the loss rates decrease with the guaranteed rate for low guarantees seems surprising at a first glance, intuitively, it can be explained as follows. Note that the return rate of the Merton strategy will be positive if the terminal price of the underlying is equal to its level at issue date. The same effect is given by a guaranteed rate $g > 0.0$ %

for a Best Garant Certificate. Thus, the return rate distribution is closer to the Merton strategy when a positive guaranteed rate is used. Finally, this could result in a lower loss rate.

We now plot the corresponding payoff profiles for varying terminal asset prices (underlying prices) in the case of the fixed strike setting and the Merton strategy, cf. Figure 4.11. The left hand side of Figure 4.11 is based upon a guaranteed rate above 0.0 %, while the right hand side is based upon a guaranteed rate of $g = 0.0$ %. Note that the deviation from the optimal Merton payoff can be viewed as much lower in the case of the positive guaranteed rate compared with the zero guaranteed rate. Essentially, this explains that the loss rate is lower for $g = 0.5$ % than for $g = 0.0$ %. In Figure 4.12, we plot the distribution of the

Figure 4.11: Merton strategy vs. fixed strike Best Garant Certificates - BS model

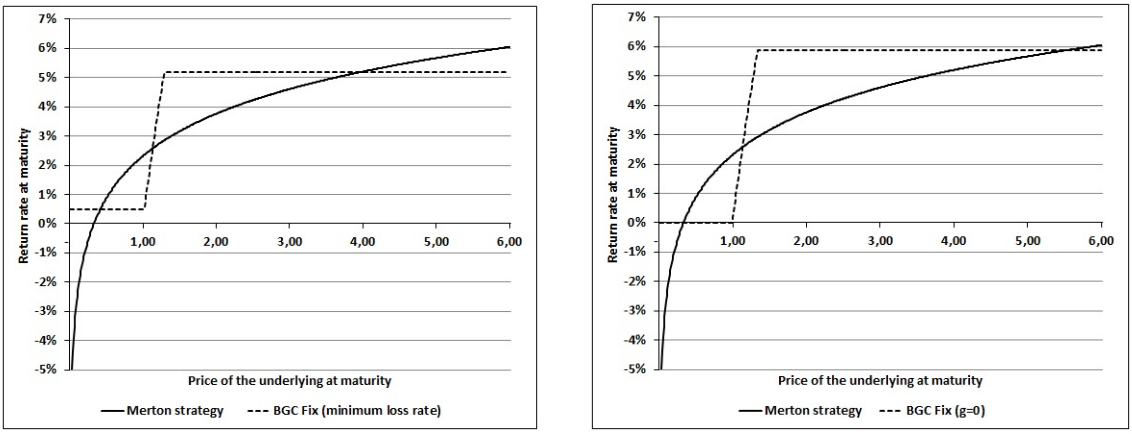

Comparison of the Merton strategy with two fixed strike BGCs, a drift parameter $\mu = 9.0$ % (benchmark case) and $g = 0.5$ % (minimal loss rate, left plot) and $g = 0.0$ % (right plot).

Merton strategy compared with the $\text{BGC}^{(\text{fix})}$, whereby the circles specify the point mass depending upon the given guaranteed and cap rates. Upon first glance, we do not identify a significant difference. With the knowledge of Figure 4.11, we will assume that this results since the point mass is not perfectly illustrated.

4.3.5 Expected utilities and loss rates in the Heston model

In the Heston model, we have to waive a closed-form solution Proposition 5 provided for the Black and Scholes framework, whereby we revert to simulation technics. In addition, the proportion of risky assets in the optimal portfolio strategy is not constant. Therefore,

Figure 4.12: Merton strategy vs. fixed strike Best Garant Certificates - BS model II

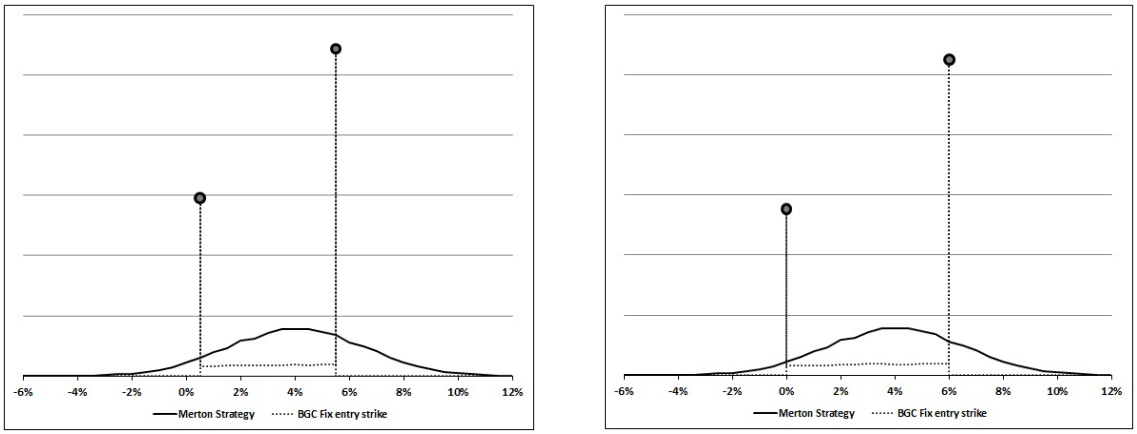

Comparison of the probability Distribution of the Merton strategy with two fixed strike BGCs, a drift parameter $\mu = 9.0$ % (benchmark case) and $g = 0.5$ % (minimal loss rate, left plot) and $g = 0.0$ % (right plot).

we apply to Lui [Lui07], who proved that the optimal portfolio process π_t^* is independent of the path of the variance process and simply changes with the time. To find this optimal portfolio process, Lui [Lui07] follows Merton [Mer71] with an indirect utility function and the application of the Hamilton-Jacobi-Bellmann equation. (The main ideas and the calculation are illustrated in Appendix B.4)

We adopt the following auxiliary variables from Lui [Lui07]:

$$\begin{aligned}
\delta &= -\frac{1-\gamma}{2\gamma^2}\overline{\lambda}^2 \\
\widetilde{\kappa} &= \kappa - \frac{1-\gamma}{\gamma}\overline{\lambda}\sigma\rho \\
\xi &= \sqrt{\widetilde{\kappa}^2 + 2\delta\left(\rho^2 + \gamma\left(1-\rho^2\right)\right)\sigma^2} \text{ and} \\
\zeta &= -i\xi
\end{aligned} \tag{4.26}$$

Using these auxiliary variables, we can define the function d_t by:
For $\xi^2 \geq 0$ holds

$$d_t = -\frac{2\left(exp\left[\xi(T-t)\right]-1\right)}{\left(\widetilde{\kappa}+\xi\right)\left(exp\left[\xi(T-t)\right]-1\right)+2\xi}\delta \tag{4.27}$$

and for $\zeta^2 \geq 0$ is

$$d_t = -\frac{2}{\widetilde{\kappa} + \zeta \frac{cos\left(\frac{\zeta(T-t)}{2}\right)}{sin\left(\frac{\zeta(T-t)}{2}\right)}}\delta \tag{4.28}$$

where T denotes the length of the investment period. With our assumption of the market parameter, we are able to concentrate on formular (4.27) since the condition for ξ^2 always holds. Finally, the portfolio process π_t^* will be the optimal solution in the Heston model:

$$\pi_t^* = \frac{1}{\gamma}\overline{\lambda} + \rho\sigma d_t \tag{4.29}$$

This deterministic process is specified in Chiarella et al. [Chi10] as the sum of an optimal static investment and an intertemporal hedging. The static investment can be compared with the constant proportion in the Merton strategy. The algebraic sign of the intertemporal hedging depends upon the correlation coefficient ρ. For a negative correlation, the intertemporal hedging is a positive term. If we assume that the optimal static investment is equal to the optimal Merton proportion as well as a negative correlation, the investor will invest a higher amount in the risky assets at the beginning of the investment horizon in the Heston model. We see in a numerical example that π_t^* in (4.29) refers to relative small changes in long time periods (cf. Appendix B.4).
However, with the optimal portfolio strategy referring to Lui [Lui07] we are able to simulate the return distribution by means of a Monte Carlo method, since the optimal weight of the risky asset at each reallocating time t is noted. To apply (4.25), we first calculate the expected utility and the certainty equivalent of the portfolio strategy by

$$EU_T^{(*,\text{Heston})} = \frac{1}{k}\sum_{i=1}^{k}\frac{(V_T^{\pi_i})^{(1-\gamma)}}{1-\gamma} \text{ and } CE_T^{(*,\text{Heston})} = \left((1-\gamma)EU_T^{(*,\text{Heston})}\right)^{\left(\frac{1}{1-\gamma}\right)} \tag{4.30}$$

where $V_T^{\pi_i}$ describes the terminal wealth of the i-th path of the simulated strategy π_t^*, considering the equity path S_t^i and the variance path V_t^i.
The relevant expected utility of the BGCs is calculated by

$$EU_T^{(BGC^{(\text{w})},\text{Heston})} = \frac{1}{k}\sum_{i=1}^{k}\frac{(BGC_T^{((\text{w}),\text{Heston})}(\omega_i))^{(1-\gamma)}}{1-\gamma} \tag{4.31}$$

$$CE_T^{(BGC^{(\text{w})},\text{Heston})} = \left((1-\gamma)EU_T^{(BGC^{(\text{w})},\text{Heston})}\right)^{\left(\frac{1}{1-\gamma}\right)} \tag{4.32}$$

We now illustrate the loss rates referring to the Heston model. Since we are unable to vary the drift parameter directly, in Figure 4.13 we plot the loss rate for the benchmark case $\overline{\lambda} = 1.2$ and $\overline{\lambda} = 0.85$, which approximate the lower drift parameter in the Black and Scholes model. This results to a static investment proportion of 24.0 % and 17.0 %, respectively, which can be compared to the calculation in the Black and Scholes model.

The loss rates in the Heston model arise from the same characteristics as the Black and Scholes model. For the benchmark case with $\overline{\lambda} = 1.2$, which could be compared to the Black and Scholes model with a drift parameter of $\mu = 9.0$ %, it is seen that the corresponding loss rate is above that regarding the Black and Scholes model. Furthermore, the minimum loss rate is calculated for a lower guaranteed rate than in the Black and Scholes model. We pass on a figure comparing the distribution of the optimal portfolio

Figure 4.13: Analysis of the loss rates for fair BGCs - Heston model

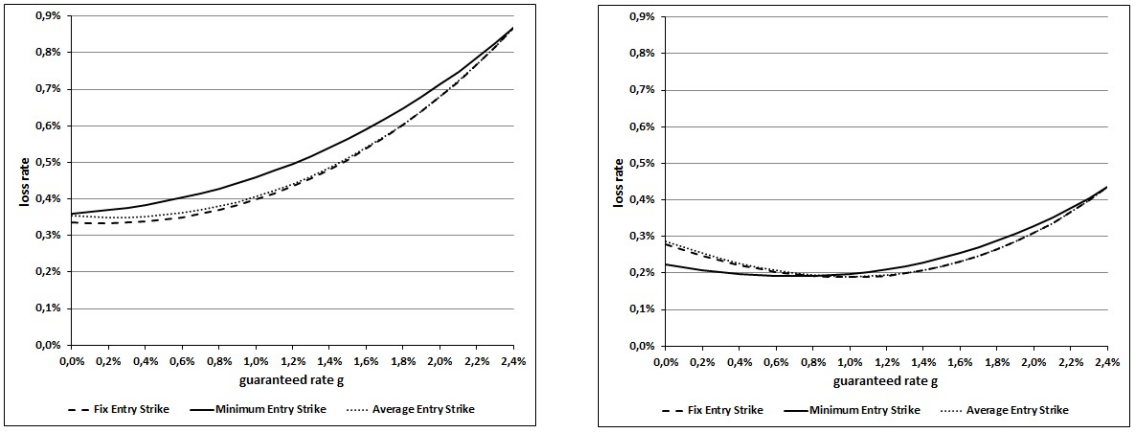

Loss rates for a risk aversion of $\gamma = 5$; $\overline{\lambda} = 1.2$ (benchmark case, on the left) and $\overline{\lambda} = 0.85$ (on the right).

strategy and the BGC with a fixed entry strike, since we do not find any new results.

4.4 Comparison of model and market prices

We now consider real data, i.e. traded Best Garant Certificates[15] issued between October 2009 and February 2010 and compare their issue prices to the model prices given by the Black and Scholes model and the Heston model from Section 4.2.

15 We decide to simply illustrate one certificate for each best-entry feature. Overall we analyzed 10 BGCs issued between October 2008 and May 2010.

Table 4.5 summarizes the contract specifications of the three certificates. The first one belongs to the class of fixed strike and is called $\text{BGC}^{(\text{fix})}$ in the following. The second certificate will be denoted as $\text{BGC}^{(\text{min})}$, because its best-entry strike is calculated by the minimum of 26 observation dates. Finally, the last observed Best Garant Certificate has an average strike feature and thus is called $\text{BGC}^{(\text{ave})}$ in the following. The Startlevel of the

Table 4.5: Best Garant Certificates - termsheet data

Key data	$BGC^{(\text{fix})}$	$BGC^{(\text{min})}$	$BGC^{(\text{ave})}$
Issuer rating [16]	A1, A+	A1, A+	A1, A+
Issue date (ID)	26 Oct 2009	21 Dec 2009	22 Feb 2010
Valuta	28 Oct 2009	23 Dec 2009	24 Feb 2010
Underlying	DJ Euro Stoxx 50	DJ Euro Stoxx 50	DJ Euro Stoxx 50
Startlevel	closed price at ID	see definition	see definition
Nominal amount (N)	EUR 100.00	EUR 1,000.00	EUR 1,000.00
capital protection	100 % of N	100 % of N	100 % of N
Caplevel	138 % of N	130 % of N	135 % of N
Valuation date	31 Oct 2014	16 Dec 2014	17 Feb 2015
Maturity date	07 Nov 2014	23 Dec 2014	24 Feb 2015

Product specification from the termsheets

$BGC^{(\text{min})}$ will be calculated by the minimum of 26 closed prices of the underlying at 26 observation dates from 28 December 2009 to 18 June 2010 (observation period). At the end of the last observation date (18 June 2010), the start level is fixed. For the $BGC^{(\text{ave})}$, the observation period is slightly different. The length of the observation period is only five months (24 Feb 2010 - 26 Jul 2010) and the observation dates have a monthly frequency. Since all certificates guarantee the nominal amount, i.e. $g = 0.0$ % we simply have to transfer the maximum payoff to obtain the cap rate $c^{(\text{w})}$.

In Table 4.6, the cap rates and all model prices (based upon the formula derived in Sec. 4.2.2) are illustrated. It is seen that the model prices for the Black and Scholes model and the Heston model are situated above the nominal amount of EUR 100 and EUR 1,000, respectively. These unrealistic model prices could result from our assumed parameter.[18]

16 All certificates are issued by the same issuer.

17 For these $\text{BGC}^{(\text{ave})}$, a margin of 4.0 % is illustrated in the termsheet.

18 The unrealistic model prices could also result by the assumption that the issuer is solvent at maturity of the certificates in any case. An analysis which allows a default of the BGC issuer is made in Chapter 6.

Table 4.6: Calculated t_0-prices - BS and Heston model

	$BGC^{(\text{fix})}$	$BGC^{(\min)}$	$BGC^{(\text{ave})17}$
Time to maturity T (in years)	5.0	5.0	5.0
Best-in period t_N (in years)	X	0.5	0.42
Nominal amount N (in EUR)	100	1,000	1,000
Maximum payoff (in EUR)	138	1,300	1,350
Cap rate $c^{(\text{w})}$ in %	6.42	5.25	6.02
BS model: t_0-price in % of N	100.87	101.17	100.07
Heston model: t_0-price in % of N	102.15	102.16	101.31

Relevant product specifications and the Black & Scholes and the Heston model prices

We know from the loss rate calculation in Section 4.3 that all observed fair Best Garant Certificates with neither a path-dependent nor a path-independent payoff are suboptimal for an investor with a CRRA utility. With the given subnormal t_0-prices of the certificate, we now consider the loss rate calculation. However, we want to illustrate the efficiencies and inefficiencies of the corresponding Best Garant Certificates with a special loss rate. Since the BGCs are not issued at the fair model price, we will split the loss rate introduced in proportion 5 in two parts. We define

$$l_T^{(\text{w})} = \frac{\ln\left(\frac{CE_T^*}{C\tilde{E}_T}\right)}{T} + \frac{\ln\left(\frac{C\tilde{E}_T}{CE_T^{\text{BGC,w}}}\right)}{T} \tag{4.33}$$

where $C\tilde{E}_T$ describes the certainty equivalent of the fair BGC$^{(\text{w})}$, calculated with the fair cap rate for $g = 0.0$ % and $CE_T^{\text{BGC,w}}$ is the certainty equivalent of the traded BGC with the parameter of the termsheet. CE_T^* still illustrates the certainty equivalent of the optional Merton strategy. With this definition, we are able to separate a loss rate depending upon the specific structure of the BGC (loss rate by structure), which is comparable to Figure 4.10 and Figure 4.13 and a loss rate resulting from the price at issue date (loss rate by market price). Although Table 4.6 shows that our model prices are above the nominal amount, with the applied loss rate calculation we identify that most of the trade certificates are suboptimal for the CRRA investors, despite the undervaluation at issue date. The result are illustrated in Table 4.7.

If we first look at the results based upon the Black and Scholes model, we identify that each loss rate by structure is positive (cf. Figure 4.10) and is located between 0.252 % and 0.275 %. The calculated loss rates by market price are all negative (-0.014 %--0.227 %),

Table 4.7: Separated loss rate - BS and Heston model

BS model	$BGC^{(\text{fix})}$	$BGC^{(\text{min})}$	$BGC^{(\text{ave})}$
Loss rate by structure in %	0.256	0.252	0.275
Loss rate by market price in %	-0.150	-0.227	-0.014
Sum of both loss rates in %	0.106	0.025	0.256
Heston model			
Loss rate by structure in %	0.327	0.346	0.347
Loss rate by market price in %	-0.370	-0.401	-0.211
Sum of both loss rates in %	-0.04	-0.05	0.140

The special loss rate calculation for the relevant product specifications and the Black & Scholes and the Heston model

although they are so small that the summation of both loss rates is positive.[19] This means that the traded certificates are inefficient for the CRRA investor despite being issued above their nominal amount, and their model prices are above their nominal amount.

The results in the Heston model are different, whereby the loss rates by structure are higher than in the Black and Scholes model. However, the loss rates by market price are 0.2 % lower than in the Black and Scholes model on average and are located between -0.211 % and -0.401 %. Consolidated, we find two negative loss rates after the summation for the fixed and the average entry strike. Nonetheless, the loss rate is more-or-less zero as in the case of the $\text{BGC}^{(\text{min})}$ in the Black and Scholes model, whereby we cannot mark any efficiencies or inefficiencies. Only the calculated loss rate for the $\text{BGC}^{(\text{ave})}$ allows us to note an inefficient structure for the investor.

4.5 Conclusion

Although Best Garant Certificates are advertised as offering attractive return characteristics achieved by so-called best-entry strikes, the answer to the question of *is best entry really better* is ambiguous. The BGC investor pays an implicit premium for the entry strike (and the guarantee), whereby she gives up some of her upward participation, i.e. her return is capped. The cap rate is lower, the lower the entry strike tends to be. Thus, a minimum price setting can imply a cap rate that is unfavorably low. In addition to the pricing issues of the contracts under consideration, we discuss the optimality (suboptimality) of the

19 The difference in the case of the minimum strike setting is marginal, whereby the following conclusion only holds for the $\text{BGC}^{(\text{fix})}$ and $\text{BGC}^{(\text{ave})}$.

best-entry strike settings and the overall product design for an expected utility maximizing CRRA investor. While all observed BGC payoff profiles differ from the overall optimal product design of a CRRA investor, we find that within the class of BGCs the optimal guaranteed rate is not necessarily equal to zero. In addition, it emerges that the BGC investor suffers from the minimum strike setting compared to a fixed strike setting.
Regarding the observed market prices, we find that the Best Grant Certificates are undervalued at their issue date. However, we use a special loss rate calculation and ascertain that some certificates seem to be inefficient for the CRRA investor, despite being issued below their fair model price. A comparison of the model prices and the market prices suggest that the issuer uses path-dependent certificates with more complex payoff structures, which are difficult to understand, to gain a higher margin.

CHAPTER 5

Investors' preference concerning Locally Capped Garant Certificates

5.1 Introduction

The market for structured products has been increasing in recent years. Besides the volume invested in structured products, the variety has also significantly risen. Considering the different classes of structured products, it is seen that the main focus is on garant certificates resp. structured product with capital protection. Most of the certificates guarantee the investor's nominal amount, which she invested at the issue date. Furthermore, the investor receives an addition amount depending on the performance of an underlying. In general, such certificates combine a guarantee and an upward participation. Over time, many variations of classical garant certificates have been developed whereby the final payoff depends on complex calculations, including minimum guarantees (floors), caps or path-dependence. Exemplary representatives of this class are Locally Capped Garant Certificates (LCGC) as well as Globally Capped Garant Certificates (GCGC), which we will analyze in the following.

The class of certificates was first analyzed by Bernard et al. [Ber11b]. Thus, Bernard et al. [Ber11b] provide the preparatory work for our analysis.[1]
The main feature of a LCGC is the combination of a floor, cap and path-dependent underlying observation. More precisely, the payoff is floored at the nominal amount or above, whereby the investor receives - independently from the underlying performance - an amount greater or equal to her initial investment. With an additional amount, the

1 They focus on different aspects of locally capped globally floored Certificates issued in the United States. They mention that the observed products are very complicated to understand for retail investors. Furthermore, they show that the illustrated payoffs in the products prospectus are extremely optimistic, meaning that an investor has an unrealistic view about the certificate. Finally, they prove that the observed certificates were highly overpriced at issue date, on average.

investor participates in the performance of the underlying, e.g. an equity index. Instead of a calculation of the excess return of the underlying between the issue date and maturity, a fix number of sub-period returns is observed and finally combined. As a special feature, each observed return of the underlying is bounded, whereby a combination of effective returns and a number of capped returns is taken into account in the final calculation.

The product specification can be simplified by the following parameter. Assuming the nominal amount N and a time to maturity T, the investor's payoff is at least $N + G$ resp. Ne^{gT}, where G describes the addition guarantee and g presents the guaranteed rate, which could be compared with a continuous interest rate over the entire investment period of the certificate. In addition, there is a set of observation dates $\{t_0 = 0, t_1, ..., t_n = T\}$ where the periodical underlying returns are calculated. Each calculated return between two observation dates t_i and t_{i+1} is bounded by a maximum return C (cap resp. locally cap). The final additional amount will be calculated from the observed return by a mathematical method. This method could include a simple summation or a calculation based upon a compounded string.

There are many possible variations of LCGC and naturally the guarantee resp. the guaranteed rate has a huge influence on the certificate. Obviously, the price of the certificate rises with higher G or g. For the additional amount, the number of calculations as well as the level of the cap is very important. However, there is a positive relation between the cap and the price of the certificate since the additional payment is higher with higher caps. Finally, the calculation period, which defines the number of calculated returns, also has a huge influence on the pricing.

Our main contribution is as follows. We analyze five different calculation sequences: monthly, quarterly, semi-annual, annual and globally. The globally sequence includes no sub-periodical calculation, e.g. only the terminal return at maturity is taken into account for the payoff of the certificate. We calculate fair combination of guarantee rates g and locally caps C for all observed certificates. For the analysis, we refer to the Black and Scholes model, as well as the Heston model, which allow stochastic volatility. Here, we assume that the financial market is complete for the issuer. More precisely, the issuer can generate any payoff profile by a dynamic strategy in the risky and risk-free assets.

It is seen that shorter observation periods (more sub-period returns are calculated) include

higher fair locally caps. Furthermore the maximum payoffs at maturity is higher. Of course, the fair locally caps decrease with higher guaranteed rates.
Furthermore, we analyze the optimality and suboptimality of these payoffs for an expected CRRA utility maximizing investor. Here, we assume incomplete market conditions for the investor. Thus, the investor can only choose between the offered LCGCs. However, within the restricted class of LCGCs, the investor can choose her optimal one. On the one hand, we ascertain that the LCGC investor could suffer from short observation periods in terms of a high loss rate. On the other hand, there is an optimal guaranteed rate above zero whereby the loss rate is minimal.

Furthermore, we consider the influences of different volatility (resp. variance) levels, whereby a higher volatility includes higher locally caps as well as higher theoretical maximum payoffs. However, simulated return rates under the real world measure show that the payoff distribution at maturity significantly changes. For instance, the number of the simulated payoffs only paying the guarantee amount rises with higher volatility, which could be interpreted as suboptimal for the investor.
Note that there is no closed-form solution for the class of LCGC, and thus the calculation relies on Monte Carlo methods. An overview of the relating literatur is given in Section 2.2.

The remainder of this chapter is as follows. In Section 5.2, we show the payoff structure of the observed certificates. The corresponding model setting as well as the assumption used are illustrated in Section 5.3. The fair tuple of guaranteed rate and locally caps are analyzed in Section 5.4. The illustration under the real world measure, e.g. the payoff distribution at maturity and additional loss rate calculation, are shown in Section 5.5, which is divided into the following two parts: Section 5.5.1 focuses on the Black and Scholes model, before the calculations based on Heston model are illustrated in Section 5.5.2. Finally, Section 5.6 concludes this chapter.

5.2 Payoff of the certificates

With the analysis of the different types of Best Garant Certificates in Chapter 4, we identify some interesting characteristics that depend on the combination of three product features: guarantee, cap and path-dependence. Especially in market conditions with low interest rates, an issuer of certificates has to include caps (and sometimes also specific path-dependent features) to finance a nominal guarantee the investors required. In addition, we will see that there are path-dependent features that proceed over the entire investment

period of the certificates. Thus, for the LCGC, the level of path-dependence is higher than for the Best Garant Certificates.

Bernard et al. [Ber11b] focus on Structured Investment Product with Caps and Floors (resp. Guarantees), mentioning that these types of product most are used by investment banks, as well as insurance companies. More precisely, they observe three different structures of Guarantee Certificates: a globally capped globally floored certificate and two versions of locally capped globally floored certificates. For a better comparison, we will denote the product by Globally Capped Garant Certificates (GCGC) and by Locally Capped Garant Certificates (LCGC) in the following.
While globally capped structures show the same characteristics as the Best Garant Certificates with a fixed entry strike setting (cf. Chapter 4), the LCGCs payoffs differ from the Best Garant Certificates with a minimum or average entry strike analyzed in Chapter 4.

According to Bernard et al. [Ber11b], the payoff of the LCGC depends on a deterministic number of returns, each of which is calculated between two observation dates t_i and t_{i+1} of a set $\{t_0 = 0,t_1,...,t_n = T\}$ of observation dates, where T denotes the corresponding time to the maturity. However, each return is bounded by the locally cap. In particular, the observation of the path of the underlying holds until maturity.
Finally, the payoff deviates from the summed or compounded string of the capped returns.

The payoff of the Globally Capped Garant Certificate (GCGC) is described in the following way[2]:

$$GCGC_T = (1+G) + \max\left(0,\min\left(C,\frac{S_T - S_0}{S_0}\right) - G\right) \tag{5.1}$$

where G is the absolute guarantee that the investor receives in addition to the nominal amount, while C describes the cap, which limits each calculated return (of course, only one calculated return in the case of a GCGC).

If we set $G = e^{gT} - 1$, $C = e^{cT} - 1$ and $S_0 = K$, the observed payoff will lead us to the same formula that describes the payoff of the $\text{BGC}^{(\text{fix})}$ (cf. Chapter 4) using a

2 We use the same description as in Bernard et al. [Ber11b].

guarantee rate g and a cap rate c rather than absolute rates G and C. Let

$$\begin{aligned} GCGC_T &= (1+G) + \max\left(0,\min\left(C,\frac{S_T - S_0}{S_0}\right) - G\right) \\ &= e^{gT} + \max\left(0,\min\left(e^{cT}-1,\frac{S_T-K}{K}\right) - (e^{gT}-1)\right). \end{aligned} \tag{5.2}$$

With $\min\{a,b\} = a - [a-b]^+$ and $\max\{a,b\} = a + [b-a]^+$ follows immediately

$$\begin{aligned} & e^{gT} + \max\left(0,\frac{S_T-K}{K} - \left[\frac{S_T-K}{K} - e^{cT} + 1\right]^+ - (e^{gT}-1)\right) \\ &= e^{gT} + \max\left(0,\frac{S_T}{K} - e^{gT} - \left[\frac{S_T}{K} - e^{cT}\right]^+\right) \\ &= e^{gT} + \left[\frac{S_T}{K} - e^{gT} - \left[\frac{S_T}{K} - e^{cT}\right]^+\right]^+ \\ &= e^{gT} + \left[\frac{S_T}{K} - e^{gT}\right]^+ - \left[\frac{S_T}{K} - e^{cT}\right]^+. \end{aligned} \tag{5.3}$$

It is evident that we have exactly the same certificate ($\text{BGC}^{(\text{fix})}$), albeit only with a different description of the guarantee and the cap. Nonetheless, the main focus is on LCGC. Thus, before proceeding with the analysis, we have to summarize the two forms of Locally Capped Garant Certificates (LCGC).

The two locally capped certificates only offer one significant disparity. On the one hand, the final payoff will be calculated by the sum of the observed returns until maturity: this Locally Capped Garant Certificate with summation will be denoted $\text{LCGC}^{(\text{sum})}$ in the following. On the other hand, we will use the denomination $\text{LCGC}^{(\text{com})}$ where a compounded string of returns calculates the final payoff.
The payoff functions are the following[3]:

$$LCGC_T^{(\text{sum})} = (1+G) + \max\left(0,\sum_{i=1}^{n}\min\left(C,\frac{S_{t_i}-S_{t_{i-1}}}{S_{t_{i-1}}}\right) - G\right) \tag{5.4}$$

3 In analogy to the GCGC, we refer exactly to the description illustrate by Bernard et al. [Ber11b]

and

$$LCGC_T^{(\text{com})} = (1+G) + \max\left(0, \left(\prod_{i=1}^{n} \min\left(1+C, \frac{S_{t_i}}{S_{t_{i-1}}}\right)\right) - 1 - G\right) \tag{5.5}$$

where $\{t_0 = 0, t_1, ..., t_n = T\}$ denotes the set of observation dates and n is the number of returns observed for the calculation of the payoff at maturity.

For the further analysis, we mention the definition of a fair contract so that the product specifications can be easily compared to other certificates.

We call a GCGC contract fair if

$$1 = PV_{t_0,T}\left((1+G) + \max\left(0, \min\left(C, \frac{S_T - S_0}{S_0}\right) - G\right)\right). \tag{5.6}$$

where $PV_{t_0,T}(.)$ denotes the arbitrage free t_0–value of a payoff receives at time T. In analogy, we define a fair contract for a LCGC$^{(\text{sum})}$ and LCGC$^{(\text{com})}$ refering to (5.4), as well as (5.5).

Thus, the (G^*, C^*)-tuple satisfying condition (5.6) defines a fair contract. In analogy, we define a fair tuple for the two Locally Capped Garant Certificates, although we change the denomination whereby we observe (g, C)-tuple.
First, we illustrate some pricing attributes of the certificates. Furthermore, we show the basic result with a focus on return distribution and utility attributes under the real world measure.

5.3 The model and additional assumption

For the analysis of the illustrated certificates, we refer to the well-known Black and Scholes and the Heston model. In the following, we provide a brief overview of the corresponding model settings. Furthermore, we give our assumption about the relevant market parameters required in the models.

5.3.1 Model description

For both model settings, we use r as the risk-free interest rate and $t \in [0, T]$ as the corresponding time parameter in the continuous market models.

The standard Black and Scholes assumptions are as follows. The price of the underlying S_t

satisfies the stochastic differential equation

$$dS_t = \mu S_t dt + \sigma S_t dW_t, \tag{5.7}$$

where $(W_t)_{t\geq 0}$ is a standard Brownian motion under the real world measure P. σ denotes the volatility parameter and μ describes the market drift. (5.7) implies that the dynamics of the stock prices under the risk-neutral measure P^* are[4]

$$dS_t = rS_t dt + \sigma S_t dW_t^* \tag{5.8}$$

where $(W_t^*)_{t\geq 0}$ is a standard Brownian motion under the equivalent martingale measure P^*. Additionally, we assume no dividend payments of the underlying.

The Heston model allows stochastic volatility resp. stochastic variance. The underlying price and the volatility dynamics under the real world measure P are given by

$$dS_t = S_t \left((r + \lambda_t)dt + \sqrt{V_t} d\widehat{W}_t^{(2)} \right) \tag{5.9}$$

$$dV_t = \kappa \left(\theta - V_t \right) dt + \sigma_v \sqrt{V_t} d\widehat{W}_t^{(1)} \tag{5.10}$$

where $(\widehat{W}^{(1)})_{t\geq 0}$ and $(\widehat{W}^{(2)})_{t\geq 0}$ denote two one–dimensional correlated Brownian motions with correlation coefficient ρ. The parameter θ describes the long-term variance of the underlying. κ is the rate that controls how fast V_t reverts to the long-term variance θ. In addition, σ_V specifies the volatility of the particular variance process and r again represents the risk-free interest rate.
In addition, $(r + \lambda_t)$ can be interpreted as the counterparty of the Black and Scholes drift parameter μ. We define the process λ_t by $\lambda_t := \overline{\lambda} V_t$ with $\overline{\lambda} \in \mathbb{R}$.

In this context, the market price of risk ε_t is unbounded with

$$\varepsilon_t := \frac{\lambda_t}{\sqrt{V_t}} = \overline{\lambda} \sqrt{V_t}. \tag{5.11}$$

To attain to the dynamics under the risk-neutral measure, we use the equivalent Cholesky decomposition and apply the Girsanov theorem. The related calculations are illustrated in Appendix B.2. Finally, the dynamics of underlying price and variance under the risk-neutral

4 cf. Harrison et al. [Har79] and Harison et al. [Har81]

measure P^* are described by

$$dS_t = rS_t dt + S_t\sqrt{V_t}(\rho dW_t^{(1)} + \sqrt{1-\rho^2}dW_t^{(2)}) \tag{5.12}$$

$$dV_t = \kappa^*\left(\theta^* - V_t\right)dt + \sigma_V\sqrt{V_t}dW_t^{(1)}. \tag{5.13}$$

Here, $(W^{(1)})_{t\geq 0}$ and $(W^{(2)})_{t\geq 0}$ denote two independent one–dimensional Brownian motions.

5.3.2 Additional assumption

In this chapter, we assume a risk-free interest rate $r = 2.4$ % and time to maturity $T = 5$ for all certificates. In Section 5.4, where we analyze the pricing of the certificates that we use in the Black and Scholes model, the volatility is 25.0 %. For the Heston model, we use $\kappa^* = 2.06$, $V_0 = 0.0625$, $\theta^* = 0.0608$, $\rho = -0.3$, as well as $\sigma_v = 1.0$. Here, we choose the variance parameter in a way that it could be compared to the volatility in the Black and Scholes model. The remaining parameters are chosen in analogy to Broadie et al. [Bro06]. Since the analysis in Section 5.5 depends on the investor's perspective, we use the parameter calculated by real market data according to Chapter 4, which differs from the previous assumption[5].

Thus, in the Black and Scholes model, we change the volatility parameter from 25.0 % to 23.5 % and use a drift parameter $\mu = 9.0$ % based upon the observed risk premium. Besides the benchmark drift, we make also calculation for a comparable lower drift of $\mu = 7.0$ %. In the Heston model, we use $\overline{\lambda} = 1.2$ to approximate this benchmark drift and $\overline{\lambda} = 0.85$ for the lower drift parameter. The other parameters are $\kappa = 2.00$, $V_0 = 0.0552$, $\theta = 0.0552$, $\rho = -0.3$ and $\sigma_v = 1.0$.

For the calculation of the loss rates, we use a risk aversion parameter of $\gamma = 5$ in both models. The results in Section 5.5 are based upon the simulation of 50,000 sample-paths.

5.4 Pricing of fair locally caps

In order to allow a conditional comparison with the existing results from Chapter 4, we illustrate fair (g,C)-tuple, where g is the corresponding guaranteed rate to the guarantee G, with $e^{gT} - 1 = G$ and C is the locally cap. Here, we know the development of the (g,C)-tuple of the GCGC (cf. Chapter 4), since the only difference is the scaling of the y-axis with $\frac{ln(C)}{T} = c$. However, we are content with the calculations of the fair tuple for the

5 Although these kinds of certificates were issued in a different period than those observed in Chapter 4, they offer the opportunity to compare the distribution of these different types of path-dependent and path-independent payoffs.

two Locally Capped Guarant Certificates. We illustrate four different methods of return calculation: monthly, quarterly, semi-annual and annual.
In the following, we show the calculations for the $\text{LCGC}^{(\text{sum})}$. Owing to the small difference in the results between the $\text{LCGC}^{(\text{sum})}$ and the $\text{LCGC}^{(\text{com})}$, we decide to focus on the calculated results of the $\text{LCGC}^{(\text{sum})}$ in the first place. A summary of the results referring to the $\text{LCGC}^{(\text{com})}$ can be found in Appendix B.7.

The left plot of Figure 5.1 illustrates the results for a $\text{LCGC}^{(\text{sum})}$ with a monthly calculation[6]. The fair locally caps calculated in the Black and Scholes model are above the locally caps calculated in the Heston model.[7]

Upon first glance, the fair locally cap of $C = 9.0$ % (resp. $C = 8.5$ %) for the guaranteed rate $g = 0.0$ % seems attractive for an investor. Here, the maximum payoff of the $\text{LCGC}^{(\text{sum})}$ is 540 % (resp. 510 %), which can be compared with a maximum return rate of 33.7 % (resp. 32.6 %). Considering our analysis of the simulated return rates at maturity in the next section, we will see that the average returns as well as the medians of the return significantly differ from the maximum payoff, quite contrary to the returns of the GCGC.
Considering the right plot of Figure 5.1 and the two plots of Figure 5.2, we reach the result that the shorter the calculation frequence, the lower the fair locally caps.[8] However, the maximum payoff rises with a shorter observation period, since there are more returns to be summed in the final calculation at maturity.
It is also observed that a higher guaranteed rate g has different influences on the ratio of the calculated Black and Scholes and Heston locally caps C. In the case of a semi-annual or annual calculation, the fair caps seem to be converging for higher g. For the monthly observation, where the fair caps are near to each other for the guaranteed rate $g = 0.0$ %, the two charts enlarge their gap with an increasing guaranteed rate. The relative difference in the quarterly observation is more or less constant in comparison to the other plots.
The same development of the fair locally caps is observed for the $\text{LCGC}^{(\text{com})}$. Overall, the

6 For this type of certificates, with a locally cap and a globally guarantee, it is not possible to assign a unique solution for a fair cap C if the global guarantee is equal to the risk-free interest rate return. Thus, with $G = e^{rT} - 1$, the sum in the case of a $\text{LCGC}^{(\text{sum})}$ or the product in the case of a $\text{LCGC}^{(\text{sum})}$ have to be lower than or equal to zero. For example, for a $\text{LCGC}^{(\text{sum})}$, it holds for $C = 0$ % as well for $C = \frac{G}{n}$ %.

7 We should mention that the same difference is observed in Chapter 4. This highlights our assumption that the difference relies on the assumed parameter.

8 cf. Bernard et al. [Ber11b]

Figure 5.1: Fair (g,C)-tuple in the BS and Heston model - LCGC$^{(\text{sum})}$ monthly vs. quarterly

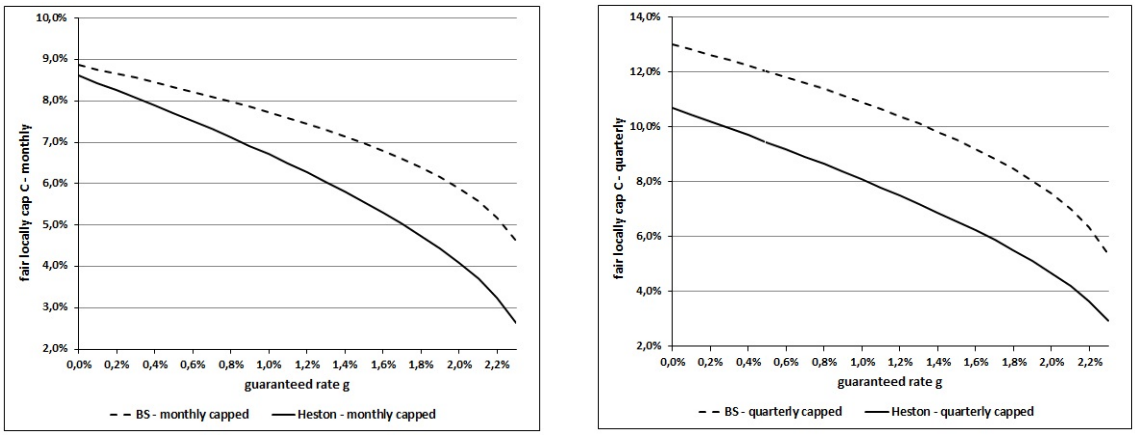

Comparison of model based fair (g,C)-tuple with monthly (left plot) and quarterly (right plot) capped returns for the LCGC$^{(\text{sum})}$.

level of the fair locally caps is above the level of the locally caps for LCGC$^{(\text{sum})}$. This result emerges due to the calculation with compounded string overweight large negative returns. As previously mentioned, we illustrate the four plots of the fair (g,C)-tuple for the LCGC$^{(\text{com})}$ in the Appendix B.7.

As previously mentioned, we assume that the volatility of the underlying has a crucial influence on the fair locally caps. For the Black and Scholes model, Table 5.1 shows for a fixed guaranteed rate $g = 0.0$ % the corresponding fair locally caps, while we use three different volatility levels. Besides the benchmark volatility of $\sigma = 25.00$ %, we choose $\sigma = 10.00$ % as an example for a very low volatility and, on the contrary, $\sigma = 40.00$ %.

Table 5.1: Influences of different volatility levels on the fair locally caps - BS model

BS-model	monthly	quarterly	semi-ann.	annual	globally
C for $\sigma = 10.00$ %	4.73	7.44	10.01	13.61	28.57
C for $\sigma = 25.00$ %	8.86	13.02	16.49	20.97	34.69
C for $\sigma = 40.00$ %	12.76	18.24	22.76	28.07	41.61

Fair locally caps for a guaranteed rate of $g = 0.0$ % and varied volatility level in the Black and Scholes model.

We could identify that for a lower volatility, the caps look less attractive than in the

Figure 5.2: Fair (g,C)-tuple in the BS and Heston model - LCGC$^{(\text{sum})}$ semi-annual vs. annual

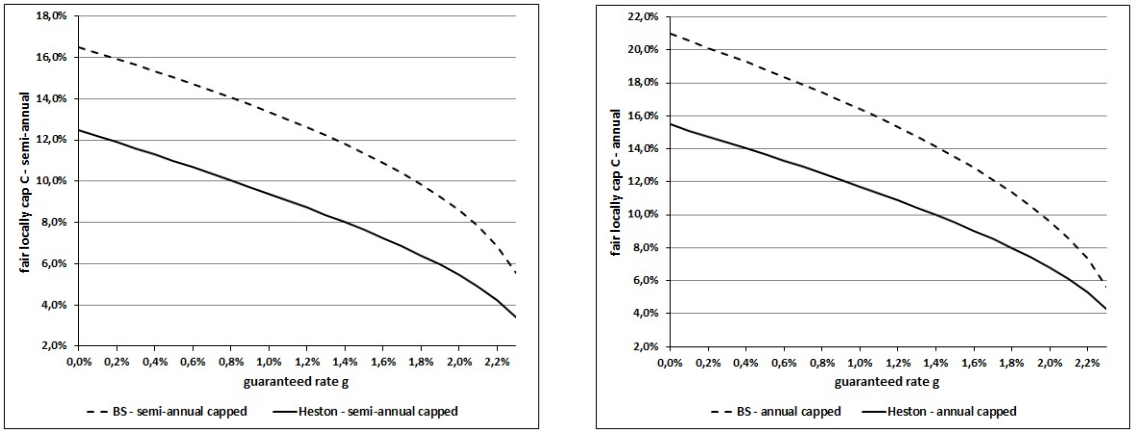

Comparison of model based fair (g,C)-tuple with semi-annual (left plot) and annual (right plot) capped returns for the LCGC$^{(\text{sum})}$.

benchmark case ($\sigma = 25.00$ %). For the monthly observation, the locally caps are around half as large as for the benchmark volatility. We should mention that the percentual difference is reduced with a lower number of observation dates. The other way around, the assumed higher volatility of $\sigma = 40.00$ % is followed by significantly larger locally caps for all types of observation. Remember that large negative returns are never floored by a locally guarantee. Thus, with a higher volatility, the probability of large negative return increases, so that the positive return should be capped at a higher level.

The volatility analysis is more complicated in the Heston model. In the first rows of Table 5.2, it is illustrated how the locally caps change if we vary the long-term variance θ, as well as the initial variance V_0 in a comparable way to the Black and Scholes model. We see that the locally caps for the higher variance change in the same way as in the Black and Scholes model, although the results for the lower variance significantly differ. The shorter the observation period, the smaller the difference between the calculations for lower variance compared with the benchmark variance.
While this seems illogical upon first glance, taking a closer look at the parameter used, it is evident that we also have to adjust the third variance parameter in the Heston model: the vol of vol σ_v. In the last rows, we calculate locally caps exemplary for $\sigma_v = 0.2$ (instead of $\sigma_v = 1.0$), while the other parameters are unchanged. We observe that for these parameter

Table 5.2: Influences of different variance levels on the fair locally caps - Heston Model

Heston-model	monthly	quarterly	semi-ann.	annual	globally
C for $\theta = V_0 = 0.01$	8.71	10.64	11.46	12.89	24.07
C for $\theta = V_0 = 0.0608$	8.61	10.70	12.47	15.47	29.60
C for $\theta = V_0 = 0.16$	11.20	14.52	17.52	21.74	36.08
C for $\theta = V_0 = 0.01$, $\sigma_v = 0.2$	4.85	6.99	8.95	11.83	26.34

Fair locally caps for a guaranteed rate of $g = 0.0$ % and varied variance parameter in the Heston model

combinations, the results of the Black and Scholes model and the Heston model are more comparable with each other.

Overall, we find that the volatility resp. the variance has a crucial influence on the fair locally caps. In the Heston model, all variance relating parameters (V_0, θ and σ_v) has to been observed. The shorter the calculation period for the locally caps, the greater the influence of the volatility or variance of the observed LCGC. Furthermore, we should mention that the change of the fair locally caps is small in the case of the GCGC, since the payoff is completely path-independant.

5.5 Distribution and utility under the real world measure

Bernard et al. [Ber11b] mention that the probability of the maximum payoff highlighted in the prospectus is very low. This result should disillusion investors, since the probability of such events is sometimes almost certainly zero. We will enlarge this observation by quantifying the effect.
Here, we have to understand the highest payoff for a LCGC$^{(\text{sum})}$ with monthly observation results of a summation of 60 monthly returns, which has to be almost larger than or equal to 9 %. Typical up- and downturns in the underlying should be analyzed, whereby we simulated the payoff of the different certificates under the real world measure. Furthermore, we used the fair locally caps, which depend on the new assumption calculated for the guaranteed rate $g = 0.0$ %.

5.5.1 The Black and Scholes model

Figure 5.3 shows the distribution of the simulated return rates at maturity for the benchmark case and a lower drift parameter ($\mu = 7.0$ %). Both observations illustrate that the four path-dependent certificates do not significantly differ in their distribution. The maximum payoff of the GCGC without any path-dependence is much lower than the

maximum payoff of the other certificates.
The probability distribution of the GCGC has most of its weight on the guarantee and the maximum payoff (globally cap).[9] By contrast, the LCGCs also have an accumulation at the guaranteed rate, although there is no point mass at a specific positive return rate. In comparison to the GCGC, the distribution shows that the return rates vary below and above the cap rate of the GCGC.

Figure 5.3: Simulated return rates for the LCGC$^{(\text{sum})}$ - BS model

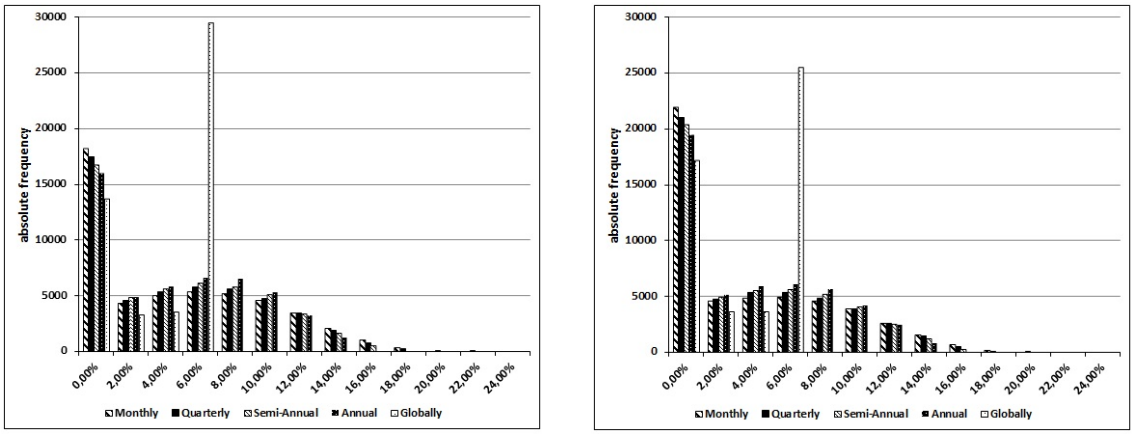

Simulated return rates for the different features of the LCGC$^{(\text{sum})}$ and the GCGC for $\mu = 9.0$ % (benchmark case, left plot) and for $\mu = 7.0$ % (right plot).

Although the characteristic of the fair LCGC$^{(\text{sum})}$ are more or less the same, we ascertain the following for the monthly observation.
On the one hand, it is observed that the LCGC$^{(\text{sum})}$ with the monthly observation has more weight on the guarantee level and the return rates above 12.0 %. On the other hand, all other calculation methods have more weight in the range between 0.0 % and 12.0 %. Overall, it can be stated that the shorter the calculation period, the lower the weights for the return rates between 0.0 % to 12.0 %. It is evident that with a higher probability of very attractive return rates above 12.0 %, the probability of only obtaining the nominal amount increases. The investor has to decide whether she is confident about a good return or if she requires a very high return, whereby the probability of only getting the nominal amount is higher. It is seen that the investor's choice is different to the question illustrated

9 The result is along the lines of the observation of the BGCs in Chapter 4.

in Chapter 4.[10]

Table 5.3: Overview of the simulated return rates - BS model

$\mu = 9.0$ %	monthly	quarterly	semi-ann.	annual	globally
average return rate in %	4.27	4.20	4.14	4.06	3.69
median in %	2.95	3.13	3.24	3.39	5.90
return = guaranteed rate (in %)	36.47	34.89	33.44	31.99	27.38
max. return rate in %	20.63	19.87	17.66	14.03	5.90
theo. max. return rate in %	36.14	25.09	19.07	14.03	5.90
$\mu = 7.0$ %					
average return in %	3.50	3.48	3.44	3.41	3.23
median in %	1.36	1.70	1.86	2.14	4.26
return = guaranteed rate (in %)	43.83	41.95	40.76	38.88	34.34
max. return rate in %	19.04	18.57	17.37	14.03	5.90
theo. max. return rate in %	36.14	25.09	19.07	14.03	5.90

Overview of the calculated figures relying on the simulated return rates for $\mu = 9.0$ % (first part) and $\mu = 7.0$ % (second part), with a fixed volatility of $\sigma = 23.50$ %.

To confirm our observation, Table 5.3 illustrates the main results of the simulation. For the benchmark case ($\mu = 9.0$ %), we identify that the average return decreases with a longer observation period, while the number of the sample-paths that only pay the guaranteed rate also declines. In addition to these results, we can mention that the median of the return rates increases with the length of the calculation period.

Furthermore, we show the simulated maximum return rates in comparison to the theoretical maximum return rates. In the Black and Scholes model, it is observed that none of the 50,000 sample-paths for the monthly, quarterly and semi-annual observations yield the maximum payoff. Only for the annual observation and the GCGC$^{(\text{sum})}$ does the simulated maximum return rate correspond with the theoretical maximum rate. Even if we quintuple the drift parameter to 45.0 %, only the maximum return rate of the semi-annual calculation will achieve the maximum payoff level. However, across all observation methods, the monthly observation leads to the best payoff.

In comparison to the benchmark case, the second part of Table 5.3 shows detailed results for the lower drift parameter. It is observed that the average return and the median are

10 The investor who is restricted to BGCs decides with the different entry strike features if she wants a fixed and relatively good return more often or a more attractive one less often.

significantly lower for the drift parameter of $\mu = 7.0$ %. Of course, the number of the simulated return rates that only pay the guarantee is also higher for the smaller drift parameter (cf. Figure 5.3 for all certificates). Compared to the average return and the median, the changes in the simulated maximum payoffs of the certificates are relatively small. In the special cases of the GCGC$^{(\text{sum})}$ and the LCGC$^{(\text{sum})}$ with the annual observation, the maximum payoffs are equal to the benchmark case. This result shows that the payoff of the certificates with longer observation periods (respectively without an observation period in the case of the GCGC) are less influenceable regarding the assumed drift parameter than the LCGC$^{(\text{sum})}$ with monthly or quarterly observation, for instance.

As mentioned in Section 5.4, the volatility seems to have a crucial influence on the simulated return rates. Since the observed returns are capped at the top but do not have a floor at the bottom, it is perspicuous that the return rates decrease with a higher volatility. If we change the volatility in analogy to the previous observation to $\sigma = 10.00$ % or $\sigma = 40.00$ %, we will find some interesting developments concerning the return rates at maturity.

Table 5.4: Volatility analysis - BS model

$\sigma = 10.00$ %	monthly	quarterly	semi-ann.	annual	globally
average return in %	6.23	6.08	5.93	5.71	4.51
median in %	6.42	6.29	6.16	6.02	5.03
return = guaranteed rate (in %)	3.51	3.31	3.16	2.95	2.75
max. return rate in %	15.74	14.80	13.06	10.38	5.03
theo. max. return rate in %	26.91	18.23	13.87	10.38	5.03
$\sigma = 40.00$ %					
average return in %	3.20	3.19	3.21	3.17	3.10
median in %	0.0	0.00	0.00	0.00	1.06
return = guaranteed rate (in %)	59.57	57.56	55.74	53.55	47.74
max. return rate in %	24.34	24.14	20.93	17.54	6.96
theo. max. return rate in %	43.17	30.73	23.73	17.54	6.96

Overview of the calculated figures relying on the simulated return rates for the benchmark case ($\mu = 9.0$ %) with $\sigma = 10.00$ % (first part) and $\sigma = 40.00$ % (second part) and the corresponding fair caps calculated from Table 5.1.

Table 5.4 confirms our assumption by using the changed volatility parameter and the corresponding fair locally caps (cf. Table 5.1).
With the low volatility of $\sigma = 10.00$ %, the average return and the median are higher. More precisely, we identify for all LCGC$^{(\text{sum})}$ an average return that is approximately 2.0 %

higher. Furthermore, we state that the median rises over the average return, which belongs to a significant change of the payoff distribution. Finally, we should mention that only a few of the simulated payoffs are equal to the guarantee (cf. $2.75 - 3.51$ %), although the observed maximum payoff decreases with the lower volatility.
The volatility of $\sigma = 40.00$ % changes the simulated results in a complete different way, whereby all medians aside from the $\text{GCGC}^{(\text{sum})}$ are equal to zero and the average return is also significantly lower. In addition, we notice that for all $\text{LCGC}^{(\text{sum})}$, over 50 % of the simulated payoff only pays the guarantee. However, the maximum payoff is marginally higher than in the benchmark case. For a better analysis, we also show the two return rate Figures depending on the volatility analysis in the Appendix B.8.
Finally, Figure 5.4 and Figure 5.5 illustrate the simulated return rates relating to the

Figure 5.4: Simulated return rates w.r.t. the monthly and quarterly $\text{LCGC}^{(\text{sum})}$ - BS model

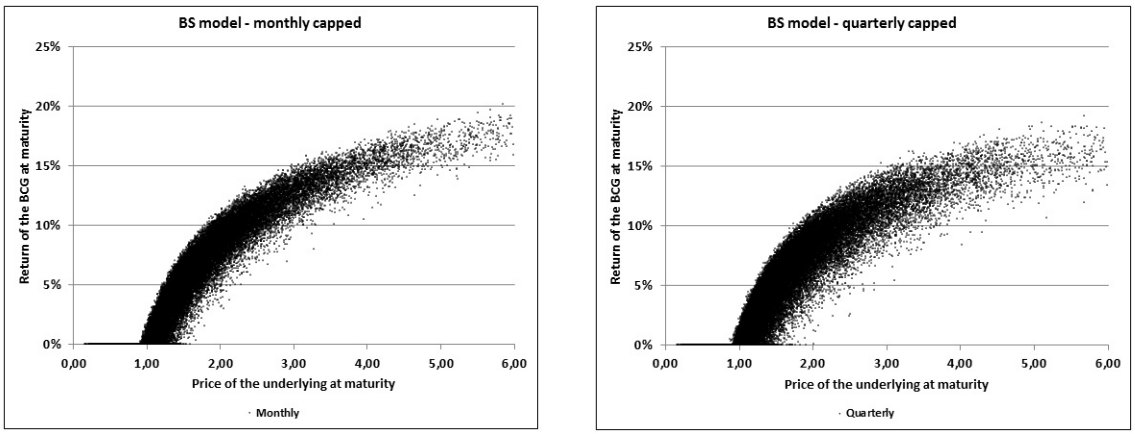

Simulated return rates at maturity for the monthly observation (left plot) andthe quarterly observation (right plot) depending on the simulated underlying price with $\mu = 9.00$ % and $\sigma = 23.50$ %. The monthly locally cap is C= 8.48 % and the quarterly locally cap is C= 12.53 %.

simulated terminal prices of the underlying at maturity. With a shorter observation period (and thus a higher number of observed returns) follows a higher maximum return rate in the simulation. While the chart flattens with a longer observation period, it is also obvious that the mass of positive and relative good returns rises with a longer observation frequency.

In a final step, we calculate the loss rates for an exemplary CRRA investor. For this reason, we use the (overall) optimal investment decision in a complete Black and Scholes

Figure 5.5: Simulated return rates w.r.t. the semi-annual and annual LCGC$^{(\text{sum})}$ - BS model

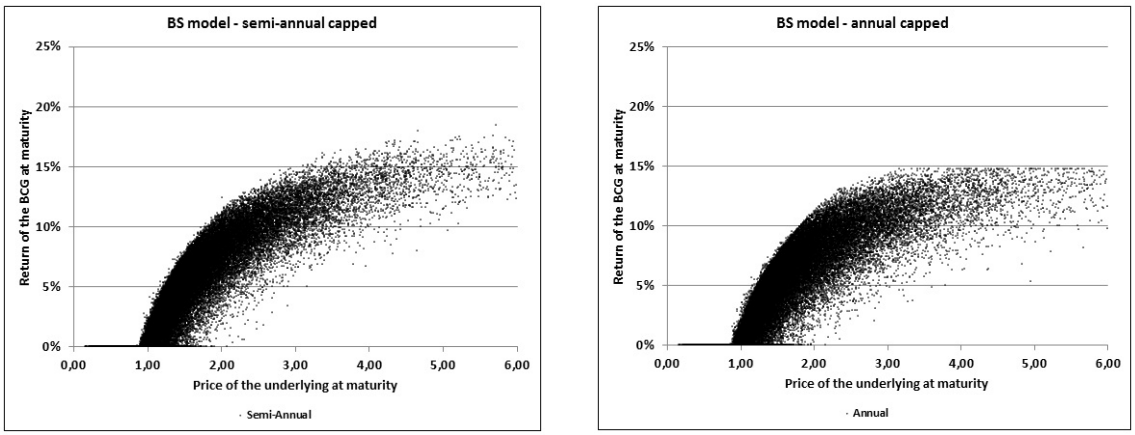

Simulated return rates at maturity for the semi-annual observation (left plot) and the annual observation (right plot) depending on the simulated underlying price with $\mu = 9.00$ % and $\sigma = 23.50$ %. The semi-annual cap is C= 15.95 % and the annual cap is C= 20.34 %.

model, which is well known for the special case of a CRRA utility function with $u(w) = \frac{w^{1-\gamma}}{1-\gamma}$ for $w > 0$ and $u(w) = -\infty$ for $w \leq 0$. Here, the optimal proportion of wealth φ^* invested in the risky asset S is constant during the observed period [0,T], i.e.

$$\varphi^* = \frac{\mu - r}{\gamma \sigma^2} \tag{5.14}$$

The terminal value V_T^{φ} of a so-called Constant-Mix strategy, which is characterized by a constant investment faction of φ and initial wealth V_0, is given by

$$V_T^{\varphi} = V_0 \, e^{\left(r + \varphi(\mu - r) - \frac{1}{2}\varphi^2\sigma^2\right)T + \varphi\sigma W_T}$$

The expected utility (under the real world measure P) is

$$E_P\left[u(V_T^{\varphi})\right] = \frac{(V_0)^{1-\gamma}}{1-\gamma} e^{(1-\gamma)\left(r + \varphi(\mu - r) - \frac{1}{2}\gamma\varphi^2\sigma^2\right)T}.$$

The certainty equivalent CE_T^{φ}, which is defined by the certain amount that makes the investor indifferent between achieving this certain amount (at T) or using the strategy π,

i.e.

$$u\left(CE_T^{\varphi})\right) = E_P\left[u\left(V_T^{\varphi}\right)\right]$$

then is

$$CE_T^{\varphi} = V_0 e^{\left(r+\varphi(\mu-r)-\frac{1}{2}\gamma\varphi^2\sigma^2\right)T}.$$

In particular, the benchmark certainty equivalent is

$$CE_T^{*} = V_0 e^{\left(r+\frac{1}{2\gamma}\left(\frac{\mu-r}{\sigma}\right)^2\right)T}. \tag{5.15}$$

Second, we consider the expected utility derived by an investment in a LCGC and GCGC, respectively. The following proposition yields a simplified procedure to approximate the expected utility by means of the Monte Carlo method.

Definition 7 (LCGC$^{(\mathrm{sum})}$: Expected utility, certainty equivalent and loss rate)

(i) For a set $\{t_0 = 0,t_1,...,t_n = T\}$ of observation dates, the expected utility $EU^{LCGC^{(sum)}}$ of a Locally Capped Garant Certificate is calculated within the following simulation. In order to approximate the expected utility, we rely on the Monte Carlo method and simulate k sample-paths of the tuple $(S_{t_0},S_{t_1},\ldots,S_T)$. We obtain for $j = 1,\ldots k$ and $i = 1,\ldots n$ the underlying price $S_{t_i}(\omega_j)$ to calculate the corresponding payoff for each sample-path. Subsequently, for $j = 1,\ldots k$ holds

$$\begin{aligned} &LCGC_T^{(sum)}(\omega_j) \\ &= (1+G) + \max\left(0, \sum_{i=1}^{n} \min\left(C, \frac{S_{t_i}(\omega_j) - S_{t_{i-1}}(\omega_j)}{S_{t_{i-1}}(\omega_j)}\right) - G\right) \end{aligned} \tag{5.16}$$

and the overall expected utility is given by the mean of the expected utility of each sample path

$$EU_T^{LCGC^{(sum)}} = \frac{1}{k}\sum_{j=1}^{k} \frac{\left(LCGC_T^{(sum)}(\omega_j)\right)^{1-\gamma}}{1-\gamma}. \tag{5.17}$$

(ii) The certainty equivalent $CE_T^{LCGC^{(sum)}}$ *of a LCGC is given by*

$$CE_T^{LCGC^{(sum)}} = \left[(1-\gamma)EU_T^{LCGC^{(sum)}}\right]^{\frac{1}{1-\gamma}}. \tag{5.18}$$

(iii) The loss rate l_T *of a LCGC (benchmarked on the certainty equivalent of the optimal Merton strategy) is given by*

$$l_T = \frac{\ln\left(\frac{CE_T^*}{CE_T^{LCGC^{(sum)}}}\right)}{T} \tag{5.19}$$

where $CE_T^* = V_0 e^{\left(r+\frac{1}{2\gamma}\left(\frac{\mu-r}{\sigma}\right)^2\right)T}$ *and* $V_0 = LCGC_{t_0}^{(sum)}$.

We decide to illustrate the calculated loss rates for the two drift parameters used in Table 5.3. Remember that we assume an investor with a risk aversion parameter $\gamma = 5$.
Hence, Figure 5.6 shows in the left plot the benchmark case where the loss rates for the four LCGCs as well as the GCGC are calculated with an assumed drift parameter of $\mu = 9.0$ %. In the right plot, we state the results for the lower drift parameter of $\mu = 7.0$ %.

Figure 5.6: Loss rates for all observation types - BS model

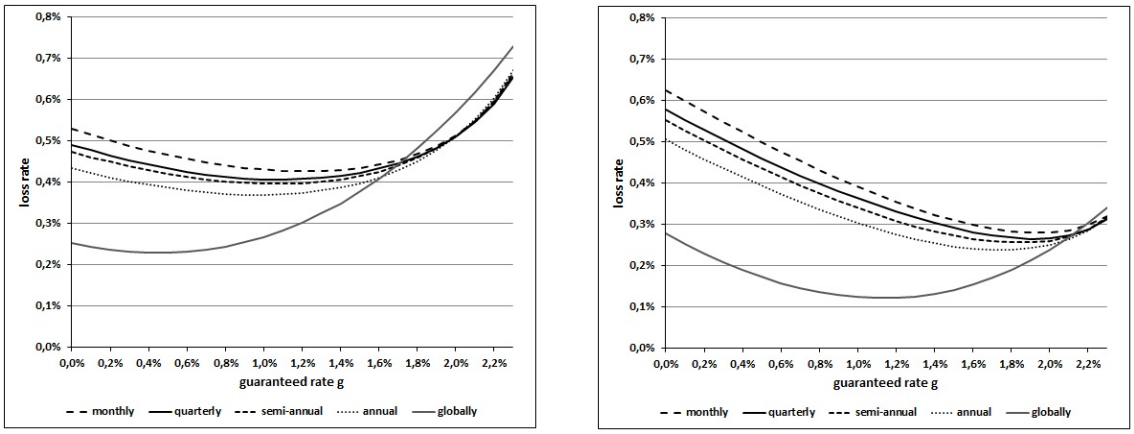

Loss rates in the Black and Scholes model for a risk aversion of $\gamma = 5$; $\mu = 9.0$ % (benchmark case, left plot) and $\mu = 7.0$ % (right plot).

It is seen that all loss rates in the benchmark case find a minimum significant above the guaranteed rate (resp. guarantee) of $G = g = 0.0$ %. More precisely, the GCGC investor has a minimum loss rate at a guaranteed rate of $g = 0.5$ %. For each of the LCGCs, the corresponding minimum is situated between $g = 1.0$ % and $g = 1.2$ %. Of course, the

path-dependent certificates have a different development from the path-independent GCGC: while the loss rates for the LCGCs are higher for all guaranteed rates below $g = 1.6$ %, we identify a turning point where the loss rates for the GCGCs rises above the loss rate regarding the LCGCs.
Comparing the Locally Capped Garant Certificates to each other, we can mention the following results. On the one hand, it is seen that the shorter the observation period, the higher the loss rate. Since the benchmark certainty equivalent CE_T^* is path-independent, it looks like the level of path-dependence (number of observation dates) is responsible for the difference. On the other hand, all LCGCs seem to be converging with a guaranteed rate increasing to the risk-free interest rate. This can be explained by the notion that there will be only a minimal difference in the payoff distribution since all certificates have relatively low fair locally caps, thus all offering more or less a bond-like payoff.

Looking at the right plot of Figure 5.6, where we assume a lower drift parameter, it is evident that some results differ from the benchmark case. First, the position of the minimum loss rates change in a way whereby a higher guaranteed rate is observed in each case. Second, the overall loss rates for the path-dependent certificates start at a significant higher level. Finally, they all continuously decrease with a higher guaranteed rate until they find their minimum at around $g = 2.0$ %. The observed investor (with $\gamma = 5$) seems to feel confident with less upward participation when she receives a higher guaranteed rate.

5.5.2 The Heston model

With the findings of the previous sections, we assume the following for the $\text{LCGC}^{(\text{sum})}$ regarding the Heston model. Since it is illustrated in Section 5.4 that the certificates in the Heston model have lower fair locally caps, we also assume that the simulated return rates at maturity as well as the average return and the median are lower than in the Black and Scholes model.
The simulated results are shown in Figure 5.7, where the simulated return rates at maturity for the different certificates in Heston model are illustrated. The following Table 5.5 provides a detailed overview of the figures regarding the simulated return rates. To allow a comparison to the Black and Scholes model, two drifts are applied. We use $\overline{\lambda} = 1.2$ as the benchmark case. Furthermore, the results based on the calculation with $\overline{\lambda} = 0.85$ can be

Figure 5.7: Simulated return rates for the $\text{LCGC}^{(\text{sum})}$ - Heston model

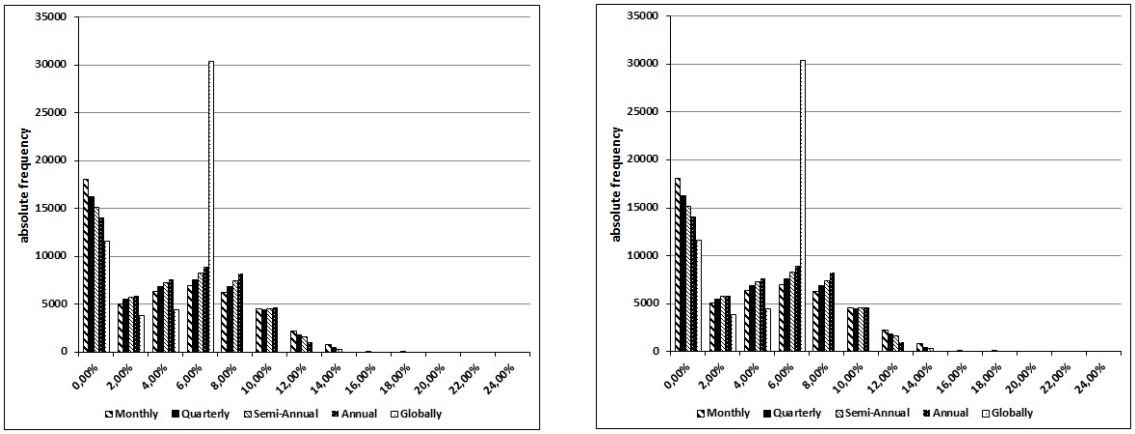

Simulated return rates for the different features of the $\text{LCGC}^{(\text{sum})}$ and the $\text{GCGC}^{(\text{sum})}$ for $\overline{\lambda} = 1.2$ (benchmark case, left plot) and $\overline{\lambda} = 0.85$ (right plot).

used for a comparison with the lower drift parameter.[11]

With the results illustrated in Figure 5.7, we recognize that our assumptions regarding the average return and the median are correct. In the benchmark case, the average return in the case of a monthly observation is about 0.7 % lower, although this difference is reduced with the length of the observation period. For the annual observation, a difference of almost 0.4 % is observed and less than 0.3 % for the GCGC. For the monthly, quarterly and semi-annual observations, the median is lower compared to the Black and Scholes benchmark case. In the case of the annual observed LCGC and the GCGC, the median calculated in the Heston model is above the median calculated by the Black and Scholes model.

This return rate distribution could be explained by two reasons. First, we mentioned that the fair locally caps calculated in the Heston model are below the fair caps in the Black and Scholes model; thus, as a natural result, the average returns in the Heston model are lower. Regarding the differences between the lengths of the observation periods, the stochastic volatility seems to have an influence on the median. In Section 5.4, it is observed that higher volatility has a huge influence on the fair locally caps. Assuming the calculated

11 According to the definition in Lui [Lui07] $\overline{\lambda} = 1.2$ results in a drift parameter, which can be compared to $\mu = 9.00$ % in the Black and Scholes model. The drift calculated by $\overline{\lambda} = 0.85$ is comparable to the low drift parameter. (cf. Appendix **??**).

fair locally caps, the variation of the volatility has a negative influence since the positive returns are capped and the negative returns are not floored.

Now, we should consider the change of the described return rate distribution. Overall, we see less weight at the guaranteed rate in the Heston model whereat the difference is very low in the case of a monthly observation. The longer the observation period, the lower the weight at the guaranteed rate in the Heston model. In addition, we recognize a shift in the distribution to range of *good positive* returns ($2.00 - 8.00$ %), which means that there are fewer simulated payoffs only paying the guaranteed rate, but there are also less very high return rates in comparison to the benchmark case of the Black and Scholes model.
In addition to the benchmark case, we also make a calculation for $\overline{\lambda} = 0.85$. In comparison to the Heston model benchmark case, all relevant figures are lower, aside from the weight at the guarantee. Looking at the calculation of the Black and Scholes model with the lower drift parameter, we notice that the development of the median changes, whereby all calculated medians in the Heston model are above the calculation in the Black and Scholes model.

Table 5.5: Overview of the return rates - Heston model

$\overline{\lambda} = 1.2$	monthly	quarterly	semi-ann.	annual	globally
average return in %	3.57	3.59	3.61	3.62	3.43
median in %	2.67	2.99	3.20	3.41	5.14
return = guaranteed rate (in %)	36.00	32.55	30.23	28.12	23.05
max. return rate in %	18.35	17.25	14.75	11.26	5.14
theo. max. return rate in %	36.08	22.56	15.91	11.26	5.14
$\overline{\lambda} = 0.85$					
average return in %	3.09	3.12	3.14	3.17	3.09
median in %	1.72	2.10	2.38	2.60	4.78
return = guaranteed rate (in %)	41.21	38.17	36.07	33.79	28.94
max. return rate in %	18.00	16.27	14.73	11.26	5.14
theo. max. return rate in %	36.08	22.56	15.91	11.26	5.14

Overview of the calculated figures relying on the simulated return rates for $\overline{\lambda} = 1.2$ (first part) and $\overline{\lambda} = 0.85$ (second part)

In analogy to the Black and Schloles model, we will analyze different volatility resp. variance levels in the Heston model. Since the Heston model takes into account stochastic volatility, the variation that can be compared to the Black and Scholes model is complicated. First,

it seems meaningful to value the simulated payoffs for different levels of variance in terms of V_0 and θ. Nonetheless, by varying the variance, we have to change $\overline{\lambda}$ so that we can calculate a comparable drift parameter (cf. Appendix B.2).
For the case of low variance, we use $V_0 = \theta = 0.01$ and the corresponding parameters $\overline{\lambda} = 6.6$ and $V_0 = \theta = 0.16$, as well as $\overline{\lambda} = 0.4125$ for the high variance simulation.[12] Additionally, we calculate a third simulation where we change the vol of vol from $\sigma_v = 1$ to $\sigma_v = 0.2$ (cf. Table 5.2). The results are illustrated in Table 5.6.[13]

Table 5.6: Variance analysis - Heston model

$V_0 = \theta = 0.01$	monthly	quarterly	semi-ann.	annual	globally
average return in %	4.85	4.56	4.36	4.19	3.69
median in %	4.24	4.20	4.18	4.16	4.31
return = guaranteed rate (in %)	1.76	1.63	1.53	1.47	1.51
max. return rate in %	25.02	20.09	14.62	9.95	4.31
theo. max. return rate in %	36.57	22.81	15.28	9.95	4.31
$V_0 = \theta = 0.16$,$\overline{\lambda} = 0.4125$					
average return in %	2.80	2.84	2.90	2.93	2.96
median in %	0.00	0.00	0.00	0.00	2.29
return = guaranteed rate (in %)	60.41	57.17	54.46	52.09	44.57
max. return rate in %	21.42	21.59	19.84	14.72	6.16
theo. max. return rate in %	40.87	27.24	20.25	14.72	6.16
$V_0 = \theta = 0.01$, $\sigma_v = 0.2$,$\overline{\lambda} = 6.6$					
average return in %	5.85	5.67	5.52	5.31	4.29
median in %	6.01	5.84	5.73	5.58	4.68
return = guaranteed rate (in %)	3.44	3.10	2.86	2.59	2.19
max. return rate in %	14.94	13.76	11.83	9.30	4.68
theo. max. return rate in %	27.27	17.49	12.79	9.30	4.68

Overview of the calculated figures relying on the simulated return rates for different levels of variance.

The change to a higher and lower variance has a significant influence on the payoff of the certificates. As presented in the previous section, a low variance (or a low volatility in the BS-model) has a positive influence on the left side of the distribution, whereby the weight at the guaranteed rate is halved. However, with a smaller average return as

12 Applying the equation $\mu = \overline{\lambda} V_0$, we have to assume that a changed $\overline{\lambda}$ is comparable with the drift parameter by higher or lower variance.

13 The plots illustrating the change in the return rate distribution at maturity for the different levels of variance are presented in Appendix B.8, where we also illustrate the same figures in analogy to the Black and Scholes model.

well a smaller maximum return, it is observed that the probability of very attractive returns also decreases. A tighter price range of the underlying is followed by observed returns that are below the fair locally caps. At once, the amount of negative returns decreases.

The simulation with a higher variance of $\theta = 0.16$ shows positive and negative changes from the investor's perspective. Of course, the number of simulated payoffs that only pay the guaranteed amount is higher than in the benchmark case, which implicates an explicit smaller median. In opposite to the Black and Scholes calculation the average return is higher for all $\text{LCGC}^{(\text{sum})}$ than in the benchmark case. This effect can be explained by the fact that the realized variance over the entire investment period of the certificate can significantly vary between V_0 and the long-term variance θ.

Finally, the loss rates for the $\text{LCGC}^{(\text{sum})}$ and the GCGC in the Heston model are illustrated in Figure 5.8. For this calculation, we refer to the optimal portfolio process introduced in Lui [Lui07]. The optimal portfolio process replaces the Merton strategy (used in the Black and Scholes model) since we take into account stochastic volatility. The optimal portfolio process π_t in the Heston model is separated into an optimal static investment and an inter-temporal hedging. The static investment could be compared to the constant proportion for the investment in the risky assets in the Black and Scholes model. However, the optimal portfolio process will result in a higher investment fraction if the inter-temporal hedging is positive. In the benchmark case, the optimal static investment proportion is given by 24.0 % and 17.0 %. A brief overview of the derivation of the optimal portfolio process in the Heston model is provided in Appendix B.4.
For the optimal portfolio strategy we calculate the expected utility and the certainty equivalent by Monte Carlo methods applying Definition 7 on the Heston model with

$$EU_T^{(*,\text{Heston})} = \frac{1}{k}\sum_{i=1}^{k}\frac{(V_T^{\pi_i})^{(1-\gamma)}}{1-\gamma} \text{ and } CE_T^{(*,\text{Heston})} = \left((1-\gamma)EU_T^{(*,\text{Heston})}\right)^{(\frac{1}{1-\gamma})} \tag{5.20}$$

where $V_T^{\pi_i}$ describes the terminal wealth of the i-th path of the simulated strategy π_t^*, considering the equity path S_t^i and the variance path V_t^i (cf. Chapter 4).

The corresponding expected utility of the LCGCs are calculated by

$$EU_T^{(LCGC^{(\mathrm{w})},\mathrm{Heston})} = \frac{1}{k}\sum_{i=1}^{k}\frac{(LCGC_T^{i((\mathrm{w}),\mathrm{Heston})})^{(1-\gamma)}}{1-\gamma} \tag{5.21}$$

$$CE_T^{(LCGC^{(\mathrm{w})},\mathrm{Heston})} = \left((1-\gamma)EU_T^{(LCGC^{(\mathrm{w})},\mathrm{Heston})}\right)^{\left(\frac{1}{1-\gamma}\right)} \tag{5.22}$$

where w $\in$ {sum,com} Finally, the loss rate is calculated by

$$l_T = \frac{\ln\left(\frac{CE_T^{(*,\mathrm{Heston})}}{CE_T^{(LCGC^{(\mathrm{w})},\mathrm{Heston})}}\right)}{T}. \tag{5.23}$$

Figure 5.8: Loss rates for all observation types - Heston model

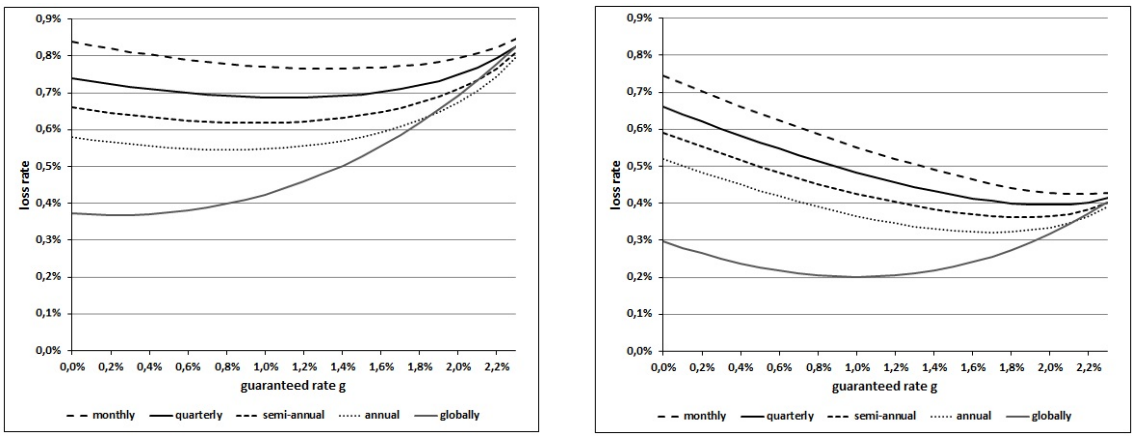

Loss rates in the Heston model for a risk aversion of $\gamma = 5$; $\overline{\lambda} = 1.2$ (benchmark case, left plot) and $\overline{\lambda} = 0.85$ (right plot).

The illustration in Figure 5.8 definitely features some comparable characteristics to the results in the Black and Scholes model. However, we will first analyze the properties concerning the different observed cases in the Heston model.

The left plot of Figure 5.8, which illustrates the Heston model benchmark case, shows loss rates that tend to be higher for a shorter observation period. The GCGC illustrates the lowest loss rates for almost all guaranteed rates, while the LCGC with the monthly observation has the highest loss rates. For the lowest assumed guaranteed rate $g = 0.0$ %, the difference between the calculated minimum and maximum loss rate is almost 0.5 %.

This range becomes significantly smaller for higher guaranteed rates, whereby the difference is only marginal for the highest assumed guaranteed rate.
Depending on the observation frequency, the corresponding loss rates finds a minimum at a guaranteed rate between 0.3 % and 1.3 %. Since the graphs for the Locally Capped Garant Certificates are very flat, the difference between the minimum loss rate and the loss rate for $g = 0.0$ % is marginal. By contrast, the spread between the minimum and the maximum loss rate of the GCGC is significantly larger.
The observation of the loss rates regarding the lower drift related to $\overline{\lambda} = 0.85$ do not show new attitudes in the developments of the certificates. Only the overall level of the loss rates should be mentioned: for all certificates and almost all guaranteed rates, the loss rates are lower than in the benchmark case. Looking at the two plots, we also identify a kind of a converging point, which is significantly higher in the benchmark case ($l_T \approx 0.8$ %) than in this calculation ($l_T \approx 0.4$ %).

Finally, we compare the loss rates based on the Black and Scholes model with the loss rates regarding the Heston model. We can mention that the overall development is comparable, given that both benchmark cases find their minimum loss rate for comparable guaranteed rates. However, in the Heston model, the absolute differences between the loss rates of the four path-dependent certificates are clearly higher than in the Black and Scholes model. Morever, the position of the relevant Globally Capped Garant Certificate is different.
In the Black and Scholes model, we identify a swiftover in the level of the GCGC. For low guaranteed rates, the corresponding loss rates are considerably below the other loss rates. However, after a turning point, they are higher than the loss rates of the LCGC.
Indeed, in the Heston model, the loss rates for the path-independent certificates are higher than the loss rates of the Locally Capped Garant Certificates with an annual or semi-annual observation when the guaranteed rate is very high. Nonetheless, overall, it holds that the loss rates are higher with the degree of path-dependence.

The second case shows the same characteristics, with the exception that the loss rates based on the lower drift parameter in the Black and Scholes model are above the loss rates from the benchmark case at the beginning and subsequently decrease below the comparable ones. In the Heston model, the calculated loss rates based on the $\overline{\lambda} = 0.85$ are always below the benchmark case loss rates.
Since the loss rates in the Heston model differ more among each other, we should mention that this development could result from the stochastic volatility, whereby the variance and

the drift parameters are non-constant during the observation.

5.6 Conclusion

We observe the class of Globally Capped Garant Certificates as well as different observation periods of the path-dependent Locally Capped Garant Certificates. Focusing on the fair locally caps, which define the maximum payoff at maturity, we observe that the shorter the observation periods (and thus the higher the number of observed returns), the higher the fair locally caps.

However, it is evident that the optimality of the derived payoff distribution for each combination of guaranteed rate and locally caps depends on the investor's preference. Since we assume a CRRA investor who can only choose of the restricted set of LCGCs (resp. GCGCs), the financial market is incomplete from the investor's perpective. Knowing the overall optimal payoff profile of the CRRA investor, we illustrate that the observed certificates differ from the overall optimal product. However, the investor can select a optimal LCGC resp. GCGC.

By investing in a specific LCGC (resp. GCGC), the investor decides if she is confident about a good return or if she requires a very high return, whereby the probability of simply getting the guaranteed amount is higher. The analysis of the return rates shows that the probability of a very high return rate is almost zero for LCGC with short observation periods. Furthermore, the simulations illustrate that the weight at the guaranteed rate significantly increases with the higher return rates. Finally, we calculate the loss rates for a CRRA utility maximizing investor with $\gamma = 5$ and mention that she suffers from higher locally caps based on short observation periods. Furthermore, we identify an optimal guaranteed rate above $g = 0.0$ %, which leads to a minimum loss rate.

Comparing the results regarding the Black and Scholes model to those of the Heston model, the following should be mentioned. The overall developments in the pricing as well as the analysis under the real world measure do not significantly differ. Moreover, the difference could naturally result from the assumed model parameter. Only the loss rate calculated in the Heston model slightly differs, possibly due to the stochastic volatility, which also influence the drift parameter.

CHAPTER 6

Issuers default risk and Best Garant Certificates

6.1 Introduction

In 2008, the financial world was prompted to realize that financial institutions such as the Lehman Brothers Investment Bank could become insolvent. Accordingly, default risk returned into the minds of the market participants.
In particular, the traded volume in the structured product market strongly increased. Interestingly, however, default risk had been analyzed a long time before the financial crises began.
We now aim to combine the analysis of issuer default risk with one class of structured products that has become increasingly popular during the last decade. Therefore, we focus on structured products that give an upward participation on the excess return of an underlying while simultaneously granting a guarantee. Our main focus is on products that are also advertised as granting a special return feature.
Here, the return of the underlying is not measured in terms of the initial price of the underlying; rather, the entry price is determined according to the minimum (or average) price based upon a certain observation period.[1] These certificates are called Best Garant Certificates (including Best-In and Best-Entry Garant Certificates) and they belong to the family of Garant Certificates. Normally, the underlying of a Best Garant Certificate is an equity index; for example, traded Best Garant Certificates are written on DJ Euro Stoxx 50.

In general, the protection feature refers to the nominal amount of the certificate. In

1 As illustrated in Chapter 4, the length of the observation period of the Best Garant Certificates is generally between three and six months, whereby the price of the underlying is observed weekly or monthly. The entire investment period varies between three and five years.

the case of the Best Garant Certificate, the payoff is floored by the guarantee amount, which could be higher than the nominal amount. Finally, the amount will be paid regardless of how the underlying evolves during the investment horizon.[2] In addition, the investor participates in the excess return of the underlying. A special feature is given by determining the excess return with respect to a *best* (resp. minimum) entry or average entry price. In the case of the best entry price, the return is measured in terms of the quotient implied by the terminal price of the underlying and the minimum price of the underlying with respect to a certain observation period. Alternatively, there are also variants of Best Garant Certificates for which the return is measured with respect to the average price determined during the observation period. However, neither the guarantee nor the additional feature in the form of the *entry strike* come for free; rather, the investor pays an implicit premium by giving up some of her upward participation, i.e. the payoff is also capped. In particular, the return of the underlying (the upward participation) is capped at a cap rate c, which is higher than the guaranteed rate g. In summary, the payoff of a Best Garant Certificate is specified in terms of the observation period $\underline{T}^{\text{obs}}$ (with the last observation date t_N), the contract horizon T with $T > t_N$, the guaranteed rate g and the cap rate c with $c > g$. In addition, the contract also specifies how the entry strike is determined, whereby we distinguish between a fixed strike $K^{(\text{fix})}$, average strike $K^{(\text{ave})}$ and minimum strike $K^{(\text{min})}$ setting.[3]

Regarding the characteristics of the issuing company, we use the recovery rate R and the initial debt D_{t_0}, which describes the debt of the issuer at the corresponding issue date.
We should mention that the value for all defaultable Best Garant Certificate (DBGC) is significant influenced by the issuer depending parameter. The value of the DBGC decreases with a higher initial debt D_{t_0} of the issuer and increases with a higher recovery rate R.
Of course, we could refer to the analysis in Chapter 4, since some developments are comparable for constant D_{t_0} and R. Thus, the contract value with average entry strike $K^{(\text{ave})}$ is, ceteris paribus, lower than the one implied by a minimum strike $K^{(\text{min})}$ ($K^{(\text{min})} \leq K^{(\text{ave})}$), since the price of a call option increases with the strike. Independent of the model assumptions, the value of a defaultable Best Garant Certificate increases with the guaranteed rate g, although it decreases with the cap rate c.
However, we also ascertain additional characteristics that rely on taking into account

2 Of course, the guarantee only prevails if the issuer remains solvent at maturity; otherwise, the payoff at maturity depends, amongst other things, on the recovery rate of the issuer and could be significant below the nominal amount.

3 Unless mentioned otherwise, the nominal value is set equal to one, i.e. $N = 1$.

default risk. For example, we calculate fair (g,c)-tuple for varying recovery rate R and initial debt D_{t_0}. Furthermore, we also focus on the the influence of default risk on the return rate distribtion. Besides the standard payoff profiles used for marketing such certificates, we illustrate the return rates in the case of an optional issuer's default regarding the guaranteed rate, the cap rate and the entry strike setting.
Finally, we try to answer the question of which parameter influences the product design most.

For our analysis, we assume that the financial market is complete from the perspective of the the issuer. Thus, the issuer knows her solvency at issue date and can offer fair DBGCs including her probability of default. With the application of the model and the complete market assumption for the issuer, we are able to compare payoff profiles for different solvencies. Assuming that the optimal Constant-Mix strategy is not affected by any default risk, the investor could suffer from the suboptimal structure of the offered product and an optional default of the issuer, although the payoff profile looks more attractive.
Our main contributions are as follows. We derive and analyze fair combinations of guaranteed and cap rates in a Black and Scholes model with default risk. Based upon the observation that both an entry price that tends to be lower and a higher guaranteed rate afford a lower (fair) cap rate, the *best* entry strike does not necessarily improve the return distribution of the Best Garant Certificate in the context of fair contracts. Therefore, we consider the question of whether an investor benefits from the best entry strike setting and the guarantee.

Furthermore, we illustrate the risk associated with an issuing company that could become insolvent during the entire investment period. We analyze the optimality (sub-optimality) of different DBGCs for an expected utility maximizing CRRA investor who is restricted to the class of DBGCs. Interestingly, it emerges that a defaultable Best Garant investor could profit from a higher guarantee, which results in a lower cap rate. In the case of a fair cap rate, the utility of a DBGC increases with the guaranteed rate. This could be explained by the fact that with a higher guaranteed amount, the amount calculated by the recovery rate in the case of an issuer's default is also higher.
In addition, we show that the *best* entry feature, i.e. the minimum strike setting and the average strike setting, are suboptimal compared to the fixed strike setting. We illustrate our results by means of real market data and take into account default risk. We consider the model prices at issue date and loss rates that are implied by traded DBGCs. It is

observed that all certificates are highly overvalued at issue date, although in relative terms the path-dependent DBGCs are more overvalued than the DBGC with the fixed strike setting.
The loss caused by a suboptimal product design, which results from the comparison to the *non-defaulable* Constant-Mix strategy, is significantly higher compared to the loss due to the fact that the certificates includes margins. We compare the results to the product design of currently offered Best Garant Certificates.
Our observations concerning the comparison of model prices and marked prices are unsurprising. When we take into account default risk, it emerges that the prices at the corresponding issue date of the certificates are highly overvalued. Furthermore, the prices of the DBCG regarding the minimum strike and the average strike setting are more overvalued than the price of DBGC with fixed strike settings. This may be explained by the common observation that a more complex and, for the investor, difficult to understand product provides the issuer with the opportunity to gain a higher margin. This result is along the lines of Carlin [Car09], who illustrates that institutions could try to rise their profits by making their product more complex. An overview of relating literature concerning structured products is given in Section 2.2. Furthermore, we refer to Section 2.3 where we illustrate some related literature regarding default risk.

The remainder of this chapter is organized as following. In Section 6.2.1, we illustrate the payoff structure of DBGCs and introduce the three settings: fixed strike, average strike and minimum strike. The model description is illustrated in Section 6.2.2 and the assumed market data are summarized in Section 6.3. In Section 6.4, we consider the pricing of BGCs with fixed, average and minimum strike settings regarding a defaultable Black and Scholes model setup. We change to the perspective of the investor in Section 6.5, before we focus on the return rate distribution under the real world measure (Sec. 6.5.1) and illustrate the corresponding loss rates (Sec. 6.5.2). Illustrative results based upon market prices under issuer risk can be found in Section 6.6. Finally, Section 6.7 concludes the chapter.

6.2 Model assumptions and Product Specification

In this section, we introduce the relevant product specification of the observed Best Garant Certificate. Additionally, we illustrate the Black and Scholes model with default risk. Finally, we show the necessary adjustments of the product specification which result by the default risk.

6.2.1 Standard product specification

As mentioned in the introduction, the payoff of a BGC is specified in terms of the observation period $\underline{T}^{\text{obs}}$ (with the last observation date t_N), the contract horizon T ($T > t_N$), the guaranteed rate g and the cap rate c ($c > g$). The guaranteed rate and the cap rate prevail regarding the nominal contract value N. In general, the investor receives at least a payoff equal to the guaranteed amount Ne^{gT}. However, she does not receive a payoff higher than the maximal amount Ne^{cT} ($c > g$). The entry strike is determined according to an observation period denoted by $\underline{T}^{\text{obs}}$, where

$$\underline{T}^{\text{obs}} = \{t_0 = 0 < t_1 \ldots < t_N\} \tag{6.1}$$

and ($t_N < T$). In the following, we consider three possibilities concerning how the entry strike is determined, i.e. we distinguish between a fixed strike $K^{(\text{fix})}$, minimum strike $K^{(\text{min})}$ and average strike $K^{(\text{ave})}$setting. In particular, we use the conventions

$$K^{(\text{fix})} := K^* > 0 \tag{6.2}$$

$$K^{(\text{ave})} := \frac{1}{N+1} \sum_{i=0}^{N} S_{2,t_i} \tag{6.3}$$

$$\text{and } K^{(\text{min})} := \min_{i=0,\ldots,N} S_{2,t_i} \tag{6.4}$$

where S_{2,t_i} denotes the price of the underlying at time t_i ($t_i \in [0,t_N]$). For the sake of simplicity, we normalize $S_{2,t_0} = 1$. In the case of an issuer default, the calculated payoff has to be multiplied by the recovery rate R with $0 \leq R \leq 1$. In the following Definition we illustrate the payoff function without observing the optimal default of the issuer.[4]

Definition 8 (Payoff of a Best Garant Certificate) *The payoff of a Best Garant Certificate with a nominal amount N, observation period $\underline{T}^{obs}$, maturity T, guaranteed rate g and cap rate c ($c \geq g$) is given by*

$$h(S_{2,t_0},\ldots,S_{2,t_N},S_{2,T}) = N\left(e^{gT} + \left[\frac{S_{2,T}}{K^{(w)}} - e^{gT}\right]^+ - \left[\frac{S_{2,T}}{K^{(w)}} - e^{cT}\right]^+\right) \tag{6.5}$$

where $w \in \{fix, ave, min\}$.

4 In practice, Definition 8 is the basis for the illustrations in marketing prospectus. However, we will use Definiton 8 to derive the relevant payoff function for the DBGC.

6.2.2 The Black and Scholes model with default risk

We use the model from Goetz et al. [Goe10], which expands the standard Black and Scholes framework by a second Stochastic Differential Equation (SDE), modelling the value per share resp. the equity price of the issuer to take into account default risk. The model of Goetz et al. [Goe10] uses two correlated stochastic processes: first, the underlying dynamics are modeled as in the Black and Scholes framework; and second, the second stochastic process illustrates the equity price of the issuer, referring to their total debt to equity ratio. For such a calculation, many parameters of the issuer are needed.
In contrast to Goetz et al. [Goe10], we will not take into account any dividend payments from the issuer, so that the system of SDE has the form

$$\begin{aligned} dS_{1,t} &= rS_{1,t}dt + \sigma_1 \left(D_{1,t} + S_{1,t}\right) dW^1 \\ dS_{2,t} &= rS_{2,t}dt + \sigma_2 S_{2,t} dW^2 \end{aligned} \tag{6.6}$$

where ρ describes the correlation between the two Brownian motions W^1 and W^2. Furthermore, $D_{1,t}$ is the total debt per share of the issuer at time t and σ_1 describes the corresponding volatility of the issuer's equity price $S_{1,t}$. The parameter of the other SDEs are well-known from the standard Black and Scholes model, although we change the denomination of the volatility of the underlying to σ_2. As always, the risk-free interest rate is given by r.
Finally, we define the time to default by a stopping time

$$\xi = \inf \left\{ t > 0 : S_{1,t} \leq 0 \right\} \tag{6.7}$$

This event has a positive probability, since the stock price dynamics of the issuer follows a shifted log-normal distribution.
To be more precise, we take a brief look at the derivation of these formulae. Let

$$\frac{dV_{1,t}}{V_{1,t}} = rdt + \sigma_1 dW^1 \text{ and } V_{1,0} = S_{1,0} + D_{1,0} \tag{6.8}$$

the dynamics of the asset value per share at time t of the issuer. We assume a deterministic issuer's debt by

$$D_{1,t} = D_{1,0} e^{rt} \tag{6.9}$$

By this definition, the default of the issuer can be expressed by the stopping time

$$\tau = \inf \{t > 0 : V_{1,t} \leq D_{1,t}\} \tag{6.10}$$

For $\tau > t$, we denote the equity per share by $S_{1,t} = V_{1,t} - D_{1,t}$ and $S_{1,t} = 0$ if $\tau \leq t$. Finally, we are able to characterize the default event by the above equation (cf. (6.10)).
For completeness, we list the two Propositions derived from GOETZ et al. [Goe10], which give the closed form solution for the defaultable zero bond and the defaultable call option.

Proposition 6 (Price of a defaultable zero bond and call option) *Let r be the constant risk-free interest rate, T the time to maturity, $S_{2,t}$ the price of the underlying and $S_{1,t}$,$D_{1,t}$ and σ_1 describes the corresponding parameter of the issuer. Subsequently, for each time $t \leq T$, it holds that*

(i) The price Z_t^D of a zero bond guaranteed by the issuer who is defaultable with recovery rate zero is given by

$$Z_t^D = e^{-r(T-t)} \left(\mathcal{N}(d_3) - e^{x_1}\mathcal{N}(d_4)\right) \tag{6.11}$$

where $\mathcal{N}(\cdot)$ denotes the standard cumulative normal distribution function, and

$$x_1 = \ln\left(\frac{S_{1,t} + D_{1,t}}{S_{1,t}}\right),\ \chi = \sigma_1\sigma_2\,(T-t)\,,\ d_3 = \frac{x_1}{\sqrt{\chi}} - \frac{1}{2}\sqrt{\chi},\ d_4 = -\frac{x_1}{\sqrt{\chi}} - \frac{1}{2}\sqrt{\chi}$$

(ii) The price C_t^D of a defaultable call option, where the payoff is guaranteed by the issuer with recovery rate zero, is given by

$$\begin{aligned} C_t^D = K e^{(\alpha-r)(T-t)+\beta_1 x_1+\beta_2 x_2} \Big(& e^{-\frac{1}{2}\chi\left({\delta_1}^2+2\rho\delta_1\delta_2+{\delta_2}^2\right)} \Big(e^{(\delta_1\eta_1+\delta_2\eta_2)\sqrt{\chi}}\mathcal{N}_2\left(\eta_1,\eta_2,\rho\right) \\ & - e^{(\delta_1\nu_1+\delta_2\nu_2)\sqrt{\chi}}\mathcal{N}_2\left(\nu_1,\nu_2,\rho\right)\Big) \\ & - e^{-\frac{1}{2}\chi\left({\delta_1^-}^2+2\rho\delta_1^-\delta_2^-+{\delta_2^-}^2\right)} \Big(e^{\left(\delta_1^-\eta_1^-+\delta_2^-\eta_2^-\right)\sqrt{\chi}}\mathcal{N}_2\left(\eta_1^-,\eta_2^-,\rho\right) \\ & - e^{\left(\delta_1^-\nu_1^-+\delta_2^-\nu_2^-\right)\sqrt{\chi}}\mathcal{N}_2\left(\nu_1^-,\nu_2^-,\rho\right)\Big)\Big) \end{aligned} \tag{6.12}$$

where $\mathcal{N}_2\left(\cdot,\cdot,\rho\right)$ is the standard bivariate normal distribution function with correlation

ρ, and in addition to the definition in (i)

$$\begin{aligned}
&\alpha = -\frac{1}{4}\frac{\sigma_1^2 - 2\sigma_1\sigma_2\rho + {\sigma_2}^2}{2\left(1-\rho^2\right)},\ \beta_1 = \frac{\sigma_1 - \rho\sigma_2}{2\sigma_1(1-\rho^2)},\ \beta_2 = \frac{\sigma_2 - \rho\sigma_1}{2\sigma_2(1-\rho^2)}\\
&\delta_1 = -\sqrt{\frac{\sigma_1}{\sigma_2}}\beta_1,\ \delta_2 = -\sqrt{\frac{\sigma_2}{\sigma_1}}(1-\beta_2),\ \delta_1^- = -\sqrt{\frac{\sigma_1}{\sigma_2}}\beta_1,\ \delta_2^- = -\sqrt{\frac{\sigma_2}{\sigma_1}}\beta_2\\
&z_1 = \sqrt{\frac{\sigma_2}{\sigma_1}}x_1,\ \eta_1 = \frac{z_1}{\sqrt{\chi}} + \sqrt{\chi}\left(\delta_1 + \rho\delta_2\right),\ \nu_1 = -\frac{z_1}{\sqrt{\chi}} + \sqrt{\chi}\left(\delta_1 + \rho\delta_2\right)\\
&\eta_1^- = \frac{z_1}{\sqrt{\chi}} + \sqrt{\chi}\left(\delta_1^- + \rho\delta_2^-\right),\ \nu_1^- = -\frac{z_1}{\sqrt{\chi}} + \sqrt{\chi}\left(\delta_1^- + \rho\delta_2^-\right)\\
&x_2 = \ln\left(\frac{S_{2,t}}{K}e^{r(T-t)}\right),\ z_2 = \sqrt{\frac{\sigma_1}{\sigma_2}}x_2,\ \eta_2 = \frac{z_2}{\sqrt{\chi}} + \sqrt{\chi}\left(\delta_2 + \rho\delta_1\right)\\
&\eta_2^- = \frac{z_2}{\sqrt{\chi}} + \sqrt{\chi}\left(\delta_2^- + \rho\delta_1^-\right),\ \nu_2 = -\frac{2\rho z_1 - z_2}{\sqrt{\chi}} + \sqrt{\chi}\left(\delta_2 + \rho\delta_1\right)\\
&\nu_2^- = -\frac{2\rho z_1 - z_2}{\sqrt{\chi}} + \sqrt{\chi}\left(\delta_2^- + \rho\delta_1^-\right)
\end{aligned} \tag{6.13}$$

Proof 6 *The proof of (i) can be found in* Sepp *[Sep06]. (ii) is given in* Goetz *et al. [Goe10].*

6.2.3 Application of the model on Best Garant Certificates with default risk

We now expand the given formula of a participation guarantee certificate from Goetz et al. [Goe10] to describe our defaultable fixed entry strike BGC (DBGC$^{(\text{fix})}$). For this propose, we refer to the relevant Proposition 4 in Chapter 4 (here Proposition 7), which illustrates a pricing formula for Best Garant Certificates where no default risk is observed.

Proposition 7 (Pricing) *For an entry strike setting $K^{(w)}$ where $w \in \{$fix, ave, min$\}$, the no–arbitrage t_0–price of the BCG is given by*

$$\begin{aligned}
BGC_{t_0}^{(w)} &= e^{(g-r)T} \\
&+ e^{-rt_N}E_*\left[\frac{1}{K^{(w)}}\left(\mathcal{B}^{Call}\left(S_{t_N},t_N,r,e^{gT}K^{(w)},T\right) - \mathcal{B}^{Call}\left(S_{t_N},t_N,r,e^{cT}K^{(w)},T\right)\right)\right]
\end{aligned} \tag{6.14}$$

$\mathcal{B}^{Call}(S_t,t,r,K,T)$ denotes the t–price of a European call–option with underlying S, maturity T and strike K, i.e.

$$\begin{aligned}
&\mathcal{B}^{Call}(S_t,t,r,K,T)\\
=&S_t\mathcal{N}\left(h^{(1)}\left(t,\frac{S_t}{e^{-r(T-t)}K}\right)\right) - e^{-r(T-t)}K\mathcal{N}\left(h^{(2)}\left(t,\frac{S_t}{e^{-r(T-t)}K}\right)\right)
\end{aligned} \tag{6.15}$$

$\mathcal{N}(.)$ *denotes the one–dimensional cumulative distribution function of the standard normal distribution and*

$$h^{(1)}(t,z) := \frac{\ln z + \frac{1}{2}\sigma^2(T-t)}{\sigma\sqrt{T-t}},\ h^{(2)}(t,z) := h^{(1)}(t,z) - \sigma\sqrt{T-t} \tag{6.16}$$

Proof 7 *The proof is given in Appendix B.1.*

For the embedment, we need the parameter D_{t_0}, the initial level of debt of the issuer, as well as R the recovery rates.

However, we start with w = fix. The formula of the defaultable fix entry strike BGC ($\text{DBGC}^{(\text{fix})}$) at time $t_0 = 0$ is given by

$$\begin{aligned}
&DBGC_{t_0}^{(\text{fix})} = \\
&= e^{-rT} E_q \left\{ e^{gT} + \frac{1}{K^{(\text{fix})}} \max\left(S_{2,T} - K^{(\text{fix})} e^{gT}, 0\right) - \max\left(S_{2,T} - K^{(\text{fix})} e^{cT}, 0\right) \right\} \\
&- (1-R) e^{-rT} \\
&E_q \left\{ e^{gT} + \frac{1}{K^{(\text{fix})}} \max\left(S_{2,T} - K^{(\text{fix})} e^{gT}, 0\right) - \max\left(S_{2,T} - K^{(\text{fix})} e^{cT}, 0\right) 1_{\{\xi \le T\}} \right\}
\end{aligned} \tag{6.17}$$

where ξ denotes the time to default. We define Z and Z^{D} as the zero bond and the defaultable zero bond, which pays e^{gT} at maturity. Thus, we could convert the formula to

$$\begin{aligned}
&DBGC_{t_0}^{(\text{fix})} \\
&= R\left(Z_{t_0} + \frac{1}{K^{(\text{fix})}} \left(\mathcal{B}^{\text{Call}}\left(S_{2,t_0}, t_0, r, K^{(\text{fix})} e^{gT}, T\right) - \mathcal{B}^{\text{Call}}\left(S_{2,t_0}, t_0, r, K^{(\text{fix})} e^{cT}, T\right)\right)\right) \\
&+ (1-R)\left(Z_{t_0}^{\text{D}} + \frac{1}{K^{(\text{fix})}} \mathcal{B}^{\text{D,Call}}\left(S_{2,t_0}, S_{1,t_0}, D_{1,t_0}, t_0, r, K^{(\text{fix})} e^{gT}, T\right)\right) \\
&- (1-R)\left(\frac{1}{K^{(\text{fix})}} \mathcal{B}^{\text{D,Call}}\left(S_{2,t_0}, S_{1,t_0}, D_{1,t_0}, t_0, r, K^{(\text{fix})} e^{cT}, T\right)\right)
\end{aligned} \tag{6.18}$$

where $\mathcal{B}^{\text{Call}}$ is the notation of Proposition 7 for a standard Black and Scholes call option at time t and maturity T. Z^{D} and $\mathcal{B}^{\text{D,Call}}$ denotes the corresponding elements for the case of a defaultable issuer.[5]

5 As the construction of the defaultable BGC differs from the calculation of a bullish vertical spread. However, the margin of difference is so small that our calculation is not influenced, cf. Appendix C.1.

Since half of the formula are known from Proposition 7, we are able to write[6]

$$DBGC_{t_0}^{(\text{fix})} = R \cdot BGC_{t_0}^{(\text{fix})} + (1-R) \underbrace{\left(Z_{t_0}^{\text{D}} + \frac{1}{K^{(\text{fix})}} \left(\mathcal{B}_{t_0}^{\text{D,Call,fix}}(g) - \mathcal{B}_{t_0}^{\text{D,Call,fix}}(c) \right) \right)}_{D_0 BGC_{t_0}^{(\text{fix})}} \tag{6.19}$$

For simplicity, we will use the following three notations. $\text{BGC}_{\text{t}}^{(\text{w})}$ describes the class of Best Garant Certificates where the default of the issuer is impossible. In the case where a default event is possible, we differ between $\text{D}_0\text{BGC}_{\text{t}}^{(\text{w})}$ and $\text{DBGC}_{\text{t}}^{(\text{w})}$. The description $\text{D}_0\text{BGC}_{\text{t}}^{(\text{w})}$ is used for the special case where the recovery rate of the issuer is equal to zero. This component of the DBGC is generated directly from the components in Proposition 6. However, in the following, we are interested in the DBGCs ($\text{DBGC}_{\text{t}}^{(\text{w})}$) with a varying recovery rate $R \in (0,1)$, which we calculated through a linear combination of $\text{BGC}_{\text{t}}^{(\text{w})}$ and $\text{D}_0\text{BGC}_{\text{t}}^{(\text{w})}$(cf. (6.19)).

Thus, we split the pricing formulae into the different basic parts. If we want to calculate the model prices for the $\text{DBGC}^{(\min)}$ and the $\text{DBGC}^{(\text{ave})}$, we use Monte Carlo simulation to evaluate the corresponding strike $K^{(\min)}$ (resp. $K^{(\text{ave})}$). In particular, we observe

$$\begin{aligned} DBGC_{t_0}^{(\min)} &= R \cdot BGC_{t_0}^{(\min)} + (1-R) \left(Z_{t_0}^{\text{D}} + \frac{1}{K^{(\min)}} \left(\mathcal{B}_{t_0}^{\text{D,Call,min}}(g) - \mathcal{B}_{t_0}^{\text{D,Call,min}}(c) \right) \right) \\ &= R \cdot BGC_{t_0}^{(\min)} + (1-R) D_0 BGC_{t_0}^{(\min)} \end{aligned} \tag{6.20}$$

$$\begin{aligned} DBGC_{t_0}^{(\text{ave})} &= R \cdot BGC_{t_0}^{(\text{ave})} + (1-R) \left(Z_{t_0}^{\text{D}} + \frac{1}{K^{(\text{ave})}} \left(\mathcal{B}_{t_0}^{\text{D,Call,ave}}(g) - \mathcal{B}_{t_0}^{\text{D,Call,ave}}(c) \right) \right) \\ &= R \cdot BGC_{t_0}^{(\text{ave})} + (1-R) D_0 BGC_{t_0}^{(\text{ave})} \end{aligned} \tag{6.21}$$

6.2.4 Modified Product Specification with default risk

Now, we state the modified product specification of a "defaultable" BGC which result by the applied model.

6 We describe the corresponding components by mentioning only the relevant parameter. For the calculation method as well as the explicit strike price, we illustrate whether the feature is based upon a fixed, minimum or average strike setting. Furthermore, we show whether the guaranteed rate g or the cap rate c is taken into account for the corresponding option.

Definition 9 (Payoff of a defaultable Best Garant Certificate) *The payoff of a defaultable Best Garant Certificate with a nominal amount N, observation period $\underline{T}^{obs}$, maturity T, guaranteed rate g,cap rate c ($c \geq g$), ξ the time to default and a recovery rate R is given by*

$$\bar{h}(S_{2,t_0},\ldots,S_{2,t_N},S_{2,T},\xi) = \begin{cases} R \cdot N \left(e^{gT} + \left[\frac{S_{2,T}}{K^{(w)}} - e^{gT} \right]^+ - \left[\frac{S_{2,T}}{K^{(w)}} - e^{cT} \right]^+ \right) & \text{if } \xi \leq T \\ N \left(e^{gT} + \left[\frac{S_{2,T}}{K^{(w)}} - e^{gT} \right]^+ - \left[\frac{S_{2,T}}{K^{(w)}} - e^{cT} \right]^+ \right) & \text{else} \end{cases} \tag{6.22}$$

where $w \in \{$fix, ave, min$\}$.

Finally, we call a contract fair if

$$1 = PV_{t_0,T}\left(\bar{h}(S_{2,t_0},\ldots,S_{2,t_N},S_{2,T},\xi)\right). \tag{6.23}$$

where $PV_{t_0,T}(.)$ denotes the arbitrage free t_0–value of a payoff received at time T.

6.3 Assumed Market Data

We try to derive the parameter from real market data, if possible. For a realistic set, we focus on the observed data during the time when the certificates were issued.
For the standard market date, we use the following data set. We use the risk-free interest rate $r = 2.4$ %, calculated as the average of the five-year Germany government bonds return, which we identify with the risk-free investment. To define the drift parameter μ, we need to assume a realistic risk premium. Based upon the CAPM (Capital Asset Price Model), the data provider FACTSET calculates a risk premium for the Dow Jones Euro Stoxx 50 on a monthly basis. The average risk premium between the three different issue dates is fixed at 6.6 %, so that we finally use $\mu = 9.0$ %.

The underlying (e.g. Euro Stoxx 50) volatility is specified by the following parameter. We calculate a realistic estimation for the volatility in the Black and Scholes setting, observing the implied volatility of traded option on the underlying between the issuing period of the certificates, which results in $\sigma = 23.5$ %

For simplicity, we assume that the volatility of the issuer is equal to that of the underlying.[7] Regarding the recovery rates, we consider historical data in the case of a company's default. Appropriating the figures of a Moody's Research Paper paper, we use $R = 0.5$ in the following calculation.[8] Since the historical recovery rates significantly fluctuate, we will make an additional calculation for a more conservative recovery rate of $R = 0.6$ and sometimes for the lower recovery rate of $R = 0.4$.

To achieve a realistic approach for the initial debt D_{t_0}, we refer to HULL [Hul07] where the probability of default is calculated by the use of credit spreads (resp. Credit Default Swaps (CDS)). First, we discover the corresponding default probabilities. Second, we use a monto Carlo simulation to identify the initial debts D_{t_0}, which results in the same default probabilities by applying the formula from GOETZ et al. [Goe10]. An explanation of the practical formula in HULL [Hul07] is shown in Appendix C.2. Accordingly, we can concentrate on the range between $D_{t_0}^{(\text{low})} = 64.00$ and $D_{t_0}^{(\text{high})} = 82.00$. For the sake of convenience, we use the following equidistant parameters, $D_{t_0} = 65$, $D_{t_0} = 75$ and $D_{t_0} = 85$, since they meet our requirement for the analysis.
Finally, we use the known product specification offered in the termsheets as the further parameter. We will take into account that the time to maturity of each observed DBGC is $T = 5$ years. Unless otherwise specified, we assume $t_N = 0.5$ and a monthy observation period for the minimum and average strike setting.

When we finally come to the analysis of the investors utility, we choose a risk aversion parameter of $\gamma = 5$, since we presume that the investor of a structured product with a capital guarantee is much less risk seeking.

6.4 Pricing

We analyze the class of defaultable Best Garant Certificates in analogy to Chapter 4, where we focus on the pricing of these certificates using the Black and Scholes as well as the Heston model. Now, we apply a Black and Scholes with default risk which takes into account the possibility that the issuer could become insolvent over the entire investment

7 If the underlying is an equity index, this generally means an undervaluation of risk, since a single equity stock is on average more volatile than a corresponding equity index. Of course, the issuer does not have to be listed.

8 Based upon the Moody's Research Paper Corporate Default and Recovery Rates, 1920-2010, we observed the following figure: for senior unsecured bonds, the average corporate debt recovery rates measured by ultimate recoveries from 1987-2010 is 49.2 %.

period of the certificate.
In the following we focus on the three entry strike settings.

6.4.1 Pricing of the fixed entry strike DBGC

Now, we calculate fair (g,c)-tuple in the case of a fixed strike setting, i.e. for w = fix, we simply have $K^{(\text{fix})} = K^*$ Thus, our calculation rely on

$$DBGC_{t_0}^{(\text{fix})} = R \cdot BGC_{t_0}^{(\text{fix})} + (1-R)D_0 BGC_{t_0}^{(\text{fix})}. \tag{6.24}$$

Using the former condition (6.23) gives the fair (g,c)-tuple, as illustrated in Figure 6.1, for $K^{(\text{fix})} = S_{t_0} = 1$, different initial debt D_{t_0} and two recovery rates $R = 0.5$ and a more conservative one ($R = 0.6$).

Figure 6.1: Fair (g,c)–tuple for a fixed strike DBGC for different initial debt and recovery rates

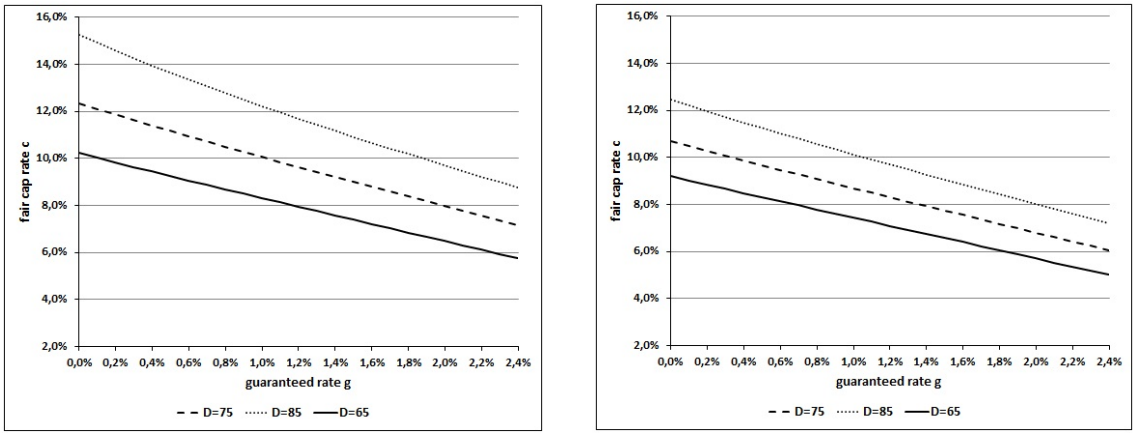

Fair (g,c)–tuple for a DBGC with a fixed entry strike setting for different initial debt level D_{t_0} and a recovery rate of $R = 0.5$ (left plot) and a more conservative recovery rate $R = 0.6$ (right plot).

Unsurprisingly, the fair cap rates in the left plot of Figure 6.1 are always higher than the fair caps rates illustrated in the right plot. Of course, this results according to definition, since the value of the non-defaultable BGCs is always higher.
Furthermore, we observe decreasing fair cap rates for higher guaranteed rates g. If we assume a guarantee rate equal to the risk-free interest rate of $r = 2.4$ %, we could identify a kind of risk premium of the issuer, who could become insolvent over the entire investment period of the certificate. The corresponding lowest fair cap rate is $c = 5.0$ %, observed for

$R = 0.6$ and $D_{t_0} = 0.65$.
For the lower recovery rate and the highest initial debt, the cap rate is significantly higher, at the level of $c = 8.8$ %.
Of course, we find the absolute highest fair cap levels for the guaranteed rate of $g = 0.0$ %. They lie between 9.2 % and 15.2 %, which means that under the given consideration the investors are able the double the invested nominal amount.
In Chapter 4, we show the fair (g,c)-tuple in the case where the default of the issuer is impossible. Thus, it is observed that the fair cap rates are significantly higher when we take into account default risk. In the case without the observation of an issuer's default, the cap rates converge to the risk-free interest rate with a growing guarantee rate g. By contrast, this calculation shows that regardless of the guaranteed rate being $g = r = 2.4$ %, the cap rate is obviously above the risk-free interest rate.
We use a volatility of $\sigma = 23.5$ % for the underlying as well as for the assets of the issuer. It is meaningful to analyze the development under different levels of volatility given that we know that the volatility has an influence on the option prices. Furthermore, the corresponding volatility is also responsible for the probability of default. Thus, a higher volatility seems to have a leveraged effect on the fair (g,c)-tuple.

For this analysis (cf. Figure 6.2), we take into account the fact that the model includes two different volatility parameters, σ_1 the volatility of the issuer asset price, and σ_2, the underlying volatility. We explore the different sensitivities by varying σ_1 and σ_2.
On the one hand, we know that the fair cap rates increase if we increase the assumed volatility σ_2. Thus, we show that the concave part of the embedded bullish vertical spread dominates the payoff profile. On the other hand, we know that the tendency with increasing issuer asset price volatility will be the same (cf. (6.6)). However, we have to calculate whether a higher issuer asset price volatility dominates the underlying volatility, or vice versa.
For the following overview, we choose two initial debts, $D_{t_0} = 65$ and $D_{t_0} = 45$, as well as a recovery rate of $R = 0.5$. In this step, we compare the results whereby we assume a volatility that is 5.0 % higher.

The left plot of Figure 6.2 shows that increasing σ_1 is followed by a significantly higher fair cap rate. The calculated fair cap rates in the scenario where we assume a higher underlying volatility σ_2 are always below those that result from a higher σ_1. For example, this means for the guaranteed rate of $g = 0.0$ %, that the fair cap rate increases from $c = 10.2$ % to

$c = 13.2$ % with the higher issuer asset price volatility σ_1. With $\sigma_2 = 28.5$ %, the fair cap rate is given by $c = 12.3$ %.

Although we focus on the range of $D_{t_0} \in \{65{,}85\}$, the right plot of Figure 6.2 illustrates the results for an initial debt of $D_{t_0} = 45$. This result shows a turning point referring to the initial debt D_{t_0}, where the underlying volatility has a greater influence than the issuer asset price volatility. On the one hand, we could explain this relation technically by (6.6), whereby the level of the initial debt defines the shift of the process. Depending on the shift, a possible default event occurs with the deviation influenced by the volatility. Remember that only a shifted Brownian motion could result negative asset prices. Accordingly, it is an interaction between the two parameters. However, we should highlight that the probability of hitting the barrier does not significantly increase with a higher volatility if the shift is very low.
By contrast, the economic interpretation suggests that if the issuing company is in a healthy financial situation, which means that they do not have much debt, the probability of a default is very low independently from the volatility of the asset prices.

Figure 6.2: Fair cap rates for different initial debt and volatilities

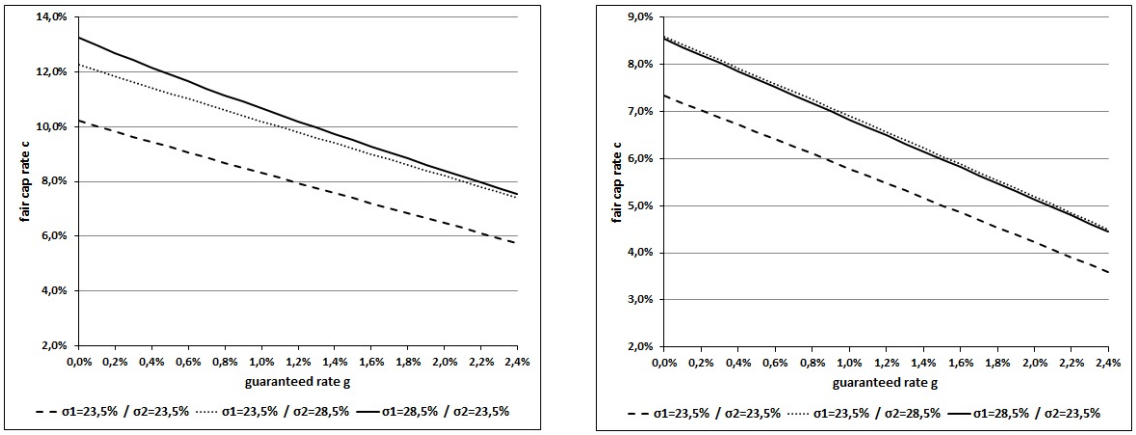

Fair (g,c)–tupel for an initial debt $D_{t_0} = 65$ (left plot) and an unrealistic low initial dept of $D_{t_0} = 45$ (right plot) for a recovery rate of $R = 0.5$.

As we can see above, the initial debt is an important parameter in the calculation of the fair (g,c)-tuple. Thus, we should have a separated look at the influence of the level of D_{t_0}. As previously mentioned, only in an event of a default is the recovery rate important for the payoff at maturity. Hence, we assume that a lower recovery rate does not influence

the price of the certificate if the initial debt level is so low that a default event is almost impossible.

To show this effect, we calculate the fair cap rates of the defaultable fixed entry strike Best Garant Certificate for a given guaranteed rate of $g = 0.0$ %. We vary the initial level of debt from $D_{t_0} = 10$ to $D_{t_0} = 90$. The results are shown for $\sigma_1 = \sigma_2 = 23.5$ % and three different recovery rates.

Figure 6.3: Fair cap rates for varying initial debt as well as varying recovery rates

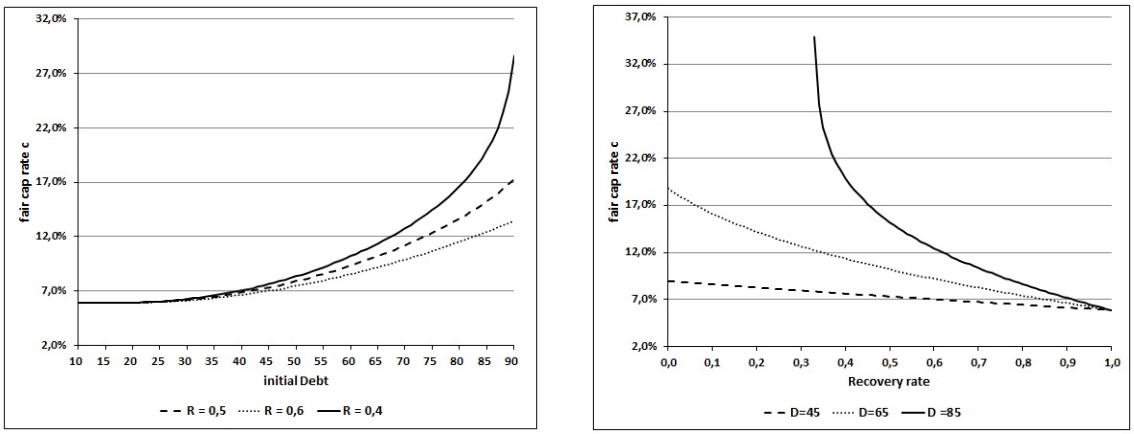

The cap rates are calculated for varying initial debt D_{t_0} and three different recovery rates R (left plot) and for varying recovery rates R and three different initial debt D_{t_0} (right plot) where the guaranteed rate is $g = 0.0$ %.

Considering the left plot of Figure 6.3, we identify a disproportionately high growth of the fair cap rates with increasing initial debt D_{t_0}. Since the different recovery rates illustrate the ratio between the defaultable and non-defaultable parts of the corresponding DBGC, it is seen how important the assumed recovery rate could be, especially in the case of large initial debts. For initial debts $D_{t_0} \leq 30$, the fair cap rates seem to be stable independent of the recovery rate. In the range between $30 < D_{t_0} \leq 60$, the difference between the fair cap rates for different R growth to about 1 %. Finally, $(D_{t_0} > 60)$, the fair cap rates diverge for the three assumed recovery rate R.

For the sake of completeness, we also illustrate in the right plot of Figure 6.3 the fair cap rates for varying recovery rates. We choose three characteristic initial debt levels $D_{t_0} \in \{45,65,85\}$, as already used before.

Of course, the fair cap rates decrease with a higher recovery rate. Surprisingly, we cannot calculate fair cap rates for the initial debt of $D_{t_0} = 85$ in the range of $R \in [0,0.33]$. This

is possible if the sum of the zero bond and the long call component is below the nominal amount $N = 1$. In other words, even the price of an upcapped defaultable garant certificate lies under the fair condition illustrated in (6.23). Finally, it is evident that the fair cap rates converge with recovery rates going to 1. This means that regardless whether the issuing company is solvent at maturity of the certificate, the calculated payoff is guaranteed.

6.4.2 Pricing of the minimum entry strike DBGC

In order to calculate the t_0–price regarding the minimum strike DBGC given by

$$DBGC_{t_0}^{(\min)} = R \cdot BGC_{t_0}^{(\min)} + (1-R) D_0 BGC_{t_0}^{(\min)} \tag{6.25}$$

we rely on a Monte Carlo method. Thus, for k sample paths of $(S_{2,t_1}, \ldots, S_{2,t_N})$, we obtain (for $j = 1, \ldots k$) $\hat{y}_j = S_{2,t_N}(\omega_j)$ and $\hat{x}_j = \min_{i=0,\ldots,N} S_{2,t_i}(\omega_j)$ and use

$$BGC_{t_0}^{(\min)} \approx Z_{t_0} + \frac{1}{k} \sum_{j=1}^{k} \frac{e^{-rt_N}}{\hat{x}_j} \left(\mathcal{B}^{\text{Call}} \left(\hat{y}_j, t_N, r, e^{gT} \hat{x}_j, T \right) - \mathcal{B}^{\text{Call}} \left(\hat{y}_j, t_N, r, e^{cT} \hat{x}_j, T \right) \right) \tag{6.26}$$

resp. with the use of $\hat{z}_j = S_{1,t_n}(\omega_j)$

$$\begin{aligned} & D_0 BGC_{t_0}^{(\min)} \\ & \approx Z_{t_0}^{D} + \frac{1}{k} \sum_{j=1}^{k} \frac{e^{-rt_N}}{\hat{x}_j} \left(\mathcal{B}^{\text{D,Call}} \left(\hat{y}_j, \hat{z}_j, D_{1,t_N}, t_N, r, e^{gT} \hat{x}_j, T \right) - \mathcal{B}^{\text{D,Call}} \left(\ldots, e^{cT} \hat{x}_j, \ldots \right) \right). \end{aligned} \tag{6.27}$$

Figure 6.4 illustrates the fair (g,c)-tupel for the defaultable minimum strike BGC. In the same sense as Figure 6.1, we use two different recovery rates as well as different initial debt levels in each plot. The observation shows the identical development as identified for the defaultable fixed entry strike BGC, i.e. the fair cap level decreases with the guaranteed rate. However, it is seen that all fair cap rates are lower than the corresponding rate in the case of the fix entry strike. Since the risk of an issuer default event is more or less the same, the difference is a result of the strike setting. Here, the strike $K^{(\min)}$ is always lower than or equal to the fixed strike $K^{(\text{fix})}$. Thus, the payoff has to be capped earlier.

In the following, we do not illustrate the additional calculation for the defaultable fixed entry strike BGC, since there are no significant added values to highlight. In particular,

Figure 6.4: Fair (g,c)-tuple for a minimum strike DBGC for different initial debt and recovery rates

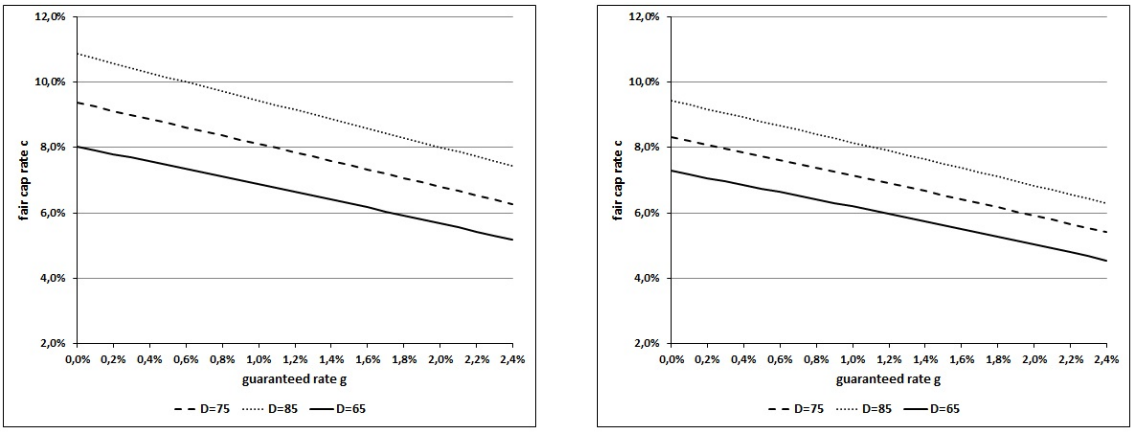

Fair (g,c)-tuple for a DBGC with minimum entry strike setting for different initial debt level D_{t_0} and a recovery rate of $R = 0.5$ (left plot) and a more conservative recovery rate $R = 0.6$ (right plot).

the analysis of the initial debt and the recovery rate has its main focus on the value of the nominal amount, rather than the path-dependent payoff feature.

6.4.3 Pricing of the average entry strike DBGC

The defaultable average entry strike setting is illustrated in the same sense as the defaultable minimum entry strike BGC, whereby again we apply Monte Carlo methods. We use the same approximation by the use of Monte Carlo methods (6.26) and (6.27) where we calculate $\hat{x}_j = \frac{1}{N+1}\sum_{i=0}^{N} S_{2,t_i}(\omega_j)$ rather than the minimum $\hat{x}_j = \min_{i=0,\dots,N} S_{2,t_i}(\omega_j)$. In analogy to the illustration of the fixed and minimum strike setting, the resulting fair (g,c)–tuples are illustrated in Figure 6.5. Intuitively, it is expected that the average strike setting does not imply results that are significantly different from a fixed strike setting where $K^{(\text{fix})} = S_{t_0}$.

Figure 6.5: Fair (g,c)-tuple for a average strike DBGC for different initial debt and recovery rates

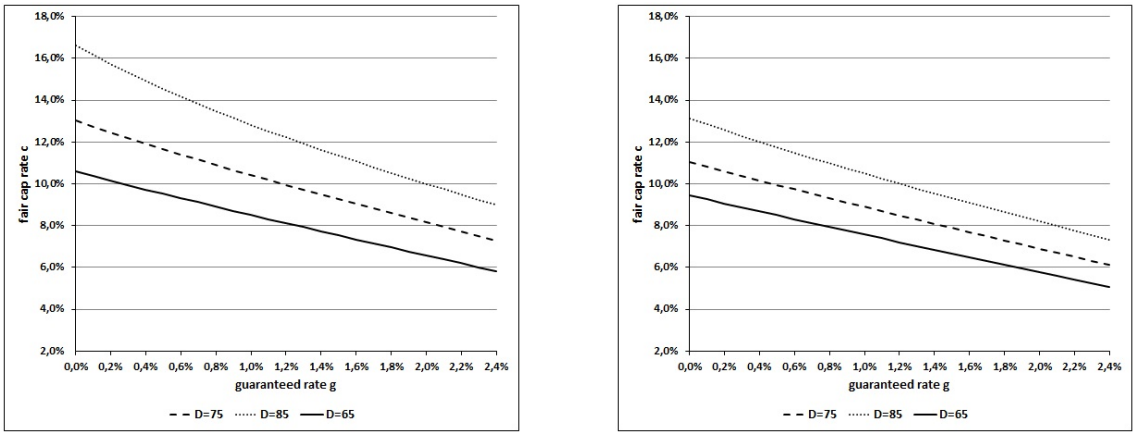

Fair (g,c)–tuple for a DBGC with average entry strike setting for different initial debt level D_{t_0} and a recovery rate of $R = 0.5$ (left plot) and a more conservative recovery rate $R = 0.6$ (right plot).

6.5 Perspective of the investor

Referring to the results from Section 6.4, an investor who is restricted to the class of DBGC has to choose among different return distributions. Additionally, with the focus on the issuer default risk, the investor also has to decide if she runs the risk of an issuer default or invest directly in the underlying without a guarantee.[9] In the following, we analyze the simulated return distribution assuming the real world measure.

Thus, we switch from the risk-neutral measure (P^* resp. Q) that we used for the pricing analysis to the real world measure P. In this context, we use the introduced drift parameter $\mu = 9.0$ %, which results by summation of the risk-free interest rate r and the equity risk premium derived in Section 6.3.

6.5.1 Illustration of the simulated return distribution of defaultable BGC's

The following simulated return rates under the real world measure P in the Black and Scholes model with default risk (cf. Goetz et al. [Goe10]) are approximated by means of the Monte Carlo method. More precisely, the results in this section are based upon the simulation of 50,000 sample-paths.

9 Respectively, the investor could choose a strategy that does not contain a guarantee feature where no default risk exists.

For comparison, we use the recovery rate R and the initial debt D_{t_0} of the issuer from the previous section. For each one, we focus on the tupels $(0,c^{(\mathrm{w})})$, whereby we use the highest fair cap rate that corresponds to the guaranteed rate $g = 0.0$ %. We start with the illustration of the return rate distribution of the three defaultable certificates (fix, minimum and average) with initial debt $D_{t_0} = 75$ and the two different recovery rates $R = 0.5$ and $R = 0.6$ in Figure 6.6.

Figure 6.6: Simulated return rates w.r.t the DBGCs

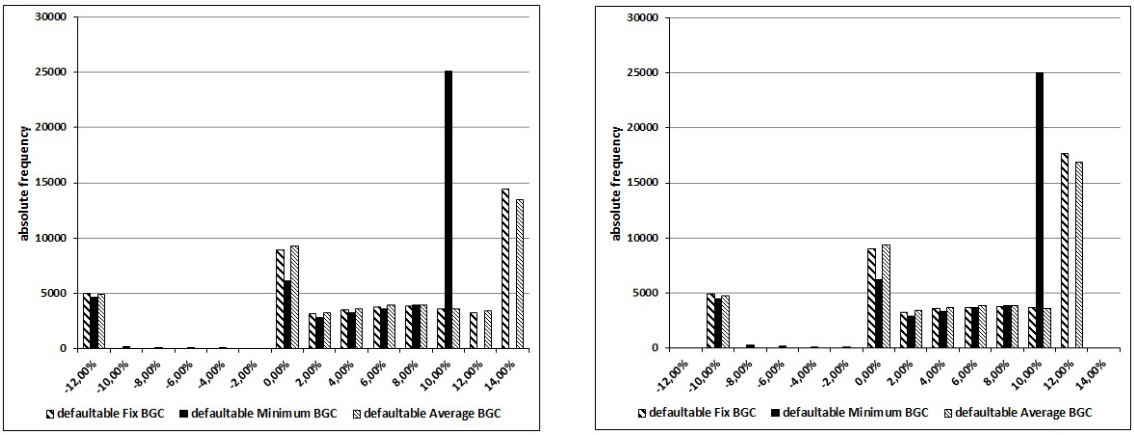

Simulated return rate distribution for the different features of the DBGC, with $c^{(\mathrm{fix})} = 12.34$ %, $c^{(\mathrm{min})} = 9.38$ % and $c^{(\mathrm{ave})} = 13.02$ % for $R = 0.5$ (left plot) and in the more conservative case $c^{(\mathrm{fix})} = 10.67$ %, $c^{(\mathrm{min})} = 8.32$ % and $c^{(\mathrm{ave})} = 11.05$ % for $R = 0.6$ (right plot).

Considering Figure 6.6, we identify some interesting developments. Focusing on the payoff structures of the three DBGCs, the distribution of the fixed and the average strike looks more or less the same, whereas the minimum strike, which is capped earlier than the two other certificates, has significantly more point mass at the cap rate. However, the minimum strike feature gives the investor less upwards participation, although the maximum payoff is paid more often. Furthermore, the number of simulated paths that only pay the guaranteed rate is lowest for the minimum strike setting, since $K^{(\mathrm{min})} \leq \min\left(K^{(\mathrm{fix})},K^{(\mathrm{ave})}\right)$. Overall, more than 50 % of the simulated paths pay either the cap rate or the guaranteed rate.

Additionally, we observe that the simulation also results in negative return rates, due to the model assumption whereby the default of the issuer is possible. Hence, we identify a third point mass, besides the accumulation point at the guaranteed rate and the cap rate,

which results from taking into account default risk. Since we do not vary the initial debt in this calculation, the overall point mass in both plots is more or less the same, although the level of the return rate is different, owing to the assumed recovery rates.
We should note that a return rate of -10.22 % is identical with the payoff of 60 % of the nominal amount and the payoff of 50 % of the nominal amount corresponds with a return rate of -13.86 %. On the one hand, the recovery rate defines the worst case return rate, which appears when a default event occurs and the underlying price is below the appropriate strike $K^{(\mathrm{w})}$ (only the nominal amount would be paid). On the other hand, the fair cap rates are higher for a lower recovery rate, whereby the point mass at the cap rates shift to the right if the recovery rate decreases.
For a better overview, we illustrate the relevant statistics of this calculation in Table 6.1.
We know that the assumed parameters significantly influence the distribution. For a higher

Table 6.1: Overview of the return rate distribution of the DBGCs for different recovery rates

$R = 0.5$	fixed	minimum	average
fair cap rate in %	12.34	9.38	13.02
average return in %	4.74	4.46	4.76
median in %	6.14	8.06	5.80
return = recovery rate (in %)	9.89	9.12	9.69
return = guarenteed rate (in %)	17.93	12.28	18.59
return = cap rate (in %)	28.95	46.33	23.98
$R = 0.6$	fixed	minimum	average
fair cap rate in %	10.67	8.32	11.05
average return in %	4.59	4.32	4.57
median in %	6.12	8.01	5.71
return = recovery rate (in %)	9.80	8.98	9.60
return = guarenteed rate (in %)	18.06	12.20	18.77
return = cap rate (in %)	35.46	49.80	30.35

Calculated figures for the three DBGCs for the initial debt $D_{t_0} = 75$, $\mu = 9.0$ % and $\sigma = 23.50$ % and the two recovery rates $R = 0.5$ and $R = 0.6$.

risk premium (resp. a higher μ), we find significant more weight on the right hand sight at the cap rates. Furthermore, we know that the variation of the volatility changes the figures: with a low volatility, the average return and the median increases. In addition, the point mass shifts from the guaranteed rate to the fair cap rate.[10] In an additional analysis, we

10 All these results do not depend on the possible issuer default. Thus, for this observation, we can also refer to Chapter 4.

explore the influence of the adjusted initial debt of the issuer. We assume that the change will be evident at the third point mass, which is defined by the recovery rate. Figure 6.7 illustrates the results.

Figure 6.7: Simulated return rates for all DBGCs by varied initial debt D_{t_0}

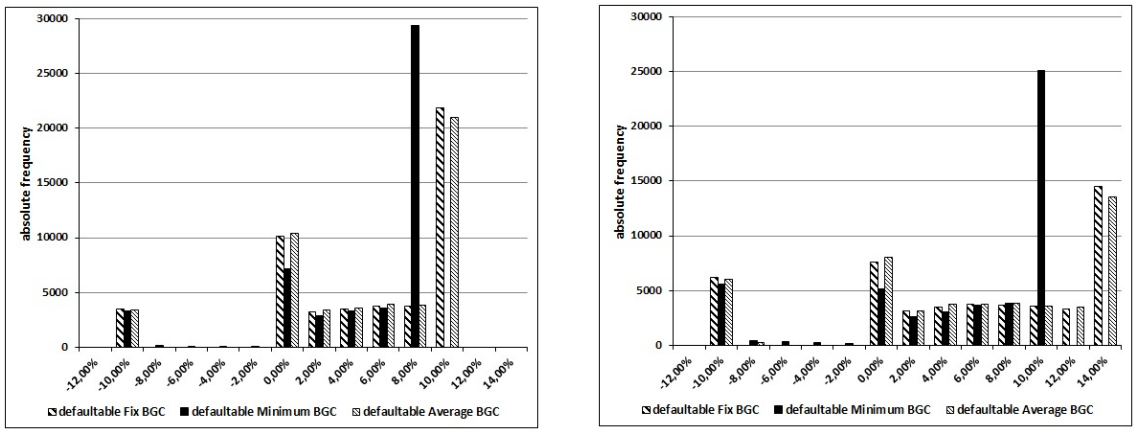

Simulated return rate distribution for the different features of the DBGC, with $c^{(\text{fix})} = 9.20$ %, $c^{(\text{min})} = 7.28$ % and $c^{(\text{ave})} = 9.44$ % for $D_{t_0} = 65$ (left plot) and in the more conservative case $c^{(\text{fix})} = 12.45$ %, $c^{(\text{min})} = 9.43$ % and $c^{(\text{ave})} = 13.13$ % for $D_{t_0} = 85$ (right plot). The recovery rate is fixed by $R = 0.6$.

It is realized that the weight at the recovery rate depends on the level of the issuer's initial debt. This is meaningful since the probability of default is positively correlated to the initial debt D_{t_0}. While for the initial debt of $D_{t_0} = 75$, almost 5.000 of the sample paths of the certificates (>10 %) pay only the amount depending of the recovery rate, the number of sample paths rise significantly above 5.000 for the initial debt of $D_{t_0} = 85$. By contrast, the left plot of Figure 6.7 shows for $D_{t_0} = 65$ a considerable lower weight at this mass point.

However, we should mention that the complete distribution changes. On the one hand, the maximum payoff for each DBGC changes since the fair cap rates are higher for higher initial debt (cf. Section 6.4). Thus, the weights at the cap rates also vary. On the other hand, the number of sample paths that only pay the guaranteed rate increases in the case of the lower initial debt of $D_{t_0} = 65$. While this is remarkable upon first glance, it is meaningful to mention that the number of sample paths where no underlying performance is measured ($S_T^{(\text{w})} \leq K^{(\text{w})}$) independently from the initial debt of the issuer. Accordingly,

the overall number of payoffs with $g \leq 0.0$ % is fixed in contrast to the number of payoffs that pay only the recovery rate. Finally, it is obvious that the weight at the guaranteed rate has to fall if a higher initial debt is assumed, and vice versa.

Table 6.2: Influence of the initial debt on the return rates distribution of the DBGCs

$D_{t_0} = 65$ / $D_{t_0} = 85$	fixed	minimum	average
fair cap rate %	9.20 / 12.45	7.28 / 9.43	9.44 / 13.13
average return in %	4.45 / 4.83	4.15 / 4.54	4.43 / 4.85
median in %	6.34 / 6.11	7.28 / 8.05	5.98 / 5.79
return = recovery rate (in %)	7.06 / 12.45	6.62 / 11.15	6.93 / 12.17
return = guarenteed rate (in %)	20.32 / 15.18	14.30 / 10.26	20.81 / 16.08
return = cap rate (in %)	40.00 / 29.10	54.94 / 46.41	38.26 / 24.10

Illustration of the return rate distribution for the DBGCs for $\mu = 9.0$ % and different level of the initial debt D_{t_0} of the issuer.

The derivation of the simulated return rates are also shown in Table 6.2. While the fair cap rates are different, the average returns of the three DBGCs only marginally change. The average returns are around 0.4 % higher in the case where the initial debt is higher. Interestingly, the median for the fixed and average strike setting is lower for $D_{t_0} = 85$ than for $D_{t_0} = 65$. For the minimum strike setting, the median is higher for $D_{t_0} = 85$. However, the weight at the cap rate decreases below 50 %, whereby the median is lower than the corresponding cap rate.
It is also interesting that the weight at the recovery rates differ between the three DBGCs. In most cases where the issuer becomes insolvent, we assume that the underlying also has a negative performance due to the positive correlation of $\rho = 0.3$ between the two strochastic processes. However, simulating 50,000 sample paths shows many specifications exist in which we see a different development. The following Figure 6.8 and Figure 6.9 illustrate these scenarios.

First, we illustrate the distribution of the return rates at maturity for a defaultable fixed entry strike BGC depending on the final underlying price, assuming an initial debt of $D_{t_0} = 75$ and the two recovery rates $R = 0.5$ and $R = 0.6$. We use the fair cap rate $c^{(\text{fix})} = 12.34$ % for $g = 0.0$ % and $R = 0.5$. For the more conservative recovery rate ($R = 0.6$), we assume $c^{(\text{fix})} = 10.67$ %. Second, we analyze the discussed development for the path-dependent payoff structures.
Figure 6.8 now shows the announced plots. On the one hand, it is seen how the payoff

takes course in the case where no default occurs. For the recovery rate of $R = 0.5$, the payoff is capped at the return rate of $c^{(\text{fix})} = 12.34$ %. For the more conservative recovery rate, the payoff is capped early at $c^{(\text{fix})} = 10.67$ %. For an underlying performance rate below 10.67 %, the two structures have the identical return rate if the issuer is solvent during the time to maturity.
On the other hand, it seems realistic that the structure that is capped later offers more risk in the case of a default event. While the investor who is capped at $c^{(\text{fix})} = 10.67$ % receives a return rate of -10.22 % in the worst case, the investor who decide to be capped at $c^{(\text{fix})} = 12.34$ % takes the risk of a lower return rate of -13.86 %.
Additionally, we observe in both plots that a default event is not a byword for a high negative return rate, since the payoffs are calculated by the multiplication of the non-default payoff times the recovery rate in the case of a default. It is meaningful to mention that in the calculation for the recovery rate $R = 0.6$, the probability exists whereby the investor receives a return rate above the guaranteed rate despite the issuer being insolvent. Nonetheless, this probability is very low.

Figure 6.8: Simulated return rates w.r.t. the fixed strike DBGC

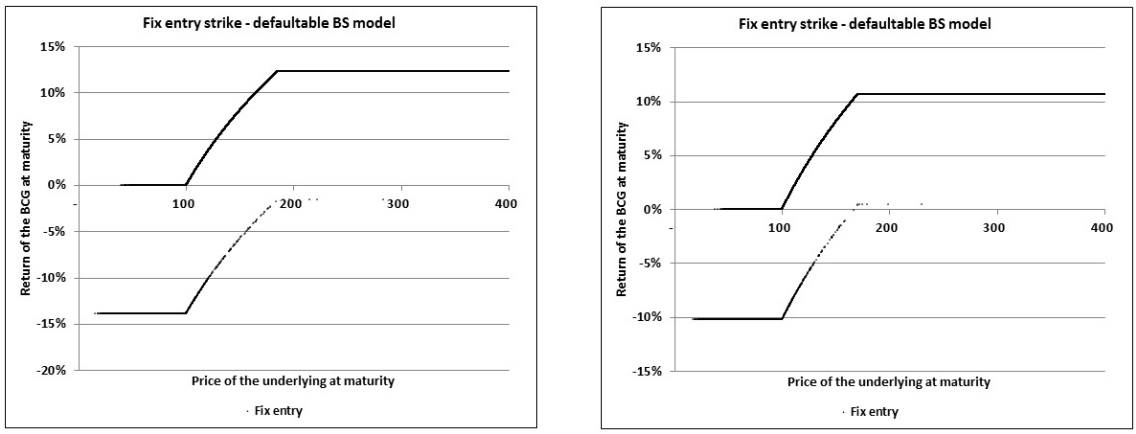

Simulated return rate distribution for the defaultable fixed entry strike DBGC with initial debt of $D_{t_0} = 75$ and a recovery rate $R = 0.5$ (left plot) and $R = 0.6$ (right plot).

Finally, we explore the simulated return rates of the defaultable minimum and the average strike BGC, as illustrated in Figure 6.9. While the overall difference between the payoffs in the case of a default and without a default are the same for the two path-dependent structures, the plots show other interesting characteristics. For instance, the DBGC$^{(\text{min})}$

Figure 6.9: Simulated return rates w.r.t. the minimum and average strike DBGC

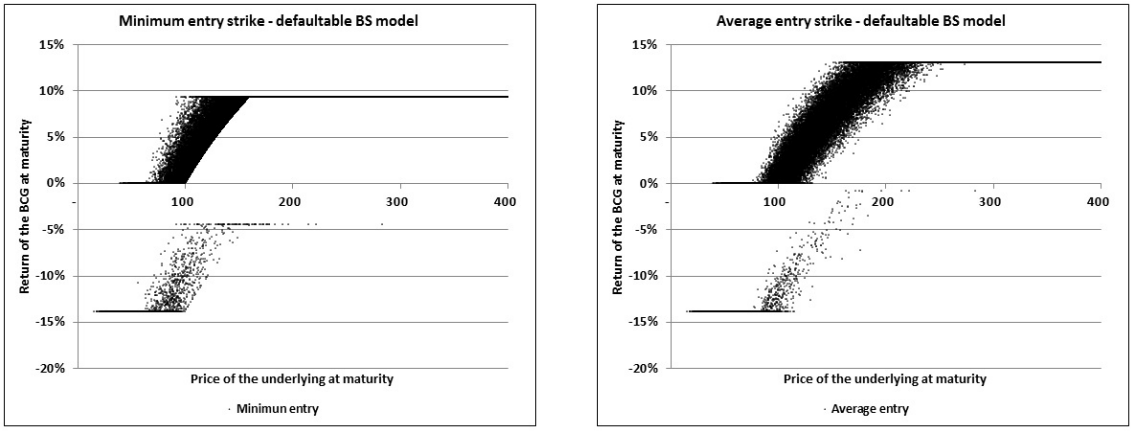

Simulated return rate distribution for the defaultable minimum (left plot) and the average (right plot) entry strike setting, with an initial debt of $D_{t_0} = 75$ and a recovery rate $R = 0.5$ is used

applies that the return rates are always higher than or equal to the fix entry strike if the underlying performance is below the minimum entry strike cap rate.
Graphically, this is seen in the scatter diagram by the points of from the linear development, which can be compared to the scatter diagram of the fix strike setting. For example, this means that while the final underlying performance could be the same, due to the lower strike $K^{(\min)}$ (with $K^{(\min)} \leq K^{(\min)}$) the return rate of the DBGC$^{(\min)}$ is higher.
These development cannot be tranferred to the average entry strike as the strike $K^{(\text{ave})}$ could be above or below the start level. However, we see that the derivation of the return rates is significantly higher for the average strike setting than for the other settings.

To summarize the results we have to expose two import aspects. In a simplified manner, the investor has two decision problems: first, she has to choose between the different entry strike settings, whereby she prefers a certificate that gives a moderately good return relatively often or one that can obtain a higher good return, but less often (cf. Chapter 4); and second, if the investor has a choice, she could select an issuer under consideration of their financial strength. Since there is no way to analyze a hypothetical recovery rate, the investor could only focus on the parameter that influences a possible default event.

The next section tackles the optimality of the strike price setting mechanism on a more

solid basis, i.e. we consider an expected CRRA utility maximizing investor.

6.5.2 Expected utilities and loss rates

We consider an expected CRRA utility maximizing investor with utility function $u(w) = \frac{w^{1-\gamma}}{1-\gamma}$ for $w > 0$ and $u(w) = -\infty$ for $w \leq 0$. As already mentioned, we assume that the financial markets is incomplete for the investor, e.g. she has to resort to the restricted class of BGC. However, we benchmark the expected utility obtained by an investment in the DBGC against the expected utility obtained by the so–called *Merton strategy*, which is optimal regarding a complete Black and Scholes model and a CRRA utility function. Furthermore, we assume that the investor's optimal Merton resp. Constant-Mix portfolio is not exposed to default risk.[11] In the following, we give an overview of some basic results concerning the optimal investment in complete market conditions of a CRRA investor in a Black and Scholes model. The Black and Scholes case is used as a benchmark case, i.e. we subsequently define the loss rate implied by the defaultable Best Garant Certificate regarding the certainty equivalent, which is implied by the optimal certainty equivalent given by the *Merton strategy*, cf. MERTON [Mer71].
In the case of a Black and Scholes model, the overall optimal investment process is given by a constant investment fraction

$$\varphi^* = \frac{\mu - r}{\gamma \sigma^2}. \tag{6.28}$$

The terminal value V_T^{φ} of a Constant-Mix strategy, which is characterized by a constant investment faction of φ and initial wealth V_0, is given by

$$V_T^{\pi} = V_0 \, e^{\left(r + \varphi(\mu - r) - \frac{1}{2}\varphi^2\sigma^2\right)T + \varphi\sigma W_T}.$$

The expected utility (under the real world measure P) is

$$E_P\left[u(V_T^{\varphi})\right] = \frac{(V_0)^{1-\gamma}}{1-\gamma} e^{(1-\gamma)\left(r + \varphi(\mu - r) - \frac{1}{2}\gamma\varphi^2\sigma^2\right)T}.$$

11 For example, we compare the certificates with an investment in a mutual fund where the default of the issuer has no influence of the wealth (resp. utility) of the retail investor.

The certainty equivalent CE_T^{φ}, defined by the certain amount that makes the investor indifferent between achieving this certain amount (at T) or using the strategy π, i.e.

$$u\left(CE_T^{\varphi}\right)) = E_P\left[u\left(V_T^{\varphi}\right)\right]$$

then is

$$CE_T^{\varphi} = V_0 e^{\left(r+\varphi(\mu-r)-\frac{1}{2}\gamma\varphi^2\sigma^2\right)T}.$$

In particular, the benchmark certainty equivalent is

$$CE_T^{*} = V_0 e^{\left(r+\frac{1}{2\gamma}\left(\frac{\mu-r}{\sigma}\right)^2\right)T}. \tag{6.29}$$

Now, we consider the expected utility derived by an investment in a DBGC. In the case of a fixed strike K^*, the expected utility of the BGC can be calculated in closed-form. In addition, the following proposition also yields a simplified procedure to approximate the expected utility by means of the Monte Carlo method.

Definition 10 (DBGC$^{(\mathbf{fix})}$: Expected utility, certainty equivalent and loss rate)

(i) The expected utility $EU^{DBGC,fix}$ of a defaultable fixed strike Best Garant Certificate is calculated by the following simulation. In order to approximate the expected utility, we rely on the Monte Carlo method, i.e. for k sample paths of $(S_{2,t_0},S_{2,t_1},\ldots,S_{2,T})$, we obtain (for $j=1,\ldots k$) $\hat{y}_j = S_{2,T}(\omega_j)$ for the underlying price as well as the stopping time ξ_j (time to default) for the sample paths $(S_{1,t_0}(\omega_j),S_{1,t_1}(\omega_j),\ldots,S_{1,T}(\omega_j))$ of the correlated asset price process (cf. (6.6)). For $j=1,\ldots,k$ holds

$$DBGC_T^{(fix)}(\omega_j) = \begin{cases} R\left(e^{gT} + \left[\frac{\hat{y}_j}{K^*} - e^{gT}\right]^+ - \left[\frac{\hat{y}_j}{K^*} - e^{cT}\right]^+\right) & \text{if } \xi \le T \\ e^{gT} + \left[\frac{\hat{y}_j}{K^*} - e^{gT}\right]^+ - \left[\frac{\hat{y}_j}{K^*} - e^{cT}\right]^+ & \text{else} \end{cases} \tag{6.30}$$

and the overall expected utility is given by the mean of the expected utility of each sample path

$$EU^{DBGC,fix} = \frac{1}{k}\sum_{j=1}^{k} \frac{\left(DBGC_T^{(fix)}(\omega_j)\right)^{1-\gamma}}{1-\gamma} \tag{6.31}$$

(ii) The certainty equivalent $CE_T^{DBGC,fix}$ *of a defaultable fixed strike Best Garant Certificate is given by*

$$CE_T^{DBGC,fix} = \left[(1-\gamma)EU^{DBGC,fix}\right]^{\frac{1}{1-\gamma}} \tag{6.32}$$

(iii) The loss rate l_T *of a defaultable fixed strike Best Garant Certificate (benchmarked on the certainty equivalent of the optimal Constant-Mix strategy is given by*

$$l_T = \frac{\ln\left(\frac{CE_T^*}{CE_T^{DBGC,fix}}\right)}{T} \tag{6.33}$$

where $CE_T^* = V_0 e^{\left(r+\frac{1}{2\gamma}\left(\frac{\mu-r}{\sigma}\right)^2\right)T}$ *and* $V_0 = DBGC_{t_0}^{fix}$.

Using the methodology introduced in Definition 10, we can also calculate the expected utility, the certainty equivalent and the loss rate for the path-dependent average and minimum DBGC. We simply have to calculate the minimum strike $K^{(\min)}$ and the average strike $K^{(\min)}$ by the subset of the sample path, e.g. $(S_{2,t_0}, S_{2,t_1}, \ldots, S_{2,t_N})$. More precisely, we calculate for $j = 1, \ldots k$ the relevant minimum strike by $x_j = \min_{i=0,\ldots,N} S_{2,t_i}(\omega_j)$ resp. $\hat{x}_j = \frac{1}{N+1}\sum_{i=0}^{N} S_{2,t_i}(\omega_j)$ for the average entry strike to assign the corresponding payoffs.

We analyze the loss rates l_T of the three DBGCs regarding the combination of the recovery rates $R = 0.5$ and $R = 0.6$, as well as the initial debt levels $D_{t_0} = 65$ and $D_{t_0} = 75$. For each calculation, we assume that the contracts are fair. Figures 6.10 and 6.11 show the loss rates for a CRRA investor for $\mu = 9.0$ %, volatility of $\sigma_1 = \sigma_2 = 23.5$ % and a risk aversion of $\gamma = 5$. Based upon the assumed risk aversion parameter γ and the drift parameter μ, the optimal proportion of a risky asset in the optimal Constant-Mix strategy is 23.9 %.

The two figures show that the recovery rate and the initial debt have a significant influence on the loss rate for a CRRA investor. Upon first glance, we observe that investors do not necessarily suffer from a lower cap rate in combination with a higher guaranteed rate. Since we assume that a risk aversion investor has a higher guaranteed rate, which also defines the determination base in a case of a default, is more important than the optional upward participation.

Starting with the assume parameter $R = 0.6$ and $D_{t_0} = 65$, it is seen that the loss rates for the defaultable fixed entry strike and the defaultable average entry strike are concurrent, whereas the graphs for the defaultable minimum entry strike clearly proceed below the others, although the difference reduces with a higher guaranteed rate g. In comparison

Figure 6.10: Analysis of the loss rates for all DBGCs

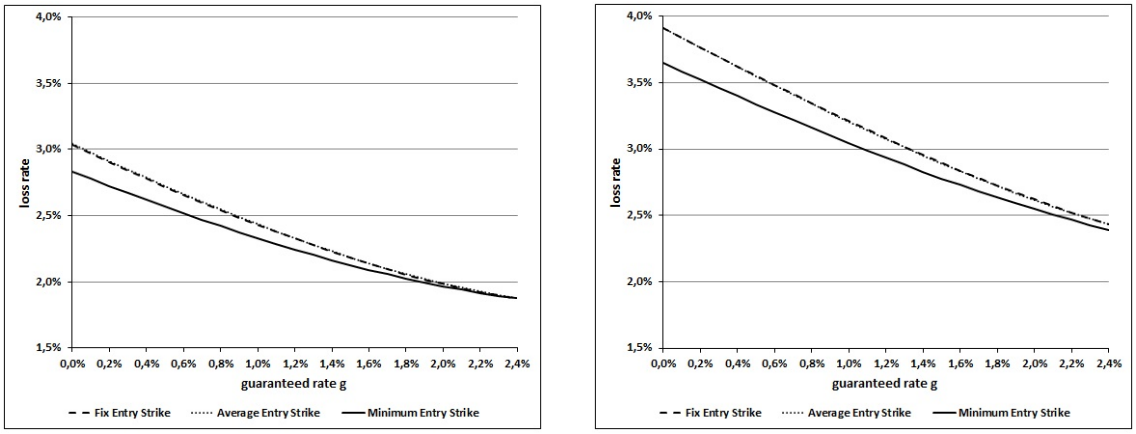

Loss rates calculated for the DBGC for a risk aversion of $\gamma = 5$; $R = 0.6$, $D_{t_0} = 65$ (left plot) and $D_{t_0} = 75$ (right plot).

to the other plots, we have to mention that the overall loss rates are the lowest for this parameter combination.

We identify that the loss rates in the right plot of Figure 6.10 are between 1.0 % and 0.5 % above the loss rate in the left plot, where a lower initial debt $D_{t_0} = 65$ is assumed. In

Figure 6.11: Analysis of the loss rates for all DBGCs - II

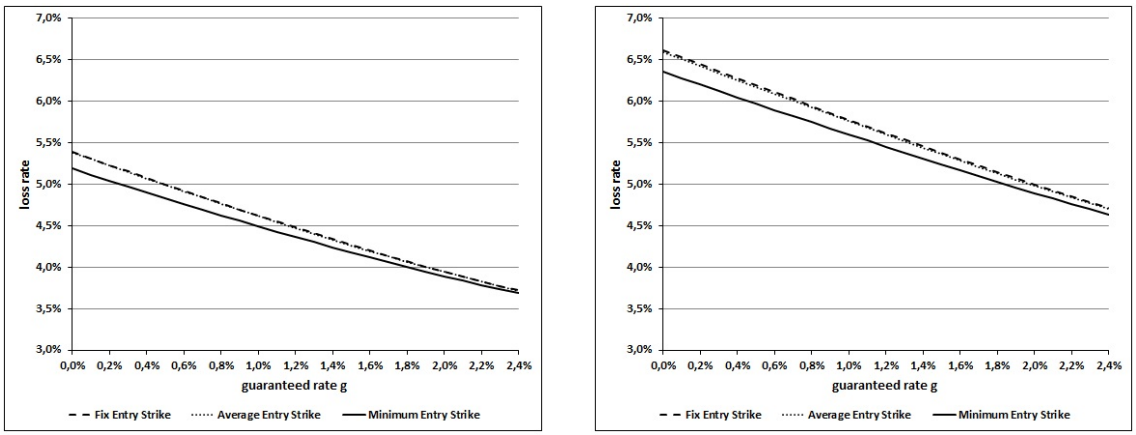

Loss rates calculated for the DBGC for a risk aversion of $\gamma = 5$; $R = 0.5$, $D_{t_0} = 65$ (left plot) and $D_{t_0} = 75$ (right plot).

contrast, the changing of the recovery rate has a greater influence in our observation. For the guaranteed rate of $g = 0.0$ %, the loss rate rises from $l_T = 3.0$ % to $l_T = 5.0$ % in the case of the DBGC with a fixed and average strike. A similar swift is seen for the minimum strike (cf. Figure 6.11).

We should mention that the risk aversion CRRA investor of a Constant-Mix strategy (with $\varphi^* = 23.9$ %) has a significantly lower downside risk than the investor of a DBGC where the issuer could become insolvent. Regarding the expected utility and the loss rate, the investor suffers from a probability of an issuer's default. This also explains that the loss rates are lower for the defaultable minimum strike setting, since in the case of a default the minimum strike setting has more weight above the recovery rate (cf. Table 6.1).

6.6 Comparison of model and market prices

We now consider real traded (defaultable) Best Garant Certificates[12] issued between October 2009 and February 2010 and compare their issue prices resp. their product specification at issue date to the model prices given by the Black and Scholes under default risk from Section 6.2.[13]

Table 6.3 summarizes the contract specifications of three observed certificates.[14] We observe three defaultable BGC: a $\text{DBGC}^{(\text{fix})}$, a $\text{DBGC}^{(\text{min})}$ and a $\text{DBGC}^{(\text{ave})}$. We should mention, that the corresponding best-entry period differ between the DBGC with the minimum and the average calculation. The start level of the $\text{DBGC}^{(\text{min})}$ will be calculated by the minimum of 26 Closed Prices of the underlying at 26 observation dates from 28 December 2009 to 18 June 2010 (observation period). At the end of the last observation date (18 June 2010) the start level is fixed.
For the $\text{DBGC}^{(\text{ave})}$ the observation period is slightly different. The length of the observation period is only 5 month (24 Feb 2010 - 26 Jul 2010) and the observation dates have a monthly frequence.
Notice, all certificates simply guarantee the nominal amount. Thus, we use $g = 0.0$ % for all further calculation. For the application of the pricing formula we have to transfer the

12 As in Chapter 4, we decide just to illustrate one certificate for each best-entry feature. Overall we analyzed 10 BGCs issued between October 2008 and May 2010.
13 Remember, that we have already done this exercise in the case without default risk (cf. Chapter 4). Therefore, we assume significant lower model prices in the following calculation.
14 All contract specification are in analogy to Chapter 4.
15 All certificates are issued by the same issuer.

Table 6.3: Best Garant Certificates - termsheet data

Key data	$\text{DBGC}^{(\text{fix})}$	$\text{DBGC}^{(\text{min})}$	$\text{DBGC}^{(\text{ave})}$
Issuer rating [15]	A1, A+	A1, A+	A1, A+
Issue date (ID)	26 Oct 2009	21 Dec 2009	22 Feb 2010
Valuta	28 Oct 2009	23 Dec 2009	24 Feb 2010
Underlying	DJ Euro Stoxx 50	DJ Euro Stoxx 50	DJ Euro Stoxx 50
Startlevel	closed price at ID	see definition	see definition
Nominal amount (N)	EUR 100.00	EUR 1,000.00	EUR 1,000.00
capital protection	100 % of N	100 % of N	100 % of N
Caplevel	138 % of N	130 % of N	135 % of N
Valuation date	31 Oct 2014	16 Dec 2014	17 Feb 2015
Maturity date	07 Nov 2014	23 Dec 2014	24 Feb 2015

Product specification from the termsheets.

maximum payoff into the relevant cap rate $c^{(\text{w})}$.

Table 6.4: Transformed parameter for the application of the pricing formula

	$\text{BGC}^{(\text{fix})}$	$\text{BGC}^{(\text{min})}$	$\text{BGC}^{(\text{ave})}$
Time to maturity T (in years)	5.0	5.0	5.0
Best-in period t_N (in years)	X	0.5	0.42
Nominal amount N (in EUR)	100	1,000	1,000
Maximum payoff (in EUR)	138	1,300	1,350
Cap rate $c^{(w)}$ in %	6.42	5.25	6.02

Relevant parameter based on the product specifications for the calculation in the Black and Scholes with default risk.

Remember, R controls the ratio of the standard and the defaultable components of the enbedded options (cf. (6.19), (6.20) and (6.21)). The second varied parameter is the initial issuer's debt D_{t_0}. It is clear, the higher the initial debt the higher is the default probability of the issuer. Thus, D_{t_0} only influence the price of the defaultable components of the pricing formula where R defines the ratio between both.
As mentioned in Section 6.3, we use the recovery rates $R = \{0.4, 0.5, 0.6\}$.

For an realistic approach for the initial debt D_{t_0}, we refer to Hull [Hul07] where the probability of default is calculated by the use of credit spreads (resp. Credit Default Swaps (CDS)) and the relevant recovery rates. After we derive the corresponding default probabilities we use Monto Carlo simulation to identify the initial debts D_{t_0} which results

to the same default probabilities by applying the formula from Goetz et al. [Goe10]. An explanation of this approach from Hull [Hul07] is shown in Appendix C.2.

Summarized, we calculate the initial debt by the observed CDS of the issuer at the issue date for the certificates in combination with an assumed recovery rate. We should mentioned, that we observe different CDS level at the corresponding issue dates of the certificates. While the CDS for the DBGC$^{(\text{fix})}$ is 88.34 basis point at the relevant issue date, the CDS for the DBGC$^{(\text{min})}$ (103.05 bp) and the the DBGC$^{(\text{ave})}$ (109.38 bp) are significant higher.
It results, that we have to concentrate on the range between $D_{t_0}^{(\text{low})} = 64.00$ and $D_{t_0}^{(\text{high})} = 82.00$. The comparison in Table 6.5 shows the t_0-prices of the three certificates in the Black and Scholes model under default risk of the issuer.

Table 6.5: Calculated t_0-price for all DBGCs

t_0-price in % of N	DBGC$^{(\text{fix})}$	DBGC$^{(\text{min})}$	DBGC$^{(\text{ave})}$
$R = 0.4$	93.98	93.34	91.97
$R = 0.5$	94.20	93.67	92.25
$R = 0.6$	94.48	93.99	92.60

The t_0-prices are calculated with the same parameter as in the calculation before. In addition, three different parameter for the recovery rate are used. The significant initial debt is derived by the CDS of the issuer.

In particular, all illustrated prices are significant lower than the nominal amount.
To sum up the effects, the t_0-prices are higher as we assume a higher recovery rate for the issuer, although this implicates a higher assumed initial debt. This could be explained due to the pricing formular where the recovery rate has a more immediate influence on the observed t_0-prices.
For all certificates, we discover a relative small price change between 0.20 % and 0.35 % if the recovery rate R varies by 0.1. According to all recovery rates and the calculated initial debts D_{t_0} for each certificate the defaultable Best Garant Certificate with the fixed strike setting shows the highest t_0-price. The defaultable minimum entry strike Best Garant Certificate is slightly more expensive than the DBGC$^{(\text{fix})}$. The lowest t_0-price is shown by the DBGC$^{(\text{ave})}$, it is on average 1.20 % shepper than the DBGC$^{(\text{min})}$. The difference to the fix entry strike is almost 2.00 %. It is evident, if we take into account default risk we will find out that all Best Garant Certificates are overvalued at issue date. As we anticipated, the level of overvaluation is also a matter on the path-dependency.

Finally, we observe a special loss rate for the corresponding defaultable Best Garant Certificates. Basically, we want to illustrate the suboptimality of the certificates by separated loss rates. Since the DBGCs are not issued at the fair model price we will split the loss rate introduced in Proportion 10 in two parts. We define

$$l_T^{(\mathrm{w})} = \frac{\ln\left(\frac{CE_T^*}{C\tilde{E}_T}\right)}{T} + \frac{\ln\left(\frac{C\tilde{E}_T}{CE_T^{\mathrm{DBGC,w}}}\right)}{T} \tag{6.34}$$

where $C\tilde{E}_T$ describes the certainty equivalent of the fair DBGC$^{(\mathrm{w})}$, calculated with the fair cap rate assuming $g = 0.0$ % and the given combination of R and D_{t_0} and $CE_T^{\mathrm{DBGC,w}}$ is the certainty equivalent of the traded defaultable DBGC with the parameter of the termsheet. CE_T^* still illustrates the certainty equivalent of the optional Constant-Mix Strategy. With this definition, we are able to separate a loss rate depending on the specific structure of the DBGC (loss rate by structure) and a loss rate as a result of the overvalued price at issue date which results e.g. from the embedded margins (loss rate by market price).
For each DBGC, we will calulate the illustrated loss rates for a recovery rate of $R = 0.5$, the more conservative assumed recovery rate $R = 0.6$ and the lowest assumption of $R = 0.4$ and the corresponding initial debt D_{t_0}.

Of course, the loss rates for the defaultable fixed entry strike BGC depend on the fair cap rates which we calculate by applying (6.19) for the relevant parameter combination. The following calculations are based on the tuples $\big(R = 0.6,\, D_{t_0} = 0.7475,\, c^{(\mathrm{fix})} = 10.63\ \%\big)$, $(0.5,\, 0.685,\, 10.90\ \%)$ and $(0.4,\, 0.64,\, 11.07\ \%)$, where c describes the fair model based cap rate. At first, Figure 6.12 illustates the calculated loss rates for the traded DBGC$^{(\mathrm{fix})}$.

With a look on Figure 6.12, we will distinguish between the 'loss rate by structure', the 'loss rate by market price' and finally the summation of both. First, we identify that the overall loss rate are more or less completely discribed by the 'loss rate by structure'. The 'loss rate by market price' takes only a very small proportion of the overall loss rate. Second, we recognize that the overall loss rate is rising significantly with a lower recovery rate.
Assuming $R = 0.6$, the loss rate is about $l_T = 4.0$ % while it is soar to $l_T = 6.0$ % (resp. $l_T = 9.0$ %) as we assume a recovery rate of $R = 0.5$ (resp. $R = 0.4$).
We observe, that the 'loss rate by structure' takes the dominant position, so that between 93 % and 99 % of the overall loss rate is explained the by this component. Of course, an

Figure 6.12: Composition of the loss rates for the fixed strike DBGC

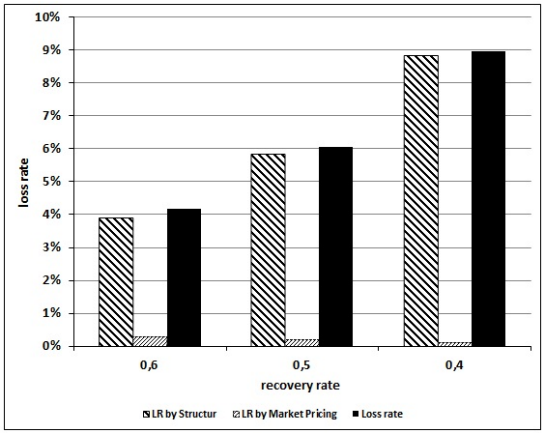

Composition of the special loss rate calculation of the traded defaultable fixed Entry Strike BGC with different recovery rates.

optional default of the issuer has no impact on the value of an investment in a Constant-Mix Strategy.[16] As anticipated, a CRRA investor suffers from an optional default of the issuer. The lower the corresponding payoff in the case of a default, which is defined by the recovery rate the higher is the 'loss rate by structure'.

At a first glance, the 'loss rate by market price' seems to be a small amount between 0.10 % and 0.30 %. But, we can use the 'loss rate by market Price' as a measure for the overvaluation and the mispricing of the traded certificates. Thus, it is meaningful to look on the this special loss rate in comparison with the results of the other defaultable Best Garant Certificates.

In analogy to the calculations before, we calculate the fair cap rates for the path-dependent DBGCs by (6.21). The relevant tuples for the defaultable minimum strike setting are $\big(R = 0.6,\, D_{t_0} = 0.7975,\, c^{(\min)} = 8.42\ \%\big)$, (0.5, 0.7275, 8.61 %) and (0.4, 0.6775, 8.76 %). Finally, we use for the DBGC$^{(\text{ave})}$ the three tuples $\big(R = 0.6,\, D_{t_0} = 0.82,\, c^{(\text{ave})} = 12.27\ \%\big)$, (0.5, 0.7475, 12.71 %) and (0.4, 0.6950, 13.04 %).

Now, we illustrated the calculated loss rates for the DBGC$^{(\min)}$ and DBGC$^{(\text{ave})}$. It is

16 Of course, the correspoding developments are not completly independent, since we assume a positive correlation between the issuers underlying and the underlying of the certificate.

seen, that the leading development are the same, this should be a result by the dominance of the default risk in the loss rate calculation.

Figure 6.13: Composition of the loss rates of the minimum and average strike DBGC

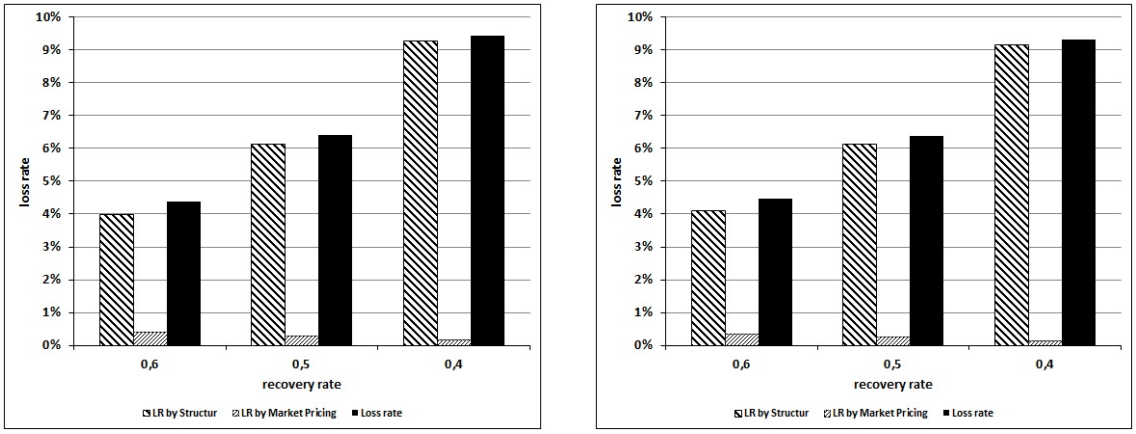

Composition of the special loss rate calculation of the traded minimum and average entry strike DBGC with different recovery rates.

Figure 6.13 shows the relevant results of the special loss rate calculation for the two path-dependent DBGCs. The tendency of the different loss rates is equal, but they differ in their loss rate levels. In particular, all calculated loss rates depending on the minimum and average strike setting are higher than the loss rates for the fixed entry strike DBGC. Interestingly, we do not find a explicit result which best-entry feature has the highest loss rate. It holds for the recovery rate $R = 0.6$, that the DBGC$^{(\text{ave})}$ has a loss rate of $l_T^{(\text{ave})} = 4.46$ % compared to $l_T^{(\text{min})} = 4.39$ %, the loss rate of the minimum entry strike DBGC. But, for the lowest observed recovery rate $R = 0.4$ the rank changes, so that $l_T^{(\text{min})} = 9.43$ % is higher than $l_T^{(\text{ave})} = 9.31$ %.

In addition, the 'loss rate by market price' is obivously higher for the path-depentent certificates. The difference is 0.28 % resp. 0.25 % for the minimum and average strike DBGC in comparison with fix strike setting with 0.20 %. Hence, it follows that the ratio between the 'loss rate by structure' and the 'loss rate by market price' is different. The porportion of the 'loss rate by market price' is clearly higher in the case of the path-dependent certificate. This can be interpreted as in indicator for our presumption that a more complex and, for the investor, difficult to understand product provides the issuer the opportunity to gain a

higher margin.

6.7 Conclusion

We analyze defaultable Best Garant Certificates in a Black and Scholes model which allows a default of the issuer. We find out, that the fair cap rate are significant higher than in the case where the default event is impossible (cf. Chapter 4). However, most result regarding the pricing of fair (g,c)-tuple are in analogy to the non-defaultable case, only the overall level is different. In addition, it holds that the investor pays an implicit premium for the entry strike (and the guarantee).

With regard on the optimality (suboptimality) of the best-entry strike settings and the overall product design for an expected utility maximizing CRRA investor, we discover further aspects. We could mention, by analying of the return rates at maturity, that the investor has different choices. Regarding the different payoff structures of the certificates (resp. entry-strikes), the investor could decide if she like to have a good return more often with selecting the minimum DBGC or a better return less often with the other structures. Furthermore, we find out that the investor, if possible, could select an issuer who is more solvent than an other issuer to reduce the probability of an issuers default. In other word, depending on the financial strenght of the issuer the event of default is more or less probable. If the issuer is less solvent the investor could require better product specification, i.e a higher guaranteed rate or higher cap rates. Nevertheless, if the an issuer default event occurs the payoff of at maturity will depend on the recovery rate which is always unknown at issue date.

Regarding the observed market prices, it is proved, that the traded Best Grant Certificates are highly overpriced at issue date. In a special loss rate calculation we illustrate that the CRRA investor will suffer more from the optimal default of the issuer instead of the overpricing at issue date. In addition, our results show that the issuer could profit by issuing path-dependent certificates which have more complex payoff structures. Since this certificates are difficult to understand for the investor, the issuer could gain a higher margin.

CHAPTER 7

Optimal product design for products with guarantees and caps under margin constraints

7.1 Introduction

In this chapter, we explore the optimal product design of products with guarantees and caps from both the investor and the issuer's perspective, allowing an embedded margin. We assume that an issuer does not offer any products for free. Thus, we consider an adjustment of the fair product design depending upon embedded margins. Nevertheless, we suggest that the issuer tries to offer products that fit to the investor's preference.

We will observe two sources of embedded margin. On the one hand, we presume a sales margin that is given exogenously. This margin could be economically required by a third party, which we note as the distribution company.[1]
On the other hand, we assume a hedging margin, which the issuer has to apply. Although there are many opportunities to define such a hedging margin, we will assume that the corresponding margin results from internal hedging requirements. Since it is impossible to hedge an offered product in many cases, issuers have to use sub-hedges or quantile hedging methods.[2] In our observation, we assume a hedging margin that increases with the Value-at-Risk of the return rate distribution of the product. Put simply, if the optional maximum return rate for the investor is very high, the issuer will require a high hedging

1 For example, distribution companies could be banks, insurance companies, investment managers or a relevant distribution department of the issuing company.
2 In practice, the product hedging depends upon different effects, such as the trade book of the issuer, the liquidity of the underlying, etc. We refer to Foellmer et al. [Foe99] and Foellmer et al. [Foe00] who motivates the method of quantile hedging, where only a fix part of the liabilities are hedged.

margin, which influences the product specification. Thus, the overvaluation of the product depends upon a VaR approach, which describes the unhedged part of the return rate distribution. The adjustment of this problem ends in a loop of changing the parameter since an adjustment of the cap rate or the participation rate is followed by a new return rate distribution.
We observe products characterized by a guaranteed rate g, a participation rate α and a cap rate c.[3] While the guaranteed rate and the cap rate define constant amounts (Ne^{gT} resp. Ne^{cT}), α determines the proportion to which the product participates in the underlying performance. In our analysis, we allow two different underlying assets where both can be interpreted as a value process given by Constant-Mix strategies. V_t is defined by the optimal Constant-Mix strategy for the risk aversion $\gamma = 2$ and S_t describes the process of a Constant-Mix strategy that invests the complete amount in the risky asset.[4]
However, we try to find the optimal product design under the constraint of an embedded margin. To classify the preference of the investor, we presume that her utility could be described by a constant relative risk aversion (CRRA) utility function.
The embedded margins define an addition source of suboptimality for the investor. However, we differ between two margins: an exogenous given sales margin $M_{(sales)}$ and an issuer's hedging margin $M_{(hedge)}$. As previously mentioned, we motivate the hedging margin by method of quantile hedging[5], where the issuer will only perfectly hedge a given quantile of the optimal liabilities at maturity. Depending upon the remaining risk - which we calculate by a Value-at-Risk approach - the issuer will calculate $M_{(hedge)}$, which serves as a buffer if the worst-case payoffs occurs. Accordingly, we can assume that the higher the remaining risk, the higher the embedded hedging margin.

For the investor, it follows indirectly that a higher optional return rate is followed by a higher margin. As a result, the margin impairs the product specification, e.g. a lower guaranteed rate.

All of our analysis rely on a formulated optimization problem where we calculate the (g,c,α)-tuple, which maximizes the CRRA investor utility under three constraints. The constraints are given by the fair product design or an adjusted product design with embedded margins.

3 By contrast to Chapter 3, we allow a variable participation rate α.
4 The underlying S_t can be compared to an equity index, which is often used in practice.
5 cf. Foellmer et al. [Foe99] and Foellmer et al. [Foe00]

We start to calculate the optimal fair product design of the corresponding products. For each underlying asset, we calculate the corresponding certainty equivalent for a range of risk aversion parameters and compare the results to the optimal certainty equivalent.[6] Furthermore, we illustrate the theoretical hedging margin of the optimal fair product design using the Value-at-Risk approach.
Based upon the theoretical margin, a variety of product adjustments are possible. Note that by changing the guaranteed rate g, the hedging margin is untouched. The adjustment of the participation rate or the cap rate will influence the hedging margin in a way, since the right-hand side of the return rate distribution is changed.

Beyond the fair product design, the application of the optimization problem results in an adjustment of the product specification. Thus, we calculated the optimal (g,c,α)-tuple generated under the embedded margin constraints. It results that all investors suffer from the embedded margin, albeit in their optimal product design. However, it is seen that a constant sales margin influences all observed products in the same way, while a hedging margin is followed by different product adjustments. Here, it is proven that a change of the relevant underlying could result in a higher certainty equivalent of the investor.

7.2 Summary of the product description and further assumptions

In this section, we provide an overview of the related assumptions used in our analysis. We observe products with guarantees and caps. As the underlying assets, we observe the value process V_t based upon the optimal Constant-Mix Strategy φ^* for $\gamma = 2$, as well as the stock price process S_t.
We illustrate the class of investors and give a closed-form solution to calculate the expected utility regarding the products.

7.2.1 Related assumption for market model and the product used

We assume the market model with two assets: the risky asset and the risk-free asset.[7] Thus, for the assumed stock price process S_t and for the risk-free asset B_t holds

$$dS_t = \mu S_t dt + \sigma S_t dW_t \quad \text{and} \tag{7.1}$$

$$dB_t = B_t r dt \tag{7.2}$$

6 The optimal certainty equivalent results from the relevant Constant-Mix strategy, depending upon the risk aversion of the investor.
7 The assumption is analogous to Chapter 3.

where $(W_t)_{0\leq t\leq T}$ is a standard Brownian motion under the real world measure P. μ is the drift of the risky asset and σ is the corresponding volatility of the process. Furthermore, r is the risk-free interest rate. In this model setup, we assume that μ, σ and r are constant. For pricing issues, we rely on the dynamics of the stock prices under the equivalent martingale measure (resp. the risk neutral measure)[8] P^*, which is given by

$$dS_t = rS_t dt + \sigma S_t dW_t^*, \tag{7.3}$$

For the observed products, we allow two underlying assets.
On the one hand, we use the value process V_t of the Constant-Mix strategy that is optimal for the assumed investor with risk aversion parameter $\gamma = 2$.[9] Remember that the corresponding dynamics are given by

$$dV_t = V_t \left((r + \varphi(\mu - r))\, dt + \varphi\sigma dW_t \right) \tag{7.4}$$

In addition, we are able to describe the value process with

$$V_t = V_0 e^{(1-\varphi)\left(r+\varphi\frac{1}{2}\sigma^2\right)t} \left(\frac{S_t}{S_0}\right)^{\varphi}. \tag{7.5}$$

On the other hand, we assume the stock price process S_t, which is comparable with an equity index. Of course, S_t could be identified as the value process of a Constant-Mix strategy V_t with $\varphi = 100$ %. Since both underlyings can be defined by their volatility σ, we write V_t^σ to describe the general case.
The payoff of the corresponding product with guarantee G_T and cap C_T is stated with

$$X_T^\sigma = G_T + (\alpha V_T^\sigma - G_T)^+ - (\alpha V_T^\sigma - C_T)^+ \tag{7.6}$$

where $G_T = e^{gT}$ the guarantee amount, $C_T = e^{cT}$ the maximum payoff amount, α the participation rate and V^σ is the underlying asset. We use the Black and Scholes model to

8 cf. Harrison et al. [Har79] and Harison et al. [Har81]
9 This is comparable with investor Γ from Chapter 3

illustrate the t-price of the products by[10]

$$X_t^\sigma = e^{(g-r)(T-t)} + \alpha \left(Call^{V^\sigma} \left(t, \frac{e^{gT}}{\alpha} \right) - Call^{V^\sigma} \left(t, \frac{e^{cT}}{\alpha} \right) \right) \tag{7.7}$$

where $Call^{V^\sigma}(t, \frac{e^{gT}}{\alpha})$ describes the t-call price on V^σ with strike $K = \frac{e^{gT}}{\alpha}$, an initial time to maturity of T and remaining time $(T-t)$. In the following, we focus on different combinations of g, c, and α regarding pricing issues, the hedging margin and investor's utility.

Of course, we need a fair product design in our calculation. For this reason, we use the following definition.

Definition 11 (Fair product) *Let N be the nominal amount of the product at time $t_0 = 0$ and r the risk-free interest rate. The product X^σ written on the underlying V^σ with maturity T is called fair if the no-arbitrage t_0-price of the corresponding payoff X_T^σ at maturity is equal to the nominal amount, whereby*

$$N = E_{P^*} \left\{ e^{-r(T-t_0)} X_T^\sigma \right\} \tag{7.8}$$

where E_{P^*} denotes the expectation under the equivalent martingale measure. Furthermore, we assume $N = 1$ in the following.

7.2.2 Description of the investor's utility

We assume that the expected utility of the investor could be described by a CRRA utility function, which is given by

$$u(X_T^\sigma) = \frac{(X_T^\sigma)^{1-\gamma}}{1-\gamma} \tag{7.9}$$

with $\gamma > 1$. For the observed products and a CRRA utility function, we can use the closed-form solution for the expected utility EU given in Proposition 8.

Proposition 8 (Expected utility and certainty equivalent) *For an expecting CRRA utility maximizing investor with investment horizon T, it holds in the Black and Scholes model*

(i) For the guaranteed rate g, the cap rate c and the participation rate α the expected

10 The description is also given in Chapter 3.

utility $EU^{X_T^\sigma}$ *for the product* X^σ *is given by*

$$
\begin{aligned}
EU^{X_T^\sigma} &= E_P\left[u\left(e^{gT} + \left[\alpha V_T^\sigma - e^{gT}\right]^+ - \left[\alpha V_T^\sigma - e^{cT}\right]^+\right)\right] \qquad (7.10)\\
&= \frac{1}{1-\gamma}\left[e^{(1-\gamma)gT}\mathcal{N}\left(\frac{gT + \ln\alpha - (\mu - \frac{1}{2}\sigma^2)T}{\sigma\sqrt{T}}\right)\right.\\
&+ e^{(1-\gamma)cT}\mathcal{N}\left(-\frac{cT + \ln\alpha - (\mu - \frac{1}{2}\sigma^2)T}{\sigma\sqrt{T}}\right) \quad + \alpha^{1-\gamma}e^{(1-\gamma)\left(\mu - \frac{1}{2}\gamma\sigma^2\right)T}\\
&\left.\left(\mathcal{N}\left(\frac{cT + \ln\alpha - (\mu + (\frac{1}{2} - \gamma)\sigma^2)T}{\sigma\sqrt{T}}\right) - \mathcal{N}\left(\frac{gT + \ln\alpha - (\mu + (\frac{1}{2} - \gamma)\sigma^2)T}{\sigma\sqrt{T}}\right)\right)\right]
\end{aligned}
$$

(ii) The certainty equivalent $CE_T^{X^{(gen)}}$ *of a product is given by*

$$CE_T^{X^{(gen)}} = \left[(1-\gamma)EU^{X^{(gen)}}\right]^{\frac{1}{1-\gamma}} \qquad (7.11)$$

Proof 8 *The proof is given in Appendix A.3.*

For the observation, we define the following. We use a risk-free interest rate of 2.4 % and a time to maturity of $T = 5$. The volatility of underlying V_t is $\sigma = 14.04$ % and $\sigma = 23.5$ % for S_t. Additionally, the drift parameter of the value process V_t for the optimal Constant-Mix strategy is given by $\mu = 6.34$ %. For S_t, the drift is assumed by $\mu = 9.0$ %.

7.3 Optimization problem and embedded margin

In this section, we formulate the optimization problem and introduce how the assumed margins are calculated. We assume that the issuer will require a margin for each corresponding product, which is built by a sales margin and a hedging margin. While we assume that the sales margin is fixed as well as exogenously given, the hedging margin depends upon a dynamic calculation of the issuer.

7.3.1 Optimization problem

We describe the optimization problem, which relies on the fair product design. Assuming all parameters except the guaranteed rate g, the cap rate c and the participation rate α are fixed. Using our assumption, we can calculate all combination of (g,c,α) so that the product design is fair. Using (7.7), we will write for the fair product design

$$X_{t_0}^\sigma(g,c,\alpha) = e^{(g-r)T} + B^{Call}\left(\alpha, t_0, r, e^{gT}, T, \sigma\right) - B^{Call}\left(\alpha, t_0, r, e^{cT}, T, \sigma\right) = 1 \qquad (7.12)$$

with $S_{t_0} = V_{t_0} = 1$ and σ the corresponding volatility of the underlying.

Note that each combination results in a return rate distribution at maturity under the real world measure, which illustrates the optional liabilities of the issuer.
Thus, based upon the fair product design, the issuer can calculate a margin M. More precisely, we define M as the sum of a hedging margin $M_{(hedge)}$ and a sales margin $M_{(sale)}$. Assuming that the sales margin is given exogenously, we implement $M_{(sale)}$ as a constant in the calculation of the overall margin.[11] For a better understanding of the influence parameter, we will denote the overall margin by $M(g,c,\alpha)$.

Hereby, it results that the issuer has to calculated adjusted parameter (g^*,c^*,α^*) (differing from the theoretical fair parameter (g,c,α)) if she requires a margin. It is meaningful to assume that the issuer will apply the margin in such a way that the fair issue price decreases. Finally, it should hold for $t_0 = 0$ that

$$X^{\sigma}_{t_0}(g^*,c^*,\alpha^*) + M(g^*,c^*,\alpha^*) = 1 \tag{7.13}$$

Of course, this is a dynamic problem since by changing the parameter g,c and α, the value of the M also changes.

Now, we focus on the investor's utility. We observe the investors certainty equivalent given by $CE^{X^{\sigma}}(g,c,\alpha)$ and formulate the optimization problem by

$$\begin{aligned} &\max_{(g,c,\alpha)} CE^{X^{\sigma}}(g,c,\alpha) \\ &\text{with} \quad X^{\sigma}_{t_0}(g^*,c^*,\alpha^*) + M(g^*,c^*,\alpha^*) = 1 \end{aligned} \tag{7.14}$$

In the following, we will always rely on this optimization problem. According to our analysis, we can apply the constraint with $M = 0$, M fixed or M dynamical derived.

7.3.2 Calculation of the margin

We mention that the issuer has different opportunities to calculate her relevant hedging margin $M_{(hedge)}$. We assume a Value-at-Risk approach to estimate her optional liabilities

11 We should also mention that the sales margin could be variable e.g. in the case where a high sales margin is required for product with a longer time to maturity. Nonetheless, we focus on one constant $M_{(sale)}$.

at maturity. Using the VaR approach, she can derive the corresponding hedging margin $M^{VaR_q}_{(hedge)}(g,c,\alpha)$ using

$$VaR_q = \inf\{x|F(x) \geq q\} \tag{7.15}$$

where F describes the cumulative distribution function of the return rates at maturity of a given product and q the assumed quantile that the issuer uses. In the standard Black and Scholes framework, the Value-at-Risk can be calculated analytically.
Using the Value-at-Risk approach with a fixed quantile q, the hedging margin can be calculated by

$$M^{VaR_q} = a\,(VaR_q)^b + \bar{a} \tag{7.16}$$

where $a,b,\bar{a} \in \mathbb{R}$ describes how the Value-at-Risk influences the overall margin. Of course, the constant parameter $\bar{a}$ could be implemented as the exogenous sales margin $M_{(sale)}$, which is independent from the type of hedging.

In the following, we use the 0.05-quantile for our calculation. Thus, our approach applies the $VaR(95\ \%)$, which is often used in practice.

7.4 Calculation of the optimal product design

In this section, we observe different opportunities to determine the optimal tuple of the guaranteed rate g, the cap rate c and the participation rate α. For our calculation, we use two underlying assets: V_t and S_t.
On the one hand, we calculate the optimal fair (g,c,α)-tuple assuming that the issuer does not require a margin. Additionally, we illustrate the resulting certainty equivalents for the investors. However, we also calculate a theoretical hedging margin to classify the optimal product design from the perspective of the issuer.

On the other hand, we observe two cases with embedded margins. First, we presume a fixed sales margin that is constant for all product specification. Thus, we calculate the optimal adjusted product specification for the investors. Second, we take into account a hedging margin that relies on the illustrated Vaule-at-Risk approach. We present the adjusted (g,c,α)-tuples that are optimal for the CRRA investor. For both calculations, we highlight the result by illustrating the calculated certainty equivalents and the margins to allow a comparison with the optimal fair product design.

7.4.1 Optimal fair product design

In this section, we assume a fair product design with margin $M(g^*,c^*,\alpha^*) = 0$. Thus, the optimal product design could be calculated by the illustrated optimization formula in (7.14). Here, the constraint is given by the fair product design without a margin. We rely on risk aversion parameter of $\gamma \in [2,5]$ and derive the fair (g,c,α)-tuple, as well as the resulting certainty equivalents. In our calculation, we focus on both introduced underlying asset for the product $X_t^{(fair)}$. Thus, Figure 7.1 shows the results for the underlyings S_t and V_t.

The results based upon the value process V_t are illustrated in the left plot of Figure 7.1, while we calculate the optimal solution in the right plot for the underlying S_t.

Overall, we identify that the guaranteed rates increase with higher risk aversion, while the cap rates decrease. For the participation rate, we cannot find a clear trend.

Remember that we use the value process V_t of the optimal Constant-Mix strategy for an investor with $\gamma = 2$ in the left plot. Thus, the optimal guaranteed rate is very small and the cap rate is extremely high. Furthermore, for $\gamma = 2$, we identify a participation rate of $\alpha = 100$ %.

However, an investor with a higher risk aversion requires a higher guaranteed rate. At once, the cap rate has to be lower. Interestingly, the participation rate neither increases nor decreases with higher γ. In comparison to the guaranteed and the cap rates, the variation of the participation rates is margin between $\alpha = 99.968$ % and $\alpha = 100.144$ %.

The right plot of Figure 7.1 illustrates the results relying on the underlying S_t. We should mention that S_t is more risky than V_t.[12] Thus, we observe a significantly higher guaranteed rate starting with $g = -5.53$ % for $\gamma = 2$. Furthermore, the maximum cap rate is identified at $c = 12.01$ %. By contrast to the observation relying on V_t, we find a strictly increasing participation rate.

Summarized, both plots show a comparable development concerning the guaranteed and cap rates, although they differ in the overall level of the parameters. The observation of the participation rates highlights a small discrepancy regarding the underlyings. For S_t, the participation rate strictly increases in γ. Observing the underying V_t, the participation rate neither increases nor decreases in the range of the assumed risk aversion and finds a minimum for $\gamma = 2.75$.

12 We mention in Chapter 3 that S_t is optimal for an investor with $\gamma = 1.195$.

Figure 7.1: Optimal fair (g,c,α)-tuple

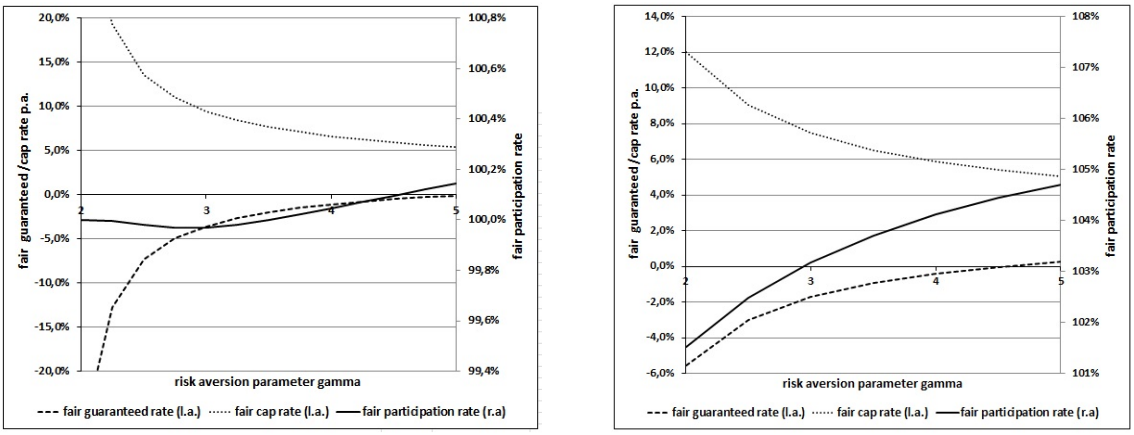

The optimal fair (g,c,α)-tuples for $X_t^{(fair)}$ from the investor's perspective are illustrated for varied risk aversion parameter γ and assumed underlying V_t (left plot), as well as S_t (right plot).

Next, we compare the corresponding optimal certainty equivalents of the products $X_t^{(fair)}$ with the certainty equivalents relying on the optimal Constant-Mix strategies (for each risk aversion γ). Figure 7.2 shows the corresponding developments. Of course, all calculated certainty equivalents decrease in γ. We identify that the calculated certainty equivalents for $X_t^{(fair)}$ written on V_t are always higher than the results relying on underlying S_t. However, the difference is reduced with higher risk aversion.

In the left plot of Figure 7.2, it is seen that the calculated certainty equivalent of $X_t^{(fair)}$ for $\gamma = 2$ is almost equal to the optimal Constant-Mix certainty equivalent. In particular, the corresponding product specification is very close to the relevant value process of the Constant-Mix strategy due to the low guaranteed and high cap rate. Obviously, the difference rises for higher γ.

Intuitively, we assume that we could find an intercept point in the right plot of Figure 7.2 if we allow lower risk aversion parameter γ. However, the range of $\gamma = 2$ and $\gamma = 5$ the calculated certainty equivalent is on average 0.25 % lower.

Looking ahead for the following calculation (which takes into account the embedded margin), we also calculate the theoretical hedging margin depending upon the optimal fair (g,c,α)-tuple in Figure 7.2. Since the hedging margin depends upon a VaR approach, it is higher for higher cap rates and higher participation rate. In general, this is given for low risk aversion parameters. However, the theoretical hedging margin calculated for

Figure 7.2: Certainty equivalents relying on the optimal fair products

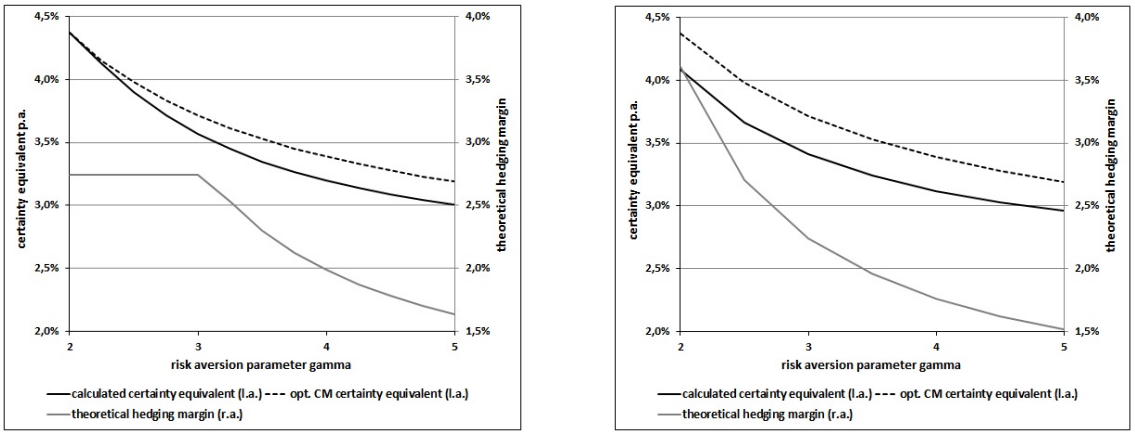

A comparison between the calculated optimal certainty equivalents and the optimal Constant-Mix certainty equivalents is shown for the products $X_t^{(fair)}$ with underlying V_t (left plot) and S_t (right plot) for varied risk aversion parameter γ.

the underlying V_t is constant in the range of $\gamma \in [2,3]$. Such a development holds if the VaR(95 %) of the corresponding return rate distribution of the products $X_t^{(fair)}$ is equal at the right hand side. Nevertheless, for risk aversion parameter $\gamma > 3$ as well as all γ for the products relying on S_t, the theoretical hedging margin decreases with γ. Note that even the calculated certainty equivalents are always higher for $X_t^{(fair)}$ written on V_t, whereby we identify that the theoretical hedging margins are also higher for $\gamma > 2.5$. This development can be important when the issuer has to adjust the product specification owing to this margin.

7.4.2 Optimal adjusted product design

In our observation, the issuer has to handle internal requirements regarding the liabilities at maturity of the offered products. Additionally, we allow a sales margin that is completely independent from the issuer requirements.

For this reason, we introduce the margin M calculated by the sum of a exogenous sales margin $M_{(sale)}$ and a hedging margin $M_{(hedge)}$, which we calculate by the illustrated Value-at-Risk approach. In this section, we observe exemplary methods to calculate the margin. We illustrate how the issuer will change the product design to meet the hedging requirements and at the same time offer *relative* optimal product designs. We assume that

especially the level of the cap rates influence the hedging margin of the issuer. However, the Value-at-Risk also depends upon the participation rate α.
For each observation, we calculate the adjusted (g,c,α)-tuples that are optimal for the CRRA investors and also fit to the relevant constraint. The results are highlighted with a focus on the calculated certainty equivalents.

Definition of the scenarios

We use the margin M defined in Section 7.3.2 by

$$M = aVaR(95\%)^b + \bar{a} \tag{7.17}$$

In the following, we observe two cases. First, we provide an overview concerning how an exogenous sales margin given by $\bar{a} = 2.0$ % influences the optimal product design. Of course, we use a,$b = 0$ to focus on the influence of the sale margin separately.

Second, we explore a hedging margin that only relies on the VaR approach; thus, we assume $\bar{a} = 0$. For example, we choose $b = 1$ and $a = 0.3$ for our calculation. This means economically that the issuer adjusts the product parameter in such a way that the embedded margin depends upon 30 % of the corresponding VaR(95 %) of the return rate distribution of the product X_t.

Influence of the sales margin

By observing the influence of a sales margin, we highlight that this amount is completely independent of the issuer's hedging requirements. Put simply, the fair product design that results in a nominal amount ($N = 1$) will change to an amount of $1 - M = 1 - \bar{a}$. Since we know that $\bar{a} = 2.0$ %, the calculated product specification will lead to a t_0-price of 0.98. This adjustment will be consummate by changing one or more of the three product parameters.

Of course, the adjustments are made within the optimization problem formulated in (7.14). Thus, all resulting combinations are optimal for the corresponding investor under the constraint of an embedded margin.
The adjusted product specification for both assumed underlyings (V_t and S_t) are illustrated in Figure 7.3. By analyzing the influence of the sales margin on the optimal adjusted

Figure 7.3: Optimal adjusted (g,c,α)-tuple resulting from embedded sales margin

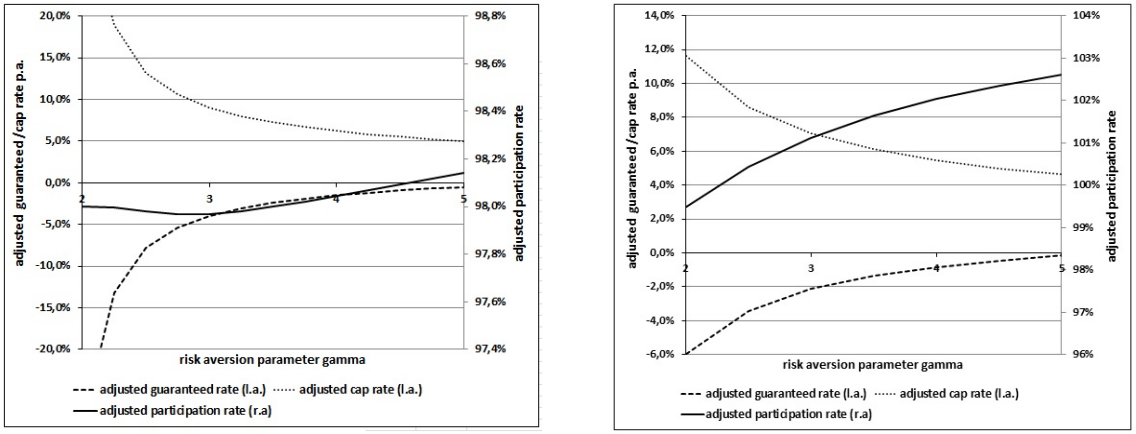

The optimal adjusted (g,c,α)-tuple $X_t^{(sales)}$ resulting from an embedded sales margin is illustrated for varied risk aversion parameter γ and assumed underlying V_t (left plot), as well as S_t (right plot).

product design, we identify an identical development for both underlying assets. The adjustment of the guaranteed and the cap rate are given by a shift of almost -0.4 % for all risk aversion parameters. Furthermore, we notice that all participation rates are 2.0 % lower. However, this means that the overall relation of the three parameter to each other is unchanged. This development is a direct result of the assumed utility function of the investors. The sales margin only reduces the investment amount to 0.98, which does not change the preferences of the CRRA investors. Thus, the adjusted product design the CRRA investor requires must be the same.

Applying this result, we assume that the calculated certainty equivalents make a parallel shift. The results highlighting this assumption are shown in Figure 7.4.

We identify that all calculated certainty equivalents are almost 0.4 % lower than for the optimal fair product $X_t^{(fair)}$. It results that – aside from the investor with $\gamma = 2$ who invests in the product written on V_t - all investors suffer from two sources of suboptimality. On the one hand, the structure of the product is suboptimal since it combines guarantees and caps that are not required by a CRRA investor. On the other hand, the sales margin leads to a parallel swift of the certainty equivalent p.a., which is finally 0.4 % lower. In our example, the utility loss caused by the sales margin is always higher than that relying on the suboptimal product specification. However, this development can also change with varying assumptions.

Figure 7.4: Certainty equivalents relying on the optimal adjusted products resulting from embedded sales margin

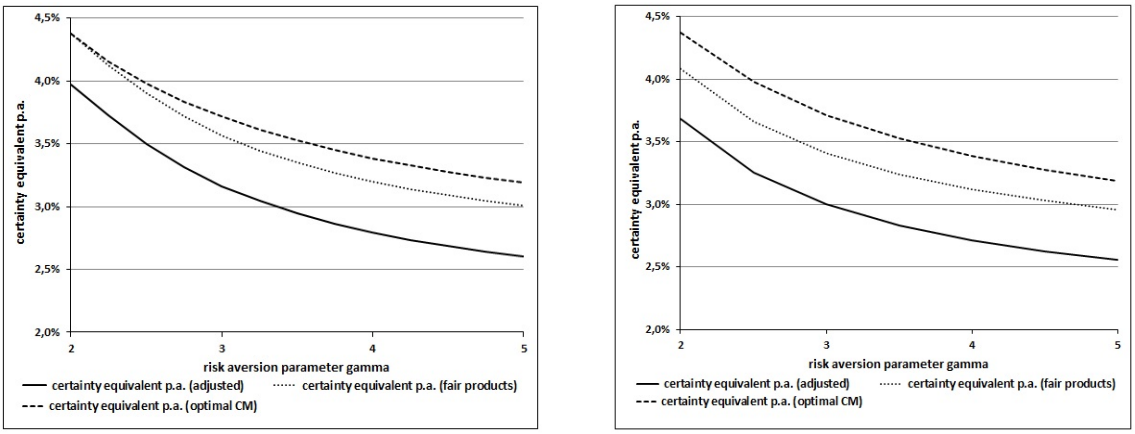

A comparison between the calculated optimal adjusted certainty equivalents as a result of an embedded sales margin and the optimal Constant-Mix certainty equivalents are shown for the products $X_t^{(sales)}$ with underlying V_t (left plot) and S_t (right plot) for varied risk aversion parameter γ.

Influence of the hedging margin

In the following, we will analyze the optimal product adjustment regarding a hedging margin derived by the Value-at-Risk approach. Thus, we assume that $\bar{a} = 0$. The parameters describing the influence of the VaR(95 %) are determined by $a = 0.3$ and $b = 1$.

We illustrate in Figure 7.5 the optimal adjusted (g,c,α)-tuple where a hedging margin of the issuer is considered. Interestingly, the two underlying assets result in completely different developments concerning the adjustment of the product design. In the left plot of Figure 7.5, the optimal adjusted parameter for the product $X_t^{(hedge)}$ relying on the underlying V_t are illustrated. We identify that the guaranteed and the cap rates marginal increase. Instead, it emerges that the participation rate is significantly lower than in the optimal fair product design.

First, we consider the lowest assumed risk aversion parameter ($\gamma = 2$). While $\alpha = 100$ % in the optimal fair product design, the optimal adjusted participation rate is $\alpha = 97.41$ %. More precisely, the hedging margin of the product $X_t^{(hedge)}$ is identical to an optional investment in the underlying V_t, since the low guaranteed rate and the high cap rate do not influence the Value-at-Risk. Thus, the adjustment is calculated by the Value-at-Risk of the underlying asset V_t itself. This effect is already illustrated in Figure 7.2, where a

Figure 7.5: Optimal adjusted (g,c,α)-tuple resulting from embedded hedging margin

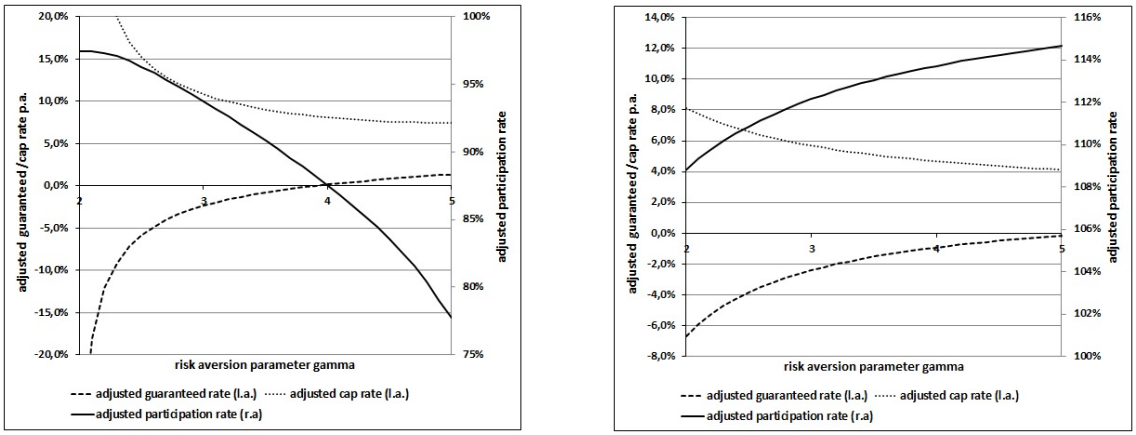

The optimal adjusted (g,c,α)-tuple for $X_t^{(hedge)}$ resulting by an embedded hedging margin is illustrated for varied risk aversion parameter γ and assumed underlying V_t (left plot), as well as S_t (right plot).

constant theoretical hedging margin is observed for a range of low risk aversion.
Second, we focus on a higher risk aversion parameter. It is proven that both the guaranteed rate and the cap rate are on average 1.32 % resp. 1.56 % higher according to the adjustment, respectively. However, the participation rate is significantly lower for all observed risk aversion parameters. Starting with $\alpha = 97.41$ %, the participation rate reaches a minimum of $\alpha = 77.70$ % for $\gamma = 5$. However, the investor profits from a higher cap rate in combination with a lower participation rate. More precisely, the required hedging margin of the issuer is about 0.21 % lower than the theoretical hedging margin in the fair product design, which we illustrate in the following Figure (cf. Figure 7.6).
Now, focusing on the underlying S_t, the results are the other way around, namely the adjusted guaranteed and cap rates are lower than those in the fair product design. However, the participation rate is clearly higher. For $\gamma = 2$, we calculate a fair tuple of ($g = -5.53$ %, $c = 12.01$ %, $\alpha = 101.52$ %). By taking into account the VaR approach, the guaranteed and cap rate decreases to $g = -6.66$ % and $c = 8.13$ %. At the same time, the participation rate increases to $\alpha = 108.84$ %. Furthermore, the difference in the participation rate increases with higher γ, whereby we compare a fair $\alpha = 104.70$ % to the adjusted one with $\alpha = 114.65$ % for $\gamma = 5$. However, in the observation, all adjusted cap rates are on average 1.68 % lower.

Note that the underlying S_t has significantly higher volatility and drift than V_t. It is obvious that both parameters are positively correlated with the Value-at-Risk. However, focusing on the corresponding products $X_t^{(hedge)}$, it is evident that the optimization leads to different results depending upon the assumed underlying assets.

Finally, we explore the adjusted certainty equivalents in Figure 7.6. However, since the shift in the certainty equivalents depends upon the margin, we also illustrate the embedded hedging margin. As anticipated, the adjusted certainty equivalents are significantly below

Figure 7.6: Certainty equivalents relying on the optimal adjusted products resulting from embedded hedging margin

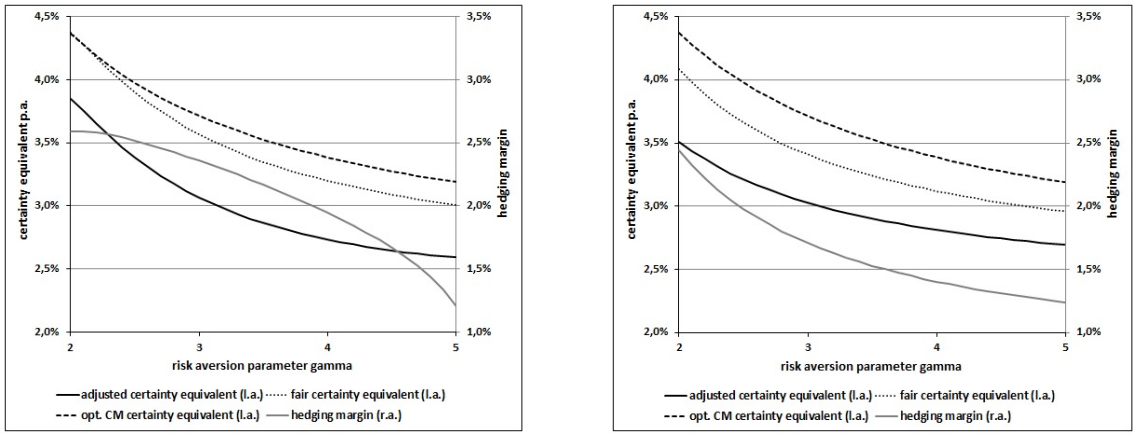

A comparison between the calculated optimal adjusted certainty equivalents as a result of an embedded hedging margin and the optimal Constant-Mix certainty equivalents is shown for the products $X_t^{(hedge)}$ with underlying V_t (left plot) and S_t (right plot) for varied risk aversion parameter γ.

the optimal CM certainty equivalents, as well as the fair certainty equivalents. Through the embedded hedging margin, we identify a certainty equivalent that is on average 0.63 % lower than the corresponding optimal solution. A comparison with the relevant fair certainty equivalent highlights that the certainty equivalents relying upon the products written on V_t decrease more than those based upon the underlying S_t. Here, the average decrease is 0.48 % for the underlying V_t and 0.36 % for the underlying S_t.
Nonetheless, an investor with lower risk aversion will prefer a product written on V_t. However, for a risk aversion of $\gamma > 3.3$, the certainty equivalents are higher for the products with underlying S_t. More precisely, although the utility loss caused by the suboptimal product specification is higher than for the comparable underlying V_t, the overall certainty

equivalent including the hedging margin adjustment is higher.
Additionally, Figure 7.6 shows the development of the hedging margin. Of course, the hedging margin decreases with the risk aversion of the investor. The observation of the two underlyings illustrates that the level of the hedging margin is almost identical for $\gamma = 2$ and $\gamma = 5$. Nonetheless, in between, the hedging margin differs. While the hedging margin depending upon the underlying V_t results in a concave development, it is convex for S_t. Thus, the hedging margin relying on the underlying V_t is always higher than that relying on S_t. The difference is very large for the mean γ.

7.5 Conclusion

We analyze the optimal product design of a product with guarantees and caps assuming an expected CRRA utility maximizing investor. In our observation, we focus on the suboptimality resulting from an embedded margin in the product.
Since we assume that the product description is defined by the issuer, we observe an optimization problem that focuses on a maximum utility for the investor under the issuer margin constraint. Furthermore, the issuer offers products written on two different underlying assets, namely V_t and S_t.

First, we explore the fair product design where no margin exists. In the calculation of the fair (g,c,α)-tuple, it emerges that the optimal solution can result in such low guaranteed and high cap rates, which have only a margin influence in the payoff distribution of the product. For example, this will appear if we assume an underlying which is almost optimal for an investor. Thus, the investor does not suffer from any suboptimality. However, all other observed investors find an optimal solution for the assumed product, although their certainty equivalents are lower than the optimal one. In general, this development results from the guaranteed and cap rate. Thus, even when we assume a fair product design, the investor suffers from a lower certainty equivalent, which depends upon the product specification using guarantees and caps.

We subsequently allow an embedded margin and analyze how the optimal product design changes. If we assume a fixed sales margin, we identify that the adjustments are identical for all risk aversion parameters. Compared to the optimal fair product design, the guaranteed rate, the cap rate and the participation rate decrease by a fixed amount for each risk aversion parameter. Thus, the adjusted certainty equivalents also result from a parallel swift. Nonetheless, all investors suffer from the sales margin in the same way, although

the utility loss can be smaller or larger than that occurring from the suboptimal product design. Of course, we ascertain that the grade of suboptimality depends upon the level of the sales margin.

Finally, we assume an embedded margin that the issuer requires regarding her optional liabilities at maturity. More precisely, our observation assumes a hedging margin that tends to be higher for a higher Value-at-Risk of the product. In this observation, we identify different results depending upon the assumed underlying asset. In the case of the underlying V_t, it is optimal for the investor if the issuer increases the cap rate and the guaranteed rate yet decreases the participation rate. Here, we find a lower hedging margin compared to the theoretical hedging margin of the optimal fair product. As previously mentioned, the adjustment is completely different for the underlying S_t. Thus, we observe a lower guaranteed and cap rate, while the participation rate is higher. Of course, this development results from the characteristics of the underlying asset. However, it is meaningful to mention that the adjusted certainty equivalents are higher for V_t if we focus on the lower risk aversion parameter. Nevertheless, for higher risk aversion, the products written on S_t are better for the investors.

CHAPTER 8

Conclusion and Future Research

The main focus of this thesis is to analyze different sources of suboptimality and their influence on the investor's utility. Based upon the assumption that the financial market is only complete for the issuer of retail products, we determine suboptimal retail products from the investor's perspective, since she can only choose one of the offered products. In general, the corresponding payoff profiles differ from the overall optimal product.
We illustrate that this restriction on the products offered brings different sources of suboptimality. More precisely, we analyze the problem of disposability, the suboptimal product design and an embedded margin.

Chapter 3 focuses on stylized products and structured stylized products. For all analyzed products, we quantify the suboptimality by a loss rate illustrating the utility loss of an investor who invests in a suboptimal product. We analyze the suboptimality pertaining to the problem of disposability of the optimal stylized products. It turns out that the corresponding utility loss can be huge if only a small number of stylized products are available.
For structured stylized products, we use guarantees and caps to distort the optimal payoff profile. Additionally, we combine the observed product with path-dependent payoff features and allow for an embedded margin. In the case of path-independent products, we ascertain that a loss rate close to zero is possible. However, all calculated loss rates for path-dependent products are significantly above zero. Finally, we prove that an embedded margin is followed by a more-or-less parallel shift of the loss rate. Thus, all investors suffer almost the same utility loss.
For future research, it can be interesting to consider different investors' utility functions. For example, we anticipate a dissenting result if an investor with a subsistence level is

assumed. Moreover, there are further payoff profiles that can be analyzed.

In Chapters 4 and 5, we consider two existing classes of structured stylized products that use an equity index as the underlying asset. More precisely, we analyze the class of Best Garant Certificates (BGCs) as well as the class of Locally Capped Garant Certificates (LCGC).[1] Both classes of certificates are characterized by guaranting at least the nominal amount of the product, although they differ in the application of the cap and the path-dependence. It emerges that none of the observed products offer an overall optimal payoff profile. Nonetheless, we find that for each observed product specification the optimal guaranteed rate is above zero, whereas an unrestricted CRRA investor does not require a guarantee. Furthermore, it is evident that the loss rate increases with the level of path-dependence. Finally, we illustrate that embedded margins of the observed products seem to be higher for path-dependent certificates when we refer to real market data.

Future analysis could validate our observations by studying further garant certificates. Again, varying the assumed investor's utility function can also be meaningful since all observed certificates offer a guarantee.

In Chapter 6, we generalize our analysis of Best Garant Certificates to a Black and Scholes model with default risk. We ascertain that many results only differ in their overall level compared to Chapter 4. For example, the observed fair cap rates are significantly higher, although their development regarding the entry strike settings and the guaranteed rates is identical. Furthermore, we identify how the possible default of an issuer influences the return rate distribution and the loss rates. Here, the main driver of higher loss rates seems to be the substantial loss in reference to a recovery rate if the issuer is insolvent at maturity. In case of a default, an amount significantly below the guarantee amount is paid. By taking into account default risk, we are able to repeat the analysis of real traded DBGC under more realistic assumptions. By contrast to Chapter 4, it turns out that all DBGC are highly overpriced at their issue date. Finally, we illustrate that the investor suffers more from the suboptimality of the product design (which includes the default risk) than from the unfair and suboptimal price at issue date.

This analysis demonstrates that a change of the model can be an interesting alternative for further observations. Moreover, it highlights that we should try to use model setups that explain the financial market as well as possible when we want to compare real traded products.

1 This includes the class of Globally Capped Garant Certificates (GCGC) with a path-independent payoff profile. Remember that a GCGC is identical to a BGC with fixed entry strike setting.

In Chapter 7, we study products with guarantees and caps and analyze how the utility of a CRRA investor is influenced by an embedded margin; thus, the optimal product design depends upon different constraints. Here, we introduce a sales margin as well as a hedging margin. While the sales margin is constant, the hedging margin that an issuer requires depends upon an Value-at-Risk approach.
We apply an optimization approach, which focuses on a maximum utility of the investor under a margin constraint. Assuming fair product design, it emerges that the optimal solution can result in so low guaranteed and so high cap rates, that they only have a marginal influence on the payoff distribution of the product. Thus, the investor will not suffer from any suboptimality if we assume an underlying that is already optimal for an investor. In particular, even if we assume a fair product design, the investor suffers from a lower certainty equivalent, which depends upon the product specification using guarantees and caps.
If we assume a fixed sales margin, all investors will suffer in the same way. However, the utility loss can be smaller or larger than that occurring from the suboptimal product design. Of course, the degree of suboptimality depends upon the level of the sales margin.
Finally, we assume a hedging margin that tends to be higher for a higher Value-at-Risk of the product. Here, the result depends upon the assumed underlying asset. Sometimes, it is optimal to increase the cap rate as well as the guaranteed rate, but at the same time decrease the participation rate. However, the adjustment is the opposite for another underlying; thus, we cannot ascertain consistent evidence for the optimal product design assuming a hedging margin.
Since the results regarding the hedging margin are significantly influenced by the assumed underlying, further analysis can pick up this issue.

In summary, we identify two areas of additional research. First, since our analysis assumes an expected CRRA maximizing investor, it is meaningful to validate the given results for varying classes of utility functions. For instance, for the class of garant certificates an investor with a DRRA utility function could be assumed. Here, interesting results can follow from the combination of the guaranteed rate of the products and the required guaranteed amount of the DRRA investor. However, the products can be also observed under a behavioral finance model. Besides the assumed guarantee amount, the optional default of the issuer can also be investigated.
Second, it is possible to study additional payoff profiles. For example, the suboptimality of a Buy-and-Hold as well as a CPPI strategy can be compared and quantified for a CRRA

investor. Furthermore, there is a variety of potential Structured Stylized Products that can be integrated in our analysis.

Bibliography

[And06] Anderson, L.: *Efficient Simulation of the Heston Stochastic Volatility Model*. Tech. rep. Banc of America Securities, 2006 (cit. on pp. 26, 100, 228).

[Bal09] Balder, S., M. Brandl, and A. Mahayni: 'Effectiveness of CPPI strategies under discrete-time trading'. *Journal of Economic Dynamics and Control* (2009), vol. 33: pp. 204–220 (cit. on p. 37).

[Bal10] Balder, S. and A. Mahayni: *How Good are Portfolio Insurance Strategies? in Alternative Investments and Strategies*. Ed. by Kiegel, Rüdiger, Matthias Scherer, and Rudi Zagst. World Scientific, 2010 (cit. on pp. 35, 37, 217).

[Bas02] Basak, S.: 'A comparative study of portfolio insurance'. *Journal of Economic Dynamics and Control* (2002), vol. 26: pp. 1217–1241 (cit. on pp. 21, 22, 42).

[Bau93] Baubonis, C., G.L. Gastineau, and D. Purcell: 'The Banker's Guide to Equity-Linked Certificates of Deposit'. *The Journal of Derivatives* (1993), vol. 1(2): pp. 87–95 (cit. on p. 23).

[Bau08] Baule, R., O. Entrop, and M. Wilkens: 'Credit Risk and Bank Margins in Structured Financial Products. Evidence from the German Secondary Market for Discount Certificates'. *The Journal of Futures Markets* (2008), vol. 28(4): pp. 376–397 (cit. on p. 27).

[Ber12] Bernard, C, P. P. Boyle, and S. Vanduffel: *Explicit Representation of Cost-Efficient Strategies*. Tech. rep. 2012 (cit. on p. 20).

[Ber11a] Bernard, C, M. Maj, and S. Vanduffel: 'Improving the Design of Financial Products in a Multidimensional Black-Scholes Market'. *North American Actuarial Journal* (2011), vol. 15: pp. 77–96 (cit. on p. 20).

[Ber11b] Bernard, C., P. P. Boyle, and W. Gornall: 'Locally-Capped Investment Products and the Retail Investor'. *The Journal of Derivatives* (2011), vol. 18(4): pp. 72–88 (cit. on pp. 7, 14, 25, 26, 121, 124, 125, 129, 132).

[Bin04] Bingham, N. H. and R. Kiesel: *Risk-Neutral Valuation, Pricing and Hedging of Financial Derivatives*. 2nd ed. Springer, 2004 (cit. on p. 226).

[Bjo96] Bjoerk, T.: 'Interest Rates Theory'. *Financial Mathemathics*. Ed. by Rung-galdier, W. J. 1996 (cit. on p. 30).

[Bla87] Black, F. and R. Jones: 'Simplifying portfolio insurance'. *The Journal of Portfolio Management* (1987), vol. 14: pp. 48–51 (cit. on pp. 22, 37).

[Bla73] Black, F. and M. Scholes: 'The Pricing of Options and Corporate Liabilities'. *Journal of Political Economics* (1973), vol. 81: pp. 637–657 (cit. on p. 21).

[Bla92] Black, F. and A. F. Perold: 'Theory of constant proportion portfolio insurance'. *The Journal of Economic Dynamics and Control* (1992), vol. 16(3-4): pp. 403–426 (cit. on pp. 22, 37).

[Bra10] Branger, N., A. Mahayni, and J.C. Schneider: 'On the optimal design of insurance contracts with guarantees'. *Insurance: Mathematics and Economics* (2010), vol. 46: pp. 485–492 (cit. on pp. 21, 22, 33, 42, 43).

[Bra11] Branger, N., A. Mahayni, and J.C. Schneider: 'Pricing and Upper Price Bounds of Relax Certificates'. *Review of Managerial Science* (2011), vol. 5: pp. 309–336 (cit. on p. 236).

[Bro06] Broadie, M. and Ö. Kaya: 'Exact Simulation of Stochastic Volatility and Other Affine Jump Diffusuin Processes'. *Operations Research* (2006), vol. 54(2): pp. 217–231 (cit. on pp. 101, 103, 128).

[Bur01] Burth, S., T. Kraus, and H.P. Wohlwend: 'The Pricing of Structured Products in the Swiss Market'. *The Journal of Derivatives* (2001), vol. 9: pp. 30–40 (cit. on p. 23).

[Car09] Carlin, B.I.: 'Strategic price complexity in retail financial market'. *Journal of Financial Economics* (2009), vol. 91: pp. 278–287 (cit. on pp. 2, 152).

[Car99] Carr, M. and D. B. Madan: 'Option valuation using the fast Fourier transform'. *Journal of Computational Finance* (1999), vol.: pp. 61–72 (cit. on p. 228).

[CFA13] CFA Institute: *Packaged Retail Investment Products - Investor Disclosure Considerations for a Key Information Document*. Tech. rep. CFA Institute, 2013 (cit. on p. 25).

[Cha10] Chang, E. C., D. Y. Tang, and M. Zhang: *Household Investments in Structured Financial Products: Pulled or Pushed?* Tech. rep. The 2010 Annual Meeting of the Financial Management Association (FMA), 2010 (cit. on p. 24).

[Che90a] Chen, A. H. and J. W. Kensinger: 'An Analysis of Market-Index Certificates of Deposit'. *Journal of Financial Services Research* (1990), vol. 4: pp. 93–110 (cit. on p. 23).

[Che90b] Chen, A.H. and R.S. Sears: 'Pricing the SPIN'. *Financial Management* (1990), vol. Sommer: pp. 36–47 (cit. on p. 23).

[Chi11] Chiappori, P.-A. and M. Paiella: 'Relative Risk Aversion is Constant: Evidence from Panel Data'. *Journal of the European Economic Association* (2011), vol. 9: 1021–1052 (cit. on p. 48).

[Chi10] Chiarella, C and C-Y Hsiao: 'Optimal Investment Strategies under Stochastic Volatility -Estimation and Applications'. *Quantitative Finance Research Centre* (2010), vol. 276: pp. 1–23 (cit. on pp. 114, 235).

[Cox85] Cox, J. C., J. E. Ingersoll, and S. A. Ross: 'A Theory of the Term Structure of Interest Rates'. *Econometrica* (1985), vol. 53: pp. 385–408 (cit. on p. 235).

[Cox00] Cox, J. C. and H. E. Leland: 'On dynamic investment strategies'. *Journal of Economic Dynamics and Control* (2000), vol. 24: pp. 1859–1880 (cit. on p. 20).

[Dan07] Dana, R.-A. and M. Jeanblanc: *Financial Markets in Continuous Time*. Springer, 2007 (cit. on pp. 19, 25, 30, 236).

[Del01] Delianedis, G. and R.L. Geske: *The Components of Corporate Credit Spreads: Default, Recovery, Taxes, Jumps, Liquidity, and Market Factors*. Tech. rep. The Anderson School at UCLA, 2001 (cit. on p. 28).

[Der10] Dersch, D.: *Dynamic Portfolio Insurance without Options in Alternative Investments and Strategies*. Ed. by Kiegel, Rüdiger, Matthias Scherer, and Rudi Zagst. World Scientific, 2010 (cit. on p. 22).

[Doe13] Doehrer, B., L. Johanning, N. Steiner, and A. Voelkle: *Issuer margins for structured products in Germany*. Tech. rep. EDG Study, 2013 (cit. on p. 24).

[Dos08] Doskeland, T. M. and H. A. Nordahl: 'Optimal pension insurance design'. *Journal of Banking & Finance* (2008), vol. 32: pp. 382–392 (cit. on pp. 24, 27).

[Dyb88a] Dybvig, P. H.: 'Distributional analysis of portfolio choice'. *The Journal of Business* (1988), vol. 61(3): pp. 369–393 (cit. on p. 20).

[Dyb88b] Dybvig, P.H.: 'Inefficient Dynamic Portfolio Strategies or How to Throw Away a Million Dollars in the Stock Market'. *The Review of Financial Studies* (1988), vol. 1(1): pp. 67–88 (cit. on p. 20).

[EK05] El Karoui, N., M. Jeanblanc, and V. Lacoste: 'Optimal portfolio management with american capital guarantee'. *Journal of Economic Dynamics and Control* (2005), vol. 8(2): pp. 93–126 (cit. on pp. 21, 219).

[Emb00] Embrechts, P.: 'Actuarial versus Financial Pricing of Insurance'. *The Journal of Risk Finance* (2000), vol. 1(4): pp. 17–26 (cit. on p. 21).

[Foe00] Foellmer, H. and P. Leukert: 'Efficient hedging: Cost versus shortfall risk'. *Finance and Stochastics* (2000), vol. 4: pp. 117–146 (cit. on pp. 185, 186).

[Foe99] Foellmer, H. and P. Leukert: 'Quantile Hedging'. *Finance and Stochastics* (1999), vol. 3: pp. 251–273 (cit. on pp. 185, 186).

[Fus06] Fusai, G., I.D. Abrahams, and C. Sgarra: 'An exact analytical solution for discrete barrier options'. *Finance and Stochastics* (2006), vol. 10: pp. 1–26 (cit. on p. 91).

[Goe10] Goetz, Barbara, Rudi Zagst, and Marcos Escobar: *Pricing Certificates Under Issuer Risk in Alternative Investments and Strategies*. Ed. by Kiegel, Rüdiger, Matthias Scherer, and Rudi Zagst. World Scientific, 2010 (cit. on pp. 5, 15, 27, 154–156, 160, 167, 180, 243, 245).

[Gol79a] Goldman, M. B., H. B. Sosin, and L. A. Shepp: 'On Contingent Claims that Insure Ex-post Optimal Stock Market Timing'. *The Journal of Finance* (1979), vol. 34(2): pp. 401–413 (cit. on p. 25).

[Gol79b] Goldman, M. B., H. B. Sosin, and M. A. Gatto: 'Path Dependent Options: "Buy at the Low, Sell at the High"'. *The Journal of Finance* (1979), vol. 34(5): pp. 1111–1127 (cit. on p. 25).

[Gru05] Gruenbichler, A. and H. Wohlwend: 'The Valuation of Structured Products: Empirical Findings for the Swiss Market'. *Swiss Society for Financial Market Research* (2005), vol. 19(4): pp. 361–380 (cit. on p. 23).

[Har81] Harison, J. and S.R. Pliska: 'Martingales and stochastic integrals in the theory of continuous trading'. *Stochastic Processes and their Applications* (1981), vol. 11(3): pp. 215–260 (cit. on pp. 21, 32, 94, 127, 188).

[Har79] Harrison, J. and D. Kreps: 'Martingales and Arbitrage in Multiperiod Securities Markets'. *Journal of Economic Theory* (1979), vol. 20: pp. 381–408 (cit. on pp. 21, 32, 94, 127, 188).

[Har85] Harrison, J. M.: *Brownian Motion and Stochastic Flow Systems*. 2nd ed. John Wiley & Sons, 1985 (cit. on p. 25).

[He98] He, H., W. P. Keirstead, and J. Rebholz: 'Double lookbacks'. *Mathematical Finance* (1998), vol. 8(3): pp. 201–228 (cit. on p. 25).

[Hes93] Heston, S. L.: 'A Closed-Form Solution for Options with Stochastic Volatility with Applications to Bond and Currency Options'. *The Review of Financial Studies* (1993), vol. 6(2): pp. 327–343 (cit. on pp. 26, 226, 228).

[Hua03] Huang, J-Z and M Huang: *How Much of the Corporate-Treasury Yield Spreads is Due to Credit Risk?* Tech. rep. Stanford University, 2003 (cit. on p. 28).

[Hul09] Hull, J. C.: *Options, Futures, and other Derivatives*. 7th ed. Pearson, 2009 (cit. on p. 21).

[Hul07] Hull, J. C.: *Risk management and financial institutions*. Pearson, 2007 (cit. on pp. 160, 179, 180, 244).

[Hul95] Hull, J. C. and A. White: 'The impact of default risk on the prices of options and other derivative securities'. *Journal of Banking & Finance* (1995), vol. 19: pp. 299–322 (cit. on pp. 26, 27).

[Irl03] Irle, A.: *Finanzmathematik - Die Bewertung von Derivaten*. 2nd ed. Teubner, 2003 (cit. on p. 26).

[Jar95] Jarrow, R. A. and S. M. Turnbull: 'Pricing Derivatives on Financial Securities Subject to Credit Risk'. *The Journal of Finance* (1995), vol. 50: pp. 53–85 (cit. on p. 27).

[Jen15] Jensen, B. A. and J. A. Nielsen: *How suboptimal are linear sharing rules?* Tech. rep. 2015 (cit. on p. 20).

[Joh87] Johnson, H. and R. Stulz: 'The Princing of Options with Default Risk'. *The Journal of Finance* (1987), vol. 42(2): pp. 267–280 (cit. on pp. 26, 27).

[Kah79] Kahneman, D. and A. Tversky: 'Prospect theory: An analysis of decision under risk'. *Econometrica* (1979), vol. 47(2): pp. 263–291 (cit. on p. 24).

[Kar99] Karatzas, I. and S.E. Shreve: *Brownian Motion and Stochastic Calculus*. 2nd ed. Springer, 1999 (cit. on pp. 19, 30).

[Kas12] Kassberger, S. and T. Liebmann: 'When are path-dependent payoffs suboptinal?' *Journal of Banking & Finance* (2012), vol. 36: pp. 1304–1310 (cit. on p. 20).

[Kle96] Klein, P.: 'Pricing Black-Scholes options with correlated credik risk'. *Journal of Banking & Finance* (1996), vol.: pp. 1211–1129 (cit. on p. 27).

[Kle01] Klein, P. and m. Inglis: 'Pricing vulnerable European options when the option's payoff can increase the risk of the financial distress'. *Journal of Banking & Finance* (2001), vol. 25: pp. 993–1012 (cit. on p. 27).

[Kra05] Kraft, H.: 'Optimal portfolios and Heston's stochastic volatility model: an explizit solution for power utility'. *Quantitative Finance* (2005), vol. 5(3): pp. 303–313 (cit. on p. 233).

[Lar12] Larsen, L. S. and C. Munk: 'The Costs of Suboptimal Dynamic Asset Allocation: General Results and Applications to Interest Rate Risk, Stock Volatility Risk, and Growth/Value Tilts'. *Journal of Economic Dynamics and Control* (2012), vol. 36: pp. 266–293 (cit. on p. 20).

[Len06] Lengwiler, Y.: *Microfoundations of Financial Economics - An Introduction to General Equilibrium Asset Pricing*. Ed. by Duffie, D. and S. Schaefer. Princeton University Press, 2006 (cit. on pp. 22, 40).

[Lon05] Longstaff, F. A., S. Mithal, and E. Neis: 'Corporate Yield Spreads: Default Risk or Liquidity? New Evidence from the Credit Default Swap Market'. *The Journal of Finance* (2005), vol. 60: pp. 2213–2253 (cit. on p. 27).

[Lui07] Lui, J: 'Portfolio Selection in Stochastic Environments'. *The Review of Financial Studies* (2007), vol. 20(1): pp. 1–39 (cit. on pp. 26, 113, 114, 141, 144, 232, 234, 235).

[Mah13] Mahayni, A. and J.C. Schneider: *Minimum Return Guarantees - Information Asymmetrie and Optimal Product Design*. Tech. rep. 2013 (cit. on pp. 31, 49, 50, 219, 228).

[Mer71] Merton, R. C.: 'Optimum Consumption and Portfolio Rules in a Continuous-Time Model'. *Journal of Economic Theory* (1971), vol. 3: pp. 373–413 (cit. on pp. 3, 12, 21, 23, 40, 41, 43, 107, 113, 174, 232).

[Mik03] Mikhailov, S. and U. Nögel: 'Heston's Stochastic Volatility Model: Implematation, Calibration and some Extensions'. *Wilmott Magazine* (2003), vol.: pp. 74–79 (cit. on p. 103).

[Per88] Perold, A. F. and W. F. Sharpe: 'Dynamic Strategies for Asset Allocation'. *Financial Analysts Journal* (1988), vol. 44: pp. 16–27 (cit. on pp. 19, 33, 36).

[Pro90] Protter, P.: *Stochastic Integration and Differential Equations*. Springer-Verlag, 1990 (cit. on pp. 19, 30).

[Rob98] Robinson, B. L.: 'The Inefficiency Costs of Guarantered Investment Products'. *The Journal of Derivatives* (1998), vol. 6(1): pp. 25–37 (cit. on p. 24).

[Rog13] Rogers, L. C. G.: *Optimal Investment*. Springer, 2013 (cit. on pp. 23, 40).

[Sch11] Schneider, J. C.: 'Structured Life Insurance and Investment Products for Retail Investors'. PhD thesis. University of Duisburg-Essen, 2011 (cit. on pp. 2, 21, 22).

[Sep06] Sepp, Artur: 'Extended CreditGrades Model with Stochastic Volatility and Jumps'. *Wilmott Magazine* (2006), vol.: pp. 50–62 (cit. on p. 156).

[Shr04] Shreve, S. E.: *Stochastic Calculus for Finance II*. Springer, 2004 (cit. on p. 25).

[Tve92] Tversky, A. and D. Kahneman: 'Advances in Prospect Theory: Cumulative Representation of Uncertainty'. *Journal of Risk and Uncertainty* (1992), vol. 5: pp. 297–323 (cit. on p. 24).

[VH08] Van Haastrecht, A. and A. A. J. Pelsser: 'Efficient, Almost Exact Simulation of the Heston Stochastic Volatility Model'. *Net for Studies on Pensions, Aging and Retirement* (2008), vol. (cit. on pp. 26, 227, 228).

[Van09] Vanduffel, S., A. Chernih, M. Maj, and W. Schoutens: 'A note on the suboptimality of path-dependent payoffs in general markets'. *Applied Mathematical Finance* (2009), vol. 16: pp. 315–330 (cit. on p. 20).

[Vas04] Vassalou, M. and Y. Xing: 'Default Risk in Equity Returns'. *The Journal of Finance* (2004), vol. 59(2): pp. 831–868 (cit. on p. 28).

[VN53] Von Neumann, J and O Morgenstern: *Theory of Games and Economic Behavior*. Princeton University Press, 1953 (cit. on pp. 22, 40).

[Wal11] Wallmeier, M.: 'Beyond payoff diagrams: how to present risk and return characteristics of structured products'. *Financial Markets and Portfolio Management* (2011), vol. 15(3): pp. 313–338 (cit. on pp. 24, 27).

[Was96] Wasserfallen, W. and C. Schenk: 'Portfolio Insurence for the Small Investor in Switzerland'. *The Journal of Derivatives* (1996), vol. Spring: pp. 37–43 (cit. on p. 23).

[Wil03] Wilkens, S., C. Erner, and K. Roder: *The Pricing of Structured Products in Germany*. Tech. rep. 2003: pp. 55–69 (cit. on p. 23).

[Won06] Wong, B. and C.C. Heyde: 'On Changes of Measure in Stochastic Volatility Models'. *Journal of Applied Mathematics and Stochastic Analysis* (2006), vol.: pp. 1–13 (cit. on pp. 226, 227).

[Zhu10] Zhu, J.: *Applications of Fourier Transform to Smile Modeling*. 2nd ed. Springer, 2010 (cit. on p. 26).

Listings

APPENDIX A

Appendix to Chapter 3

A.1 Proof of Proposition 1

The proof is a straightforward calculation. First, we show that the optimal investment fraction must be constant on the entire investment period. The proof is given in Balder et al. [Bal10].

Notice, that the investment fraction of a CRRA investor does not depend on her initial wealth. Furthermore, the optimiziation problem does not rely on the current asset price S_t, because of the stationarity of ΔS_t. It is sufficient to conclude that $V_T^{\varphi^*}$ is linear with respect to V_0.

Now, we denote the optimal final value of the investment strategy at time T with $\tilde{V}(t,T)$ where the current value is given by V_t. For two observation dates t_1 and t_2 with $t_1 < t_2$ must holds

$$E_P\left\{u\left(V_{t_2}^{\varphi^*}\right)\right\} = E_P\left\{E_P\left\{u\left(V_{t_2}^{\varphi^*}\right)|\mathcal{F}_{t_1}\right\}\right\} \tag{A.1}$$

$$= E_P\left\{E_P\left\{u\left(V_{t_1}^{\varphi^*}\cdot\tilde{V}(t_1,t_2)\right)|\mathcal{F}_{t_1}\right\}\right\} \tag{A.2}$$

$$= E_P\left\{u\left(V_{t_1}^{\varphi^*}\right)\right\} E_P\left\{\left(\tilde{V}(t_1,t_2)\right)^{1-\gamma}\right\} \tag{A.3}$$

It results, that φ_t^* in $t < t_1$ has to be equal for both investment horizons. In other words, it must hold that $\varphi_t^* = \varphi_s^*$ for all $s,t \in [0,T]$. It follows that the optimal investment strategy of a CRRA investor is given by a Constant-Mix strategy.

Second, we could calculate the explicit solution using the Black and Scholes assumption

for V_t. Thus, we calculate for $\varphi = \varphi^*$

$$\max_{\varphi} E_P\left\{u(V_T^{\varphi})\right\} \tag{A.4}$$

Refering to Section 3.2.2, we observe the value process of a Constant-Mix strategy given by

$$V_T^{\varphi} = v_0\, e^{\left(r+\varphi(\mu-r)-\frac{1}{2}\varphi^2\sigma^2\right)T+\varphi\sigma W_T} \tag{A.5}$$

Now, we could write

$$\begin{aligned} E_P\left(u(V_T^{\varphi})\right) &= E_P\left(\frac{v_0^{1-\gamma}}{1-\gamma}e^{(1-\gamma)\left(r+\varphi(\mu-r)-\frac{1}{2}\varphi^2\sigma^2\right)T+(1-\gamma)\varphi\sigma W_T}\right) \\ &= \frac{v_0^{1-\gamma}}{1-\gamma}e^{(1-\gamma)\left(r+\varphi(\mu-r)-\frac{1}{2}\varphi^2\sigma^2\right)T}E_P\left(e^{(1-\gamma)\varphi\sigma W_T}\right) \\ &= \frac{v_0^{1-\gamma}}{1-\gamma}e^{(1-\gamma)\left(r+\varphi(\mu-r)-\frac{1}{2}\varphi^2\sigma^2\right)T}e^{\frac{1}{2}(1-\gamma)^2\varphi^2\sigma^2 t} \\ &= \frac{v_0^{1-\gamma}}{1-\gamma}e^{(1-\gamma)\left(r+\varphi(\mu-r)-\frac{1}{2}\gamma\varphi^2\sigma^2\right)T} \end{aligned} \tag{A.6}$$

The first order condition for a maximum in φ is given by

$$0 = \underbrace{(1-\gamma)\,T\frac{v_0^{(1-\gamma)}}{1-\gamma}}_{>0}\underbrace{e^{(1-\gamma)\left(r+\varphi(\mu-r)-\frac{1}{2}\gamma\varphi^2\sigma^2\right)T}}_{>0}\left((\mu-r)-\gamma\varphi\sigma^2\right) \tag{A.7}$$

Immediately follows that $\varphi = \frac{(\mu-r)}{\gamma\sigma^2}$.

A.2 Proof of Proposition 2

We know from Proporsition 1 that for $G = 0$ the optimal strategy is given by a Constant-Mix strategy with

$$\varphi^{*,CM} = \frac{\mu-r}{\gamma\sigma^2} \tag{A.8}$$

For $G > 0$ we have to solve

$$\max_{\varphi} E_P\left\{u(V_T^{G,\varphi})\right\} \text{ with } V_T^{G,\varphi} \geq G \text{ and } X_0 = 1 \tag{A.9}$$

The constraint results in the following payoff

$$V_T^{G,\varphi} = \max\left\{\hat{V}_T^{G,\varphi}, G\right\} = \hat{V}_T^{G,\varphi} + \left[G - \hat{V}_T^{G,\varphi}\right]^+ \tag{A.10}$$

since the required guarantee G is no for free, the initial investment has to be lower compared to the classical Merton case with $G = 0$. Here, it must hold that

$$\hat{V}_0^{G,\varphi} \leq V_0^{G,\varphi}. \tag{A.11}$$

El Karoui et al. [EK05] show that the constrained solution is given by

$$V_T^{G,\varphi} = \hat{V}_T^{\varphi^*,CM} + \left[G - \hat{V}_T^{\varphi^*,CM}\right]^+. \tag{A.12}$$

Due to linearity of terminal wealth with respect to initial wealth it follows

$$V_T^{G,\varphi} = \lambda V_T^{\varphi^*,CM} + \left[G - \lambda V_T^{\varphi^*,CM}\right]^+ \tag{A.13}$$

where λ have to satisfy the initial budget constraint

$$V_0^{G,\varphi} = \lambda V_0^{\varphi^*,CM} + B^{Put}\left(\lambda V_t^{\varphi^*,CM}, G\right) \tag{A.14}$$

Obviously, this can be interpreted as a CG schema.

A.3 Proof of Proposition 3(i)

The proof is made in analogy to Mahayni et al. [Mah13]. Remember the oherenge between the stock price process S_t and the value process of the Constant-Mix Strategy V_t. Thus, we can write the stochastic differential equation

$$dV_t = V_t\left(\mu^\varphi dt + \sigma^\varphi dW_t\right) \tag{A.15}$$

where μ^φ and σ^φ result for the corresponding parameter of the stock price process, so that $\mu^\varphi = r + \varphi\left(\mu^S - r\right)$ and $\sigma^\varphi = \varphi\sigma^S$. However, for the following prove, we will define $\mu := \mu^\varphi$ and $\sigma := \sigma^\varphi$.

For the prove we show that

$$
\begin{aligned}
EU^{X^{(gen)}} &= E_P\left[u\left(e^{gT} + \left[\alpha V_T - e^{gT}\right]^+ - \left[\alpha V_T - e^{cT}\right]^+\right)\right] \qquad \text{(A.16)}\\
&= \frac{1}{1-\gamma}\left[e^{(1-\gamma)gT}\mathcal{N}\left(\frac{gT + \ln\alpha - (\mu - \frac{1}{2}\sigma^2)T}{\sigma\sqrt{T}}\right)\right.\\
&+ e^{(1-\gamma)cT}\mathcal{N}\left(-\frac{cT + \ln\alpha - (\mu - \frac{1}{2}\sigma^2)T}{\sigma\sqrt{T}}\right) \quad + \alpha^{1-\gamma}e^{(1-\gamma)\left(\mu - \frac{1}{2}\gamma\sigma^2\right)T}\\
&\left.\left(\mathcal{N}\left(\frac{cT + \ln\alpha - (\mu + (\frac{1}{2} - \gamma)\sigma^2)T}{\sigma\sqrt{T}}\right) - \mathcal{N}\left(\frac{gT + \ln\alpha - (\mu + (\frac{1}{2} - \gamma)\sigma^2)T}{\sigma\sqrt{T}}\right)\right)\right]
\end{aligned}
$$

holds. For simplification we define A, B and C by

$$
\begin{aligned}
A &= \mathcal{N}\left(\frac{gT + \ln\alpha - (\mu - \frac{1}{2}\sigma^2)T}{\sigma\sqrt{T}}\right)\\
B &= \mathcal{N}\left(-\frac{cT + \ln\alpha - (\mu - \frac{1}{2}\sigma^2)T}{\sigma\sqrt{T}}\right)\\
C &= \alpha^{1-\gamma}e^{(1-\gamma)\left(\mu - \frac{1}{2}\gamma\sigma^2\right)T}\\
&\quad\left(\mathcal{N}\left(\frac{cT + \ln\alpha - (\mu + (\frac{1}{2} - \gamma)\sigma^2)T}{\sigma\sqrt{T}}\right) - \mathcal{N}\left(\frac{gT + \ln\alpha - (\mu + (\frac{1}{2} - \gamma)\sigma^2)T}{\sigma\sqrt{T}}\right)\right)
\end{aligned}
$$

The prove will be separately focused on each of the three summands of the following equation

$$
E_P\left[u\left(e^{gT} + \left[\alpha V_T - e^{gT}\right]^+ - \left[\alpha V_T - e^{cT}\right]^+\right)\right] = \frac{1}{1-\gamma}\left[e^{(1-\gamma)gT}A + e^{(1-\gamma)cT}B + C\right] \qquad \text{(A.17)}
$$

Notice that

$$
\begin{aligned}
&E_P\left[u\left(e^{gT} + \left[\alpha V_T - e^{gT}\right]^+ - \left[\alpha V_T - e^{cT}\right]^+\right)\right]\\
=&\frac{1}{1-\gamma}E_P\left[e^{(1-\gamma)gT}1_{\{\alpha V_T \le e^{gT}\}} + (\alpha V_T)^{1-\gamma}\,1_{\{e^{gT} < \alpha V_T \le e^{cT}\}} + e^{(1-\gamma)cT}1_{\{\alpha V_T > e^{cT}\}}\right]\\
=&\frac{1}{1-\gamma}\left[e^{(1-\gamma)gT}P\left\{\alpha V_T \le e^{gT}\right\} + (\alpha V_T)^{1-\gamma}\,1_{\{e^{gT} < \alpha V_T \le e^{cT}\}} + e^{(1-\gamma)cT}P\left\{\alpha V_T > e^{cT}\right\}\right] \qquad \text{(A.18)}
\end{aligned}
$$

It holds for the first probability that

$$\begin{aligned}
&P\left\{\alpha V_T \le e^{gT}\right\} = P\left\{\ln\left(\alpha V_T\right) \le gT\right\} \\
=&P\left\{\ln V_T \le gT - \ln\alpha\right\} = P\left\{\left(\mu - \frac{1}{2}\sigma^2\right)T + \sigma W_T \le gT - \ln\alpha\right\} \\
=&P\left\{W_T \le \frac{gT - \ln\alpha - (\mu - \frac{1}{2}\sigma^2)T}{\sigma}\right\} = P\left\{\frac{W_T}{\sqrt{T}} \le \frac{gT - \ln\alpha - (\mu - \frac{1}{2}\sigma^2)T}{\sigma\sqrt{T}}\right\} \\
=&\mathcal{N}\left(\frac{gT - \ln\alpha - (\mu - \frac{1}{2}\sigma^2)T}{\sigma\sqrt{T}}\right) = A
\end{aligned} \tag{A.19}$$

And it also holds that

$$\begin{aligned}
P\left\{\alpha V_T > e^{cT}\right\} =&1 - P\left\{\ln V_T \le cT - \ln\alpha\right\} \\
=&1 - P\left\{\frac{W_T}{\sqrt{T}} \le \frac{cT - \ln\alpha - (\mu - \frac{1}{2}\sigma^2)T}{\sigma\sqrt{T}}\right\} \\
=&\mathcal{N}\left(-\frac{cT - \ln\alpha - (\mu - \frac{1}{2}\sigma^2)T}{\sigma\sqrt{T}}\right) = B
\end{aligned} \tag{A.20}$$

with $\mathcal{N}(-x) = 1 - \mathcal{N}(x)$ for the cumulative distribution function of the normal distribution.

In addition, we have

$$\begin{aligned}
E_P\left[\left(\alpha V_T\right)^{1-\gamma} 1_{\{e^{gT} < \alpha V_T \le e^{cT}\}}\right] &= E_P\left[\left(\alpha V_T\right)^{1-\gamma} 1_{\{e^{gT} < \alpha V_T \le e^{cT}\}}\right] \\
&= E_P\left[\left(\alpha v_0\right)^{(1-\gamma)} \left(e^{\left(\mu - \frac{1}{2}\sigma^2\right)T + \sigma W_T}\right)^{(1-\gamma)} 1_{\{e^{gT} < \alpha V_T \le e^{cT}\}}\right] \\
&= \left(\alpha v_0\right)^{(1-\gamma)} E_P\left[e^{(1-\gamma)\left(\mu - \frac{1}{2}\sigma^2\right)T + (1-\gamma)\sigma W_T} 1_{\{e^{gT} < \alpha V_T \le e^{cT}\}}\right]
\end{aligned} \tag{A.21}$$

Now we define $\hat{P}$ as a Radon-Nykodym measure by

$$\left(\frac{d\hat{P}}{dP}\right)_T = L \text{ with } L_T := e^{-\frac{1}{2}(1-\gamma)^2\sigma^2 T + (1-\gamma)\sigma W_T} \tag{A.22}$$

Finally it follows that

$$\begin{aligned}
&E_P\left[e^{(1-\gamma)\left(\mu-\frac{1}{2}\sigma^2\right)T+(1-\gamma)\sigma W_T}1_{\{e^{gT}<\alpha V_T\leq e^{cT}\}}\right]\\
&=E_{\hat{P}}\left[\frac{dP}{d\hat{P}}\quad e^{(1-\gamma)\left(\mu-\frac{1}{2}\sigma^2\right)T+(1-\gamma)\sigma W_T}1_{\{e^{gT}<\alpha V_T\leq e^{cT}\}}\right]\\
&=E_{\hat{P}}\left[e^{\frac{1}{2}(1-\gamma)^2\sigma^2T-(1-\gamma)\sigma W_T}\quad e^{(1-\gamma)\left(\mu-\frac{1}{2}\sigma^2\right)T+(1-\gamma)\sigma W_T}1_{\{e^{gT}<Z_T\leq e^{cT}\}}\right]\\
&=E_{\hat{P}}\left[e^{(1-\gamma)\left(\mu-\frac{1}{2}\gamma\sigma^2\right)T}1_{\{e^{gT}<\alpha V_T\leq e^{cT}\}}\right]\\
&=e^{(1-\gamma)\left(\mu-\frac{1}{2}\gamma\sigma^2\right)T}\left(\hat{P}\left\{\alpha V_T\leq e^{cT}\right\}-\hat{P}\left\{\alpha V_T\leq e^{gT}\right)\right\}
\end{aligned}\tag{A.23}$$

Now Girsanov's theorem implies that $\hat{W}_t = W_t - (1-\gamma)\sigma t$ is a $\hat{P}$–Brownian motion. Using

$$S_T = s_0 e^{(\mu-\frac{1}{2}\sigma^2)T+\sigma W_T} = s_0 e^{(\mu+(\frac{1}{2}-\gamma)\sigma^2)T+\sigma\hat{W}_T}$$

and (A.19) immediately gives

$$\begin{aligned}
\hat{P}\left\{\alpha V_T\leq e^{gT}\right\} &= \hat{P}\left\{\ln V_T\leq gT-\ln\alpha\right\}\\
&= \hat{P}\left\{\frac{\hat{W}_T}{\sqrt{T}}\leq\frac{gT-\ln\alpha-(\mu+(\frac{1}{2}-\gamma)\sigma^2)T}{\sigma\sqrt{T}}\right\}\\
&= \mathcal{N}\left(\frac{cT-\ln\alpha-(\mu+(\frac{1}{2}-\gamma)\sigma^2)T}{\sigma\sqrt{T}}\right)
\end{aligned}\tag{A.24}$$

and

$$\begin{aligned}
\hat{P}\left\{\alpha V_T\leq e^{cT}\right\} =&\hat{P}\left\{\frac{\hat{W}_T}{\sqrt{T}}\leq\frac{cT-\ln\alpha-(\mu+(\frac{1}{2}-\gamma)\sigma^2)T}{\sigma\sqrt{T}}\right\}\\
=&\mathcal{N}\left(\frac{gT-\ln\alpha-(\mu+(\frac{1}{2}-\gamma)\sigma^2)T}{\sigma\sqrt{T}}\right)
\end{aligned}\tag{A.25}$$

With (A.23),(A.24) and (A.25) follows

$$E_P\left[(\alpha V_T)^{1-\gamma}1_{\{e^{gT}<\alpha V_T\leq e^{cT}\}}\right] = C.$$

A.4 Additional calculation for the GCP

We illustrate in section 3.6.5 that investor Γ can reduce her utility loss by choosing an corresponding underlying asset (Constant-Mix strategy) with higher volatility. This result is in contrast to the analysis of the GP and CP where the optimal Constant-Mix V_t

is always the best choice. However, the same development will be seen for the GCP if we observe lower guaranteed rates. Figure A.1 enlarge the illustration of section 3.6.5 by assuming different guaranteed rate. It is seen, that lower guaranteed rate leads to a

Figure A.1: Calculated loss rates for GCPs with different guaranteed rates and varying underlying asset

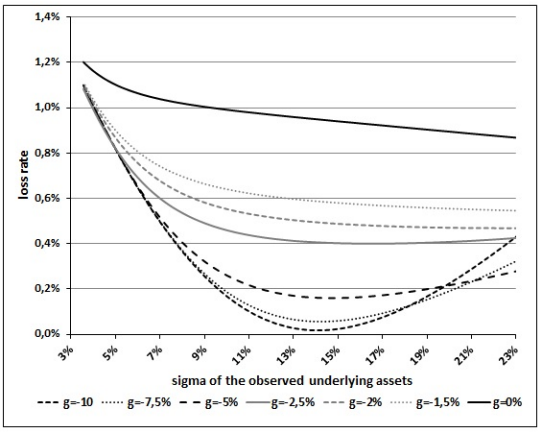

Calculated loss rate for GCP with different guaranteed rates between $g = -10$ % $g = 0$ % for different underlying asset resp. different volatility levels.

development which is compareable with the calculations for GP and CP. To be more precise, for $g < -7.5$ % the mimimum loss rate is calculated for $\sigma = 14.04$ % which is the volatility of the optimal Constant-Mix strategy for investor Γ. Intuitively, the development of the product is dominated by the underlying instead of the guaranteed rate in combination with the cap rate. But, the higher the guaranteed rate ($g > -7.5$ %) the more important are the calculated (g,c)-tuple. For higher g, each mimimum loss rate is calculated for higher σ. Finally, if we assume a guaranteed rate above $g = -1{,}5$ % we will find the lowest loss rate for the market volatility of $\sigma = 23.5$ % which is identical to a Constant-Mix strategy with $\varphi = 100$ %.

APPENDIX B

Appendix to Chapter 4 and 5

B.1 Proof of Proposition 4

Notice the t_0–price of the Best Garant Certificate (BGC) is given by

$$\begin{aligned} BGC_{t_0} &= E_* \left[e^{-rT} h(S_{t_0}, \ldots, S_{t_N}, S_T) \right] \\ &= E_* \left[e^{-rt_N} E_* \left[e^{-r(T-t_N)} h(S_{t_0}, \ldots, S_{t_N}, S_T) \middle| \mathcal{F}_{t_N} \right] \right] \end{aligned} \tag{B.1}$$

where E_* denotes the expectation under the martingale measure P^* and where $\mathcal{F}_{t_N}$ denotes the information at t_N. Observe that $K^{(\mathrm{w})} = g(S_{t_0}, \ldots, S_{t_N})$ is $\mathcal{F}_{t_N}$–measurable such that

$$\begin{aligned} & E_* \left[e^{-r(T-t_N)} h(S_{t_0}, \ldots, S_{t_N}, S_T) \middle| \mathcal{F}_{t_N} \right] \\ =& E_* \left[e^{-r(T-t_N)} \left(e^{gT} + \left[\frac{S_T}{K^{(\mathrm{w})}} - e^{gT} \right]^+ - \left[\frac{S_T}{K^{(\mathrm{w})}} - e^{cT} \right]^+ \right) \middle| \mathcal{F}_{t_N} \right] \\ =& e^{-r(T-t_N)} e^{gT} \\ &+ E_* \left[e^{-r(T-t_N)} \left(\left[\frac{S_T}{K^{(\mathrm{w})}} - e^{gT} \right]^+ - \left[\frac{S_T}{K^{(\mathrm{w})}} - e^{cT} \right]^+ \right) \middle| \mathcal{F}_{t_N} \right] \end{aligned} \tag{B.2}$$

For the expectation we have

$$\begin{aligned} & E_* \left[e^{-r(T-t_N)} \frac{1}{K^{(\mathrm{w})}} \cdot \left(\left[S_T - e^{gT} K^{(\mathrm{w})} \right]^+ - \left[S_T - e^{cT} K^{(\mathrm{w})} \right]^+ \right) \middle| \mathcal{F}_{t_N} \right] \\ =& \frac{1}{K^{(\mathrm{w})}} \cdot \mathcal{B}^{\mathrm{Call}} \left(S_{t_N}, t_N, r, e^{gT} K^{(\mathrm{w})}, T \right) - \mathcal{B}^{\mathrm{Call}} \left(S_{t_N}, t_N, r, e^{cT} K^{(\mathrm{w})}, T \right) \end{aligned} \tag{B.3}$$

Notice that, for a realized strike, the payoff under consideration is given in terms of the payoff of a *vertical bull spread*, i.e. the payoff of a long position in a call option with strike

$K_1 = e^{gT}K^{(\mathrm{w})}$ and a short position in a call with strike $K_2 = e^{cT}K^{(\mathrm{w})}$. Here, the well known Black and Scholes pricing formula applies which gives the result.

B.2 Heston model – implementation

First, we illustrate the change to the equivalent martingale measure. For the change of measure we go to the equivalent Cholesky decomposition with two independent Brownian motion W_t^1 and W_t^2, $\mu_t := (r + \overline{\lambda}V_t)$ and the stochastic differential equation

$$dS_t = \mu_t S_t dt + S_t\sqrt{V_t}(\rho dW_t^1 + \sqrt{1-\rho^2}dW_t^2) \tag{B.4}$$

$$dV_t = \kappa\left(\theta - V_t\right)dt + \sigma_v\sqrt{V_t}dW_t^1. \tag{B.5}$$

Since we are only able to trade S_t and B_t (where B_t describes the risk free investment), we face an incomplete market with a non-tradeable volatility.
We assume that the following inequality (cf. Wong et al. [Won06])

$$2\kappa\theta \geq \sigma_v^2 \tag{B.6}$$

holds, so that the volatility process is strictly positive. A further necessary condition for the existence of an equivalent martingale measure is

$$\mu_t - r = \sqrt{V_t}\left(\rho\gamma_t^{(1)} + \sqrt{1-\rho^2}\gamma_t^{(2)}\right), \tag{B.7}$$

which guarantees that the discounted stock price is a local martingale (cf. Bingham et al. [Bin04]; Risk Neutral Valuation 6.2 (6.5)).
Following Heston [Hes93], we ssume that $\gamma_t^{(1)}$ is proportional to the variance process

$$\gamma_t^{(1)} = \overline{\lambda}\sqrt{V_t} \tag{B.8}$$

with a constant $\overline{\lambda}$. This results to the following expresion for $\gamma_t^{(2)}$:

$$\begin{aligned} \mu_t - r &= \sqrt{V_t}\rho\overline{\lambda}\sqrt{V_t} + \sqrt{V_t}\sqrt{1-\rho^2}\gamma_t^{(2)} \\ \Rightarrow \mu_t - r - \rho\overline{\lambda}V_t &= \sqrt{V_t}\sqrt{1-\rho^2}\gamma_t^{(2)} \\ \Rightarrow \gamma_t^{(2)} &= \frac{1}{\sqrt{1-\rho^2}}\left(\frac{\mu_t - r}{\sqrt{V_t}} - \overline{\lambda}\sqrt{V_t}\right) \end{aligned} \tag{B.9}$$

With these choices of $\gamma_t^{(1)}$ and $\gamma_t^{(2)}$ we define the Girsanov density (according to Wong et al. [Won06]) by

$$\begin{aligned}\frac{dQ}{dP} = L_T = \exp\left(-\left(\int_0^T \gamma_s^{(1)} dW_s + \int_0^T \gamma_s^{(2)} dW_s\right)\right) \\ \cdot \exp\left(-\frac{1}{2}\int_0^T \left((\gamma_s^{(1)})^2 + (\gamma_s^{(2)})^2\right) ds\right)\end{aligned} \tag{B.10}$$

Thus, the change of measure for the variance process follows by

$$\begin{aligned}dV_t &= \kappa\left(\theta - V_t\right) dt + \sigma_v \sqrt{V_t} dW_t^1 \\ &= \kappa\left(\theta - V_t\right) dt + \sigma_v \sqrt{V_t} dW_t^{*(1)} - \overline{\lambda}\sqrt{V_t} dt \\ &= \left(\kappa\left(\theta - V_t\right) - \sigma_v \overline{\lambda}\sqrt{V_t}\right) dt + \sigma_v \sqrt{V_t} dW_t^{*(1)} \\ &= \left(\kappa\theta - (\kappa + \sigma_v\overline{\lambda})V_t\right) dt + \sigma_v \sqrt{V_t} dW_t^{*(1)} \\ &= \underbrace{(\kappa + \sigma_v\overline{\lambda})}_{:=\kappa^*} \cdot \left(\underbrace{\frac{\kappa\theta}{\kappa + \sigma_v\overline{\lambda}}}_{:=\theta^*} - V_t\right) dt + \sigma_v \sqrt{V_t} dW_t^{*(1)} \\ &= \kappa^* \cdot \left(\theta^* - V_t\right) dt + \sigma_v \sqrt{V_t} dW_t^{*(1)}\end{aligned} \tag{B.11}$$

Similarly, for the stock price process we have

$$\begin{aligned}dS_t &= \mu S_t dt + S_t \sqrt{V_t}(\rho dW_t^1 + \sqrt{1-\rho^2} dW_t^2) \\ &= \mu S_t dt + S_t \sqrt{V_t} \rho dW_t^{*(1)} - \overline{\lambda}\sqrt{V_t} dt \\ &+ \sqrt{1-\rho^2} dW_t^{*(2)} - \frac{1}{\sqrt{1-\rho^2}}\left(\frac{\mu - r}{\sqrt{V_t}} - \overline{\lambda}\rho\sqrt{V_t}\right) dt \\ &= r S_t dt + S_t \sqrt{V_t}(\rho dW_t^{*(1)} + \sqrt{1-\rho^2} dW_t^{*(2)})\end{aligned} \tag{B.12}$$

A lot of research has studied time-efficient algorithms for Monte Carlo simulation of the Heston model, cf. for example Van Haastrecht et al. [VH08]. The following dynamics of S_t and V_t are given by

$$dS_t = S_t\left(r dt + \sqrt{V}\left(\sqrt{1-\rho^2} dW_t^{*(1)} + \rho dW_t^{*(2)}\right)\right) \tag{B.13}$$

$$dV_t = \kappa^*\left(\theta^* - V_t\right) dt + \sigma_v \sqrt{V_t} dW_t^{*(1)} \tag{B.14}$$

where $W^{*(1)}$ and $W^{*(2)}$ denote two independent one–dimensional Brownian motions. It is well known that the mean-reverting square-root process implies that the distribution of V is given by non-central chi-squared distribution. In particular,

$$F_{\chi'^2}(z;\nu,\widetilde{\lambda}) = e^{-\frac{\widetilde{\lambda}}{2}} \sum_{j=0}^{\infty} \frac{(\frac{\widetilde{\lambda}}{2})^2}{j!2^{(\frac{\nu}{2}+j)}\Gamma(\frac{\nu}{2}+j)} \int_0^z z^{\frac{\nu}{2}+j-1} e^{-\frac{x}{2}} dx \tag{B.15}$$

is the cumulative distribution function for the non-central chi-squared distribution with ν degrees of freedom and non-centrality parameter $\widetilde{\lambda}$. For $T > t$, let

$$d = \frac{4\kappa^*\theta^*}{\sigma_v^2}; \qquad n(t,T) = \frac{4\kappa^* e^{-\kappa^*(T-t)}}{\sigma_v^2(1-e^{-\kappa^*(T-t)})} \tag{B.16}$$

Then, it holds that

$$P\{V(T) < x|V(t)\} = F_{\chi'^2}\left(\frac{x \cdot n(t,T)}{e^{-\kappa^*(T-t)}}; d, V(t) \cdot n(t,T)\right) \tag{B.17}$$

Basically, we simulate V by means of the above distribution and use, in the next step, the Euler-scheme to determine S. For details, we refer the reader to Anderson [And06] or Van Haastrecht et al. [VH08].

A detailed description of the quasi closed form solutions $\mathcal{B}^{\text{Call, Heston}}$ is illustrated in Heston [Hes93]. For a more efficient solution using Fourier transform techniques we refer to [Car99].

B.3 Proof of Proposition 5

For Proposition 5 we only have to prove (i). The proof is made in analogy to Mahayni et al. [Mah13], who illustrated the Proportion in a more general case. Note, the proof of the more general case is illustrated in A.3. However, we also mention a solution for the minimum and average strike BGC.

We have to show that

$$
\begin{aligned}
EU^{\mathrm{BGC,fix}} &= E_P\left[u\left(e^{gT}+\left[\frac{S_T}{K}-e^{gT}\right]^+-\left[\frac{S_T}{K}-e^{cT}\right]^+\right)\right] \qquad \text{(B.18)}\\
&= \frac{1}{1-\gamma}\left[e^{(1-\gamma)gT}\mathcal{N}\left(\frac{gT+\ln K-(\mu-\frac{1}{2}\sigma^2)T}{\sigma\sqrt{T}}\right)\right.\\
&+ e^{(1-\gamma)cT}\mathcal{N}\left(-\frac{cT+\ln K-(\mu-\frac{1}{2}\sigma^2)T}{\sigma\sqrt{T}}\right) \quad + \left(\frac{s_0}{K}\right)^{1-\gamma} e^{(1-\gamma)\left(\mu-\frac{1}{2}\gamma\sigma^2\right)T}\\
&\left.\left(\mathcal{N}\left(\frac{cT+\ln K-(\mu+(\frac{1}{2}-\gamma)\sigma^2)T}{\sigma\sqrt{T}}\right)-\mathcal{N}\left(\frac{gT+\ln K-(\mu+(\frac{1}{2}-\gamma)\sigma^2)T}{\sigma\sqrt{T}}\right)\right)\right]
\end{aligned}
$$

holds. For simplification we define A, B and C by

$$
\begin{aligned}
A &= \mathcal{N}\left(\frac{gT+\ln K-(\mu-\frac{1}{2}\sigma^2)T}{\sigma\sqrt{T}}\right)\\
B &= \mathcal{N}\left(-\frac{cT+\ln K-(\mu-\frac{1}{2}\sigma^2)T}{\sigma\sqrt{T}}\right)\\
C &= \left(\frac{s_0}{K}\right)^{1-\gamma} e^{(1-\gamma)\left(\mu-\frac{1}{2}\gamma\sigma^2\right)T}\\
&\quad\left(\mathcal{N}\left(\frac{cT+\ln K-(\mu+(\frac{1}{2}-\gamma)\sigma^2)T}{\sigma\sqrt{T}}\right)-\mathcal{N}\left(\frac{gT+\ln K-(\mu+(\frac{1}{2}-\gamma)\sigma^2)T}{\sigma\sqrt{T}}\right)\right)
\end{aligned}
$$

The proof calculates each of the three summands of the following equation separately

$$
E_P\left[u\left(e^{gT}+\left[\frac{S_T}{K}-e^{gT}\right]^+-\left[\frac{S_T}{K}-e^{cT}\right]^+\right)\right] = \frac{1}{1-\gamma}\left[e^{(1-\gamma)gT}A+e^{(1-\gamma)cT}B+C\right] \qquad \text{(B.19)}
$$

Let $Z_T := \frac{S_T}{K}$ and notice that

$$
\begin{aligned}
&E_P\left[u\left(e^{gT}+\left[Z_T-e^{gT}\right]^+-\left[Z_T-e^{cT}\right]^+\right)\right]\\
=&\frac{1}{1-\gamma}E_P\left[e^{(1-\gamma)gT}1_{\{Z_T\le e^{gT}\}}+(Z_T)^{1-\gamma}1_{\{e^{gT}<Z_T\le e^{cT}\}}+e^{(1-\gamma)cT}1_{\{Z_T>e^{cT}\}}\right]\\
=&\frac{1}{1-\gamma}\left[e^{(1-\gamma)gT}P\left\{Z_T\le e^{gT}\right\}+E_P\left[(Z_T)^{1-\gamma}1_{\{e^{gT}<Z_T\le e^{cT}\}}\right]+e^{(1-\gamma)cT}P\left\{Z_T>e^{cT}\right\}\right] \qquad \text{(B.20)}
\end{aligned}
$$

For the first probability in (B.20) it hold that

$$\begin{aligned}
&P\left\{Z_T \leq e^{gT}\right\} \\
&= P\left\{\ln S_T \leq gT + \ln K\right\} = P\left\{\left(\mu - \frac{1}{2}\sigma^2\right)T + \sigma W_T \leq gT + \ln K\right\} \\
&= P\left\{\frac{W_T}{\sqrt{T}} \leq \frac{gT + \ln K - (\mu - \frac{1}{2}\sigma^2)T}{\sigma\sqrt{T}}\right\} = \mathcal{N}\left(\frac{gT + \ln K - (\mu - \frac{1}{2}\sigma^2)T}{\sigma\sqrt{T}}\right) = A \quad \text{(B.21)}
\end{aligned}$$

Moreover, we have

$$\begin{aligned}
P\left\{Z_T > e^{cT}\right\} =& 1 - P\left\{\ln S_T \leq cT + \ln K\right\} \\
=& 1 - P\left\{\frac{W_T}{\sqrt{T}} \leq \frac{cT + \ln K - (\mu - \frac{1}{2}\sigma^2)T}{\sigma\sqrt{T}}\right\} \\
=& \mathcal{N}\left(-\frac{cT + \ln K - (\mu - \frac{1}{2}\sigma^2)T}{\sigma\sqrt{T}}\right) = B \quad \text{(B.22)}
\end{aligned}$$

with $\mathcal{N}(-x) = 1 - \mathcal{N}(x)$ for the cumulative distribution function of the normal distribution.

In addition, we have

$$\begin{aligned}
E_P\left[(Z_T)^{1-\gamma} 1_{\{e^{gT} < Z_T \leq e^{cT}\}}\right] &= E_P\left[\left(\frac{S_T}{K}\right)^{1-\gamma} 1_{\{e^{gT} < Z_T \leq e^{cT}\}}\right] \\
&= E_P\left[\left(\frac{1}{K}\right)^{1-\gamma} s_0^{1-\gamma}\left(e^{(\mu - \frac{1}{2}\sigma^2)T + \sigma W_T}\right)^{1-\gamma} 1_{\{e^{gT} < Z_T \leq e^{cT}\}}\right] \\
&= \left(\frac{s_0}{K}\right)^{1-\gamma} E_P\left[e^{(1-\gamma)(\mu - \frac{1}{2}\sigma^2)T + (1-\gamma)\sigma W_T} 1_{\{e^{gT} < Z_T \leq e^{cT}\}}\right] \quad \text{(B.23)}
\end{aligned}$$

Now we define $\hat{P}$ as a Radon-Nykodym measure by

$$\left(\frac{d\hat{P}}{dP}\right)_T = L_T \text{ with } L_T := e^{-\frac{1}{2}(1-\gamma)^2\sigma^2 T + (1-\gamma)\sigma W_T} \quad \text{(B.24)}$$

Then, it follows that

$$\begin{aligned}
&E_P\left[e^{(1-\gamma)\left(\mu-\frac{1}{2}\sigma^2\right)T+(1-\gamma)\sigma W_T}1_{\{e^{gT}<Z_T\le e^{cT}\}}\right]\\
&=E_{\hat{P}}\left[\frac{dP}{d\hat{P}}\quad e^{(1-\gamma)\left(\mu-\frac{1}{2}\sigma^2\right)T+(1-\gamma)\sigma W_T}1_{\{e^{gT}<Z_T\le e^{cT}\}}\right]\\
&=E_{\hat{P}}\left[e^{\frac{1}{2}(1-\gamma)^2\sigma^2T-(1-\gamma)\sigma W_T}\quad e^{(1-\gamma)\left(\mu-\frac{1}{2}\sigma^2\right)T+(1-\gamma)\sigma W_T}1_{\{e^{gT}<Z_T\le e^{cT}\}}\right]\\
&=E_{\hat{P}}\left[e^{(1-\gamma)\left(\mu-\frac{1}{2}\gamma\sigma^2\right)T}1_{\{e^{gT}<Z_T\le e^{cT}\}}\right]\\
&=e^{(1-\gamma)\left(\mu-\frac{1}{2}\gamma\sigma^2\right)T}\ \left(\hat{P}\left\{Z_T\le e^{cT}\right\}-\hat{P}\left\{Z_T\le e^{gT}\right)\right\} \qquad \text{(B.25)}
\end{aligned}$$

Now Girsanov's theorem implies that $\hat{W}_t = W_t - (1-\gamma)\sigma t$ is a $\hat{P}$–Brownian motion. Using

$$S_T = s_0 e^{(\mu-\frac{1}{2}\sigma^2)T+\sigma W_T} = s_0 e^{(\mu+(\frac{1}{2}-\gamma)\sigma^2)T+\sigma\hat{W}_T}$$

and (B.21) immediately gives

$$\begin{aligned}
\hat{P}\left\{Z_T\le e^{gT}\right\} &= \hat{P}\left\{\ln S_T\le gT+\ln K\right\}\\
&= \hat{P}\left\{\frac{\hat{W}_T}{\sqrt{T}}\le\frac{gT+\ln K-(\mu+(\frac{1}{2}-\gamma)\sigma^2)T}{\sigma\sqrt{T}}\right\}\\
&= \mathcal{N}\left(\frac{cT+\ln K-(\mu+(\frac{1}{2}-\gamma)\sigma^2)T}{\sigma\sqrt{T}}\right) \qquad \text{(B.26)}
\end{aligned}$$

and

$$\begin{aligned}
\hat{P}\left\{Z_T\le e^{cT}\right\} &= \hat{P}\left\{\frac{\hat{W}_T}{\sqrt{T}}\le\frac{cT+\ln K-(\mu+(\frac{1}{2}-\gamma)\sigma^2)T}{\sigma\sqrt{T}}\right\}\\
&= \mathcal{N}\left(\frac{gT+\ln K-(\mu+(\frac{1}{2}-\gamma)\sigma^2)T}{\sigma\sqrt{T}}\right) \qquad \text{(B.27)}
\end{aligned}$$

With (B.25),(B.26) and (B.27) follows

$$E_P\left[(Z_T)^{1-\gamma}\,1_{\{e^{gT}<Z_T\le e^{cT}\}}\right] = C.$$

For the calculation based on the minimum and the average entry strike setting holds

$$S_T = S_0 \exp\left(\mu - \frac{1}{2}\sigma\right) T + \sigma W_T = S_{t_n} \exp\left(\mu - \frac{1}{2}\sigma\right)(T - t_n) + \sigma W_{T-t_n} \tag{B.28}$$

So, for the calculation of A_{t_n} follows

$$\begin{aligned}
&P\left\{Z_T \leq e^{gT}\right\} = P\left\{\frac{S_T}{K} \leq e^{gT}\right\} = P\left\{\ln\left(\frac{S_T}{K}\right) \leq gT\right\} \\
=&P\left\{\ln S_T \leq gT + \ln K\right\} = P\left\{\ln S_{t_n} + \left(\mu - \frac{1}{2}\sigma^2\right)(T - t_n) + \sigma W_{T-t_n} \leq gT + \ln K\right\} \\
=&P\left\{W_{T-t_n} \leq \frac{gT + \ln K - \ln S_{t_n} - (\mu - \frac{1}{2}\sigma^2)(T - t_n)}{\sigma}\right\} \\
=&P\left\{\frac{W_{T-t_n}}{\sqrt{T - t_n}} \leq \frac{gT + \ln K - \ln S_{t_n} - (\mu - \frac{1}{2}\sigma^2)(T - t_n)}{\sigma\sqrt{T - t_n}}\right\} \\
=&\mathcal{N}\left(\frac{gT + \ln K - \ln S_{t_n} - (\mu - \frac{1}{2}\sigma^2)(T - t_n)}{\sigma\sqrt{T - t_n}}\right) = \mathrm{A}_{t_n}
\end{aligned} \tag{B.29}$$

B_{t_n} and C_{t_n} are derived analogously, Thus, we are able to calculated $EU^{\mathrm{BGC,min}}$ as well as $EU^{\mathrm{BGC,ave}}$.

B.4 Derivation of the optimal portfolio process in the Heston model

As we mentioned before, the derivation of the optimal portfolio process in Lui [Lui07] depends on different complex mathematical operations. With our assumptions on the market model, we have to maximize the given utility

$$\max_{\pi} E\left(\frac{(X_T^{\pi})^{1-\gamma}}{1-\gamma}\right) \tag{B.30}$$

where X_T^{π} describes the terminal value of the portfolio strategy π_t at time T. To solve this problem we use the approach of Merton [Mer71]. We define the indirect utility function $J(t,X,V)$, which leads us to the familiar Hamilton-Jacobi-Bellmann equation for J (cf. Lui [Lui07]):

$$\max_{\pi} \frac{\partial J}{\partial t} + \frac{1}{2}X^2\pi^2 V\frac{\partial^2 J}{\partial X^2} + X\left(\pi(\overline{\lambda}V) + r\right)\frac{\partial J}{\partial X} + X\pi\rho\sigma_v V\frac{\partial^2 J}{\partial X\partial V} + \frac{1}{2}\sigma_v V\frac{\partial^2 J}{\partial V^2} + (r+\overline{\lambda}V)\frac{\partial J}{\partial V} \tag{B.31}$$

with the boundary condition

$$J(T,X,V) = \frac{(X_T^{\pi})^{1-\gamma}}{1-\gamma} \tag{B.32}$$

which is also used by KRAFT [Kra05]. The above equation use the description e.g. $\frac{\partial J}{\partial t}$ for the derivation of J with respect to t. We conjecture that the indirect utility function has the form

$$J(t,X,V) = \frac{X^{1-\gamma}}{1-\gamma}\left[f\left(V,t\right)\right]^{\gamma} \tag{B.33}$$

and assume the following portfolio process

$$\pi^* = \frac{\overline{\lambda}}{\gamma} + \rho\sigma_v\frac{\partial lnf}{\partial X} \tag{B.34}$$

The explicit solution for $\frac{\partial lnf}{\partial X} = \frac{1}{f}\frac{\partial f}{\partial V}$ and the following derivation are used

$$\begin{aligned}
\frac{\partial J}{\partial t} &= \frac{\gamma X^{1-\gamma}}{1-\gamma} f\left(V,t\right)^{\gamma-1}\frac{\partial f}{\partial t} \\
\frac{\partial J}{\partial X} &= \left[f\left(V,t\right)^{\gamma}\right]X^{-\gamma} \\
\frac{\partial^2 J}{\partial X^2} &= -\gamma\left[f\left(V,t\right)^{\gamma}\right]X^{-\gamma-1} \\
\frac{\partial^2 J}{\partial X\partial V} &= \gamma X^{-\gamma}\left[f\left(V,t\right)^{\gamma-1}\right]\frac{\partial f}{\partial V} \\
\frac{\partial J}{\partial V} &= \frac{\gamma X^{1-\gamma}}{1-\gamma}\left[f\left(V,t\right)^{\gamma-1}\right]\frac{\partial f}{\partial V} \\
\frac{\partial^2 J}{\partial V^2} &= \frac{\gamma X^{1-\gamma}}{1-\gamma}\left((\gamma-1)\left[f\left(V,t\right)\right]^{\gamma-2}\frac{\partial f}{\partial V}\frac{\partial f}{\partial V} + \left[f\left(V,t\right)^{\gamma-1}\right]\frac{\partial^2 f}{\partial V^2}\right).
\end{aligned} \tag{B.35}$$

This simplifies the above equation to

$$\begin{aligned} 0 = {} & \gamma \frac{X^{1-\gamma}}{1-\gamma} f^{\gamma-1} \frac{\partial f}{\partial t} + \frac{1}{2} X^2 \pi^2 V(-\gamma) f^{\gamma} X^{-\gamma-1} \\ & + X \left[\pi(\overline{\lambda} V) + r \right] f^{\gamma} X^{-\gamma} + X \pi \rho \sigma_v V \gamma X^{-\gamma} f^{\gamma-1} \frac{\partial f}{\partial V} \\ & + \frac{1}{2} \sigma_v^2 V \gamma \frac{X^{1-\gamma}}{1-\gamma} \left((\gamma-1) f^{\gamma-2} f^{\gamma-1} \frac{\partial f}{\partial V} \frac{\partial f}{\partial V} + \frac{\partial^2 f}{\partial V^2} \right) \\ & + \left(r + \overline{\lambda} V \right) \gamma \frac{X^{1-\gamma}}{1-\gamma} f^{\gamma-1} \frac{\partial f}{\partial V}. \end{aligned} \tag{B.36}$$

By division of γ, $X^{1-\gamma}$, $f^{\gamma-1}$ and multiplication of $(1-\gamma)$ we obtain:

$$\begin{aligned} 0 = {} & \frac{\partial f}{\partial t} + \frac{1}{2} \sigma_v^2 V \frac{\partial^2 f}{\partial V^2} + \left[(r + \overline{\lambda} V) + \frac{1-\gamma}{\gamma} \rho \sigma_v (\overline{\lambda} V) \right] \frac{\partial f}{\partial V} \\ & + \frac{1}{2f} (\gamma - 1) \left(\sigma_v^2 V - \sigma_v^2 V \rho^2 \right) \frac{\partial f}{\partial V} \frac{\partial f}{\partial V} \\ & + \left[\frac{1-\gamma}{2\gamma^2} \overline{\lambda} V + \frac{1-\gamma}{\gamma} r \right] f \end{aligned} \tag{B.37}$$

Lui [Lui07] follows an approach which leads to a general solution of the portfolio problem. He also takes into account intertemporal consumption as well as different properties of the state process X. We just focus on the solution for the Heston model. Since the variance process belongs the the family of affine processes and we do not assume intertemporal consumption, we can rely on Lui [Lui07] and just have to solve

$$\begin{aligned} 0 = {} & \frac{d}{dt} d_v - \left(\kappa - \frac{1-\gamma}{\gamma} \overline{\lambda} \sigma_v \rho \right) d_v \\ & + \frac{\sigma_v^2}{2} \left[1 - (1-\gamma)(1-\rho^2) \right] d_v^2 + \frac{1-\gamma}{2\gamma^2} \overline{\lambda}^2 \end{aligned} \tag{B.38}$$

with $d_v(T) = 0$. To solve the above equation we first define $\widetilde{\kappa} := \kappa - \frac{1-\gamma}{\gamma} \overline{\lambda} \sigma_v \rho$ and $\delta := -\frac{1-\gamma}{2\gamma^2} \overline{\lambda}^2$. Now the equation has the form

$$0 = \frac{d}{dt} d_v - \widetilde{\kappa} d_v + \frac{1}{2} \left[\rho^2 + \gamma(1-\rho^2) \right] \sigma_v^2 d_v^2 - \delta \tag{B.39}$$

with $d_v(T) = 0$. If we now write

$$0 = \frac{d}{dt} \frac{d_v}{\delta} - \widetilde{\kappa} \frac{d_v}{\delta} + \frac{1}{2} \delta \left[\rho^2 + \gamma(1-\rho^2) \right] \sigma_v^2 \left(\frac{d_v}{\delta} \right)^2 - 1 \tag{B.40}$$

with $d_v(T) = 0$, we obtain a non-linear ordinary differential equation by defining $D(t) = \frac{d_v(t)}{\delta}$ and $\widehat{\sigma}^2 = \delta \left[\rho^2 + \gamma(1-\rho^2)\right] \sigma_v^2$ (B.40) then becomes

$$0 = \frac{d}{dt} D - \widetilde{\kappa} D + \frac{1}{2} \widehat{\sigma}^2 D^2 - 1. \tag{B.41}$$

(B.41) is a Riccati equation, which is solved in Cox et al. [Cox85]. They find the solution

$$D(t) = -\frac{2\left[\exp\left(\xi\tau\right) - 1\right]}{\left(\widetilde{\kappa} + \xi\right)\left[\exp\left(\xi\tau\right) - 1\right] + 2\xi} \tag{B.42}$$

where $\xi = \sqrt{\widetilde{\kappa}^2 + 2\widehat{\sigma}^2}$. In a last step we substitute $D(t)$ and $\widehat{\sigma}^2$ so that we have

$$d_v(t) = -\frac{2\left[exp\left(\xi\tau\right) - 1\right]}{\left(\widetilde{\kappa} + \xi\right)\left[exp\left(\xi\tau\right) - 1\right] + 2\xi} \delta \tag{B.43}$$

with $\xi = \sqrt{\widetilde{\kappa}^2 + 2\delta\left[\rho^2 + \gamma(1-\rho^2)\right]\sigma_v^2}$.

Additionally, we show the optimal portfolio process in Figure B.1. This result is in line with Lui [Lui07] and Chiarella et al. [Chi10]. Chiarella et al. [Chi10] interpret the positive intertemporal hedging position as a result of the negative correlation. If there is a positive correlation between the underlying and the variance process the relevant parameter d_v would be positive so that the optimal portfolio process is always below the static investment weight.

Figure B.1: Optimal portfolio process - Heston model

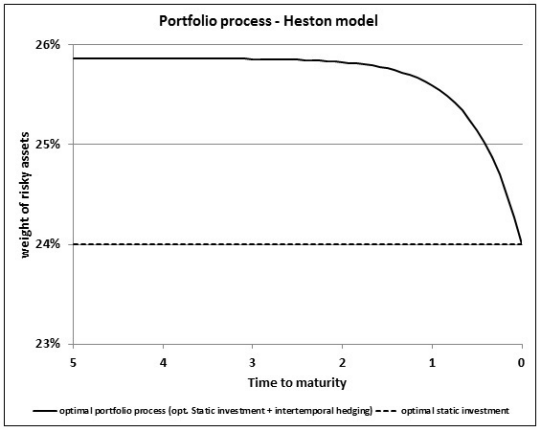

The weight of risky assets in the optimal portfolio process in the Heston model is illustrated.

B.5 Joint distrubution

First, we review some well known results.

Proposition 9 *Let $X_t = \mu t + \sigma W_t$, with constant μ, σ and $\sigma > 0$. $m_t^X = \min_{0\leq s\leq t} X_s$ describes the running minimum of the process X. Then for $y \leq x$ and $y \leq 0$ holds*

$$P\left\{X_t \geq x, m_t^X \geq y\right\} = \mathcal{N}\left(\frac{-x+\mu t}{\sigma\sqrt{t}}\right) - e^{\frac{2\mu y}{\sigma^2}}\mathcal{N}\left(\frac{2y+\mu t-x}{\sigma\sqrt{t}}\right) \tag{B.44}$$

Proof 9 *A proof can be found e.g. in* Dana *et al. [Dan07].*

Straightforward derivations give the following corollary.

Corollary 1 *Let X_t and m_t^X be given as in Proposition 9, then*

$$P\left\{X_t \in dx, m_t^X \in dy\right\} = f(x,y)dxdy \tag{B.45}$$

where

$$f(x,y) = \frac{2x-4y}{\sigma^3\sqrt{t^3}}\phi\left(\frac{-x+\mu t}{\sigma\sqrt{t}}\right) exp\left(\frac{2xy-2y^2}{\sigma^2 t}\right) \tag{B.46}$$

The above results can easily be transferred to a geometric Brownian motion instead of a simple Brownian motion. The Corollar is given in Branger et al. [Bra11].

Corollary 2 *Let*

$$S_t = S_0 e^{\left(\mu-\frac{1}{2}\sigma^2\right)t+\sigma W_t} \tag{B.47}$$

where μ,σ ($\sigma > 0$) are constants. W is a Brownian motion defined on some probability space. For the running minimum $m_t^S := \min_{0\leq u\leq t} S_u$ of S_t it holds that

$$\begin{aligned}
&P\left\{S_t \geq x, m_t^S \geq y\right\} \\
&= \mathcal{N}\left(\frac{ln\frac{x}{S_0} + (\mu-\frac{1}{2}\sigma^2)t}{\sigma\sqrt{t}}\right) - e^{2\frac{(\mu-\frac{1}{2}\sigma^2)}{\sigma^2}ln\frac{y}{S_0}}\mathcal{N}\left(\frac{2ln\frac{y}{S_0} + (\mu-\frac{1}{2}\sigma^2)t - ln\frac{x}{S_0}}{\sigma\sqrt{t}}\right)
\end{aligned}$$

and

$$\begin{aligned}
&P\left\{S_t \in dx, m_t^S \in dy\right\} \\
&= \frac{2ln\frac{x}{S_0} - 4ln\frac{y}{S_0}}{\sigma^3\sqrt{t^3}xy}\phi\left(\frac{-ln\frac{x}{S_0} + (\mu-\frac{1}{2}\sigma^2)t}{\sigma\sqrt{t}}\right) exp\left(\frac{2ln\frac{x}{S_0}ln\frac{y}{S_0} - 2ln\frac{y}{S_0}^2}{\sigma^2 t}\right) dxdy.
\end{aligned}$$

Proof 10 *Let X_t denote the logarithm of the normalized asset price, i.e. $X_t := \ln \frac{S_t}{S_0} = \left(\mu - \frac{1}{2}\sigma^2\right) t + \sigma W_t$ and set $\alpha = \mu - \frac{1}{2}\sigma^2$. Then X_t is a one dimensional Brownian motion with drift α. It follows*

$$P\left\{S_t \geq x, m_t^S \geq y\right\} = P\left\{X_t \geq ln\frac{x}{S_0}, m_t^X \geq ln\frac{y}{S_0}\right\}$$
$$\mathcal{N}\left(\frac{-ln\frac{x}{S_0} + (\mu - \frac{1}{2}\sigma^2)t}{\sigma\sqrt{t}}\right) - e^{2\frac{(\mu-\frac{1}{2}\sigma^2)}{\sigma^2} ln\frac{y}{S_0}} \mathcal{N}\left(\frac{2ln\frac{y}{S_0} + (\mu - \frac{1}{2}\sigma^2)t - ln\frac{x}{S_0}}{\sigma\sqrt{t}}\right)$$

To derive the density function let $\widetilde{x} = ln\frac{x}{S_0}$ and $\widetilde{y} = ln\frac{y}{S_0}$. Notice that

$$\frac{\partial \widetilde{x}}{\partial x} = \frac{1}{x} \text{ and } \frac{\partial \widetilde{y}}{\partial y} = \frac{1}{y}$$

With Corollary 1 it follows

$$\begin{aligned}
&\frac{\partial}{\partial x}\mathcal{N}\left(\frac{-\widetilde{x} + \alpha t}{\sigma\sqrt{t}}\right) - e^{2\frac{\alpha}{\sigma^2}\widetilde{y}}\mathcal{N}\left(\frac{2\widetilde{y} + \alpha t - \widetilde{x}}{\sigma\sqrt{t}}\right) \\
&= -\frac{1}{\sigma\sqrt{t}x}\mathcal{N}\left(\frac{-\widetilde{x} + \alpha t}{\sigma\sqrt{t}}\right) - e^{\frac{2\alpha}{\sigma^2}\widetilde{y}}\left(-\frac{1}{\sigma\sqrt{t}x}\right)\mathcal{N}\left(\frac{2\widetilde{y} + \alpha t - \widetilde{x}}{\sigma\sqrt{t}}\right) \\
&= -\frac{1}{\sigma\sqrt{t}x}\phi\left(\frac{-\widetilde{x} + \alpha t}{\sigma\sqrt{t}}\right)\left[1 - exp\left(\frac{2\widetilde{x}\widetilde{y} - 2\widetilde{y}^2}{\sigma^2 t}\right)\right]
\end{aligned}$$

and

$$\begin{aligned}
&\frac{\partial}{\partial y}\left(-\frac{1}{\sigma\sqrt{t}x}\right)\phi\left(\frac{-\widetilde{x} + \alpha t}{\sigma\sqrt{t}}\right)\left[1 - exp\left(\frac{2\widetilde{x}\widetilde{y} - 2\widetilde{y}^2}{\sigma^2 t}\right)\right] \\
&= \frac{2\widetilde{x} - 4\widetilde{y}}{\sigma^3\sqrt{t^3}xy}\phi\left(\frac{-\widetilde{x} + \alpha t}{\sigma\sqrt{t}}\right) exp\left(\frac{2\widetilde{x}\widetilde{y} - 2\widetilde{y}^2}{\sigma^2 t}\right) := \widetilde{f}(x,y)
\end{aligned}$$

Inserting α, $\widetilde{x}$ and $\widetilde{y}$ gives the density, i.e.

$$f(x,y) = \frac{2ln\frac{x}{S_0} - 4ln\frac{y}{S_0}}{\sigma^3\sqrt{t^3}xy}\phi\left(\frac{-ln\frac{x}{S_0} + (\mu - \frac{1}{2}\sigma^2)t}{\sigma\sqrt{t}}\right) exp\left(\frac{2ln\frac{x}{S_0}ln\frac{y}{S_0} - 2ln\frac{y}{S_0}^2}{\sigma^2 t}\right)$$

B.6 Supplementary figures

Figure B.2 shows the fair (g,c)-tuples for the minimum strike setting w.r.t different lengths of the observation period. We assume a monthly price observation and a volatility of

$\sigma = 25.00$ %. The longer the observation period the higher is the probability that the minimum strike is (much) lower than the underlying price at the end of the observation period. Therefore, the fair cap rate c is the higher the shorter the observation period is. If the length of observation period converges to 0 ($t_n \to 0$), the fair cap rate is equal to the one of the fixed strike setting.

Figure B.2: Fair (g,c)-tuple for minimum strike setting and different observation periods

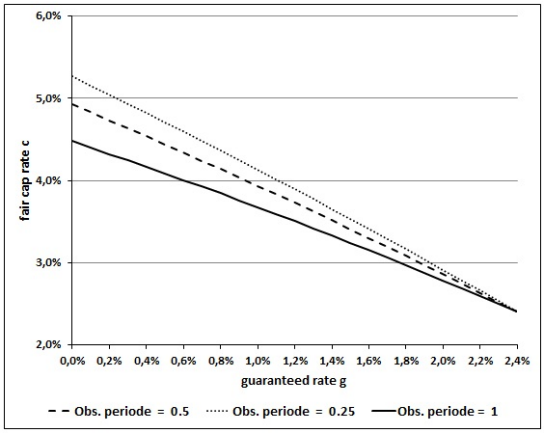

(g,c)-tuple for a BGC with minimum strike setting with variable frequence of observation

B.7 Calculated results for the LCGC$^{(com)}$

Since there is only a marginal difference in the calculated results, it is mentioned in section 5.4 that we illustrate the fair (g,C)-tuple for the LCGC$^{(com)}$ in the Appendix. Figures B.3 and B.4 show the tuple for the Black and Scholes as well as the Heston model. It is seen that the graphs do not significantly differ from the tuple calculated for the LCGC$^{(sum)}$. Overall, the fair locally caps with restrictions concerning the compounded calculation are marginally higher than the fair locally caps observed for the Locally Capped Garant Certificate where the final payoff is calculated by summation of the observed returns. This can be explained by the mathematical fact that a single high negative return has greater influence on the final payoff in the compounded method compared with the summation method.

Besides the different level of the fair locally caps, it is meaningful to mention that a comparable development is observed for all calculation frequencies.

In the monthly calculation, the fair locally caps in the Black and Scholes model differ more than those calculated in the Heston model when we assume higher guaranteed rates. An opposite development is observed in the case of a semi-annual or annual calculation.

Figure B.3: Fair (g,C)-tuple in the BS and Heston model - LCGC$^{(com)}$ monthly vs. quarterly

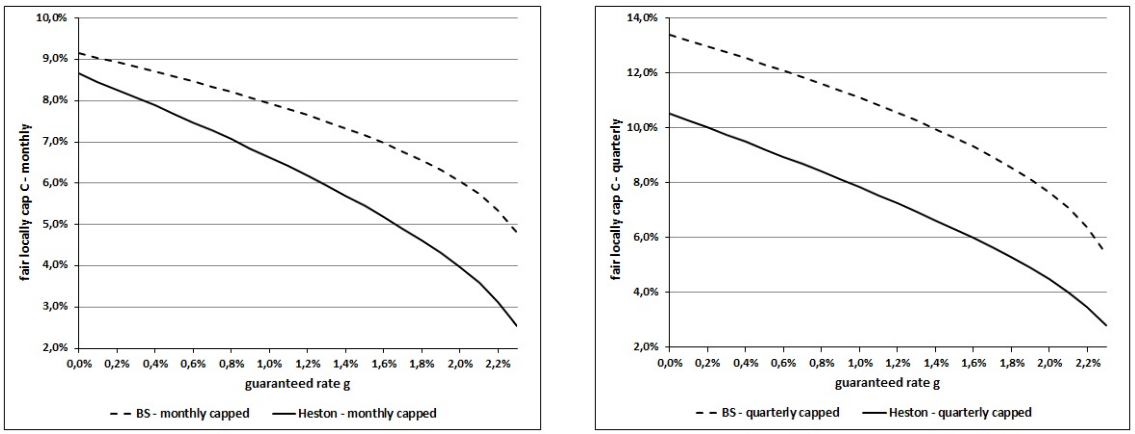

Comparison of model based fair (g,C)-tuple with monthly (left plot) and quarterly (right plot) calculation for the LCGC$^{(com)}$

Figure B.4: Fair (g,C)-tuple in the BS and Heston model - LCGC$^{(com)}$ semi-annual vs. annual

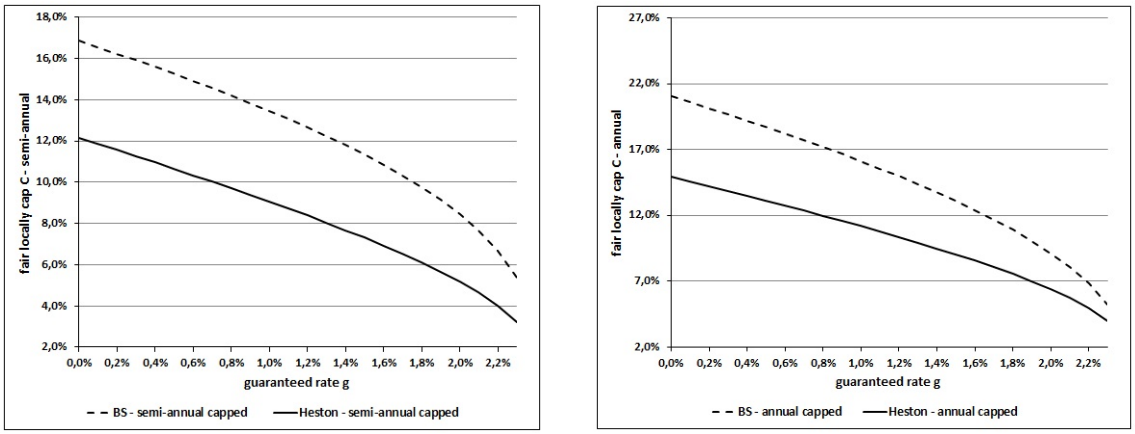

Comparison of model based fair (g,C)-tuple with semi-annual (left plot) and annual (right plot) calculation for the LCGC$^{(com)}$

B.8 Volatility / Variance influences on the payoffs at maturity

We have already mentioned that the level of volatility or variance has a crucial influence on the payoff distribution of the different certificates. Thus, we illustrated in Table 5.4 in section 5.5 the calculated figures for varying volatility in the Black and Scholes model. For a better illustration, Figure B.5 shows the distribution of the return rates at maturity. As mentioned in section 5.5, a crucial swift is identified. Furthermore, the calculation in

Figure B.5: Simulated return rates for the $\text{LCGC}^{(\text{sum})}$ influenced by volatility - BS model

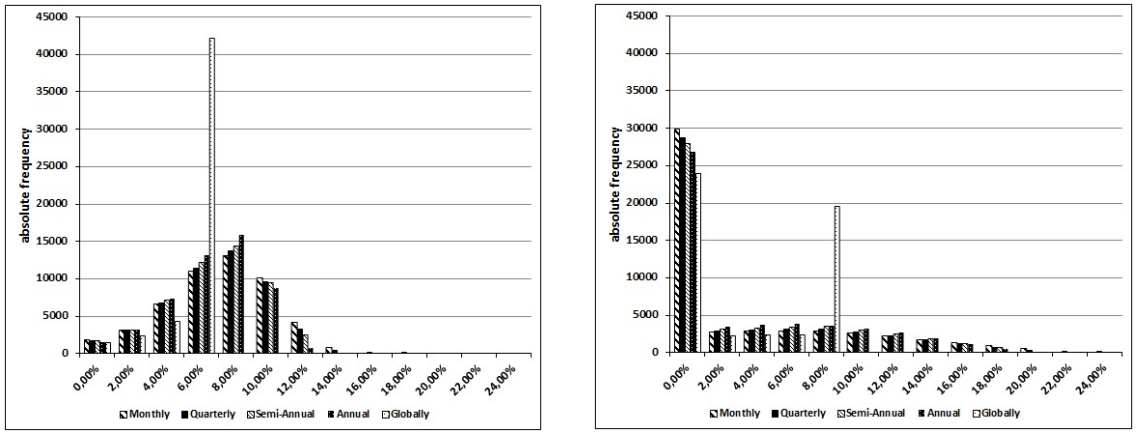

Comparison of the simulated return rates at maturity for a low volatility of $\sigma = 10.0$ % (left plot) and a high volatility of $\sigma = 40.0$ % (right plot) in the benchmark case with $\mu = 9.0$ % assuming the relevant fair locally caps ($C = 4.73$ % resp. $C = 12.76$ %) calculated with the corresponding volatility parameter σ

the Heston model shows significant changes in the characteristics of the distribution at maturity. Referring to section 5.5.2, we should mention that we choose higher and lower long-term variance θ, as well as the initial variance V_0 and the corresponding fair locally cap rates illustrated in Table 5.2. Finally, we adjust the parameter $\overline{\lambda}$ whereby the overall drift is comparable the $\mu = 9.0$ % in the Black and Scholes model.

Figure B.6: Simulated return rates for the $\text{LCGC}^{(\text{sum})}$ influenced by variance - Heston model

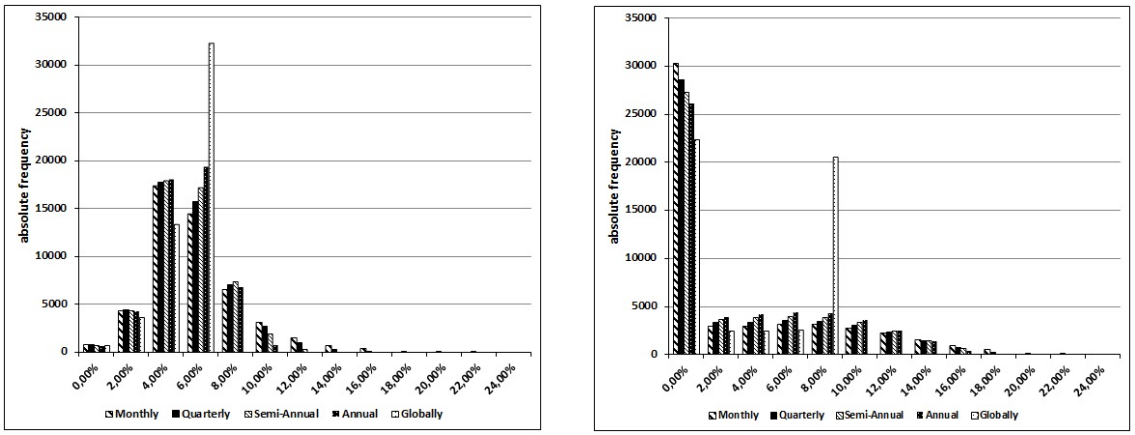

Comparison of the simulated return rates at maturity for a low variance of $\theta = 0.01$ (and $\bar{\lambda} = 6.6$; left plot) and a high variance of $\theta = 0.16$ ($\bar{\lambda} = 0.4125$; right plot) in the benchmark case assuming the relevant fair locally caps ($C = 8.71$ % resp. $C = 11.20$ %) calculated with the corresponding variance parameter θ and V_0

APPENDIX C

Appendix to Chapter 6

C.1 Approximation results

We already mentioned, that we are not able to describe the price of the defaultable Best Grant Certificate by applying the formula of the defaultable call option from Goetz et al. [Goe10]. To be more precise, we need the price of a defaultable bullish vertical spread instead of the summation of the long call and a short call with different strikes. Since we use the describe method in this paper we want to highlight that our results are well approximation for the actually case.

By construction, the illustrated results can be identify as a lower boundary w.r.t. the calculated fair cap as well as upper boundary regarding the t_0-prices. Now, we replace the position of the defaultable short call with a non-defaultable short call (resp. standard Black and Scholes call option). Of course, by this assumption the payoff could become negative if the issuer defaults and the underlying boost at the same time. Hence, the defaultable zerobond as well as the defaultable long call option are cleared with the corrsponding recovery rate. But, the investor have the liability to pay the short call, since she got the relevant premium at issue date.
Nevertheless, this case has a small probability so that we could show with the following results that the fair cap rate of the defaultable bullish vertical spread lie in the calculation range of the upper and lower boundary. In analogy, we state the lower bondary to the fair t_0-prices.
Since we identify tight range between the lower and upper bound, we feel comfortable to use the main results in the paper. We illustrate our results for the combination of $R = 0.5$ and the three initial debt of the issuer.

Figure C.1: Comparison of the fair (g,c)-tuple for a DBGC$^{(\text{fix})}$ and the theoretical constructed DBGC$^{(\text{fix})}$ (with an embedded standard short call)

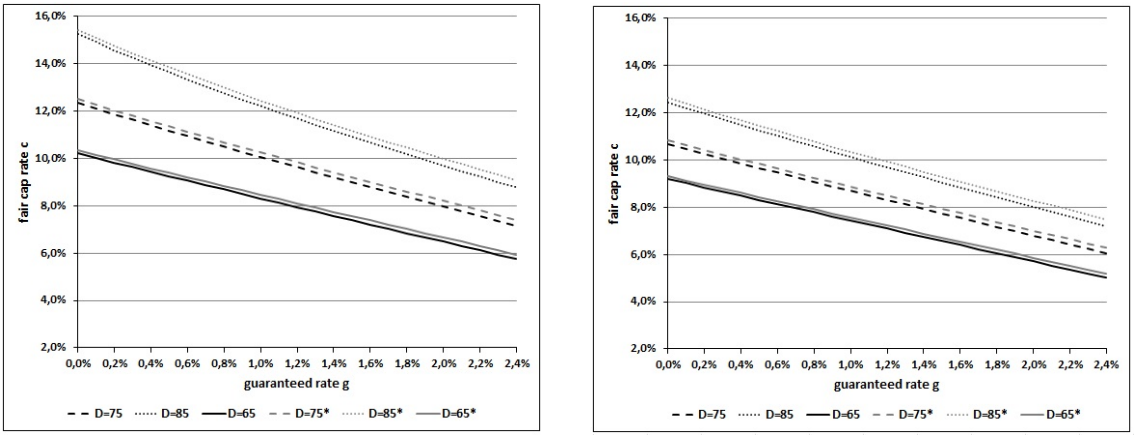

Fair (g,c)-tuple for a DBGC with a fixed entry strike setting compared to the fair tuple of the theoretical constructed DBGC$^{(\text{fix})}$ (with an embedded standard short call) for different initial debt level D_{t_0} and a recovery rate of $R = 0.5$ (left plot) and a more conservative recovery rate $R = 0.6$ (right plot).

C.2 Credit spreads and default probability

First, we apply the formula from Hull [Hul07] to get an approximation of the probability of default. For each observed certificate, we use the corresponding Credit Default Swap of the issuer at issue date. Since all Best Garant Certificates have a time to maturity of 5 years, we are able to use the well-known 5y CDS. Here, we are able to calculate the default probability for the recovery rates $R \in \{40,50,60\}$. The formula from Hull [Hul07] applied on our issue is the following:

$$PD_{t_0} = 1 - \left(\left(1 - \frac{CDS}{(1-R)} \right)^T \right) \tag{C.1}$$

where PD_{t_0} describes the probability at time t_0 that the issuer is insolvent at any time during the time to maturity T (5 years). CDS is the 5 years Credit Default Swap of the issuer at the relevant issue date and R is the recovery rate. We should clarify, that the result seems to be unnormal at the first glance as the default probability is higher for higher recovery rates. If we fix the probability of default and raise the recovery rate, the CDS will be fall since the expecting loss is lower. But, with constant CDS the default probability has to raise when we assume a higher recovery rate, since there is no other

parameter to vary. Afterwards, we use Monto Carlo simulation to identify the initial debt

Table C.1: Probability of default by CDS

PD_{t_0} in %	$BGC^{(\text{fix})}$	$BGC^{(\text{min})}$	$BGC^{(\text{ave})}$
$R = 0.4$	7.15	8.30	8.83
$R = 0.5$	8.53	9.89	10.52
$R = 0.6$	10.57	12.23	13.01

The probability of default is calculated for the three different Best Garant Certificates, where the CDS at the relevant issue date is taken and the recovery rates are varied

D_{t_0} which results to the same default probability when we apply the formula from Goetz et al. [Goe10]. Table C.2 illustrated the results.

Table C.2: Approximation of the initial debt by default probabilities

D_{t_0} in %	$BGC^{(\text{fix})}$	$BGC^{(\text{min})}$	$BGC^{(\text{ave})}$
$R = 0.4$	64.00	67.75	69.50
$R = 0.5$	68.50	72.75	74.25
$R = 0.6$	74.25	79.25	82.00

The initial debt D_{t_0} is approximated by monto carlo simulation. It is calculated for different recovery rates and the probability of default illustrated in Table C.1